Université de Montréal

Développement de modèles prédictifs de la toxicocinétique de substances organiques

par
Thomas Peyret

Département de santé environnementale et santé au travail
Faculté de Médecine

Thèse présentée à la Faculté de Médecine
en vue de l'obtention du grade de Ph.D.
en Santé Publique
option Toxicologie et analyse du risque

Février, 2013

Université de Montréal
Faculté des études supérieures et postdoctorales

Cette thèse intitulée :

Développement de modèles prédictifs de la toxicocinétique de substances organiques

Présentée par :
Thomas Peyret

a été évaluée par un jury composé des personnes suivantes :

Marc Baril, président-rapporteur
Kannan Krishnan, directeur de recherche
Ginette Truchon, membre du jury
Yumei Cecilia Tan, examinateur externe
Patrick du Souich, représentant du doyen de la FESP

Résumé

Les modèles pharmacocinétiques à base physiologique (PBPK) permettent de simuler la dose interne de substances chimiques sur la base de paramètres spécifiques à l'espèce et à la substance. Les modèles de relation quantitative structure-propriété (QSPR) existants permettent d'estimer les paramètres spécifiques au produit (coefficients de partage (PC) et constantes de métabolisme) mais leur domaine d'application est limité par leur manque de considération de la variabilité de leurs paramètres d'entrée ainsi que par leur domaine d'application restreint (c. à d., substances contenant CH_3, CH_2, CH, C, C=C, H, Cl, F, Br, cycle benzénique et H sur le cycle benzénique). L'objectif de cette étude est de développer de nouvelles connaissances et des outils afin d'élargir le domaine d'application des modèles QSPR-PBPK pour prédire la toxicocinétique de substances organiques inhalées chez l'humain. D'abord, un algorithme mécaniste unifié a été développé à partir de modèles existants pour prédire les PC de 142 médicaments et polluants environnementaux aux niveaux macro (tissu et sang) et micro (cellule et fluides biologiques) à partir de la composition du tissu et du sang et de propriétés physicochimiques. L'algorithme résultant a été appliqué pour prédire les PC tissu:sang, tissu:plasma et tissu:air du muscle (n = 174), du foie (n = 139) et du tissu adipeux (n = 141) du rat pour des médicaments acides, basiques et neutres ainsi que pour des cétones, esters d'acétate, éthers, alcools, hydrocarbures aliphatiques et aromatiques. Un modèle de relation quantitative propriété-propriété (QPPR) a été développé pour la clairance intrinsèque (CL_{int}) *in vivo* (calculée comme le ratio du V_{max} (μmol/h/kg poids de rat) sur le K_m (μM)), de substrats du CYP2E1 (n = 26) en fonction du PC *n*-octanol:eau, du PC sang:eau et du potentiel d'ionisation). Les prédictions du QPPR, représentées par les limites inférieures et supérieures de l'intervalle de confiance à 95% à la moyenne, furent ensuite intégrées dans un modèle PBPK humain. Subséquemment, l'algorithme de PC et le QPPR pour la CL_{int} furent intégrés avec des modèles QSPR pour les PC hémoglobine:eau et huile:air pour simuler la pharmacocinétique et la dosimétrie cellulaire d'inhalation de composés organiques volatiles (COV) (benzène, 1,2-dichloroéthane, dichlorométhane, *m*-xylène, toluène, styrène,

1,1,1-trichloroéthane et 1,2,4-trimethylbenzène) avec un modèle PBPK chez le rat. Finalement, la variabilité de paramètres de composition des tissus et du sang de l'algorithme pour les PC tissu:air chez le rat et sang:air chez l'humain a été caractérisée par des simulations Monte Carlo par chaîne de Markov (MCMC). Les distributions résultantes ont été utilisées pour conduire des simulations Monte Carlo pour prédire des PC tissu:sang et sang:air. Les distributions de PC, avec celles des paramètres physiologiques et du contenu en cytochrome P450 CYP2E1, ont été incorporées dans un modèle PBPK pour caractériser la variabilité de la toxicocinétique sanguine de quatre COV (benzène, chloroforme, styrène et trichloroéthylène) par simulation Monte Carlo. Globalement, les approches quantitatives mises en œuvre pour les PC et la CL_{int} dans cette étude ont permis l'utilisation de descripteurs moléculaires génériques plutôt que de fragments moléculaires spécifiques pour prédire la pharmacocinétique de substances organiques chez l'humain. La présente étude a, pour la première fois, caractérisé la variabilité des paramètres biologiques des algorithmes de PC pour étendre l'aptitude des modèles PBPK à prédire les distributions, pour la population, de doses internes de substances organiques avant de faire des tests chez l'animal ou l'humain.

Mots-clés : Toxicocinétique, Modélisation pharmacocinétique à base physiologique, Relation quantitative structure-propriété, Relation quantitative propriété-propriété, Simulation Monte Carlo, Monte Carlo par chaîne de Markov, Coefficient de partage, Métabolisme, Analyse d'incertitude, Dosimétrie cellulaire.

Abstract

Physiologically-based pharmacokinetic (PBPK) models simulate the internal dose metrics of chemicals based on species-specific and chemical-specific parameters. The existing quantitative structure-property relationships (QSPRs) allow to estimate the chemical-specific parameters (partition coefficients (PCs) and metabolic constants) but their applicability is limited by their lack of consideration of variability in input parameters and their restricted application domain (i.e., substances containing CH_3, CH_2, CH, C, C=C, H, Cl, F, Br, benzene ring and H in benzene ring). The objective of this study was to develop new knowledge and tools to increase the applicability domain of QSPR-PBPK models for predicting the inhalation toxicokinetics of organic compounds in humans. First, a unified mechanistic algorithm was developed from existing models to predict macro (tissue and blood) and micro (cell and biological fluid) level PCs of 142 drugs and environmental pollutants on the basis of tissue and blood composition along with physicochemical properties. The resulting algorithm was applied to compute the tissue:blood, tissue:plasma and tissue:air PCs in rat muscle (n = 174), liver (n = 139) and adipose tissue (n = 141) for acidic, neutral, zwitterionic and basic drugs as well as ketones, acetate esters, alcohols, ethers, aliphatic and aromatic hydrocarbons. Then, a quantitative property-property relationship (QPPR) model was developed for the *in vivo* rat intrinsic clearance (CL_{int}) (calculated as the ratio of the *in vivo* V_{max} (μmol/h/kg bw rat) to the K_m (μM)) of CYP2E1 substrates (n = 26) as a function of *n*-octanol:water PC, blood:water PC, and ionization potential). The predictions of the QPPR as lower and upper bounds of the 95% mean confidence intervals were then integrated within a human PBPK model. Subsequently, the PC algorithm and QPPR for CL_{int} were integrated along with a QSPR model for the hemoglobin:water and oil:air PCs to simulate the inhalation pharmacokinetics and cellular dosimetry of volatile organic compounds (VOCs) (benzene, 1,2-dichloroethane, dichloromethane, *m*-xylene, toluene, styrene, 1,1,1-trichloroethane and 1,2,4-trimethylbenzene) using a PBPK model for rats. Finally, the variability in the tissue and blood composition parameters of the PC algorithm for rat tissue:air and human

blood:air PCs was characterized by performing Markov chain Monte Carlo (MCMC) simulations. The resulting distributions were used for conducting Monte Carlo simulations to predict tissue:blood and blood:air PCs for VOCs. The distributions of PCs, along with distributions of physiological parameters and CYP2E1 content, were then incorporated within a PBPK model, to characterize the human variability of the blood toxicokinetics of four VOCs (benzene, chloroform, styrene and trichloroethylene) using Monte Carlo simulations. Overall, the quantitative approaches for PCs and CL_{int} implemented in this study allow the use of generic molecular descriptors rather than specific molecular fragments to predict the pharmacokinetics of organic substances in humans. In this process, the current study has, for the first time, characterized the variability of the biological input parameters of the PC algorithms to expand the ability of PBPK models to predict the population distributions of the internal dose metrics of organic substances prior to testing in animals or humans.

Keywords : Toxicokinetics, Physiologically based pharmacokinetic modeling, Quantitative structure-property relationship, Quantitative property-property relationship, Monte Carlo simulation, Markov chain Monte Carlo, Partition coefficient, Metabolism, Uncertainty analysis, Cellular dosimetry.

Table des matières

Liste des tableaux

CHAPITRE 2

CHAPITRE 3

CHAPITRE 4

CHAPITRE 5

CHAPITRE 6

Liste des figures

CHAPITRE 2

CHAPITRE 3

CHAPITRE 4

CHAPITRE 5

CHAPITRE 6

CHAPITRE 7

Abréviations

Les abréviations ci-dessous sont citées dans le texte. Certains noms de paramètres qui n'apparaissent qu'une fois dans une équation ou un tableau ne sont pas présentés dans cette liste.

[MSP] : Concentration en protéines microsomiales

[P450] : Concentration en cytochrome P450

2-D : À 2 Dimensions

3-D : À 3 Dimensions

AC : Noyau benzénique

ADME : Absorption, distribution, métabolisme et excrétion

AFSSET : Agence française de sécurité sanitaire de l'environnement et au travail

AUC : Aire sous la courbe

AUC_{24} : Aire sous la courbe de 0 à 24 heures

AUC_{Emax} : Aire sous la courbe de simulation avec taux de métabolisme maximum (égal au débit sanguin au foie)

AUC_{Emin} : Aire sous la courbe de simulation sans métabolisme

BW : Masse corporelle

C : Concentration

C=C : Deux carbones avec double liaison

CA : Concentration artérielle

CALV : Concentration alvéolaire

C_{cl} : Concentration dans la cellule hépatique

C_{ct} : Concentration dans la cellule du tissu

CF : Concentration dans le tissu adipeux

Cf_i : Contribution du fragment *i* à la valeur de la réponse

CI : Concentration inhalée

C_{ifl} : Concentration dans le liquide interstitiel hépatique

C_{ift} : Concentration dans le liquide interstitiel tissulaire

CL : Concentration dans le foie

CL_h, CLH : Clairance hépatique

CL_{int}, CLINT, CLint : Clairance intrinsèque

$CL_{intblood}$: Clairance intrinsèque en litres de sang par unité de temps

$CL_{intcell}$: Clairance intrinsèque de la cellule du foie

$CLint_{CYP2E1}$, CL_{int2E1} : Clairance intrinsèque normalisée sur le contenu en cytochrome P450 2E1

$CL_{intPL,}$ CLintPL : Clairance intrinsèque normalisée sur le contenu en phospholipides

C_m : Concentration dans la matrice *m*

C_{max} : Concentration maximale

C_{nw} : Concentration de la forme non ionique dans l'eau

COV : Composé organique volatil

CR : Concentration dans les tissus richement perfusés

CS : Concentration dans les tissus pauvrement perfusés

CV : Concentration veineuse

CVF : Concentration veineuse du tissu adipeux

CVL : Concentration veineuse hépatique

CVR : Concentration veineuse des tissus richement perfusés

CVS : Concentration veineuse des tissus pauvrement perfusés

C_{vt} : Concentration dans le sang qui quitte le tissu

CYP : Cytochrome P450

CYP2E1 : Cytochrome P450 2E1

dA_{cl}/dt : Taux de changement de la quantité dans la cellule hépatique

dA_{ct}/dt : Taux de changement de la quantité dans la cellule tissulaire

dA_{met}/dt : Taux de changement de la quantité métabolisée

E : Ratio d'extraction hépatique

EHOMO : Voir HOMO

ELUMO : Voir LUMO

E_{max} : Ratio d'extraction hépatique maximum

E_{min} : Ratio d'extraction hépatique minimum

Exp. :: Valeur expérimentale

F : Statistique de Fisher

F_{aple} : Fraction de phospholipides acides dans l'érythrocyte

F_{aplm} : Fraction de phospholipides acides dans la matrice

F_{cl} : Fraction volumique de cellules dans le foie

F_{ct} : Fraction volumique de cellules dans le tissu

F_{e} : Fraction volumique d'érythrocytes dans le sang

fi : Occurrence du fragment *i*

F_{it} : Fraction volumique de liquide interstitiel dans le tissu

F_{nl} : Fraction volumique de lipides neutres

f_{nlb} : Fraction volumique d'équivalent en lipides neutres dans le sang

F_{nlct} : Fraction volumique d'équivalent en lipides neutres dans les cellules du tissu

F_{nle} : Fraction volumique d'équivalent en lipides neutres dans l'érythrocyte

F_{nlm} : Fraction volumique d'équivalent en lipides neutres dans une matrice

F_{nlp} : Fraction volumique d'équivalent en lipides neutres dans le plasma

f_{nlt} : Fraction volumique d'équivalent en lipides neutres dans le tissu

F_p : Fraction volumique de plasma dans le sang

f_{pb} : Fraction volumique d'équivalent en protéines liantes dans le sang

F_{pr} : Fraction volumique de protéines

F_{pre} : Fraction volumique de protéines liantes dans l'érythrocyte

F_{prm} : Fraction volumique de protéines liantes dans une matrice

fu_p : Fraction libre dans le plasma

F_w : Fraction d'eau

f_{wb} : Fraction d'équivalent en eau dans le sang

F_{wct} : Fraction d'équivalent en eau dans les cellules du tissu

F_{we} : Fraction d'équivalent en eau dans l'érythrocyte

F_{wit} : Fraction d'équivalent en eau dans le liquide interstitiel

F_{wm} : Fraction d'équivalent en eau dans une matrice

F_{wp} : Fraction d'équivalent en eau dans le plasma

f_{wt} : Fraction d'équivalent en eau dans le tissu

GST : Glutathion-S-Tranférase

HDL : Lipoprotéines de haute densité

HOMO : Orbitale moléculaire occupée de plus haute énergie (*highest occupied molecular orbital*)

IDL : Lipoprotéines de densité intermédiaire

I_m : Terme d'ionisation pour la phase aqueuse d'une matrice

IP : Potentiel d'ionisation

IPCS : *International Programme on Chemical Safety* (Programme international sur la sécurité des substances chimiques, PISC)

K_{cat} : Constante catalytique

K_f, KF, KFC : Constance d'élimination de 1er ordre

K_m, Km : Constante de Michaelis-Menten (constante métabolique)

K_p : Coefficient de partage tissu:plasma

K_{pu} : Coefficient de partage tissu:libre plasma

LDL : Lipoprotéines de basse densité

LFE : énergie libre linéaire (*Linear free energy*)

LMCI : Limite inférieure de l'intervalle de confiance à la moyenne

logclint : Logarithme (base 10) de la clairance intrinsèque

LUMO : Orbitale moléculaire non-occupée de plus basse énergie (*lowest unoccupied molecular orbital*)

Max : Maximum

MC : Monte Carlo

MCMC : *Markov chain Monte Carlo*, Monte Carlo par chaîne de Markov

Min : Minimum

MM2 : *Molecular mechanics program*

MOPAC : *Molecular Orbital PACkage*

MSP : Protéine microsomiale

MW : Masse moléculaire

n : Nombre d'observations

NRC : National Research Council

NSERC : Conseil de recherche en sciences naturelles et en génie du Canada

OECD : *Organisation for Economic Co-operation and Development*; Organisation de Coopération et de Développement Économiques (OCDE)

PA_{bif} : Produit croisé de perméation entre le sang et le liquide interstitiel

PA_{cifl} : Produit croisé de perméation entre la cellule hépatique et le liquide interstitiel

PA_{cift} : Produit croisé de perméation entre la cellule tissulaire et le liquide interstitiel

P_{aplw} : Coefficient de partage phospholipide acide:eau

PB : Coefficient de partage sang:air

P_{ba} : Coefficient de partage sang:air

PBPK : *Physiologically based pharmacokinetic*; pharmacocinétique à base physiologique

PBTK : *Physiologically based toxicokinetic*; toxicocinétique à base physiologique

P_{bw} : Coefficient de partage sang:eau

PC : Coefficient de partage

P_{cift} : Coefficient de partage cellule tissulaire:liquide interstitiel

P_{clb} : Coefficient de partage cellule hépatique:sang

P_{clif} : Coefficient de partage cellule hépatique:liquide interstitiel

P_{clw} : Coefficient de partage cellule hépatique:eau

P_{ct} : Coefficient de partage cellule tissulaire:eau

P_{e} : Coefficient de partage érythocyte:eau

P_{ew} : Coefficient de partage érythrocyte:eau

PFB : Coefficient de partage tissu adipeux:air

P_{hba} : Coefficient de partage hémoglobine:air

P_{Hbw}, P_{hbw} : Coefficient de partage hémoglobine:eau

P_{ib} : Coefficient de partage liquide interstitiel:sang

P_{it} : Coefficient de partage liquide interstitiel:eau

PISC : Acronyme francais pour IPCS (Programme international sur la sécurité des substances chimiques)

P_{iw} : Coefficient de partage liquide interstitiel:eau

PK : Pharmacocinétique

PL : Phospholipide

PLB : Coefficient de partage foie:air

P_{mw} : Coefficient de partage matrice:eau

P_{oa} : Coefficient de partage octanol ou huile:air

P_{ow} : Coefficient de partage octanol ou huile:eau

P_{p} : Coefficient de partage plasma:eau

P_{pw} : Coefficient de partage plasma:eau

P_{plb}, pplb : Coefficient de partage phospholipide:sang

P_{plw} : Coefficient de partage phospholipide:eau

P_{prw} : Coefficient de partage protéine:eau

P_{prwp} : Coefficient de partage albumine plasmatique:eau

PRB : Coefficient de partage tissus richement perfusés:air

Pred. : Valeur prédite

PSB : Coefficient de partage tissus pauvrement perfusés:air

P_{ta} : Coefficient de partage tissu:air

P_{tb} : Coefficient de partage tissu:sang

P_{wa} : Coefficient de partage eau:air

Q^2 : Diagnostic de validation croisée

Qc, QC, QCc : Débit cardiaque

Qf, QF, QFc : Débit sanguin du tissu adipeux

Ql, Q_L, QL, QLc : Débit sanguin hépatique

Qp, QP, QPc : Ventilation alvéolaire

QPPR : Relation quantitative propriété-propriété

Qr, QR, QRc : Débit sanguin des tissus richement perfusés

Qs, QS, QSc : Débit sanguin des tissus pauvrement perfusés

QSAR : Relation quantitative structure-activité

QSPR : Relation quantitative structure -propriété

R^2 : Coefficient de détermination

R^2_{adj} : Coefficient de détermination ajusté par rapport aux degrés de liberté du modèle

rAF : Taux d'accumulation dans le tissu adipeux

rAL : Taux d'accumulation dans le foie

RAM : Taux de quantité métabolisée

rAR : Taux d'accumulation dans les tissus richement perfusés

rAS : Taux d'accumulation dans les tissus pauvrement perfusés

SAR : Relation structure-activité

SR : Ratio de sensibilité

SV : Volume molaire

UMCI : Limite supérieure de l'intervalle de confiance à la moyenne

US EPA : *United States Environmental Protection Agency*

VF : Volume du tissu adipeux

VFc : Volume du tissu adipeux

VIF : Facteur d'inflation de la variance

V_l, V_L, VL : Volume du foie

VLc : Volume du foie

VLDL : Lipoprotéines de très basse densité

V_{max}, Vmax : Vitesse maximale du métabolisme

VOC : Composé organique volatil

VR, VRc : Volume des tissus richement perfusés

VS, VSc : Volume des tissus pauvrement perfusés

Vt : Volume du tissu *t*

WHIM : *Weighted holistic invariant molecular*

Remerciements

Mes premiers remerciements vont au professeur Kannan Krishnan, d'abord pour avoir accepté de m'encadrer quelques années de plus pour ce doctorat. J'ai toujours apprécié vos précieux conseils, votre encadrement, votre soutien, votre patience, votre culture de l'excellence et du dépassement de soi et bien sûr, vos qualités humaines. C'est un privilège d'avoir un directeur comme vous, vous serez toujours pour moi un exemple à suivre.

Je tiens à remercier Patrick Poulin, ce fut un honneur pour moi de collaborer avec vous, dont je lisais les articles depuis des années, merci pour vos conseils et nos échanges amicaux.

Merci à vous mes collègues de laboratoire Katia, Mathieu, Michelle, Nazanin, Thérèse et Yannick. J'ai passé de très bons moments avec vous.

Merci à tous les membres du Département de santé environnementale et santé au travail. Vous êtes comme une très belle petite famille pour moi, dont je suis fier d'avoir été membre pendant sept ans. Un merci spécial aux étudiants du Département que je n'ai pas encore mentionné et avec qui j'ai passé des moments inoubliables : Maximilien, Cyril, Nolwenn, Naïma.

Merci aux organismes qui ont subventionné mes études et mes travaux de recherche: l'Agence française de sécurité sanitaire de l'environnement et du travail (remplacée par l'Agence nationale de sécurité sanitaire de l'alimentation, de l'environnement et du travail, ANSES) et le Conseil de recherche en sciences naturelles et en génie du Canada (CRSNG).

Ma famille, merci de votre soutien à quelques milliers de kilomètres de distance. Oui, mes parents, mes frères, mes grand-mères, oui tout le monde, le doctorat est terminé.

Et je finirai par mes amours : Catherine, Justin et Alizé, merci pour m'avoir soutenu jusqu'au bout.

Chapitre 1. Introduction générale

1.1. La modélisation QSAR pour les modèles pharmacocinétiques à base physiologique de contaminants environnementaux

La pharmacocinétique (PK) et la toxicocinétique (TK) consistent en l'étude de l'absorption, distribution, métabolisme et élimination (ADME) de substances toxiques ou à usage pharmacologique en fonction du temps (Gibaldi et Perrier, 1982). En analyse de risque, la connaissance de la cinétique de la dose interne permet de réduire l'incertitude dans la relation entre la dose externe et la réponse (Klaassen, 2001; Krishnan et Andersen, 2007). La pharmacocinétique peut être prédite à l'aide de modèles compartimentaux ou de modèles pharmacocinétiques à base physiologique (PBPK). Les modèles compartimentaux sont des descriptions mathématiques, comme des équations algébriques et différentielles, dont les valeurs des paramètres sont ajustées sur des données pharmacocinétiques. Les modèles PBPK consistent en un assemblage de descriptions mathématiques mécanistes des processus d'ADME. L'organisme est y décrit comme un ensemble de compartiments reliés entre eux par des flux. Les compartiments d'un modèle PBPK correspondent à des organes ou ensembles d'organes ayant des caractéristiques biochimiques, physiologiques et/ou anatomiques comparables (Reddy, 2005; Krishnan et Andersen, 2007; Krishnan et Andersen, 2010). Les modèles PBPK permettent de simuler la cinétique de molécules dans le sang et les tissus d'intérêt d'un organisme, cela à condition que le modèle conceptuel soit en accord avec la réalité et d'en connaître tous les intrants. Dans ces derniers, il y a trois catégories de paramètres : physiologiques, physicochimiques et biochimiques. Les paramètres physiologiques (p.ex. débits sanguins, volumes des tissus, débit alvéolaire, concentration en enzymes biotransformantes) sont spécifiques à l'espèce étudiée et des valeurs standards sont disponibles dans la littérature (Arms et Travis, 1988; Brown et coll., 1997; Valentin, 2002). Par contre, les paramètres physicochimiques (coefficients de partage, PC) et biochimiques (constantes métaboliques) sont spécifiques à la substance et doivent donc être caractérisés expérimentalement ou prédits à l'aide de modèles.

En modélisation PBPK, le PC représente la distribution d'une molécule entre deux phases à l'équilibre (Krishnan et Andersen, 2007). Ce paramètre physicochimique est utilisé pour prédire la distribution d'une substance chimique donnée dans les compartiments des modèles PBPK. Les PC peuvent être déterminés expérimentalement soit *in vitro* par dialyse d'équilibre (Lin et coll., 1982; Igari et coll., 1983; Sultatos, 1990; Sultatos et coll., 1990), distribution à l'équilibre (Sato et Nakajima, 1979a; Sato et Nakajima, 1979b; Fiserova-Bergerova et Diaz, 1986; Gargas et coll., 1988; Johanson et Dynésius, 1988; Gargas et coll., 1989; Kaneko et coll., 1994; Kaneko et coll., 2000) ou ultrafiltration (Lin et coll., 1982; Poet et coll., 2010), soit *in vivo* sur des données de cinétique d'infusion ou intraveineuse (Chen et Gross, 1979; Lam et coll., 1982; Gabrielsson et coll., 1984; Gallo et coll., 1987; Gueorguieva et coll., 2004).

La connaissance du taux de métabolisme est indispensable à la prédiction quantitative de la biotransformation d'une substance. Ce taux est calculé en fonction de constantes métaboliques qui peuvent aussi être déterminées expérimentalement par des méthodes *in vivo* par la méthode de captage de gaz (Filser et Bolt, 1979; Andersen et coll., 1980; Dallas et coll., 1986; Gargas et coll., 1986a; Filser et coll., 2004), par chambre d'air exhalé (Gargas et Andersen, 1989; Gargas et coll., 1990) ou en mesurant la production d'un métabolite (Gargas et coll., 1986b). Les constantes métaboliques peuvent aussi être déterminées *in vitro* à partir de tissus isolés, de tranches de foie ou autre tissu métabolisant, de cellules, de fractions sous-cellulaires, ou encore de préparations post-mitochondriales (Sato et Nakajima, 1979b; Hilderbrand et coll., 1981; Reitz et coll., 1988; Reitz et coll., 1989; DeJongh et Blaauboer, 1996a; 1996b; 1997; Mortensen et coll., 1997; Mortensen et Nilsen, 1998a; 1998b; Mortensen et coll., 2000).

Du fait que la modélisation PBPK nécessite de l'information sur des paramètres physiologiques, physiochimiques et biochimique, elle permet d'obtenir des estimés *a priori* de la TK de substances en disposant de peu ou pas de données pharmacocinétiques. Cependant, dans le cas d'une molécule nouvellement créée ou mal connue, les paramètres

physicochimiques et biochimiques sont souvent inconnus et leur caractérisation expérimentale peut s'avérer longue et coûteuse (Peyret et Krishnan, 2011). Par conséquent, la méconnaissance des valeurs des paramètres spécifiques au produit est un facteur limitant le développement de modèles PBPK pour de nouvelles substances.

Étant donné que le risque pour la santé associé à l'exposition doit être évalué pour des centaines de substances chimiques (Commission des communautés européennes, 2001), la réduction des études expérimentales de toxicité est encouragée pour des raisons éthiques et économiques et le développement de méthodes alternatives sur ordinateur (*in silico*) est fortement encouragé par des gouvernements et autres organisations travaillant à la réglementation de produits en circulation (CEPA, 1999; Commission des communautés européennes, 2001; National Research Council, 2007; OECD, 2012).

Les approches *in silico* utilisées à ce jour pour estimer de manière quantitative les paramètres des modèles PBPK peuvent être classées en deux catégories : Les modèles de relation quantitative structure-activité (QSAR) et les algorithmes à base biologique (Béliveau et Krishnan, 2003). Les modèles QSAR proprement dit sont des modèles qui prédisent des activités biologiques, comme la toxicité. Les modèles qui prédisent des propriétés, physicochimiques ou biochimiques, comme des PC ou des constantes métaboliques à partir de la structure moléculaire sont des modèles de relation quantitative structure-propriété (QSPR). Lorsqu'un paramètre du modèle prédictif d'une propriété est une propriété mesurée expérimentalement (par exemple, le coefficient de partage *n*-octanol:air d'un solvant) alors, le modèle peut être qualifié de relation quantitative propriété-propriété (QPPR). Dans la présente thèse, il arrive que le terme QSAR soit utilisé pour désigner de façon générique des modèles qui prédisent des propriétés en fonction de la structure moléculaire. Les algorithmes biologiques sont des équations prédisant des propriétés sur la base de paramètres biologiques. Par exemple l'information sur le contenu d'un tissu en termes de lipides neutres, protéines et eau peut être utilisée pour estimer la

valeur d'un coefficient de partage entre le tissu et une autre phase (Nichols et coll., 1991; Poulin et coll., 1999; Béliveau et Krishnan, 2003).

Des modèles QSPR pour des PCs et des constantes métaboliques ont été développés et intégrés dans un modèle PBPK pour des composés organiques volatils (COV, alcanes, alcènes, composés aromatiques halogénés et non halogénés) (Béliveau et coll., 2003; Béliveau et coll., 2005; Kamgang et coll., 2008; Price et Krishnan, 2011). Ces modèles QSPR-PBPK ont permis de prédire la toxicocinétique de COV inhalés chez le rat et l'humain à partir d'information simple sur la structure moléculaire. Les QSPR des modèles QSPR-PBPK été estimés à partir du nombre de fragments ou groupes structuraux de la molécule étudiée (p. ex., l'éthane contient 2 groupes CH_3) et leur contribution à la valeur de PC et les constantes métaboliques (p. ex., clairance intrinsèque). Cette méthode à contribution de groupe a cependant un domaine d'application limitée par le nombre de fragments disponibles pour décrire une molécule. Les modèles QSPR-PBPK prédisent la toxicocinétique de produits contenant les fragments suivants : CH3, CH2, CH, C, H sur C, deux carbones avec double liaison (C=C), noyau benzénique (AC), H sur le noyau benzénique, F, Cl, Br. Ces onzes fragments ne permettent donc contenant d'autres éléments que du carbone, de l'hydrogène, du chlore, du brome, et du fluor, comme des molécules oxygénées, des alcynes etc.

L'article présenté dans le chapitre 2 complète cette introduction par une revue de la littérature portant sur différentes méthodes de prédiction des PC et des constantes de métabolisme qui sont nécessaires pour le développement de modèles QSPR-PBPK.

1.2. Méthodes de prédiction de la variabilité en modélisation PBPK

Pour un polluant donné, des différences de concentration dans les matrices biologiques peuvent être observées entre les individus d'une population ayant subi exactement la même exposition. La variabilité des concentrations observées peut être expliquée par la variation entre les individus des processus d'ADME du polluant. La variabilité d'un paramètre (p.ex., débit sanguin hépatique) correspond à la variation inhérente de ce paramètre pour un même individu (variabilité intra-individuelle) ou entre les individus (variabilité interindividuelle) d'une population. L'incertitude reflète plutôt le manque de connaissance dans la valeur du paramètre (U.S. E.P.A., 1997; Bernillon et Bois, 2000).

En modélisation PBPK, un estimé de la moyenne de la dose interne d'un produit ne rend pas compte de la variabilité de cette dose dans la population. La variabilité de la dose interne peut être simulée en considérant la variabilité des paramètres du modèle (Bernillon et Bois, 2000; Krishnan et Andersen, 2007). L'analyse de variabilité ou d'incertitude permet de quantifier l'impact de la variabilité ou de l'incertitude des paramètres d'un modèle PBPK sur une dose interne. En modélisation PBPK, les trois principales méthodes développées pour l'analyse de variabilité sont : i) l'approche par intervalles de probabilité; ii) la simulation Monte Carlo (MC); et iii) la simulation Monte Carlo par chaîne de Markov (MCMC) (Krishnan et Andersen, 2007).

Le choix de l'approche à utiliser dépend principalement des informations disponibles sur la variabilité des paramètres du modèle PBPK (Krishnan et Andersen, 2007). Si l'on dispose seulement de données concernant les valeurs limites des paramètres, l'approche par intervalles de probabilités sera appliquée. L'entrée des valeurs maximales et minimales des paramètres du modèle PBPK permet d'obtenir un intervalle de probabilité de valeur de dose interne. Nong et Krishnan (2007) ont appliqué cette méthode pour déterminer des facteurs de variabilité interindividuelle de COV.

La simulation MC est celle qui a été la plus utilisée pour modéliser la toxicocinétique de population (Droz et coll., 1989; Portier et Kaplan, 1989; Woodruff et coll., 1992; Gearhart et coll., 1993; Cronin et coll., 1995; Clewell et Andersen, 1996; Cox, 1996; Thomas et coll., 1996; Clewell et coll., 1999; El-Masri et coll., 1999; Delic et coll., 2000; Vinegar et coll., 2000; Beck et coll., 2001; Clewell et coll., 2001; Sweeney et coll., 2001; Gentry et coll., 2002; MacDonald et coll., 2002; Tardif et coll., 2002; Timchalk et coll., 2002; Lipscomb et coll., 2003; Pelekis et coll., 2003; Hamelin et coll., 2005; Tan et coll., 2006; Liao et coll., 2007a; Tan et coll., 2007; Valcke et Krishnan, 2010; Valcke et Krishnan, 2011; Huizer et coll., 2012). L'agence américaine de protection de l'environnement a établi des directives pour mener une analyse Monte Carlo aux fins d'estimation du risque toxicologique lié à l'exposition à une substance (U.S. E.P.A., 1997). Cette méthode consiste à assigner des distributions aux paramètres intrants du modèle PBPK. Par cette méthode il est possible de générer des distributions pour les doses internes d'intérêt pour la population étudiée. A chaque simulation Monte Carlo, pour chaque paramètre variant dans le modèle PBPK, une valeur est échantillonnée aléatoirement dans la distribution qui est utilisée pour prédire la TK. Cette opération est repétée plusieurs fois (itérations), jusqu'à obtenir une distribution stable (c. à d. dont la forme ne change plus en ajoutant des échantillons) de dose interne. Cette méthode nécessite donc de connaître les valeurs des paramètres d'entrée (p.ex. moyenne, écart type pour les distributions normales et log normales). La forme et les valeurs des paramètres d'entrée des distributions qui sont assignées aux paramètres du modèle PBPK varient en fonction de la nature du paramètre et du niveau de connaissance actuel (Thomas et coll., 1996; Bernillon et Bois, 2000; Clewell et coll., 2001).

Au cours des dernières années, la simulation MCMC a été appliquée dans plusieurs études de modélisation PBPK (Bois et coll., 1996a; Bois et coll., 1996b; Bois, 2000a; Bois, 2000b; Jonsson et coll., 2001a; Jonsson et coll., 2001b; Jonsson et Johanson, 2001a; Jonsson et Johanson, 2001b; Jonsson et Johanson, 2002; David et coll., 2006; Marino et coll., 2006;

Allen et coll., 2007; Liao et coll., 2007b; Peyret, 2007; Lyons et coll., 2008; Nong et coll., 2008; Chiu et coll., 2009; Mörk et coll., 2009; Péry et coll., 2009; Qiu et coll., 2010; Chiu et Ginsberg, 2011; Sasso et coll., 2012). Alors que la simulation MC permet de simuler la variabilité du résultat d'un modèle en fonction de variabilité donnée pour ces paramètres d'entrée, la simulation MCMC permet de caractériser la variabilité des paramètres d'entrée du modèle à partir de données expérimentales (Bernillon et Bois, 2000; Gelman et coll., 2004). Cette approche fait appel à des modèles dit hiérarchiques, c'est-à-dire qui ont plusieurs niveaux, par exemple un niveau population et un niveau individuel. Dans le cas d'un modèle PBPK hiérarchique de la TK d'un produit donné, au niveau individuel se trouvent un modèle PBPK et des données TK de ce produit, observées chez plusieurs individus. Le niveau population contient les distributions assignées *a priori* (*prior distribution* en anglais) à des paramètres du modèle PBPK pour lesquels la variabilité est à caractériser. Pour chaque individu, les valeurs des paramètres qui varient dans le modèle PBPK sont échantillonnées de façon itérative sur les distributions du niveau population jusqu'à ajuster la prédiction du modèle aux données observées. Ainsi, pour un paramètre donné, la distribution *a posteriori* (*posterior distributions* en anglais) est définie à partie des valeurs échantillonnées sur la distribution *a priori* pour ajuster le modèle aux données observées. Cette approche a l'avantage de générer des distributions qui reflètent la variabilité des données observées, à condition que ces dernières soient assez riches en information.

Pour prédire la variabilité de la TK de polluants environnementaux par simulation MC, il est nécessaire de connaître les valeurs des paramètres des distributions utilisées. Des distributions de paramètres physiologiques utilisées dans des simulations Monte Carlo sont disponibles dans la littérature (Thomas et coll., 1996; Clewell et coll., 2001; Tan et coll., 2007). Par contre, la variabilité des paramètres biochimiques (constantes de métabolisme) et physicochimiques (PC) est plus difficile à caractériser en l'absence de données. Quelques approches, mentionnées plus bas, ont été utilisées en modélisation PBPK pour prédire la variabilité des coefficients de partage et du taux de métabolisme.

1.2.1 Prédiction de la variabilité des coefficients de partage

Les algorithmes à base biologique permettent d'estimer la variabilité des PC à travers la variabilité des paramètres physiologiques. Pelekis et coll. (1995) ont utilisé un algorithme mécaniste de coefficient de partage tissu:air, pour prédire les minima et maxima des coefficients de partage foie, muscle et tissu adipeux:air chez l'humain pour le dichlorométhane. Pour ce faire ils ont utilisé les minima et maxima des contenus tissulaires en eau, lipides neutres et phospholipides chez l'humain, recoltés dans la littérature. Pour les trois tissus étudiés, les valeurs de PC tissu:air mesurées expérimentalement chez le rat se retrouvent dans l'intervalle de valeurs prédites par l'algorithme mécaniste, bien que le PC muscle:air soit moins bien prédit. C'est la seule étude ayant fourni une estimation de la variabilité dans les prédictions de PC à base biologique.

Lowe et coll. (2009) ont utilisé la mesure du niveau en lipides plasmatiques de rats et d'humains pour calculer le coefficient de partage tissu adipeux:sang du chlorpyrifos à différents âges gestationnels. Ainsi cette étude permet de tenir compte de la variation du contenu lipidique du plasma pendant la gestation, les estimés sont assez différents entre le rat et l'humain (de 121 à 178 chez l'humain et de 156 à 250 chez le rat).

1.2.2 Prédiction de la variabilité du métabolisme

Dans le cas de substances qui sont biotransformées par le foie, le taux de métabolisme ne peut pas être supérieur au débit sanguin hépatique. Il est par conséquent possible d'estimer la TK de polluants environnementaux en faisant varier la clairance hépatique entre zéro et le débit sanguin hépatique. Ceci équivaut à utiliser les valeurs extrêmes, 0 et 1, du rapport d'extraction hépatique (Poulin et coll., 1999; Poulin et Krishnan, 1999; Krishnan et Andersen, 2007). Cette méthode permet d'évaluer l'impact de l'ignorance complète du taux de métabolisme d'un produit. Les deux courbes concentration-temps simulées en utilisant 0

et 1 comme valeur de ratio d'extraction enveloppent l'ensemble des courbes concentrations-temps possibles en faisant varier le métabolisme.

Une autre manière de considérer la variabilité interindividuelle en prédisant le métabolisme est de tenir compte de la variabilité de la concentration en enzymes (par exemple cytochrome P450) entre les individus (Lipscomb et coll., 2003; Nong et coll., 2006; Valcke et Krishnan, 2010). Pour ce faire il est possible de décrire la clairance hépatique selon l'équation (23) présentée dans la section 2.4 (Wilkinson et Shand, 1975) :

1.3. Problématique

Pour une première évaluation de la toxicité de nouvelles substances, il serait intéressant de disposer d'outils prédictifs du comportement TK à partir d'un minimum d'informations (p.ex. propriétés physicochimiques). Comme des estimés ponctuels de la TK ne fournissent pas de renseignements sur l'impact de la variabilité des déterminants de la TK dans la population, ces outils prédictifs devrait aussi permettre l'estimation de la variabilité de leur réponse.

La revue de la littérature présentée dans ce chapitre démontre que des algorithmes de coefficient de partage ont été développés pour à peu près toutes les classes de molécules. Il n'apparait pas dans la littérature de modèle prédisant adéquatement à la fois les phénomènes de distribution des polluants environnementaux et ceux des médicaments. Les polluants environnementaux utilisés dans le développement de modèles de coefficient de partage sont tous des molécules neutres et la prédiction de leur distribution est en général plus précise (à peu près 50 % de variation) que la prédiction des coefficients de partage des médicaments, qui ont des propriétés physicochimiques bien plus diverses. Les polluants du futur auront, ou ont déjà, une grande diversité de propriétés physicochimiques, comme c'est déjà le cas pour les médicaments.

La prédiction du métabolisme de substances organiques reste le facteur limitant dans la prédiction *a priori* de la dose interne des polluants environnementaux. Il est important de développer de tels modèles afin de pouvoir tester chacune des substances chimiques à différents niveaux de doses et chez différentes espèces.

Il y a actuellement un manque de modèles prédictifs de PC et de constantes métaboliques qui tiennent compte la variabilité interindividuelle et/ou l'incertitude. La variabilité interindividuelle peut être prédite en considérant la variabilité entre individus de la composition en constituants biologiques de l'organisme qui jouent un role majeur dans les phénomènes d'ADME. Les constituants biologiques utilisés pour prédire la distribution d'un produit chimique sont la composition tissulaire en lipides neutre, phospholipides neutres, eau et protéines alors que la quantité du contenu enzymatique est utilisée pour prédire le métabolisme. Aucun estimé de l'incertitude reliée aux estimés des modèles QSAR des paramètres biochimiques et physicochimiques (p.ex. PC tissu:sang, clairance intrinsèque) n'est disponible actuellement. Des modèles prédisant la variabilité et l'incertitude sur les paramètres PBPK de distribution et de métabolisme permettraient de fournir des prédictions de la TK et de sa variabilité.

1.4. Objectifs

L'objectif de cette thèse est de développer des modèles pour prédire la TK et sa variabilité pour des substances organiques sur la base de la structure moléculaire ou de propriétés physicochimiques.

L'atteinte de cet objectif repose sur l'utilisation de la modélisation PBPK et de simulations Monte Carlo pour évaluer la TK de polluants environnementaux. Les hypothèses spécifiques sont : i) La structure moléculaire et le contenu tissulaire sont déterminants pour la prédiction des paramètres spécifiques au produit; ii) La variabilité interindividuelle des coefficients de partage s'explique par la variabilité interindividuelle du contenu tissulaire

en termes de lipides, eau et protéines; et iii) La variabilité interindividuelle de la biotransformation s'explique par la variabilité interindividuelle du contenu complexes enzymatiques.

1.5. Organisation de la thèse

Les chapitres 1 et 2 dressent l'état de connaissance relatif à l'étude de modèles QSAR ainsi que pour la modélisation PBPK de la variabilité de la TK. Les chapitres 3 à 6 présentent les travaux de recherche réalisés pour atteindre l'objectif de cette thèse. Le chapitre 7 est une discussion générale sur l'ensemble des travaux rapportés.

Dans l'étude présentée au chapitre 3, un algorithme biologique a été développé pour prédire des PC de diverses classes chimiques de composés organiques. Cet algorithme unifié a été dérivé à partir d'algorithmes biologiques publiés, qui permettent de prédire des PC tissu:air, tissu:sang, tissu:plasma, tissu:fraction libre du plasma. Dans cet algorithme, le tissu est subdivisé en deux compartiments : la cellule du tissu et le liquide interstitiel alors que le sang est décrit par les compartiments érythrocytes et plasma. La combinaison de ces compartiments permet de calculer des PC aussi bien au niveau macro (c. à d. tissulaire), qu'au niveau micro (c. à d. cellule ou fluide biologique). Une analyse de sensibilité a été effectuée pour déterminer quels sont les déterminants majeurs de la valeur des PC pour tous les produits étudiés (142 médicaments et polluants environnementaux).

Le chapitre 4 rapporte le développement d'un modèle de QPPR pour la clairance intrinsèque de COV inhalés chez le rat. Dans cette étude, une nouvelle estimation de la clairance, normalisée sur le contenu en phospholipides, a servi de variable dépendante pour le QPPR. Les limites de l'intervalle de confiance à 95 % (à la moyenne) des estimés QPPR de la clairance intrinsèque ont servi comme paramètres d'entrée dans un modèle PBPK pour des COV inhalés. Ceci permet de visualiser l'ensemble des courbes concentrations-temps simulées enveloppées, par les courbes correspondant aux simulations utilisant les

valeurs supérieures et inférieures de l'intervalle de confiance de clairance intrinsèque prédite. Cet ensemble de courbes est appelé enveloppe de concentrations. Pour 37 COV, l'enveloppe des concentrations sanguines simulées en utilisant les limites de l'intervalle de confiance des prédictions du modèle QPPR a été comparée avec l'enveloppe des concentrations sanguines simulées avec les limites physiologiques du métabolisme (c. à d. avec une clairance hépatique comprise entre 0 et le débit sanguin hépatique). Une analyse de confiance dans l'application de ce QPPR pour prédire l'aire sous la courbe de concentration sanguine-temps a été effectuée, sur la base des travaux du PISC (2010).

Le chapitre 5 présente le développement de QSPR pour les paramètres physicochimiques de l'algorithme unifié (chapitre 3) pour des COV. Des QSPR pour les PC huile:air et hémoglobine:eau ont été développés. Ces QSPR, incorporés dans l'algorithme unifié, permettent de prédire les PC nécessaires à la modélisation PBPK sans avoir recours à des mesures expérimentales. Les PC prédits sur la base des QSPR ainsi que des prédictions QPPR de clairance intrinsèque, ont été incorporés dans un modèle PBPK à dosimétrie cellulaire. Ce modèle PBPK a été utilisé pour prédire la TK de 26 COVs chez le rat.

Le chapitre 6 présente le développement d'un modèle PBPK pour prédire la variabilité de la TK associée à l'inhalation de COV chez l'humain. Dans ce modèle, les PC ont été prédits par l'algorithme unifié en utilisant les QSPR pour ces paramètres d'entrée. La clairance intrinsèque a été prédite par le modèle QPPR développé dans le chapitre 4. La variabilité des paramètres physiologiques de l'algorithme de PC a été caractérisée par modélisation MCMC en utilisant des données individuelles de PC sang:air du toluène et de l'acétone chez l'humain et de données de PC tissu:air pour 76 COV. La variabilité des paramètres biologiques ainsi caractérisée a servi à prédire des distributions de PC tissu:sang et sang:air. Pour le benzène, le chloroforme, le styrène et le trichloroéthylène, les distributions de PC prédites, de contenu en cytochrome P450 CYP2E1 et des paramètres physiologiques tirées de la littérature (Clewell et coll., 2001; Lipscomb et coll., 2003) ont été incorporées dans un modèle PBPK chez l'humain. Des simulations MC ont été effectuées pour prédire la TK de

ces quatre COV. Des distributions d'aire sous la courbe concentration-temps ont été simulées. Les prédictions des enveloppes de concentration ont ensuite été comparées à des données expérimentales.

Chapitre 2. QSARs for PBPK modelling of environmental contaminants

Peyret, T. and Krishnan, K. 2011. QSARs for PBPK modelling of environmental contaminants. SAR QSAR Environ. Res. 22, 129-169.

QSARs for PBPK modelling of environmental contaminants

Thomas Peyret and Kannan Krishnan

Département de santé environnementale et santé au travail,
Université de Montréal, Montréal, Canada H3T 1A8

(Received 28 July 2010; in final form 12 November 2010)

2.1. Abstract

Physiologically-based pharmacokinetic (PBPK) models are increasingly finding use in risk assessment applications of data-rich compounds. However, it is a challenge to determine the chemical-specific parameters for these models, particularly in time- and resource-limiting situations. In this regard, SARs, QSARs and QPPRs are potentially useful for computing the chemical-specific input parameters of PBPK models. Based on the frequency of occurrence of molecular fragments (CH_3, CH_2, CH, C, C=C, H, benzene ring and H in benzene ring structure) and exposure conditions, the available QSAR-PBPK models facilitate the simulation of tissue and blood concentrations for some inhaled volatile organic chemicals. The application domain of existing QSARs for developing PBPK models is limited, due to lack of relevant data for diverse chemicals and mechanisms. Even though this approach is conceptually applicable to non-volatile and high molecular weight organics as well, it is more challenging to predict the other PBPK model parameters required for modelling the kinetics of these chemicals (particularly tissue diffusion coefficients, association constants for binding and oral absorption rates). As the level of our understanding of the mechanistic basis of toxicokinetic processes improves, QSARs to provide *a priori* predictions of key chemical-specific PBPK parameters can be developed to expedite the internal dose-based health risk assessments in data-poor situations.

Keywords: PBPK modelling; QSAR-PBPK; pharmacokinetics; in silico

2.2. Introduction

Molecular structure-based prediction of the temporal change in the concentration of environmental chemicals or their metabolites in blood and organs of exposed organisms is a challenge. Even though several investigators reported the development of quantitative structure–property relationship (QSPR) models for certain pharmacokinetic parameters (e.g. volume of distribution, half-life) of anaesthetics and pharmaceuticals [1–3], there are few efforts on the QSAR-based prediction of the pharmacokinetic or toxicokinetic profiles of chemicals. The pharmaceutical literature consists of numerous examples of 2-D QSARs, 3-D QSARs and expert systems for modelling the individual components or phases of drug disposition and pharmacokinetics (i.e. absorption, distribution, metabolism and elimination; ADME). Several reviews and reports present the advantages and limitations of the currently available algorithms and software for in silico modelling of the drug dissolution/bioavailability, oral absorption rate/fraction, volume of distribution, pathways, affinities or rates of metabolism, renal excretion rate as well as affinity for specific transporters [3–20]. These QSPRs for pharmacokinetic parameters and individual ADME processes could not be and have not been used in predictive toxicology, particularly in risk assessment, for providing *a priori* predictions of the time-course of the tissue or blood concentrations of the toxic moiety in intact animals and humans exposed to varying doses of chemicals by various routes and scenarios. Furthermore, the development of QSARs for each sampling point, dose, route and species would be an arduous task. However, *a priori* predictions can be obtained by developing QSPRs for the chemical-specific input parameters of mechanism-based models such as the physiologically-based pharmacokinetic (or toxicokinetic) models.

Physiologically-based pharmacokinetic (PBPK) modelling refers to the development and evaluation of mathematical descriptions of the ADME of chemicals in biota based on proven/hypothetical mechanistic determinants [21]. PBPK models essentially represent a systems biology approach to the study of ADME and are increasingly finding use in screening-level as well as quantitative risk assessments to reduce the uncertainties

associated with interspecies, route-to-route, and high-dose to low-dose extrapolations of tissue dose of chemicals [21–24]. These models represent the organism as a set of several tissue compartments interconnected by blood flows (Figures 1 and 2). The compartments correspond to individual organs or groups of organs exhibiting the same time-course behaviour, as simulated by solving sets of mass-balance differential equations [21]. Examples of equations commonly used in PBPK models for simulating the pharmacokinetics of inhaled volatile organic chemicals (VOCs) are listed in Table 1. The input parameters required for solving the set of PBPK model equations are either species-specific or chemical-specific. The species-specific parameters, for example, relate to alveolar ventilation rate (*Qp*), cardiac output (*Qc*), tissue blood flow rates (*Qt*) and tissue volumes (*Vt*). The chemical-specific input parameters include partition coefficients (blood:air (P_{ba}), tissue:air (P_{ta}) or tissue:blood (P_{tb})) as well as metabolic parameters such as the maximal velocity (Vmax) and Michaelis affinity constant (Km) or the intrinsic clearance (V_{max}/Km). The species- and age-specific values of several physiological parameters (*Qp*, *Qc*, *Qt*, *Vt*) are available in the biomedical and physiology literature [21,25,26]. However, the physicochemical (P_{ba}, P_{ta}, P_{tb}) and biochemical (V_{max}/Km) parameters need to be determined experimentally or predicted using animal-replacement methods for each chemical individually.

Even though *in vivo* and *in vitro* methods for determining blood:air, tissue:air, tissue:blood partition coefficients exist (e.g. equilibrium dialysis, vial equilibration, ultrafiltration, steady-state kinetic studies) [21], they are time- and resource-consuming, particularly for chemicals for which analytical method development has not been achieved. Similarly, the metabolic constants can be determined experimentally *in vivo* using the kinetic data from invasive sampling (parent chemical or metabolite), closed/open chamber, gas uptake, or exhaled chamber methods; *in vitro* data collected from isolated organ, tissue slices, cells, microsomes, etc. can be used to scale to *in vivo* conditions based on careful considerations of differences in determinants between the *in vitro* and *in vivo* systems [21,27,28]. As the experimental evaluation of the absorption, distribution and clearance parameters for each

chemical is time- and resource-consuming, it has led to exploratory work on in silico methods for parameterizing PBPK models [29,30].

If SARs, QSARs, QSPRs or QPPRs (referred to hereafter as QSARs) can be developed for predicting the numerical values, or for generating at least some initial estimates or bounds, of the chemical-specific parameters such as P_{ba}, P_{ta}, P_{tb}, V_{max} and Km, then it will be feasible to make a priori predictions of the *in vivo* kinetics of new and untested chemicals. Integration of structure- or property-based algorithms with animal anatomy and physiology information could provide a logical and scientifically-sound means of generating first-cut estimates of the pharmacokinetic behaviour of data-poor chemicals. Basically, in the case of a chemical for which pharmacokinetic parameter database is either incomplete or lacking, the internal dose cannot be reliably estimated (Figure 3A); at the outset, the internal dose measure associated with a particular exposure scenario could vary from anywhere between zero (theoretical minimum) and the potential dose (theoretical maximum). This large uncertainty is due to the fact that there is a lack of precise knowledge regarding the key chemical-specific determinants of ADME (e.g. P_{tb}, P_{ta}, P_{ba}, CL_{int}). Since these parameters, together with the physiology of the animal species, determine the pharmacokinetics (particularly the internal dose) of chemicals in biota, integrated QSAR-PBPK models can effectively predict or identify the possible range of internal dose (Figure 3B). The level of accuracy required for the QSARs then would depend not only upon the intended end-use purpose(s) but also on the sensitivity of the specific input parameters with respect to the model outcome, i.e. predicted internal dose.

This article presents (1) an overview of the QSARs available for predicting the chemical-specific pharmacokinetic determinants, specifically, the partition coefficients (PCs) and metabolic constants, as well as (2) the state-of-the-art for their integration within PBPK models to provide predictions of pharmacokinetics of environmental contaminants in biota.

2.3. QSARs of PCs for PBPK models

The tissue:plasma PCs along with the volumes of tissues and blood determine the apparent volume in which a chemical is distributed in the exposed organism [31]. On the other hand, the plasma:air or blood:air PC along with the alveolar ventilation rate determines the lung clearance of volatile chemicals [21]. Partition coefficients for PBPK modelling can be predicted following diverse approaches ranging from linear regression to biologically-based algorithms incorporating QSARs [29,30].

Several investigators have explored and established the feasibility of predicting the tissue:blood PCs or the Ostwald solubility from measurements of liposolubility such as P_{ow} and solubility in *n*-octanol or vegetable oil using the linear free energy (LFE) approach [32–48]. The LFE-type QSARs have mainly focused on using steric or hydrophobic descriptors. For example, Abraham et al. [47] developed equations for predicting hydrophobic descriptors (i.e. octanol:water, hexadecane:water, alkane:water and cyclohexane:water PCs) based on properties including the McGowan volume, an indicator of compound bulkiness:

$$\log SP = c + rR_2 + s\pi_2^H + a\alpha_2^H + b\beta_2^H + vV_X \quad (1)$$

$$\log P = 0.088 + 0.562R_2 - 1.054\pi_2^H + 0.034\alpha_2^H - 3.460\beta_2^H + 3.814V_X \quad (2)$$

$n = 613$; $r = 0.9974$; sd = 0.116; $F = 23161.6$

where SP: solute property (e.g., solute octanol:water PC); log *P*: logarithm of *n*-octanol:water PC; R_2: solute excess molar refraction; π_2^H: solute dipolarity/polarisability; α_2^H: sum of hydrogen-bond acidity of the solute; β_2^H: sum of hydrogen-bond basicity of the solute and V_X: solute McGowan's volume.

Abraham and Weathersby [48] used a multilinear equation combining the solute excess molar refraction, the solute dipolarity/polarizability and the overall hydrogen bond acidity or basicity along with the log hexadecane PC to predict the oil (n = 88), water (n = 75),

blood (n = 82), plasma (n = 32), brain (n = 41), muscle (n = 41), lung (n = 36), liver (n = 29), kidney (n = 36), heart (n = 24), and fat (n = 36):air PCs for several inorganic and organic chemicals including helium, neon, argon, krypton, xenon, hydrogen, oxygen, nitrogen, nitrous oxide, alkanes, haloalkanes, ketones, alkenes, alcohols and aromatic hydrocarbons:

$$\log L = c + rR_2 + s\pi_2^H + a\alpha_2^H + b\beta_2^H + l\log L^{16} \quad (3)$$

where L : Ostwald solubility (media:air PC); R_2: solute excess molar refraction; π_2^H: solute dipolarity/polarisability; α_2^H: sum of hydrogen-bond acidity of the solute; β_2^H: sum of hydrogen-bond basicity of the solute and L^{16}: Ostwald solubility of hexadecane at 298^{o}K.

In this study, the resulting models performed better for water (n = 75; r = 0.9974; sd = 0.182; F = 912.8) and olive oil (n = 88; r = 0.9985; sd = 0.082; F = 7079.0), rather than for kidney (n = 36; r = 0.9753; sd = 0.266; F = 117.1) and heart (n = 24; r = 0.9784; sd = 0.172; F = 117.1). Abraham and Weathersby [48] observed that non-polar solutes only needed hexadecane:air partitioning (a lipophilic descriptor) to predict the human tissue:air PCs, whereas electrostatic descriptors (i.e. solute dipolarity/polarizability, and hydrogen bond acidity or basicity) were important for functionally substituted compounds such a 1-propanol.

The development of LFE-type QSARs for blood and tissue partitioning was initially based on data for anaesthetic gases [46,49–52]. Since these compounds are relatively lipophilic, the best regression equations were observed for those containing hydrophobic parameters or measures of solubility in lipids and water. Batterman et al. [53] developed quantitative relationships between the human blood:air PCs of four trihalomethanes (chloroform, bromodichloromethane, chlorodibromomethane, and bromoform) and various descriptors including molecular weight and number of bromine atoms in the compound:

$$\log K_{ba} = 0.0072\text{MW} + 0.197 \qquad r^2 = 0.994 \tag{4}$$

where K_{ba}: blood:air PC and MW: molecular weight

$$\log K_{ba} = 0.321N + 1.06 \qquad r^2 = 0.994 \tag{5}$$

where N is the number of bromine atoms.

Since the above descriptors tend to be correlated with lipophilicity (i.e. increases in molecular weight or number of bromine tend to increase P_{ow}), these types of correlations, especially for such a reduced dataset, are also to be expected. DeJongh et al. [54], Meulenberg and Vijverberg [55] and Meulenberg et al. [56] used the hydrophobic descriptors P_{ow}, P_{oa}, and P_{wa} to relate to rat and human blood:air and tissue:air PCs of VOCs.

Meulenberg and colleagues [55,56] used the following regression for the tissue:air PCs:

$$P_{ta} = aoP_{oa} + asP_{sa} + c \tag{6}$$

where P_{ta} is the tissue:air PC; P_{oa} is the oil:air PC and P_{sa} is the saline:air PC.

This resulting model exhibited r^2 values of 0.99, 0.92, 0.98, 0.88, 0.99, and 0.98 for blood, fat, brain, liver, muscle, and kidney, respectively. However, contrary to the regression with tissue:air PCs these authors could only derive adequate regressions for blood:air PCs when a significant intercept was included. Since partitioning into lipids and water was taken into account by the hydrophobic descriptors, presence of an intercept was interpreted as being the result of significant binding to blood proteins.

Basak et al. [57] developed QSPRs to predict the human blood:air PCs using principal component regression, partial least squares and ridge regression methods for 31 low-molecular weight VOCs (18 haloalkanes, four haloalkenes, two nitroalkanes, two aliphatic hydrocarbons and five aromatic hydrocarbons) characterized by 221 topostructural (including information on distances; degree complexity; path, cluster, and chain connectivity indices; Wiener index; Balaban's index; triplet indices), topochemical

(information theoretic and neighbourhood complexity indices, bond connectivity indices; triplet indices; number of non-hydrogen atoms, number of elements in a molecule; molecular weight; Wiener number; hydrogen bond donor indices, E-state descriptors) and geometrical (Kappa zero, Kappa simple and alpha indices) molecular descriptors. The regression analyses were conducted using one or more (combined) classes of molecular descriptors and with all the chemicals or with only the haloalkanes. In general, the ridge regression that used only the topochemical parameters (i.e. molecular weight, quantifying molecular size, triplet indices, encoding information about the nature of atoms, electrotopological state indices, valence and bonding connectivity indices hydrogen bonding parameter) was found to be superior to the other QSPRs (Q^2 leave-one-out = 0.874; PRESS = 7.79). This study also reported a comparison between the QSPRs and the quantitative property–property relationships (QPPR) based on saline:air along with oil:air PCs or rat blood:air PCs. The QSPRs were found to be comparable or superior to the QPPRs using oil and saline:air PCs; furthermore the rat blood:air PC was shown to be the best predictor of the human blood:air PC. Since the value of rat blood:air PC is not routinely measured, the ridge regression QSPRs were developed to permit the prediction of the human blood:air PC based on quickly calculable molecular descriptors. A similar approach was used by these authors to develop QSPRs for predicting the tissue:air (fat, brain, liver, muscle, kidney) PCs in rats and humans [58]. The QSPRs included topostructural, topochemical, three-dimensional, and *ad initio* quantum chemical molecular descriptors as independent variables for 131 chemicals (alkanes, haloalkanes, nitroalkanes, alcohol, ketones, acetates, ethylenes, cycloalkanes, halogenated and nonhalogenated aromatic hydrocarbons). Again, the ridge regression compared to the principal component regression and partial least squares provided the best results and the most significant types of molecular descriptors in the QSPRs were: hydrogen bonding descriptors (number of hydrogen bond donors and acceptor, hydrogen bond donor and acceptor indexes), the polarity descriptor, and the molecular size and shape indices (bond and valence connectivity indexes, number of paths of length of order 1 and 2).

There have been only limited efforts towards the development and evaluation of QSARs for computing PCs of non-volatile, environmental chemicals. In this regard, Parham et al. [59] developed QSARs using steric descriptors, for estimating adipose tissue:plasma and adipose tissue:blood PCs of a congeneric series of 24 polychlorinated biphenyls (PCBs) (from bichlorophenyl to octachlorophenyl). The descriptors included in the model reflected aspects such as the planarity, the number and position of chlorines, as well as the effect of the chlorines on the adjacent carbons. After a stepwise analysis, the following QSPR (r^2 = 0.77) for the logarithm of the adipose tissue:plasma PC (log K_{fp}) was obtained:

$$\text{Log } K_{fp} = 1.9988 - 0.5004\ \text{UNS} + 0.1793\ \text{NPL} + 0.05931\ \text{DIFF}^2 \quad (7)$$

where UNS = 1 if the number of adjacent non-chlorine-substituted *ortho-meta* carbon pairs is higher than 0, UNS = 0 otherwise; NPL is the non-planarity index, equal to the number of *ortho* (2,6,2', or 6') chlorines if the number is less than 2, otherwise equal to 2; and DIFF is the difference between the number of chlorines on the most-substituted ring and the number of chlorines on the least-substituted ring (measure of polarity).

The fat:blood PC was in turn calculated based on the fat:plasma PC and the fraction of PCBs in the blood cells (*fcr*), which in turn was calculated using the following QSPR (r^2 = 0.94):

$$f_{cr} = 0.1954(\pm 0.0586) + 0.1513(\pm 0.0352)\text{NUNMP} \quad (8)$$

where NUNMP is the number of adjacent non-chlorine-substituted *ortho-meta* carbon pairs.

It was shown that the PCs depended mostly on the presence or absence of adjacent non-chlorine-substituted *meta* and *para* carbons. Since PCB congeners without unsubstituted *meta-para* pairs tended to be more slowly eliminated than those with such pairs, it was suggested that the reason for this slower elimination might be the higher adipose tissue:blood PC, leading to a greater storage of PCBs in this tissue [59].

Gargas et al. [60] used connectivity indexes and *ad hoc* descriptors in order to correlate structure with the rat tissue:air PCs of a series of 25 haloalkanes (methanes, ethanes, ethylenes with log olive oil:water PC values between 0.56 and 3.43). The following QSARs for the fat:air PC, based on higher order connectivity indices and ad hoc descriptors (QH: polar hydrogen factor; N_{Cl}, N_{Br}, N_C, N_F: number of chlorine, bromine, carbon, and fluorine atoms, respectively) were obtained in this study:

$$\log P_{fa} = 0.734(\pm 0.096)^{1}\chi^{v} - 0.029(\pm 0.003)(\chi^{v}{}_{s}) - 1.570(\pm 0.284)(1/^{1}\chi) - 0.559(\pm 0.167)(1/^{1}\chi^{v}) - 0.098(\pm 0.038)^{3}\chi_{c}^{vv} + 2.213(\pm 0.365) \quad (9)$$
$$r^2 = 0.9779;\ s = 0.1348$$

$$\log P_{fa} = 0.563(\pm 0.028)N_{Cl} + 1.028(\pm 0.065)N_{Br} + 0.467(\pm 0.060)N_C + 0.270(\pm 0.036)Q_H - 0.199(\pm 0.034)N_F - 0.097(\pm 0.121) \quad (10)$$
$$r^2 = 0.9781;\ s = 0.1341$$

These authors reported that fluorine substitution reduced the tissue solubility, with the greatest effect being observed in biological matrices with the greatest volume fraction of water (e.g. blood). On the contrary, the chlorine and bromide substituents increased solubility in all tissues. Because of the electronegativity of these atoms (F < Cl < Br), it was suggested that these atoms increased the solubility in the media via dispersion interactions. Their study results indicate that it is challenging to evaluate the 'steric' influence independent of the 'hydrophobic' influence, as they relate to tissue solubility of environmental chemicals [60]. More recent work focused on evaluating the contribution of each molecular fragment to the tissue and blood partitioning processes in a global manner. Accordingly, the Free–Wilson approach was used, reflecting the working hypothesis that each substituent in the molecular structure had an additive and constant contribution to the PC of interest [61]:

$$PC = \sum_{i=1}^{n} Cf_i \cdot f_i \qquad (11)$$

where Cf_i is the contribution of the fragment i to the value of the PC and f_i corresponds to the frequency of occurrence of the fragment in the molecule.

Using the above approach, Béliveau et al. [62] carried out linear regression analysis based on the frequency of occurrence of 11 different structural fragments (CH_3, CH_2, CH, C, C=C, H, Cl, F, Br, benzene ring (AC) and H in benzene ring (H on AC)) and the logarithm of published data on tissue:air and blood:air PCs. The experimental data corresponded to the blood:air, fat:air, muscle:air and liver:air PCs of 46 low molecular weight VOCs (16 chloroalkanes, five alkanes, five chloroethylenes, five aromatic hydrocarbons, four bromoalkanes, three bromochloroalkanes, two chlorofluoroalkanes, difluoromethane, 2-bromo-2-chloro-1,1,1-trifluoroethane, vinyl bromide, chlorobenzene, allyl chloride and isoprene). All the chemicals were described using combinations of the eleven molecular fragments listed above. Table 2 summarizes the contributions of the molecular fragments to rat blood:air, liver:air, muscle:air and fat:air PCs of low molecular weight VOCs, as determined by Béliveau et al. [62]. These QSPRs were developed using data for alkanes, haloalkanes, haloethylenes, and aromatic hydrocarbons with log *P* ranging between 0.56 and 5.44. Some classes of haloalkanes, particularly the fluorinated hydrocarbons, were poorly represented in the calibration dataset and thus the predictions of the log PCs using the group contribution represented in Table 2 can have large uncertainty for such chemicals. However, the chlorinatedhydrocarbons are well represented in the dataset; therefore the QSPR model may be more adequate for application to this sub-class of VOCs. Based on these data, for example, the predicted logarithm of the blood:air PC of the 1,2-dichlorethane would equal: (2 x 0.481) + (2 x 0.109) = 1.18.

Using a similar methodology, Kamgang et al. [63] developed QSPRs for predicting fat:air and blood:air PCs of VOCs. The linear regression analysis was conducted with published *in vitro* data of fat:air and blood:air PCs for 20 non-halogenated VOCs (alkanes, alkenes and aromatic hydrocarbons). The eight fragments used in the regression were the same as those listed in Table 2 (i.e. without the three halogens). Table 3 summarizes the fragment

contributions to the rat blood:air PCs and the fat:air PCs, as obtained by these authors. Interestingly, the group contributions that were significant in the analysis of Kamgang et al. [63] (CH_2, H, AC H on AC for blood:air PC; and CH_3, CH_2, CH, H, AC for fat:air PC) were comparable to those reported by Béliveau et al. [62] (Table 2).

Contributions of individual fragments to the model parameters are expected to be dependent on the tissue composition of the species of interest and would vary from one species to another. Accordingly then, several Free–Wilson type QSARs would be required for computing the PCs in multiple tissues and species [62–64]. Should the nature and concentrations of lipids, proteins and water be the same in two tissues of the species of interest, then the calculated molecular fragment contributions are expected to be identical in these species. Ideally then, the strategy would be to incorporate species-specific differences in tissue composition along with chemical-specific parameters reflective of liposolubility. In this regard, a number of tissue composition-based algorithms are potentially of particular use.

The mechanistic, tissue composition-based algorithms for predicting PCs for PBPK modelling were developed by considering ionization, solubility and binding in the various matrices (i.e. intracellular, interstitial, vascular) [65–79]. The fundamental principle of these mechanistic algorithms is that the concentration (or solubility) of a chemical in a biological matrix can be expressed as the sum of its concentration in the key components of the matrix (i.e. water, neutral lipids, charged phospholipids, haemoglobin and/or plasma proteins). Accordingly, for environmental chemicals, the tissue:air PCs have been computed as follows [72]:

$$P_{ta} = P_{oa} \cdot F_{nlt} + P_{wa} \cdot F_{wt} \tag{12}$$

where P_{ta} is the tissue:air PC; P_{oa} is the olive oil:air PC; F_{nlt} is the fractional content of neutral lipids equivalent in tissue; P_{wa} is the water:air PC; and F_{wt} is the fractional content of water equivalent in tissue. Equation (12) for predicting matrix:air PC is adequate only for VOCs that do not bind significantly to macromolecules. For chemicals that bind

significantly to biological macromolecules in blood or tissues, the bound concentrations should be taken into account in computing the apparent PCs [71,80]. In such cases, the prediction of PCs from molecular structure information is compounded by the difficulty of predicting the binding association constants. Béliveau et al. [81], based in the work of Poulin and Krishnan [71], used the following equation to calculate the blood:air PC:

$$P_{ba} = P_{oa} \cdot (F_{nlb} + 0.3 \cdot F_{plb}) + P_{wa} \cdot (F_{wb} + 0.7 \cdot F_{plb}) + f_b \cdot P_{pa} \cdot F_{pb} \quad (13)$$

where P_{oa} is the *n*-octanol:air or oil:air PC predicted from molecular structure information; P_{wa} is the water:air PCs predicted with molecular structure information; P_{pa} is the protein:air PCs predicted with molecular structure information; F_{nlb} is the fraction of neutral lipids in blood; F_{plb} is the fraction of phospholipids in blood; F_{wb} is the fraction of water in blood; F_{pb} is the fraction of proteins in blood and f_b is the fraction of proteins involved in binding.

In the above algorithms, the solubility of the chemical in blood and tissue is described as the sum of its solubility in neutral lipids, phospholipids and water. Here, the phospholipids are assumed to behave as a mixture of neutral lipids (30%) and water (70%), based on literature evidence of the hydrophobicity characteristics of commercial lecithin [70]. According to this approach, the numerical values of P_{ba} and P_{ta} can be predicted with knowledge of (1) blood and tissue lipid, water and protein levels (F_{nlb}, F_{nlt}, F_{plb}, F_{plt}, F_{wb}, F_{wt} and F_{pb}) and (2) the numerical values of P_{oa}, P_{wa} and P_{pa}. Species-specific data on the levels of lipids, water and proteins are available in the literature [42,69,70,73,81–83] (e.g. Table 4). Once the numerical values of these species-specific parameters are included in the above equations, P_{ta} and P_{ba} can be predicted solely fromknowledge of P_{wa} and P_{oa} (and additionally P_{pa} in the case of rat). Here, P_{oa}, the *n*-octanol:air or oil:air partition coefficient, is reflective of the chemical partitioning into the tissue lipids whereas the tissue water:air PC is considered to be the same as the inverse of the Henry's law constant.

Thus, the tissue composition-based algorithms account for both physiological and physicochemical characteristics. For example, in the algorithms for predicting tissue:air and

blood:air PCs (Equations (12) and (13)), the physiological input parameters correspond to the composition of the tissue or the blood, whereas the physicochemical parameters are the oil:air PC, the water:air PC and, additionally, protein:air PC for the blood:air PC [71,72,81]. QSARs for predicting oil:air (or *n*-octanol:air), water:air and blood protein:air PCs are available in the literature [35,81,84-86], facilitating the computation of PCs for different species for the purpose of PBPK modelling. In this regard, Béliveau et al. [81] developed QSPRs for oil, water, and protein:air PCs, and then integrated the results with the tissue and blood composition data for rats and humans to predict the tissue:air (i.e. muscle, liver, and fat), and blood:air PCs, as per Equations (12) and (13). Table 5 summarizes the findings of this QSPR analysis, specifically the contributions of the fragments to the numerical values of olive oil:air, water:air and protein:air PCs, for computing tissue and blood:air PCs. These fragment contributions and QSARs are not specific to any species because they are only used to predict the chemical-specific input parameters of the algorithm. In turn, upon inclusion of the tissue and blood composition data specific to the species (Table 4), predictions of PCs for various tissues and species become feasible - solely from the molecular structure information.

The mechanistic algorithms for predicting PCs have evolved over the years. Tables 6 and 7 summarize the input parameters and the characteristics of the compounds underlying the development of these algorithms. Most of the refinements of the PC algorithms as well as QSARs for binding to albumin have been accomplished based on data for pharmaceutical substances [65,74-76,87-97]. These advances would potentially be informative for guiding further development of QSARs for PCs of metabolites and other non-volatile environmental chemicals that are hydrophilic or that bind extensively to proteins.

2.4. QSARs of metabolic parameters for PBPK models

Metabolism in PBPK models is often described as a first order, second order or saturable process [3] (Table 8). The frequently employed description of enzymatic metabolism requires the knowledge of the maximum velocity of reaction (V_{max}) and the Michaelis

constant (*Km*, i.e. the affinity of the substrate for the metabolizing enzyme). In most situations of human exposure to environmental contaminants, the first order description, based on the use of intrinsic clearance ($CL_{int} = V_{max}/Km$) or hepatic clearance (CL_h), is sufficient. The hepatic clearance CL_h is equal to the hepatic extraction ratio (i.e. the fraction of quantity of chemical extracted by the liver) times the volume of blood perfusing the liver per unit time (Q_L) [31]. The hepatic extraction ratio, *E*, in turn can be calculated on the basis of the intrinsic clearance (CL_{int}) and Q_L as follows [31]:

$$E = \frac{CL_h}{Q_L} = \frac{CL_{int}}{Q_L + CL_{int}} \qquad (14)$$

where $CL_{int} = \frac{V_{max}}{Km + C_v}$ and C_v is the free concentration of chemical at the site of metabolism.

The *in silico* approaches for predicting metabolic rates generally focus on two aspects: (1) identification of substrate specificity and (2) prediction of V_{max}, *Km*, CL_{int} or CL_h. Much of the activity so far has focused on CYP-mediated metabolism. The literature is abundant with approaches and results regarding the modelling of protein structures and pharmacophores [3,5,12]; however, very little progress has been made in terms of QSARs for predicting metabolism parameters (e.g. CL_h, *E*, CL_{int}, V_{max}, or *Km*) required for PBPK modelling of environmental chemicals. Whereas the lessons learnt with (Q)SAR modelling of drug metabolism are useful for orienting work on the development of (Q)SARs for environmental contaminants, there are some obvious limitations. A fundamental one relates to the major isoforms of CYP involved in metabolism. Contrary to the major isozymes involved in the metabolism of pharmaceuticals (CYP2D6, CYP3A4, CYP2C19, CYP1A2), the metabolism of environmental chemicals is principally mediated by: CYP1A1 (e.g. polycyclic aromatic hydrocarbons), CYP1B1 and CYP1A2 (e.g. aromatic amines), CYP2E1 (trichloroethylene, chloroform) as well as CYP3A4 to a limited extent (e.g. larger

molecules) [98]. This aspect might be critical with regard to both qualitative prediction and quantitative prediction of the metabolism of environmental chemicals in biota.

For identifying substrates that can bind to or be metabolized by a given isozyme, a SAR component is often used. Basically, the intent here is to use the information on the active site of the enzyme (protein) and/or molecular structure or features of known substrates to infer about whether or not a particular chemical would be a substrate for a given isozyme. In this regard, visual inspection of the crystal structure, protein homology models and other descriptions of the active site are useful in understanding the structural requirements of molecules that fit into the enzymes or binding sites [99]. Mackman et al. [100] reported that the active site of CYP2E1 (an isozyme involved in the metabolism a number of low molecular weight air and water pollutants) is open to a height of 10 Å directly above the iron atom, and that the active site cavity (topologically congruent in both rats and humans) is primarily located above the pyrrole rings A and D, with the region above the pyrrole ring D being the most accessible. Lewis [101,102] proposed decision trees to identify the human CYP isozymes that can metabolize a given substrate (mostly drugs) using selected molecular descriptors (log *P*, HOMO-LUMO, molecular area, depth or volume), and these are likely to be a useful starting point for identifying isozyme specificity of the metabolism of environmental chemicals.

The results of the step above, i.e. identification of pathways(s) and/or enzyme(s) involved in the metabolism of a set of chemicals, would be useful in guiding the development of QSARs for enzymic metabolism, induction or inhibition, as learnt from past work with drugs [1,20,99-105]. QSARs have been developed to predict the hepatic clearance of benzodiazepines in humans on the basis of physicochemical, electrostatic and steric molecular descriptors such as the difference between the lowest unoccupied and highest occupied molecular orbital energies, the ionization potential, the number of potential hydrogen bond donor atoms in the molecule, the geometry-optimized minimum internal energy, and log *P* [101]. The *in vitro* intrinsic clearance and human hepatic clearance of drugs have been modelled using 10 or more molecular descriptors calculated by specialized software [106,107]. The QSAR developed by Li et al. [106] predicted the human hepatic

clearance from 13 molecular descriptors (cosmic torsional energy; inertia moment 2 length; dipole moment Z component; Kier ChiV4 (cluster) index; number of H-bond acceptors; six-membered rings; group count for methyl; ADME violations; energy of the lowest unoccupied molecular orbital (VAMP LUMO); energy of the highest occupied molecular orbital (VAMP HOMO); VAMP total dipole; VAMP dipole Z component; VAMP octupole ZZZ). Nikolic and Agababa [107] used partial least squares regression (PLSR) to select most relevant molecular descriptors for QSAR modelling of human microsomal intrinsic clearance and half-life of drugs (model 1: $r^2 = 0.84$, Q^2 leave-seven-out = 0.62; model 2: $r^2 = 0.808$, Q^2 leave-seven-out = 0.63). The models were calibrated using experimental data from 29 drugs. Model 1 used 10 molecular descriptors (molecular polarizability; bond information content; mean topological charge index of order 6; radial distribution function-4.5/weighted by atomic masses of the ligands; 3D-MoRSe-signal 24/weighted by atomic Sanderson electronegativities; third component symmetry directional weighted holistic invariant molecular (WHIM) index/unweighted; third component symmetry directional WHIM index/weighted by atomic masses; third component symmetry directional WHIM index/weighted by atomic Sanderson electronegativities; number of tertiary aromatic amines and atom centre = CR2 fragments), whereas model 2 used the same input parameters with the exception of the number of tertiary aromatic amines.

Binding to microsomal proteins is another determinant that needs to be evaluated and modelled, particularly when metabolism data from *in vitro* test systems are used for extrapolating to *in vivo* situations. In this regard, Austin et al. [108] have developed a model that predicts the extent of non-specific binding to microsomal proteins using a modified lipophilicity descriptor (log *P*/*D*) that accounts for the enhanced microsomal binding of basic compounds. This equation was calibrated for 37 drugs (20 bases, $-6.35 \leq \log P \leq 6.34$; 12 neutrals, $0.36 \leq \log P \leq 3.75$; and five acids, $2.86 \leq \log P \leq 4.81$) with less than 90% of compound unbound to microsomal proteins. Austin et al. [109] similarly modelled the extent of binding to hepatocytes based on data for 17 drugs (six bases, $1.99 \leq \log P \leq 5.14$; seven neutrals, $1.34 \leq \log P \leq 3.75$; and four acids, $3.21 \leq \log P \leq 4.81$) using either log *P*/*D* ($r^2 = 0.65$) or log *D* ($r^2 = 0.55$).

Even though there has historically been a general interest in the relationship between chemical structure and metabolic pathways of closely-related chemicals, there are only a few attempts to develop QSARs of CL_h, CL_{int}, V_{max} and Km of environmental pollutants. For example, Yin et al. [110] reported excellent correlations between biotransformation rates and calculated activation energies (ΔH_{act}) of CYP-mediated hydrogen abstractions for six halogenated alkanes (1-fluoro-1,1,2,2-tetrachloroethane, 1,1-difluoro-1,2,2-trichloroethane, 1,1,1-trifluoro-2,2-dichloroethane, 1,1,1,2-tetrafluoro-2-chloroethane, 1,1,1,2,2-pentafluoroethane, and 2-bromo-2-chloro-1,1,1-trifluoroethane) in both rat and human enzyme preparations. Loizou et al. [111] reported correlations between the rate of metabolism, log *P*, polarizability and the activation enthalpy for four 1,1,1-trihaloethanes (1,1,1-trichloroethane, 1,1-dichloro-1-fluoroethane, 1-chloro-1,1-difluoroethane, and 1,1,1-trifluoroethane). Gargas et al. [112] studied the metabolism of 14 chlorinated organic volatile compounds (methanes, ethylenes and ethanes) using the gas uptake inhalation technique. They observed a ranking of the metabolic activity of methanes as a function of their degree of chlorination ($CHCl_3 > CH_2Cl_2 > CCl_4$). Such a trend was also observed with the ethylenes and the ethanes. Mortensen et al. [113] determined the *in vitro* metabolism rates and affinities for 25 hydrocarbons (aromatics, cycloalkanes, *n*-alkanes, 2-methylalkanes and 1-alkenes) containing 6 to 10 carbons. This study reported that the aromatic compounds were metabolized faster than the aliphatic hydrocarbons in terms of CL_{int}. The CL_{int} of the hydrocarbons decreased with increasing number of carbons with no generalizable relationship between metabolic rate and the solubility of the alkanes in water [113]. The lack of more robust analyses of metabolism rates of environmental chemicals may be due to the fact that an exhaustive database on these parameters (i.e. V_{max} and Km together) obtained using the same *in vivo* or *in vitro* protocol is essentially unavailable, and that it is worse when focusing on V_{max} and Km of chemicals metabolized by a specific pathway and/or isozyme. A summary of selected quantitative analysis between chemical structure or properties and metabolism rates of environmental chemicals is provided below.

- Galliani et al. [114] reported that V_{max} for the microsomal *N*-demethylation of para-substituted *N*,*N*-dimethylanilines could be modelled as follows:

$$\log V\max = 0.39\pi - 0.94\sigma - 1.56 \qquad (15)$$

$n = 12$, $r^2 = 0.80$, $s = 0.23$

where V_{max} is the maximal velocity of the microsomal *N*-demethylation of para-substituted *N*,*N*-dimethylaniline; π is the Hansch hydrophobic constant and σ is the Hammett constant.

The above relationship indicates that the V_{max} increases with the substituent lipophilicity and electron-donating capacity of the substituent [99]. Further, this work also developed a QSAR for *Km* values essential for describing saturable metabolism associated with these V_{max} values.

- Csanady et al. [115], analysing the apparent metabolism (epoxidation) rate (mg g^{-1} per h) of a series of alkenes (ethene, 1-fluoroethene, 1,1-difluoroethene, 1-chloroethene, 1,1-dichloroethene, *cis*-1,2-dichloroethene, *trans*-1,1-dichloroethene, 1,1,1-trichloroethene, perchloroethene, propene, isoprene, 1,3-butadiene and styrene), reported that it can be explained by the following molecular parameters: ionization potential, dipole moment and π-electron density, obtained either using a quantum chemical method or from the literature.
- Parham and Portier [116] developed a QSAR model for predicting the rate of metabolism of PCBs. The resulting linear regression model contained seven independent variables describing the steric properties of PCBs (*ortho*, *para*, *meta* positions of the chlorine in different carbon pairs). Using step-wise regression analysis of first order metabolism (hydroxylation) rates of PCBs in rats, either obtained from PBPK models ($n = 9$) or rat liver microsomes ($n = 25$), these authors reported the following quantitative relationship ($r^2 = 0.9606$):

$$\begin{aligned} Log\,rate &= 0.4861(\pm 0.2034) - 0.1364(\pm 0.0267)PL \times NSIDE \\ &+ 0.5694(\pm 0.1638)UNS - 0.2433 \times (\pm 0.0487)NOM \times NOC \\ &- 0.1544(\pm 0.0384)NOM \times NMC + 0.001227(\pm 0.000236)MW \times NUNSTOT \\ &+ 0.8242(\pm 0.1297)IND - 1.1493((\pm 0.1438)MOD \end{aligned} \qquad (16)$$

where PL is a descriptor of noncoplanarity; NSIDE is the number of *meta* (3, 5, 3' or 5') chlorines plus the number of *para* (4 or 4') chlorines; UNS is an indicator variable that is equal to 1 if there are any adjacent unsubstituted *meta* and *para* carbons; NOM is the number of adjacent unsubstituted *ortho-meta* carbons pairs; NOC is the number of ortho (2,6,2' or 6') chlorines; NMC is the number of meta (3, 5, 3' or 5') chlorines; MW is the molecular weight; NUNSTOT is equal to the sum of NUNMP and NUNOM; NUNMP is the number of adjacent non-chlorine-substituted *meta-para* carbon pairs; NUNOM is the number of adjacent non-chlorine-substituted *ortho-meta* carbon pairs; IND is equal to 1 if the data point is from Aroclor-induced experiments and otherwise equal to 0; and MOD is equal to 1 if the data point is from model fit, otherwise equal to 0.

- Gargas et al. [60] attempted to develop a QSAR for the V_{max} of 16 halogenated methanes, ethanes and ethylenes using higher order molecular connectivity indices as follows:

$$Log V_{max} = 1.676(\pm 0.049)^4 \chi_c^v + 0.424(\pm 0.110)^3 \chi_c^v - 0.134(\pm 0.045)^4 \chi_{pc}^v + 1.622(\pm 0.049) \quad (17)$$

The use of first-order connectivity indexes gave relatively better results for the prediction of log V_{max} (r^2 = 0.905, s = 0.1355, n = 16, p < 0.0001) but the predictive power and robustness of the QSAR were questionable. Furthermore, since *Km* values were not successfully modelled in this study, the V_{max} alone could not be used for PBPK modelling.

- QSARs were also developed for the V_{max} (three models) and V_{max}/Km of a series of seven alkylbenzene compounds (toluene, *o*-, *m*, *p*-xylene, ethylbenzene, 1,2,4-trimethylbenzene, styrene), all substrates of CYP2E1 [117]. The input parameters used in the QSARs were the log *P* for log V_{max}/Km, the ΔE (i.e. the difference between the energy of the highest unoccupied molecular orbital, ELUMO, and the energy of the lowest unoccupied molecular orbital, EHOMO) for the log V_{max} (model versions 1 and 3) or the ionization potential (*IP*) of the compound for log V_{max} (model 2):

model 1: $\log V_{max} = 18.799 - 1.632\,(\pm 0.324)\Delta E$ (18)

$r^2 = 0.929$; $s = 0.1197$; $F = 19.08$; $n = 6$

model 2: $\log V_{max} = 18.955 - 1.741\,(\pm 0.345)IP$ (19)

$r^2 = 0.930$; $s = 0.1195$; $F = 19.14$; $n = 6$

model 3: $\log V_{max} = 44.301\,(\pm 7.803)\Delta E - 2.369\,(\pm 0.413)\Delta E^2 - 203.75$ (20)

$r^2 = 0.954$; $s = 0.0986$; $F = 40.41$; $n = 7$

- Knaak et al. [118], based on an initial analysis of the $V_{\max}$ and *Km* for the metabolism of dialkyl *p*-nitrophenyl phosphorothioates and phenyl substituted phosphorothioates to their oxons, reported the following relationships:

$$V\max = -0.05142(MV) + 18.63(xp10) + 0.279(SdsO) + 15.9665 \quad (21)$$

$r^2 = 0.981$, $n = 11$, $F = 118.4$, cross - validation RSS = 13.44

where MV is the molecular volume; xp10 is the simple connectivity index (10th-order path chi index); and SdO is the atom type E-state, sum of all (=0) in the molecule;

$$Km = -56.63(ABSQ) + 24.19(SsCH_3) + 2.222(SsF) + 40.3213 \quad (22)$$

$r^2 = 0.9522$, $n = 11$, $F = 46.48$

where ABSQ is the 3D descriptor, sum of the absolute values of charges on each atom of molecule, in electrons; $SsCH_3$ is the atom type E-state, sum of all (CH_3) E-state values in the molecule; and SsF is the atom type E-state, sum of all (*F*) E-state values in the molecule.

In this study, however, cross-validation of the *Km* model was not possible even though the overall database included relevant pesticides such as parathion, chlorpyrifos, methyl parathion and isofenphos.

- Waller et al. [119] observed that there has been little success in the use of the energy of the LUMO or the energy of the HOMO, to predict the rates of oxidative or reductive metabolism, even though the propensity of chemicals metabolized by these process is indicated by the electron affinity or the ionization potential. Applying a CoMFA analysis to a set of 12 VOCs metabolized principally by CYP2E1 (chloromethane, dichloromethane, chloroform, carbon tetrachloride, chloroethylene, 1,1-dichloroethylene, *cis*-1,2-dichloroethylene, *trans*-1,2-dichloroethylene, trichloroethylene, chloroethane, 1,2-dichloroethane, 1,2-dichloroethane), these authors reported that the combination of steric, electrostatic, LUMO and HINT hydropathicity fields was essential to adequately model the CL_{int} of this small set of environmental chemicals (r^2 = 0.953, q^2 = 0.527) [119]. Developing QSARs for CL_h in this regard would be particularly relevant, given that for highly metabolized chemicals, it is the blood flow rate and not the intrinsic clearance that would limit or determine the extent of hepatic metabolism [120-122].
- Béliveau et al. [62] developed a simpler, group contribution method to compute the *in vivo* CL_h of several relatively lipophilic VOCs (alkanes, haloalkanes, haloethylenes, and aromatic hydrocarbons) in rats. Similarly, Kamgang et al. [63] used the group contribution method to develop QSARs based on the enzyme-content normalized values of CL_{int} of alkanes, alkenes and aromatic hydrocarbons based on *in vitro* data of Mortensen et al. [113]. Table 9 presents the published values of group contributions to the hepatic and intrinsic clearance for VOCs. The intrinsic clearance normalized for P450 2E1 facilitates the extrapolation of the hepatic clearance between species by substituting the species-specific data (i.e. cytochrome P-450 content, volume of liver, hepatic blood flow) in the following equation [81]:

$$CL_h = Q_L \cdot \frac{CL_{\text{int}} \cdot [P450] \cdot V_L}{Q_L + CL_{\text{int}} \cdot [P450] \cdot V_L} \quad (23)$$

where [P450] corresponds to the concentration of cytochrome P-450 in the liver; V_L is the liver volume; Q_L is the blood flow to liver; and $CL_{\text{int, P450}}$ is the intrinsic clearance normalized for P-450 content.

Limited efforts have focused on the integration of the QSARs for partition coefficients and metabolism constants described in the preceding sections along with human or animal physiology information to predict the pharmacokinetics of environmental chemicals using the PBPK model framework, as discussed below.

2.5. QSAR-PBPK modelling

The bottleneck for developing PBPK models for emerging or known environmental contaminants is the chemical-specific input parameters. At the present time, based primarily on research and development in the pharmaceutical arena, a number of QSAR tools have become available to facilitate the prediction of drug absorption, distribution and clearance but not the actual time-course of the drug or metabolite concentration in the target site or blood for various dosing regimens and species. In this context, Blakey et al. [123] developed PBPK models for a homologous series of barbiturates in the rat, focusing on the change in pharmacokinetics and increase in lipophilicity of the congeners due to the addition of methylene group. Regarding environmental chemicals, however, there does not exist a suite of adequate *in silico* approaches to generate *a priori* the values of ADME parameters to facilitate high-throughput PBPK modelling.

Overall, the use of the PBPK modelling framework for simulating pharmacokinetics of a given chemical requires the numerical values of physiological, physicochemical and biochemical parameters [62,63,81,86,120,124]. Whereas the physiological parameters can

be obtained from the literature, the other parameters can be estimated using QSARs as detailed above. The PCs required for PBPK modelling can be estimated from molecular structure information but reliable estimates of metabolic constants for environmental chemicals are often unavailable. In such cases, a pragmatic approach involves setting the numerical value of hepatic extraction ratio, *E*, to 0 or 1 in PBPK models, along with QSAR-driven estimates of PCs. This approach, based on the use of the theoretical physiological limits of metabolism (i.e. zero and liver blood flow), has been demonstrated to be useful for inhaled environmental toxicants [120]. The resulting simulations reflect 'bounds' of the blood concentrations of chemicals reflective of the fact that the liver cannot remove more than what is delivered by the blood flowing to the tissue (i.e. the value of hepatic extraction ratio, *E*, cannot exceed 1) and that the *E* value cannot be lower than 0. The strategy here involves the specification of the values of physiological parameters and QSARs for PCs in the PBPK model and setting of *E* value to 0 or 1 in the metabolism equation. The envelope of blood concentration profiles predicted by such an approach will, in principle, encompass all experimental data [120]. For example, using the human QSAR-PBPK model [81,120], the envelope of blood concentration of trichloroethylene (1 C=C, 1 H, 3 Cl) following 7 h exposure to 12.1 ppm was simulated by setting the value of *E* equal to 0 and then to 1 (Figure 4). The use of the range of *E* is also justified by the fact that metabolic rates might be variable among individuals but will necessarily be within the range of 0 to 1. Further, this approach implicitly considers the impact of pharmacokinetic interactions during mixed exposures. When the hepatic metabolism of a chemical is reduced (or enhanced) due to enzyme inhibition (or induction), the *E* value will change but never exceed 1 or be lower than 0. Introducing the QSARs for computing route-specific absorption rates can extend the current capability of this QSAR-PBPK modelling approach, which is limited to the inhalation route. In this regard a number of algorithms and commercial software are available to provide estimates of skin permeability coefficient as well as oral absorption rates (e.g. 125-131).

A logical and more refined alternative to the prediction of the envelope of the range of blood concentrations would involve the use of QSARs to specify an appropriate or approximate value of the rate of metabolism for a given chemical in the PBPK model. When QSARs for both partition coefficients and metabolism rates are available, the prediction of the pharmacokinetic profiles and internal dose of chemicals has been accomplished with the PBPK modelling framework using one of two approaches (Figure 5). The first approach involves the development of 'species-specific' QSARs for blood:air, tissue:blood and hepatic clearance parameters, and their integration within the PBPK model such that the numerical values of these input parameters are generated automatically during simulations only from molecular structure provided as input [62,86,120]. According to this approach, then, instead of providing experimentally-determined PCs or metabolic constants as input to the PBPK model, all one has to do is to change the number and/or nature of fragments in the molecule to estimate chemical-specific input parameters required for modelling its pharmacokinetics in a specific species (i.e. rat or human). This QSAR-PBPK approach has been investigated by Béliveau et al. [62] using inhaled VOCs in the rat. These authors used Free-Wilson type QSPR models to predict the chemical-specific input parameters (liver:air, richly perfused tissues:air, poorly perfused tissues:air, and fat:air PCs and hepatic clearance), and incorporated them with the PBPK model to predict the inhalation pharmacokinetics of eight VOCs (four from the calibration set: toluene, dichloromethane, trichloroethylene, and 1,1,1-trichloroethane; four outside the calibration set: 1,2,4-trimethylbenzene, ethylbenzene, 1,3-dichloropropene, and 2,2-dichloro-1,1,1-trifluoroethane). For example, to simulate the kinetics of toluene in rat with this QSAR-PBPK model, the frequency of occurrence of molecular fragments (i.e. $1 \times CH_3$, $1 \times AC$, and $5 \times H$ on AC) was entered as input to the model along with their respective contributions to PCs (Table 2). The Free-Wilson model then yields the following blood:air and tissue:blood partition coefficients for toluene in the rat [62]:

- blood:air PC = $10^{[1 \times 0.072 + 1 \times 2.850 + 5 \times (-0.292)]} = 29$;
- liver:blood PC = $10^{[1 \times 0.016 + 1 \times 3.760 + 5 \times (-0.408)]} / 29 = 1.88$; and

- muscle:blood PC = $10^{[1 \times (-0.020) + 1 \times 3.650 + 5 \times (-0.446)]} / 29 = 0.87$.

Similarly, the metabolic clearance of toluene can be computed using the molecular fragments contained in toluene (i.e. 1 $\times CH_3$, 1 $\times$AC, and 5 $\times$H on AC) along with the group contributions listed in Table 9, as follows [62]:

- $CL_h = 1 \times 0.388 + 1 \times 0.128 + 5 \times 0.061 = 0.82$ L/h.

Using the above chemical-specific parameters along with rat physiological parameters (volumes of liver, fat, richly perfused tissues, and poorly perfused tissues respectively equal 0.012, 0.022, 0.012, and 0.174 L; blood flow to liver, fat, richly perfused tissues, and poorly perfused tissues equal 1.31, 0.47, 2.68, and 0.79 L h^{-1}, respectively; cardiac output and alveolar ventilation = 5.25 L h^{-1}), the QSAR-PBPK model simulated the toluene kinetics in blood in rats exposed to 50 ppm for 4 h (Figure 6) [62]. Since the metabolic input parameters did not correspond to V_{max} and Km, this model is of use only under first order conditions, i.e. it is not useful for conducting high dose to low dose extrapolation, to simulate the impact of metabolic saturation on internal dose of toluene.

Another methodological approach in QSAR-PBPK modelling relates to developing chemical-specific parameters that are independent of the species and then integrating them with species-specific parameters (e.g. tissue composition data) such that distribution volume and pharmacokinetic profiles can be predicted (Figure 5B). This approach is exemplified by the work of Béliveau et al. [81]. These authors conducted interspecies extrapolations of the inhalation toxicokinetics of VOCs using the same PBPK model for which the input parameters were predicted using QSARs along with species-specific biological data. Thus, the results of the QSARs for oil:air, water:air and protein:air PCs were used as input for the computation of the blood:air and tissue:blood PCs whereas the QSAR for intrinsic clearance was incorporated along with CYP content and volume of liver in an algorithm for computing hepatic clearance. For toluene, as example, the use of

occurrence of fragments in the molecule (i.e. 1 CH_3, 1 AC, and 5 H on AC) along with the group contributions listed in Table 5, the oil:air, water:air and protein:air PCs are computed as follows [81]:

- oil:air PC = $10^{[1 \times 0.354 + 1 \times 3.729 + 5 \times (-0.190)]} = 1358$;
- water:air PC = $10^{[1 \times (-0.038) + 1 \times 0.650 + 5 \times (-0.062)]} = 2$; and
- protein:air PC = $10^{[1 \times 0.306 + 1 \times 1.970 + 5 \times (-0.028)]} = 136.6$.

Then, incorporating these partition coefficients along with rat tissue and blood composition (Table 4) in the tissue composition-based algorithms (Equations (12) and (13)), the following values of PCs are obtained within the QSAR-PBPK model:

- blood:air PC = 1358 x 0.002 + 2 x 0.8423 + 137 x 0.156 = 26;
- liver:blood PC = (1358 x 0.0425 + 2 x 0.7176) / 26 = 2.3; and
- muscle:blood = (1358 x 0.0117 + 2 x 0.7471) / 26 = 0.68

The intrinsic clearance, normalized to CYP2E1 content in liver, can be calculated using the occurrence of fragments in toluene molecule and the corresponding fragment contributions (Table 10) as follows [81]:

- $CLint_{CYP2E1} = 10^{[1 \times 1.552 + 1 \times (-7.646) + 5 \times 1.535]} = 38$ L/h/μmol CYP2E1.

The QSAR-based intrinsic clearance (2.19 L h^{-1}) was then obtained by multiplying the above $CLint_{CYP2E1}$ value with the hepatic concentration of CYP2E1 (4.8 μmol L^{-1}) and the volume of liver (0.012 L) in rats.

The blood:air and tissue:blood PCs computed using QSARs and species-specific biological data feed into the various equations to provide pharmacokinetic simulations (Figure 5B). The QSAR-PBPK model was initially used to predict the blood kinetic profile of inhaled

toluene in rats (50 ppm, 4 h) (Figure 7A); thereafter by changing only the species-specific physiological data (human tissue and blood compositions reported in Table 4; hepatic concentration of cytochrome P450 2E1 = 2.482 μmol L^{-1}; volumes of liver, fat, richly perfused tissues, and poorly perfused tissues = 1.82, 13.3, 3.5, and 43.4 L, respectively; blood flows to liver, fat, richly perfused tissues, and poorly perfused tissues = 108, 20.9, 184, and 104 L h^{-1}, respectively; cardiac output and alveolar ventilation = 417 L h^{-1}), simulations of kinetics in humans (17 ppm, 7 h) were obtained with the same QSPR-PBPK model (Figure 7B) [81].

The QSAR-PBPK models developed for rats and humans can also be adopted for other species. In this regard, for example, the chemical-specific parameters of the PBPK model for chloroethanes developed for fish [42] can be replaced with the results of QSAR modelling. The log *P* as well as tissue composition data can be used together to compute PCs of 1,1,2,2-tetrachloroethane (log *P* = 2.39, blood:water = 7.8, fat:blood = 37.3, liver:blood = 1.17, muscle:blood = 1.37) in rainbow trout [42,83]. Incorporating these results with data on fish physiology within a PBPK model, it becomes possible to generate a first-cut simulation of the kinetic profile of 1,1,2,2-tetrachloroethane in fish (Figure 8).

2.6. Conclusions

The current paradigm shift in toxicology and risk assessment would benefit from the availability of tools and approaches for generating pharmacokinetic and internal dose information. For data-poor chemicals and situations, it is relevant to explore the use of QSAR-based approaches to provide simulations of pharmacokinetics. The development of SARs and QSPRs for the input parameters of PBPK models will not only facilitate the prediction of the internal dose of a given chemical but also the development of internal dose-based toxicodynamic QSARs of relevance to risk assessment (e.g. [132]). Importantly, all of this can be done solely with knowledge of molecular structure or properties and understanding of the underlying mechanisms. Until now, physicochemical and biochemical parameters required for PBPK modelling have mostly been obtained by conducting *in vivo*

or *in vitro* studies. With the more recent advances and algorithms reviewed in this article, it is clear that chemical-specific parameters such as physicochemical and biochemical constants can be estimated from information on molecular structure. *In silico* approaches for estimating PBPK model parameters have mainly centred on LFE-type QSARs and mechanistic algorithms. The application of LFE QSARs, however, is limited to the biological species in which the data are collected. It is important that mechanistic relevance of the structural descriptors used in these types of equations to the *in vivo* pharmacokinetics of chemicals be developed. The emerging mechanistically-based algorithms offer the potential of being applicable to multiple chemical families as well as multiple levels of organization (e.g. cells, organs, species, populations). However, these approaches should further evolve to account for the uncertainty and variability in input parameters, by applying a distributional rather than a deterministic approach to QSAR-PBPK modelling. Even though the development of QSAR-PBPK approaches has largely been limited to inhaled VOCs, they are conceptually applicable to non-volatile organics as well, but it becomes more challenging to predict the other PBPK model parameters required for modelling the kinetics of the latter (i.e. tissue diffusion coefficients, association constants for binding, oral absorption rates, and dermal permeability coefficients). As our level of understanding of the mechanistic determinants of each of these parameters improves, we can be optimistic of being able to develop mechanistic QSARs to provide *a priori* predictions of these parameters and ultimately the *in vivo* pharmacokinetics of new chemicals, ahead of laboratory evaluations.

2.7. Acknowledgements

The authors wish to acknowledge the grants from ANSES (EST-2007-85) and NSERC (operating grant) to pursue research on the development of QSAR-PBPK models.

2.8. References

[1] C. Hansch, A. Leo, and D.H. Hoekman, *Exploring QSAR*, American Chemical Society, Washington, DC, 1995.

[2] J.M. Mayer and H. van de Waterbeemd, *Development of quantitative structure-pharmacokinetic relationships*, Environ. Health Perspect. 61 (1985), pp. 295–306.

[3] J.K. Seydel and K.J. Schaper, *Quantitative structure–pharmacokinetic relationships and drug design*, Pharmacol. Ther. 15 (1981), pp. 131–182.

[4] A.M. Davis and R.J. Riley, *Predictive ADMET studies, the challenges and the opportunities*, Curr. Opin. Chem. Biol. 8 (2004), pp. 378–386.

[5] S. Ekins, G. Bravi, B.J. Ring, T.A. Gillespie, J.S. Gillespie, M. Vandenbranden, S.A. Wrighton, and J.H. Wikel, *Three-dimensional quantitative structure activity relationship analyses of substrates for CYP2B6*, J. Pharmacol. Exp. Ther. 288 (1999), pp. 21–29.

[6] S. Ekins and R.S. Obach, *Three-dimensional quantitative structure activity relationship computational approaches for prediction of human in vitro intrinsic clearance*, J. Pharmacol. Exp. Ther. 295 (2000), pp. 463–473.

[7] S. Ekins and J. Rose, *In silico ADME/Tox: The state of the art*, J. Mol. Graph. Model. 20 (2002), pp. 305–309.

[8] S. Ekins, C.L. Waller, P.W. Swaan, G. Cruciani, S.A. Wrighton, and J.H. Wikel, *Progress in predicting human ADME parameters in silico*, J. Pharmacol. Toxicol. Meth. 44 (2000), pp. 251–272.

[9] C. Hansch, S.B. Mekapati, A. Kurup, and R.P. Verma, *QSAR of cytochrome P450*, Drug Metab. Rev. 36 (2004), pp. 105–156.

[10] T. Hou and J. Wang, *Structure-ADME relationship: Still a long way to go?*, Expert Opinion Drug Metabol. Toxicol. 4 (2008), pp. 759–770.

[11] J. Ishizaki, K. Yokogawa, E. Nakashima, and F. Ichimura, *Relationships between the hepatic intrinsic clearance or blood cell-plasma partition coefficient in the rabbit and the lipophilicity of basic drugs*, J. Pharm. Pharmacol. 49 (1997), pp. 768–772.

[12] J. Langowski and A. Long, *Computer systems for the prediction of xenobiotic metabolism*, Adv. Drug Deliv. Rev. 54 (2002), pp. 407–415.

[13] D.F. Lewis and M. Dickins, *Baseline lipophilicity relationships in human cytochromes P450 associated with drug metabolism*, Drug Metab. Rev. 35 (2003), pp. 1–18.

[14] H. Li, J. Sun, X. Fan, X. Sui, L. Zhang, Y. Wang, and Z. He, *Considerations and recent advances in QSAR models for cytochrome P450-mediated drug metabolism prediction*, J. Comput. Aided Mol. Des. 22 (2008), pp. 843–855.

[15] N. Manga, J.C. Duffy, P.H. Rowe, and M.T.D. Cronin, *A hierarchical QSAR model for urinary excretion of drugs in humans as a predictive tool for biotransformation*, QSAR Comb. Sci. 22 (2003), pp. 263–273.

[16] D.E. Mager, *Quantitative structure-pharmacokinetic/pharmacodynamic relationships*, Avd. Drug Delivery Rev. 58 (2006), pp. 1326–1356.

[17] U. Norinder, *In silico modelling of ADMET – a minireview of work from 2000 to 2004*, SAR QSAR Environ. Res. 16 (2004), pp. 1–11.

[18] T. Wang and J. Hou, *Recent advances on in silico ADME modeling*, Ann. Reports Comput. Chem. 5 (2009), pp. 101–127.

[19] Y.-H. Wang, Y. Li, Y.-H. Li, S.-L. Yang, and L. Yang, *Modeling Km values using electrotopological state: Substrates for cytochrome P450 3A4-mediated metabolism*, Bioorg. Med. Chem. Lett. 15 (2005), pp. 4076–4084.

[20] C.W. Yap, Z.R. Li, and Y.Z. Chen, *Quantitative structure-pharmacokinetic relationships for drug clearance by using statistical learning methods*, J. Mol. Graph. Model. 24 (2006), pp. 383–395.

[21] K. Krishnan and M.E. Andersen, *Physiologically based pharmacokinetic modeling in toxicology*, in *Principles and Methods of Toxicology*, A.W. Hayes, ed., Taylor & Francis, Boca Raton, FL, 2007, pp. 231–292.

[22] M.E. Andersen, H.J. Clewell, M.L. Gargas, F.A. Smith, and R.H. Reitz, *Physiologically based pharmacokinetics and the risk assessment process for methylene chloride*, Toxicol. Appl. Pharmacol. 87 (1987), pp. 185–205.

[23] M. Reddy, R.S. Yang, M.E. Andersen, and H.J. Clewell III (eds.), *Physiologically Based Pharmacokinetic Modeling: Science and Applications*, Wiley Interscience, Hoboken, N.J., 2006, pp. 1–420.

[24] G. Loizou, M. Spendiff, H.A. Barton, J. Bessems, F.Y. Bois, M.B. d'Yvoire, H. Buist, H.J. Clewell, B. Meek, U. Gundert-Remy, G. Goerlitz, and W. Schmitt, *Development of good modelling practice for physiologically based pharmacokinetic models for use in risk assessment: The first steps*, Regul. Toxicol. Pharmacol. 50 (2008), pp. 400–411.

[25] A.D. Arms and C.C. Travis, *Reference physiological parameters in pharmacokinetic modeling*, in EPA/600/6-88/004, U.S. Environmental Protection Agency, Office of Health and Environmental Assessment, Washington, DC, 1988.

[26] R.P. Brown, M.D. Delp, S.L. Lindstedt, L.R. Rhomberg, and R.P. Beliles, *Physiological parameter values for physiologically based pharmacokinetic models*, Toxicol. Ind. Health 13 (1997), pp. 407–484.

[27] T. Lavé , P. Coassolo, and B. Reigner, *Prediction of hepatic metabolic clearance based on interspecies allometric scaling techniques and in vitro–in vivo correlations*, Clin. Pharmacokinet. 36 (1999), pp. 211–231.

[28] J.W. Nichols, I.R. Schult, and P.N. Fitzsimmons, *In vitro–in vivo extrapolation of quantitative hepatic biotransformation data for fish. I. A review of methods, and strategies for incorporating intrinsic clearance estimates into chemical kinetic models*, Aquat. Toxicol. 78 (2006), pp. 74–90.

[29] M. Béliveau and K. Krishnan, *In silico approaches for developing physiologically based pharmacokinetic (PBPK) models*, in *Alternative Toxicological Methods*, H. Salem and S.A. Katz, eds., CRC Press, Boca Raton, FL, 2003, pp. 479–532.

[30] P. Poulin, M. Béliveau, and K. Krishnan, *Mechanistic animal replacement appoaches for predicting pharmacokinetics of organic chemicals*, in *Toxicity Assessment*

Alternatives: Methods, Issues, Opportunities, H. Salem and S.A. Katz, eds., Humana Press, Totowa, NJ, 1999, pp. 115–139.

[31] M. Gibaldi and B. Perrier, *Pharmacokinetics*, Dekker, New York, 1975.

[32] M.H. Abraham, M.J. Kamlet, R.W. Taft, R.M. Doherty, and P.K. Weathersby, *Solubility properties in polymers and biological media. 2. The correlation and prediction of the solubilities of nonelectrolytes in biological tissues and fluids*, J. Med. Chem. 28 (1985), pp. 865–870.

[33] A. Falk, E. Gullstrand, A. Lo¨ f, and E. Wigaeus-Hjelm, *Liquid/air partition coefficients of four terpenes*, Br. J. Ind. Med. 47 (1990), pp. 62–64.

[34] R.M. Featherstone, C.A. Muehlbaecher, F.L. Debon, and J.A. Forsaith, *Interactions of inert anesthetic gases with proteins*, Anesthesiology 22 (1961), pp. 977–981.

[35] V. Fiserova-Bergerova and M.L. Diaz, *Determination and prediction of tissue–gas partition coefficients*, Int. Arch. Occup. Environ. Health 58 (1986), pp. 75–87.

[36] V. Fiserova-Bergerova, M. Tichy, and F.J. Di Carlo, *Effects of biosolubility on pulmonary uptake and disposition of gases and vapors of lipophilic chemicals*, Drug Metab. Rev. 15 (1984), pp. 1033–1070.

[37] M.L. Gargas, R.J. Burgess, D.E. Voisard, G.H. Cason, and M.E. Andersen, *Partition coefficients of low-molecular-weight volatile chemicals in various liquids and tissues*, Toxicol. Appl. Pharmacol. 98 (1989), pp. 87–99.

[38] J. Järnberg and G. Johanson, *Liquid/air partition coefficients of the trimethylbenzenes*, Toxicol. Ind. Health 11 (1995), pp. 81–88.

[39] T. Kaneko, P.Y. Wang, and A. Sato, *Partition coefficients of some acetate esters and alcohols in water, blood, olive oil, and rat tissues*, Occup. Environ. Med. 51 (1994), pp. 68–72.

[40] C.P.J.M.D. Larson, E.I.I.M.D. Eger, and J.W.M.D. Severinghous, *Ostwald solubility coefficients for anesthetic gases in various fluids and tissues*, Anesthesiology 23 (1962), pp. 686–689.

[41] H.J. Lowe and K. Hagler, *Determination of volatile organic anaesthetic in blood, gases, tissues and lipids: Partition coefficients*, in *Gas Chromatography in Biology*

and Medicine. A Ciba-Geigy *Foundation Symposium*, R. Porter, ed., Churchill, New York, 1969, pp. 86–103.

[42] J.W. Nichols, J.M. McKim, G.J. Lien, A.D. Hoffman, and S.L. Bertelsen, *Physiologically based toxicokinetic modeling of three waterborne chloroethanes in rainbow trout (Oncorhynchus mykiss)*, Toxicol. Appl. Pharmacol. 110 (1991), pp. 374–389.

[43] S. Paterson and D. Mackay, *Correlation of tissue, blood, and air partition coefficients of volatile organic chemicals*, British J. Indus. Med. 46 (1989), pp. 321–328.

[44] L. Perbellini, F. Brugnone, D. Caretta, and G. Maranelli, *Partition coefficients of some industrial aliphatic hydrocarbons (C5–C7) in blood and human tissues*, British J. Indus. Med. 42 (1985), pp. 162–167.

[45] A. Sato and T. Nakajima, *A structure–activity relationship of some chlorinated hydrocarbons*, Arch. Environ. Health 34 (1979), pp. 69–75.

[46] A. Steward, P.R. Allott, A.L. Cowles, and W.W. Mapleson, *Solubility coefficients for inhaled anaesthetics for water, oil and biological media*, Br. J. Anaesth. 45 (1973), pp. 282–293.

[47] M.H. Abraham, H.S. Chadha, G.S. Whiting, and R.C. Mitchell, *Hydrogen bonding. 32. An analysis of water-octanol and water–alkane partitioning and the delta log P parameter of seiler*, J. Pharm. Sci. 83 (1994), pp. 1085–1100.

[48] M.H. Abraham and P.K. Weathersby, *Hydrogen bonding. 30. Solubility of gases and vapors in biological liquids and tissues*, J. Pharm. Sci. 83 (1994), pp. 1450–1456.

[49] A.L. Cowles, H.H. Borgstedt, and A.J. Gillies, *Solubilities of ethylene, cyclopropane, halothane and diethyl ether in human and dog blood at low concentrations*, Anesthesiology 35 (1971), pp. 203–211.

[50] E.I. Eger II and C.P.J. Larson, *Anaesthetic solubility in blood and tissues: Values and significance*, Br. J. Anaesth. 36 (1964), pp. 140–149.

[51] W. Laass, *Estimation of blood/air partition coefficients of organic solvents, in QSAR in Drug Design and Toxicology: Proceedings of the Sixth European Symposium on*

Quantitative Structure-Activity Relationships, D. Hadzi and B. Jerman-Blazic, eds., Elsevier, Amsterdam; New York, 1987, pp. 131–134.

[52] R.A. Saraiva, B.A. Willis, A. Steward, J.N. Lunn, and W.W. Mapleson, *Halothane solubility in human blood*, Br. J. Anaesth. 49 (1977), pp. 115–119.

[53] S. Batterman, L. Zhang, S. Wang, and A. Franzblau, *Partition coefficients for the trihalomethanes among blood, urine, water, milk and air*, Sci. Total Environ. 284 (2002), pp. 237–247.

[54] J. DeJongh, H.J. Verhaar, and J.L. Hermens, *A quantitative property–property relationship (QPPR) approach to estimate in vitro tissue–blood partition coefficients of organic chemicals in rats and humans*, Arch. Toxicol. 72 (1997), pp. 17–25.

[55] C.J. Meulenberg and H.P. Vijverberg, *Empirical relations predicting human and rat tissue:air partition coefficients of volatile organic compounds*, Toxicol. Appl. Pharmacol. 165 (2000), pp. 206–216.

[56] C.J. Meulenberg, A.G. Wijnkerm, and H.P. Vijverberg, *Relationship between olive oil:air, saline:air, and rat brain:air partition coefficients of organic solvents in vitro*, J. Toxicol. Environ. Health A 66 (2003), pp. 1985–1998.

[57] S.C. Basak, D. Mills, D.M. Hawkins, and H.A. El-Masri, *Prediction of human blood:air partition coefficient: A comparison of structure-based and property-based methods*, Risk Anal. 23 (2003), pp. 1173–1184.

[58] S.C. Basak, D. Mills, and B.D. Gute, *Prediction of tissue:air partition coefficients – theoretical vs. experimental methods*, SAR QSAR Environ. Res. 17 (2006), pp. 515–532.

[59] F.M. Parham, M.C. Kohn, H.B. Matthews, C. Derosa, and C.J. Portier, *Using structural information to create physiologically based pharmacokinetic models for all polychlorinated biphenyls: I. Tissue:blood partition coefficients*, Toxicol. Appl. Pharmacol. 144 (1997), pp. 340–347.

[60] M.L. Gargas, P.G. Seybold, and M.E. Andersen, *Modeling the tissue solubilities and metabolic rate constant (Vmax) of halogenated methanes, ethanes, and ethylenes*, Toxicol. Lett. 43 (1988), pp. 235–256.

[61] S.M.J. Free and J.W. Wilson, *A mathematical contribution to structure–activity studies*, J. Med. Chem. 7 (1964), pp. 395–399.

[62] M. Béliveau, R. Tardif, and K. Krishnan, *Quantitative structure–property relationships for physiologically based pharmacokinetic modeling of volatile organic chemicals in rats*, Toxicol. Appl. Pharmacol. 189 (2003), pp. 221–232.

[63] E. Kamgang, T. Peyret, and K. Krishnan, *An integrated QSPR-PBPK modelling approach for in vitro-in vivo extrapolation of pharmacokinetics in rats*, SAR QSAR Environ. Res. 19 (2008), pp. 669–680.

[64] M. Béliveau and K. Krishnan, *A spreadsheet program for modeling of quantitative strucure–pharmacokinetic relationships for inhaled volatile organic chemicals in humans*, SAR QSAR Environ. Res. 16 (2005), pp. 63–77.

[65] P. Poulin and F.P. Theil, *A priori prediction of tissue:plasma partition coefficients of drugs to facilitate the use of physiologically-based pharmacokinetic models in drug discovery*, J. Pharm. Sci. 89 (2000), pp. 16–35.

[66] S. Haddad, P. Poulin, and K. Krishnan, *Relative lipid content as the sole mechanistic determinant of the adipose tissue:blood partition coefficients of highly lipophilic organic chemicals*, Chemosphere 40 (2000), pp. 839–843.

[67] M.P. Payne and L.C. Kenny, *Comparison of models for the estimation of biological partition coefficients*, J. Toxicol. Environ. Health A 65 (2002), pp. 897–931.

[68] T. Peyret, P. Poulin, and K. Krishnan, *A unified algorithm for predicting partition coefficients for PBPK modeling of drugs and environmental chemicals*, Toxicol. Appl. Pharmacol. 249 (2010), pp. 197–207.

[69] P. Poulin and K. Krishnan, *An algorithm for predicting tissue: Blood partition coefficients of organic chemicals from n-octanol: Water partition coefficient data*, J. Toxicol. Environ. Health 46 (1995), pp. 117–129.

[70] P. Poulin and K. Krishnan, *A biologically-based algorithm for predicting human tissue: Blood partition coefficients of organic chemicals*, Hum. Exp. Toxicol. 14 (1995), pp. 273–280.

[71] P. Poulin and K. Krishnan, *A mechanistic algorithm for predicting blood:air partition coefficients of organic chemicals with the consideration of reversible binding in hemoglobin*, Toxicol. Appl. Pharmacol. 136 (1996), pp. 131–137.

[72] P. Poulin and K. Krishnan, *A tissue composition-based algorithm for predicting tissue:air partition coefficients of organic chemicals*, Toxicol. Appl. Pharmacol. 136 (1996), pp. 126–130.

[73] P. Poulin and F.P. Theil, *Prediction of pharmacokinetics prior to in vivo studies. 1. Mechanism-based prediction of volume of distribution*, J. Pharm. Sci. 91 (2002), pp. 129–156.

[74] T. Rodgers, D. Leahy, and M. Rowland, *Physiologically based pharmacokinetic modeling 1: Predicting the tissue distribution of moderate-to-strong bases*, J. Pharm. Sci. 94 (2005), pp. 1259–1276.

[75] T. Rodgers and M. Rowland, *Physiologically based pharmacokinetic modelling 2: Predicting the tissue distribution of acids, very weak bases, neutrals and zwitterions*, J. Pharm. Sci. 95 (2006), pp. 1238–1257.

[76] W. Schmitt, *General approach for the calculation of tissue to plasma partition coefficients*, Toxicol. In Vitro 22 (2008), pp. 457–467.

[77] H. Zhang, *A new nonlinear equation for the tissue/blood partition coefficients of neutral compounds*, J. Pharm. Sci. 93 (2004), pp. 1595–1604.

[78] H. Zhang, *A new approach for the tissue–blood partition coefficients of neutral and ionized compounds*, J. Chem. Inf. Model. 45 (2005), pp. 121–127.

[79] H. Zhang and Y. Zhang, *Convenient nonlinear model for predicting the tissue/blood partition coefficients of seven human tissues of neutral, acidic, and basic structurally diverse compounds*, J. Med. Chem. 49 (2006), pp. 5815–5829.

[80] C.-W. Lam, T.J. Galen, J.F. Boyd, and D.L. Pierson, *Mechanism of transport and distribution of organic solvents in blood*, Toxicol. Appl. Pharmacol. 104 (1990), pp. 117–129.

[81] M. Béliveau, J. Lipscomb, R. Tardif, and K. Krishnan, *Quantitative structure–property relationships for interspecies extrapolation of the inhalation pharmacokinetics of organic chemicals*, Chem. Res. Toxicol. 18 (2005), pp. 475–485.

[82] K. Krishnan and T. Peyret, *Physiologically based toxicokinetic (PBTK) modeling in ecotoxicology*, in *Ecotoxicology Modeling*, J. Devillers, ed., Springer, Dordrecht, 2009, pp. 145–175.

[83] S.L. Bertelsen, A.D. Hoffman, C.A. Gallinat, C.M. Elonen, and J.W. Nichols, *Evaluation of log Kow and tissue lipid content as predictors of chemical partitioning to fish tissues*, Environ. Toxicol. Chem. 17 (1998), pp. 1447–1455.

[84] C. Hansch and A. Leo, *The fragment method of calculating partition coefficients, in Substituent Constants for Correlation Analysis in Chemistry and Biology*, C. Hansch and A. Leo, eds., Wiley, New York, 1979, pp. 18–43.

[85] J. Hine and P.K. Mookerjee, *The intrinsic hydrophobic character of organic compounds: Correlations in terms of structural contributions*, J. Org. Chem. 40 (1975), pp. 511–522.

[86] P. Poulin and K. Krishnan, *Molecular structure based prediction of partition coefficients of organic chemicals for physiological pharmacokinetic models*, Toxicol. Meth. 6 (1996), pp. 117–137.

[87] S. Baláž, and V. Lukáčová, *A model-based dependence of the human tissue/blood partition coefficients of chemicals on lipophilicity and tissue composition*, Quant. Struct.-Act. Relat. 18 (1999), pp. 361–368.

[88] L.M. Berezhkovskiy, *Volume of distribution at steady state for a linear pharmacokinetic system with peripheral elimination*, J. Pharm. Sci. 93 (2004), pp. 1628–1640.

[89] I. Nestorov, L. Aarons, and M. Rowland, *Quantitative structure–pharmacokinetics relationships: II. A mechanistically based model to evaluate the relationship between tissue distribution parameters and compound lipophilicity*, J. Pharmacokinet. Pharmacodyn. 26 (1998), pp. 521–545.

[90] P. Poulin, K. Schoenlein, and F.-P. Theil, *Prediction of adipose tissue: Plasma partition coefficients for structurally unrelated drugs*, J. Pharm. Sci. 90 (2001), pp. 436–447.

[91] K. Yokogawa, E. Nakashima, J. Ishizaki, H. Maeda, T. Nagano, and F. Ichimura, *Relationships in the structure–tissue distribution of basic drugs in the rabbit*, Pharm. Res. 7 (1990), pp. 691–696.

[92] G. Colmenarejo, *In silico prediction of drug-binding strengths to human serum albumin*, Med. Res.Rev. 23 (2003), pp. 275–301.

[93] G. Colmenarejo, A. Alvarez-Pedraglio, and J.L. Lavandera, *Cheminformatic models to predict binding affinities to human serum albumin*, J. Med. Chem. 44 (2001), pp. 4370–4378.

[94] E. Estrada, E. Uriarte, E. Molina, Y. Simon-Manso, and G.W.A. Milne, *An integrated in silico analysis of drug-binding to human serum albumin*, J. Chem. Inf. Model. 46 (2006), pp. 2709–2724.

[95] N.A. Kratochwil, W. Huber, F. Mu¨ ller, M. Kansy, and P.R. Gerber, *Predicting plasma protein binding of drugs: A new approach*, Biochem. Pharmacol. 64 (2002), pp. 1355–1374.

[96] J.R. Votano, M. Parham, L.M. Hall, L.H. Hall, L.B. Kier, S. Oloff, and A. Tropsha, *QSAR modeling of human serum protein binding with several modeling techniques utilizing structureinformation representation*, J. Med. Chem. 49 (2006), pp. 7169–7181.

[97] C.X. Xue, R.S. Zhang, H.X. Liu, X.J. Yao, M.C. Liu, Z.D. Hu, and B.T. Fan, *QSAR models for the prediction of binding affinities to human serum albumin using the heuristic method and a support vector machine*, J. Chem. Inf. Comput. Sci. 44 (2004), pp. 1693–1700.

[98] S. Coecke, H. Ahr, B.J. Blaauboer, S. Bremer, S. Casati, J. Castell, R. Combes, R. Corvi, C.L. Crespi, M.L. Cunningham, G. Elaut, B. Eletti, A.P. Freidig, A. Gennari, J.-F. Ghersi-Egea, A. Guillouzo, T. Hartung, P. Hoet, M. Ingelman-Sundberg, S. Munn, W. Janssens, B. Ladstetter, D. Leahy, A. Long, A. Meneguz, M.

Monshouwer, S. Morath, F. Nagelkerke, O. Pelkonen, J. Ponti, P. Prieto, L. Richert, E. Sabbioni, B. Schaack, W. Steiling, E. Testai, J.-A. Vericat, and A. Worth, *Metabolism: A bottleneck in in vitro toxicological test development. The report and recommendations of ECVAM workshop 54*, Altern. Lab. Anim. 34 (2006), pp. 49–84.

[99] J.C. Madden and M.T. Cronin, *Structure-based methods for the prediction of drug metabolism*, Expert Opinion Drug Metabol. Toxicol. 2 (2006), pp. 545–557.

[100] R. Mackman, Z. Guo, F.P. Guengerich, and P.R. Ortiz de Montellano, *Active site topology of human cytochrome P450 2E1*, Chem. Res. Toxicol. 9 (1996), pp. 223–226.

[101] D.F.V. Lewis, *On the recognition of mammalian microsomal cytochrome P450 substrates and their characteristics: Towards the prediction of human p450 substrate specificity and metabolism*, Biochem. Pharmacol. 60 (2000), pp. 293–306.

[102] D.F.V. Lewis, *Guide to Cytochromes P450: Structure and Function*, Taylor & Francis, London; New York, 2001.

[103] D.F.V. Lewis, *Quantitative structure–activity relationships (QSARs) within the cytochrome P450 system: QSARs describing substrate binding, inhibition and induction of P450s*, Inflammopharmacology 11 (2003), pp. 43–73.

[104] D.F.V. Lewis and M. Dickins, *Factors influencing rates and clearance in P450-mediated reactions: QSARs for substrates of the xenobiotic-metabolizing hepatic microsomal P450s*, Toxicology 170 (2002), pp. 45–53.

[105] D.F.V. Lewis, Y. Ito, and B.G. Lake, *Quantitative structure–activity relationships (QSARs) for inhibitors and substrates of CYP2B enzymes: Importance of compound lipophilicity in explanation of potency differences*, J. Enzyme Inhib. Med. Chem. 25 (2010), pp. 679–684.

[106] H. Li, J. Sun, X. Sui, J. Liu, Z. Yan, X. Liu, Y. Sun, and Z. He, *First-principle, structure-based prediction of hepatic metabolic clearance values in human*, Eur. J. Med. Chem. 44 (2009), pp. 1600–1606.

[107] K. Nikolic and D. Agababa, *Prediction of hepatic microsomal intrinsic clearance and human clearance values for drugs*, J. Mol. Graph. Model. 28 (2009), pp. 245–252.

[108] R.P. Austin, P. Barton, S.L. Cockroft, M.C. Wenlock, and R.J. Riley, *The influence of nonspecific microsomal binding on apparent intrinsic clearance, and its prediction from physicochemical properties*, Drug Metab. Dispos. 30 (2002), pp. 1497–1503.

[109] R.P. Austin, P. Barton, S. Mohmed, and R.J. Riley, *The binding of drugs to hepatocytes and its relationship to physicochemical properties*, Drug Metab. Dispos. 33 (2005), pp. 419–425.

[110] H. Yin, M.W. Anders, K.R. Korzekwa, L.A. Higgins, K.T. Thummel, E.D. Kharasch, and J.P. Jones, *Designing safer chemicals: Predicting the rates of metabolism of halogenated chemicals*, Proc. Natl. Acad. USA 92 (1995), pp. 11076–11080.

[111] G.D. Loizou, N.L. Eldirdiri, and L.J. King, *Physiologically based pharmacokinetics of uptake by inhalation of a series of 1,1,1-trihaloethanes: Correlation with various physicochemical parameters*, Inhal. Toxicol. 8 (1996), pp. 1–19.

[112] M.L. Gargas, H.J. Clewell, and M.E. Andersen, *Gas uptake inhalation techniques and the rates of metabolism of chloromethanes, chloroethanes and chloroethylenes in the rat*, Inhal. Toxicol. 2 (1990), pp. 295–319.

[113] B. Mortensen, I. Eide, K. Zahlsen, and O.G. Nilsen, *Prediction of in vivo metabolic clearance of 25 different petroleum hydrocarbons by a rat liver head-space technique*, Arch. Toxicol. 74 (2000), pp. 308–312.

[114] G. Galliani, B. Rindone, G. Dagnino, and M. Salmona, *Structure reactivity relationships in the microsomal oxidation of tertiary amines*, Eur. J. Drug Metabol. Pharm. 9 (1984), pp. 289–293.

[115] G.A. Csanady, R.J. Laid, and J.G. Filser, *Metabolic transformation of halogenated and other alkenes – a theoretical approach. Estimation of metabolic reactivities for in vivo conditions*, Toxicol. Lett. 75 (1995), pp. 217–223.

[116] F.M. Parham and C.J. Portier, *Using structural information to create physiologically based pharmacokinetic models for all polychlorinated biphenyls. II. Rates of metabolism*, Toxicol. Appl. Pharmacol. 151 (1998), pp. 110–116.

[117] D.F. Lewis, C. Sams, and G.D. Loizou, *A quantitative structure–activity relationship analysis on a series of alkyl benzenes metabolized by human cytochrome P450 2E1*, J. Biochem. Mol. Toxicol. 17 (2003), pp. 47–52.

[118] J.B. Knaak, C.C. Dary, F. Power, C. Thompson, and J.N. Blancato, *Physicochemical and biological data for the development of predictive organophosphorus pesticide QSARs and PBPK/PD models for human risk assessment*, Crit. Rev. Toxicol. 34 (2004), pp. 143–207.

[119] C.L. Waller, M.V. Evans, and J.D. McKinney, *Modeling the cytochrome P450-mediated metabolism of chlorinated volatile organic compounds*, Drug Metab. Dispos. 24 (1996), pp. 203–210.

[120] P. Poulin and K. Krishnan, *Molecular structure-based prediction of the toxicokinetics of inhaled vapors in humans*, Int. J. Toxicol. 18 (1999), pp. 7–18.

[121] G.R. Wilkinson and D.G. Shand, *Commentary: A physiological approach to hepatic drug clearance*, Clin. Pharmacol. Ther. 18 (1975), pp. 377–390.

[122] M.E. Andersen, *A physiologically based toxicokinetic description of the metabolism of inhaled gases and vapors: Analysis at steady state*, Toxicol. Appl. Pharmacol. 60 (1981), pp. 509–526.

[123] G.E. Blakey, I.A. Nestorov, P.A. Arundel, L.J. Aarons, and M. Rowland, *Quantitative structure–pharmacokinetics relationships: I. Development of a whole-body physiologically based model to characterize changes in pharmacokinetics across a homologous series of barbiturates in the rat*, J. Pharmacokinet. Pharmacodyn. 25 (1997), pp. 277–312.

[124] T. Yamagushi, M. Yabuki, S. Saito, T. Watanabe, H. Nishimura, N. Isobe, F. Shono, and M. Matsuo, *Research to develop a predicting system of mammalian subacute toxicity (3) construction of a predictive toxicokinetic model*, Chemosphere 33 (1996), pp. 2441–2468.

[125] B. Agoram, W.S. Woltosz, and M.B. Bolger, *Predicting the impact of physiological and biochemical processes on oral drug bioavailability*, Adv. Drug Deliv. Rev. 50 (2001), pp. S41–S67.

[126] P.V. Balimane, S. Chong, and R.A. Morrison, *Current methodologies used for evaluation of intestinal permeability and absorption*, J. Pharmacol. Toxicol. Methods 44 (2000), pp. 301–312.

[127] G.M. Grass and P.J. Sinko, *Physiologically-based pharmacokinetic simulation modelling*, Adv. Drug Deliv. Rev. 54 (2002), pp. 433–451.

[128] H. Patel, W. ten Berge, and M.T. Cronin, *Quantitative structure–activity relationships (QSARs) for the prediction of skin permeation of exogenous chemicals*, Chemosphere 48 (2002), pp. 603–613.

[129] P. Poulin and K. Krishnan, *Molecular structure-based prediction of human abdominal skin permeability coefficients for several organic compounds*, J. Toxicol. Environ. Health A 62 (2001), pp. 143–159.

[130] O.A. Raevsky and K.-J. Schaper, *Quantitative estimation of hydrogen bond contribution to permeability and absorption processes of some chemicals and drugs*, Eur. J. Med. Chem. 33 (1998), pp. 799–807.

[131] O.A. Raevsky, S.V. Trepalin, H.P. Trepalina, V.A. Gerasimenko, and O.E. Raevskaja, *SLIPPER-2001 - Software for predicting molecular properties on the basis of physicochemical descriptors and structural similarity*, J. Chem. Inf. Comput. Sci. 42 (2002), pp. 540–549.

[132] M. Debia and K. Krishnan, *Quantitative property–property relationships for computing occupational exposure limits and vapour hazard ratios of organic solvents*, SAR QSAR Environ. Res. 21 (2010), pp. 583–601.

2.9. Tables

Table 1. Equations used in PBPK models to simulate the pharmacokinetics of inhaled volatile organic chemicals (VOCs) [21]

Compartment	Input parameters	Equations
Arterial blood	Qc, Qp, $P_{ba,}$ $Cinh$	$Ca = \frac{Qc \cdot Cv + Qp \cdot Cinh}{Qc + Qp / P_{ba}}$
Metabolizing tissue (liver)	Ql, V_{max}, Km	$\frac{dAl}{dt} = Ql \cdot (Ca - Cvl) - \frac{V_{\max} \cdot Cvl}{Km + Cvl}$
Non metabolizing tissues	Qt	$\frac{dAt}{dt} = Qt \cdot (Ca - Cvt)$
Venous blood	Qt, Qc	$Cv = \frac{\sum Qt \cdot Cvt}{Qc}$

Abbreviations: Qc: Cardiac output (L/h); Qp: Alveolar ventilation rate (L/h); P_{ba}: Blood:air partition coefficient; Ql: blood flow rate to liver (L/h); Qt: blood flow rate to tissue t (L/h); Cvl: Concentration of chemical in venous blood leaving liver (mg/L or mmol/L); Ca: Arterial blood concentration (mg/L or mmol/L); $Cinh$: inhaled air concentration (mg/L or mmol/L); Cv: Venous blood concentration (mg/L or mmol/L); Al: Amount in liver (mg or mmol); V_{max}: Maximal velocity of enzymatic reaction (mg/h or mmol/h) and Km: Michaelis-Menten affinity constant (mg/L or mmol/L).

Table 2. Fragment contribution to rat partition coefficients[1]

Fragment	Fragment contribution to			
	blood:air	liver:air	muscle:air	fat:air
CH_3	0.072	0.016	-0.020	0.366
CH_2	0.109	0.234	0.122	0.435
CH	0.079	0.359	0.266	0.330
C	-0.606	0.032	-0.105	-0.285
C=C	-0.494	0.257	-0.707	0.327
H	0.236	-0.031	0.081	0.155
Br	0.834	0.700	0.622	1.170
Cl	0.481	0.384	0.322	0.735
F	0.020	-0.113	-0.911	0.075
AC	2.850	3.760	3.650	2.920
H on AC	-0.292	-0.408	-0.446	-0.0558

[1] AC: benzene ring; the fragment contributions times the frequency of their occurrence gives the logarithm of the particular partition coefficient. Based on Béliveau et al. [62]

Table 3. Fragment contributions to rat fat:air and blood:air PCs[1]

Fragment	Fragment contribution to	
	blood:air	fat:air
CH_3	-0.024	0.277
CH_2	0.105	0.369
CH	0.186	0.395
C	0.129	0.276
H	0.065	0.267
AC	2.747	3.295
H on AC	-0.252	-0.12

AC: benzene ring

[1] The group contributions times the frequency of their occurrence gives the logarithm of the particular partition coefficient. Based on Kamgang et al. [63]

Table 4. Fractional content of the key components in blood and tissues of rats and humans

Species	Component[1]	Blood	Fat	Liver	Muscle
Rat	Neutral lipids	0.002	0.8536	0.0425	0.0117
	Water	0.8423	0.1215	0.7176	0.7471
	Proteins	0.156	-	-	-
Human	Neutral lipids	0.004	0.7986	0.0473	0.0378
	Water	0.8217	0.1514	0.74	0.7573
	Proteins	0.174	-	-	

[1] "Neutral lipids" represent the sum of neutral lipid content and 30 % of phospholipids in the biological matrix. "Water" represents the sum of water content and 70 % of phospholipids in the biological matrix. Based on data compiled/reported by Poulin and Krishnan [69,70], Béliveau et al.[81] and Krishnan and Peyret [82].

Table 5. Fragment contributions to oil:air, water:air and protein:air PC[1]

Fragment	Fragment contribution to		
	oil:air	water:air	protein:air
CH_3	0.354	-0.038	0.306
CH_2	0.441	-0.223	0.182
CH	0.377	-0.477	-0.111
C	-0.354	-1.490	-1.060
C=C	0.197	-1.940	-0.877
H	0.134	0.555	0.492
Br	1.174	0.622	1.150
Cl	0.776	0.468	0.764
F	0.136	0.229	0.241
AC	3.729	0.650	1.970
H on AC	-0.190	-0.062	-0.028

[1] AC: benzene ring; the fragment contributions times the frequency of their occurrence gives the logarithm of the particular partition coefficient. Based on Béliveau et al.: [81]

Table 6. Mechanistic algorithms for predicting partition coefficients for PBPK models.

Reference	Equation	Definition of the parameters	Comments
[91]	$K_{pfu} - \frac{1}{fui} = \alpha \cdot P^{\beta}$	K_{pfu}: tissue: unbound plasma; *fui*: non-ionized fraction of the interstitial space; *P*: solvent:water PC (i.e., *n*-octanol, benzene, chloroform and trioleine: water PC)	*n*-octanol:water PC was found to be the best descriptor of the K_{pfu}; *r* values range from 0.96 for bone to 0.987 for brain
[42]	$P_{mw} = 10^{log\ P_{ow}} \times F_{nlm} + 1 \times F_{wm}$	P_{mw}: media (blood or tissue):water PC; P_{ow}: *n*-octanol:water PC; F_{nlm}: fraction of non-polar lipids in the media; F_{wm}: fraction of water in the media	The prediction/experimental data of PCs were 2.28 ± 2.27 for blood:water, 1.34 ± 0.81 for fat:blood 0.91 ± 0.38 for kidney:blood, 0.73 ± 0.09 for liver:blood, and 1.2 ± 0.44 for white muscle:blood PCs (n = 3). Poor predictions for hexachloroethane blood:water PC (298.23 predicted *vs*. 61.36 measured)

Table 6. Continued

Reference	Equation	Definition of the parameters	Comments
[70]	$P_{tb} = \frac{(S_o \cdot f_{nlt}) + (S_w \cdot 0.7 \cdot f_{plt}) + (S_o \cdot 0.3 \cdot f_{plt}) + (S_w \cdot f_{wt})}{(S_o \cdot f_{nlb}) + (S_w \cdot 0.7 \cdot f_{plb}) + (S_o \cdot 0.3 \cdot f_{plb}) + (S_w \cdot f_{wb})}$	P_{tb}: tissue:blood PC; S_o: solubility in *n*-octanol; S_w: solubility in water; f_{nl}: fraction of neutral lipids; f_{pl}: fraction of phospholipids; f_w: fraction of water; *t*: tissue; *b*: blood	For all the tissues studied the predictions were higher than the experimental values, but within a factor of 1.48 (n = 127). The partition coefficients for which more than one value was reported in the literature, the predicted/experimental ratio was 1.83. (r = 0.96)
[69]	$P_{tb} = \frac{P_t}{0.37 \cdot P_e + 0.67 \cdot P_p}$ $P_t = (P_{ow} \cdot f_{nlt}) + (1 \cdot 0.7 \cdot f_{plt}) + (P_{ow} \cdot 0.3 \cdot f_{plt}) + (1 \cdot f_{wt})$ $P_e = (P_{ow} \cdot f_{nle}) + (1 \cdot 0.7 \cdot f_{ple}) + (P_{ow} \cdot 0.3 \cdot f_{ple}) + (1 \cdot f_{we})$ $P_p = (P_{ow} \cdot f_{nlp}) + (1 \cdot 0.7 \cdot f_{plp}) + (P_{ow} \cdot 0.3 \cdot f_{plp}) + (1 \cdot f_{wp})$	P_{tb}: tissue:blood PC; P_t: tissue:water PC; P_p: plasma:water PC; P_e: erythrocyte:water PC; P_{ow}: *n*-octanol (or oil): water PC; f_{nl}: fraction of neutral lipids; f_{pl}: fraction of phospholipids; f_w: fraction of water; *t*: tissue; *e*: erythrocyte; *p*: plasma	Using P_{ow} the predicted/experimental ratio of rat tissue:blood PC was 1.01 ± 0.27 for the muscle and 0.99 ± 0.35 for the liver (n = 21). The predictions of the fat:blood PC were found to be better when using the vegetable oil:water PC as input parameter, rather than the P_{ow} (1.5 ± 0.74; n = 21)

Table 6. Continued

Reference	Equation	Definition of the parameters	Comments
[72]	$P_{ta} = P_{oa} \cdot f_{nlt} + P_{wa} \cdot 0.7 \cdot f_{plt} + P_{oa} \cdot 0.3 \cdot f_{plt} + P_{wa} \cdot f_{wt}$	P_{ta}: tissue:air PC; P_{oa}: *n*-octanol:air PC; P_{wa}: water:air PC; f_{nl}: fraction of neutral lipids; f_{pl}: fraction of phospholipids; f_w: fraction of water; *t*: tissue; *e*: erythrocyte; *p*: plasma	The predicted/experimental ratio of tissue:air PC was 0.94 ± 0.38 (n = 45) for liver, 0.93 ± 0.46 (n = 45) for muscle, and 1.1 ± 0.35 (n = 45) for fat.
[71]	$P_{ba,app} = P_{ba} + \left(1 + \frac{Ka \cdot C_p}{\left(1 + Ka \cdot Ca_{free}\right)} \right)$ $P_{ba} = P_{oa} \cdot f_{nlb} + P_{wa} \cdot 0.7 \cdot f_{plb} + P_{oa} \cdot 0.3 \cdot f_{plb} + P_{wa} \cdot f_{wb}$	$P_{ba,app}$: apparent blood:air PC; P_{ba}: solubility-based predicted blood:air PC; Ka: affinity for hemoglobin; C_p: concentration of haemoglobin in blood Ca_{free}: concentration of the free form of the compound in the erythrocyte	The blood:air PC of the hydrophilic compounds was well predicted without considering the protein binding (i.e. using P_{ba}) (predicted/experimental ratio = 0.80 ± 0.21; n = 18); the hydrophobic VOCs could not be adequately predicted without this mechanism (predicted/experimental ratio = 0.21 ± 0.07; n = 27).

Table 6. Continued

Reference	Equation	Definition of the parameters	Comments
[54]	$PCtb = \frac{V_{lt} \times K_{l:wt} + V_{w,t}}{V_{lb} \times K_{l:wb} + V_{wb}} + B$	V_l: volume of lipids; V_w: volume of water *t*: tissue; *b*: blood; $K_{l:wt}$: lipid:water PC in tissue; $K_{l:wb}$: lipid:water PC in blood; *B*: empirical constant	The $K_{l:wt}$ were calculated from octanol:water PC. $K_{l:wb}$ and *B* were fitted to the PC data. The predictions of this algorithm were more accurate with the human data than in rats. The term *B* may account for chemical-specific binding to proteins. $r^2 = 0.99$ (liver) to 1 (other tissues) for human PCs, and $r^2 = 0.24$ (muscle), 0.58 (liver), 0.98 (fat) for rat PCs. For most chemicals, the predicted/experimental ratios were 0.5-2.
[66]	$P_{fb} = \frac{F_{nef}}{F_{neb}}$	P_{fb}: fat:blood PC; F_{nef}: fractional content of neutral lipids equivalent in fat; F_{neb}: fractional content of neutral lipids equivalent in blood	For highly hydrophobic compounds (i.e. with log *P* > 6), the predicted tissue:blood PC is a constant, but species-specific.

Table 6. Continued

Reference	Equation	Definition of the parameters	Comments
[89]	$P_{tp} = f_{wt} \cdot \left[1 + \theta_{1t} \cdot 10^{\theta_{2t} \log P_{ow}}\right]$	P_{tp}: tissue:unbound plasma PC; f_{wt}: fractional content of water in tissue; θ_1 and θ_2: empirical terms; P_{ow}: *n*-octanol:water PC	θ_1 and θ_2 fitted to data. Mean prediction error (ME) between -22.48 and 61.14%. Square root of the mean square prediction error (RMSE) between 28.33 and 85.2%.
[87]	$\log P_{tb} = \log \frac{\left(\alpha \cdot \frac{f_{mt}}{f_{wt}} + \gamma \cdot \frac{f_{pt}}{f_{wt}}\right) \cdot P_{ow}^{\ \beta_t} + 1}{\left(\alpha \cdot \frac{f_{mb}}{f_{wb}} + \gamma \cdot \frac{f_{pb}}{f_{wb}}\right) \cdot P_{ow}^{\ \beta_b} + 1} + \log \frac{f_{wt}}{f_{wb}}$	P_{tb}: tissue:blood PC; $\alpha \cdot P^{\beta}$: membrane:water PC; $\gamma \cdot P^{\beta}$: association constant to proteins (Ka_{pr}); f: fractional content; t: tissue; b: blood; m: membrane; w: water ; p: protein	α and γ are chemical specific whereas β is more specific to the tissue. α, γ and β were fitted to experimental data. Worst fit for heart PCs (n = 14; r = 0.837; s = 0.080; F = 28.1), and best fit for fat PCs (n = 36; r = 0.98; s = 0.198; F = 188)

Table 6. Continued

Reference	Equation	Definition of the parameters	Comments
[81]	$P_{ba} = P_{oa} \cdot f_{nle} + P_{wa} \cdot f_{we} + fb \cdot f_p \cdot P_{pa}$	P_{ba}: blood:air PC; P_{oa}: oil:air PC; P_{wa}: water:air PC; P_{pa}: protein:air PC; f_{nle}: fraction of neutral lipid equivalent in blood; f_{we}: fraction of water equivalent in blood; f_p: fraction of proteins in blood; fb: fraction of total proteins involved in the partitioning	QSPRs were developed for P_{oa}, P_{wa}, and P_{pa}. The predicted/experimental ratio was 0.87 ± 0.44 (range: 0.21-1.88) in humans and 1.10 ± 0.53 (range: 0.24-2.69) in rats.
[65]	$P_{tp} = \frac{P_{vow} \cdot \left(V_{nlt} + 0.3 \cdot V_{plt}\right) + 1 \cdot \left(V_{wt} + 0.7 \cdot V_{plt}\right)}{P_{vow} \cdot \left(V_{nlp} + 0.3 \cdot V_{plp}\right) + 1 \cdot \left(V_{wp} + 0.7 \cdot V_{plp}\right)} \cdot \frac{fu_p}{fu_t}$	P_{tp}: tissue:plasma PC; P_{vow}: oil:water PC; V_{nl}: volume of neutral lipids; V_{pl}: volume of phospholipids; V_w: volume of water; t: tissue; p: plasma	For all tissues and species studied predicted/experimental ratio was 1.26 ± 1.40 (n = 269)
[90]	$P_{fp} = \frac{P_{vow} \cdot \left(V_{nlf} + 0.3 \cdot V_{plf}\right) + 1 \cdot \left(V_{wf} + 0.7 \cdot V_{plf}\right)}{P_{vow} \cdot \left(V_{nlp} + 0.3 \cdot V_{plp}\right) + 1 \cdot \left(V_{wp} + 0.7 \cdot V_{plp}\right)} \cdot \frac{fu_p}{1}$	P_{tp}: fat:plasma PC; V_{nl}: volume of neutral lipids; V_{pl}: volume of phospholipids; V_w: volume of water; f: fat; p: plasma	Overall predicted/experimental ratio was 1.17 ± 0.44 (n = 14) using P_{vow} corrected for the ionization

Table 6. Continued

Reference	Equation	Definition of the parameters	Comments
[88]	$P_{tp} = \frac{P_{vow} \cdot \left(f_{nlt} + 0.3 \cdot f_{plt}\right) + 0.7 \cdot f_{plt} + f_{wt}/fu_t}{P_{vow} \cdot \left(f_{nlp} + 0.3 \cdot f_{plp}\right) + 0.7 \cdot f_{plp} + f_{wp}/fu_p}$	P_{tp}: tissue:plasma PC P_{vow}: oil:water PC; f_{nl}: fraction of neutral lipids; f_{pl}: fraction of phospholipids; f_w: fraction of water; *t*: tissue; *p*: plasma	Suggested correction of the algorithm of Poulin and Theil, considering that there are no macromolecules to interact within phospholipids
[75]	$Kpu = f_{EW} + \frac{X \cdot f_{IW}}{Y} + \frac{P_{ow} \cdot f_{NL} + \left(0.3 \cdot P_{ow} + 0.7\right) \cdot f_{NP}}{Y} + Ka_{PR} \cdot [PR]_T$	*Kpu*: tissue:unbound plasma PC; P_{ow}: *n*-octanol (or oil for adipose tissue):water PC; f_{EW}: fraction of extracellular water in the tissue; f_{IW}: fraction of intracellular water in the tissue; f_{NL}: fraction of neutral lipids in the tissue; f_{NP}: fraction of neutral phospholipids in the tissue; Ka_{PR}: association constant to proteins; $[PR]_T$: concentration of plasma proteins in the tissue; *X* and *Y* are ionization correction terms for the intracellular and plasma water, respectively	Ka_{PR} derived from fraction unbound in plasma. Using experimental values of P_{ow} and *pKa* the predicted/experimental ratio was 1.62 ± 2.17 for acids, 1.09 ± 1.32 very weak bases, and 0.91 ± 0.79 for all the studied drugs

Table 6. Continued

Reference	Equation	Definition of the parameters	Comments
[77-79]	$\log PC = \log\left(10^{\log Fl + \log Plb} + 10^{\log Fp + \log Ppb} + 10^{\log Fw + \log Pwb}\right)$	*PC:* tissue:blood PC; *Fl*: fraction of lipids; *Fw*: fraction of water; *Fp*: fraction of proteins; *Plb*: lipid:blood PC; *Ppb*: protein:blood PC;; *Pwb*: water:blood PC	QSARs were developed to predict *Plb*, *Ppb* and *Pwb* of neutral (n = 166, r^2 = 0.851, s = 0.260, Q^2 = 0.833) [77], neutral and ionized (n = 201, r^2 = 0.905, s = 0.291, Q^2 = 0.890) [78] and diverse compounds (n = 248, r^2 = 0.877, s = 0.352) [79]
[74]	$Kpu = f_{EW} + \frac{1+10^{pKa-pHiw}}{1+10^{pKa-pHp}} \cdot f_{IW} + \frac{Ka \cdot \left[AP^-\right]_T \cdot 10^{pKa-pHiw}}{1+10^{pKa-pHp}} + \frac{P_{ow} \cdot f_{NL} + \left(0.3 \cdot P_{ow} + 0.7\right) \cdot f_{NP}}{1+10^{pKa-pHp}}$	*Kpu*: tissue:unbound plasma PC; P_{ow}: *n*-octanol (or oil for adipose tissue):water PC; f_{EW}: fraction of extracellular water in the tissue; f_{IW}: fraction of intracellular water in the tissue; f_{NL}: fraction of neutral lipids in the tissue; f_{NP}: fraction of neutral phospholipids in the tissue; Ka: association constant for acidic phsopholipids; $[AP^-]_T$: acidic phospholipids content in the tissue	*Ka* derived from erythrocyte:water PC. Overall predicted/experimental ratio was 1.27 ± 1.3

Table 6. Continued

Reference	Equation	Definition of the parameters	Comments
[76]	$$K_{tp} = \left(\frac{F_{\text{int}} \cdot}{fu_{\text{int}}} + K_{cell:plasma} \cdot \frac{F_{cell}}{fu_{cell}} \right) \cdot fup$$ $$\frac{1}{fu_{\text{int}}} = F_{W\,\text{int}} + \frac{F_{p\,\text{int}}}{F_{pp}} \cdot \left(\frac{1}{fu_p} - F_{Wpl} \right)$$ $$\frac{1}{fu_{cell}} = F_W + K_{NL} \cdot F_{NL} + K_{NP} \cdot F_{NP} + K_{APL} \cdot F_{APL} + K_P \cdot F_P$$	K_{tp}: tissue:plasma fu_{int}: unbound fraction in interstitium; fu_{cell}: unbound fraction in cellular space; fu_p: unbound fraction in plasma; p: plasma; int: interstitium; F_W, water fraction; F_{NL}: neutral lipid fraction; F_{NP}: neutral phospholipids fraction; F_{APL}: acidic phospholipids fraction; F_p: protein fraction K_{NL}: neutral lipids:water PC; K_{NP}: neutral phospholipids:water PC; K_{APL}: acidic phospholipids:water PC; K_p: intracellular protein:water PC	Equations to calculate K_{NP}, K_{APL}, and K_p from P_{ow} were reported in the original article. 73% of the predictions were within a factor of 3 compared with the experimental values

Table 7. Algorithms for predicting partition coefficients for PBPK modelling.

Reference	Partition coefficient	Tissues or media	Species	Compounds studied	
				Class	log P_{ow}
[91]	Tissue:plasma unbound	Lungs, brain, heart, intestine, muscle, fat, skin and bone	Rabbit	Drugs	2.21 to 5.19
[42]	Tissue:water	Muscle	Rainbow trout	Ethanes	2.39 to 4.14
[70]	Tissue:blood	Muscle, brain, adipose tissue, liver, lung, kidney	Human	Alcohols, aromatic hydrocarbons, alkanes, halogenated alkanes, acetone, diethyl ether	-0.82 to 4.83
[69]	Tissue:blood	Liver, muscle, adipose tissue	Rat	Alcohols, ketones, acetate esters, diethyl ether	-0.77 to 2.13
[72]	Tissue:air	Liver, muscle, adipose tissue	Rat	Alcohols, aromatic hydrocarbons, alkanes, halogenated alkanes, acetone, diethyl ether	-0.77 to 3.44

Table 7. Continued

Reference	Partition coefficient	Tissues or media	Species	Compounds studied	
				Class	log P_{ow}
[71]	Blood:air	Blood	Rat	Alcohols, aromatic hydrocarbons, alkanes, halogenated alkanes, acetone, diethyl ether	-0.77 to 3.44
[54]	Tissue:blood	Liver, muscle, fat, kidney and brain	Rat, human	aromatic hydrocarbons, alkanes, halogenated alkanes	0.2 to 4.66
[66]	Tissue:blood	Adipose tissue	Rat, human	Highly lipophilic compounds, PCBs, dioxins	>4
[89]	Tissue:unbound plasma	Lungs, liver, kidneys, stomach, pancreas, spleen, intestine, muscle, fat, skin, bones, heart, brain, testes, erythrocytes	Rat	Barbituric acids	0.11 to 4.04
[87]	Tissue:blood	Fat, liver, brain, kidneys, muscle, lung, and heart	Human	Alcohols, ethers, alkanes, halogenated, alkanes	-2 to 5

Table 7. Continued

Reference	Partition coefficient	Tissues or media	Species	Compounds studied	
				Class	log P_{ow}
[81]	Blood:air	Blood	Rat, human	Aromatic hydrocarbons, alkanes, halogenated alkanes	0.71 to 4.05
[65]	Tissue:plasma	Brain, heart, lung, muscle, skin, intestine, spleen, bone	Rabbit, rat, mouse	Drugs	-4.62 to 6.28
[90]	Tissue:plasma	Adipose tissue	Rabbit, rat, human	Drugs	0.04 to 4.8
[88]	Tissue:plasma	-	-	-	-
[75]	Tissue:unbound plasma	Adipose tissue, bone, brain, intestine, heart, kidney, liver, lung, muscle, pancreas, skin, spleen, thymus	Rat	Drugs	-1.2 to 4.1
[77]	Tissue:blood	Adipose tissue, liver, brain, kidney, muscle, lung, heart	Human	Alcohols, alkanes, ethers, fluorated ethers, alkenes, aromatic hydrocarbons	-0.77 to 4.66

Table 7. Continued

Reference	Partition coefficient	Tissues or media	Species	Compounds studied	
				Class	log P_{ow}
[78]	Tissue:blood	Adipose tissue, liver, brain, kidney, muscle, lung, heart	Human	Alcohols, alkanes, ethers, fluorated ethers, alkenes, aromatic hydrocarbons, drugs	-0.77 to 4.81
[79]	Tissue:blood	Adipose tissue, liver, brain, kidney, muscle, lung, heart	Human	Alcohols, alkanes, ethers, fluorated ethers, alkenes, aromatic hydrocarbons, drugs	-4.62 to 6.80
[74]	Tissue:unbound plasma	Adipose tissue, bone, brain, intestine, heart, kidney, liver, lung, muscle, pancreas, skin, spleen, thymus	Rat	Drugs	0.88 to 4.96
[76]	Tissue:plasma	Adipose tissue, bone, brain, intestine, heart, liver, lung, kidney, muscle, skin, spleen, testes	Rat	Drugs	-4.62 to 6.3

Table 8. Descriptions of the rate of metabolism in PBPK models

Metabolic constants	Description
V_{max} and Km	$\frac{V_{max} \cdot Cvl}{Km + Cvl}$
CL_{int}	$CL_{int} \cdot Cvl$
CL_h	$CLh \cdot Ca$
E	$Ql \cdot E \cdot Ca$

Abbreviations: V_{max}: Maximal velocity of enzymatic reaction (mg/h or mmol/h); Km:Michaelis-Menten affinity constant (mg/L or mmol/L); CL_{int}: Intrinsic clearance (L/h); CL_h: Hepatic clearance (L/h); E: Hepatic extraction ratio; Q_l: blood flow rate to liver (L/h); Cvl: Concentration of chemical in venous blood leaving liver (mg/L or mmol/L) and Ca: Arterial blood concentration (mg/L or mmol/L).

Table 9. Fragment-specific contributions to the hepatic and intrinsic clearance for VOCs[1]

Fragment	Contribution to	
	CL_h	CL_{int}
CH_3	0.388	-0.005
CH_2	-0.186	0.039
CH	-0.464	0.042
C	-1.440	-1.735
C=C	-1.710	0.000
H	0.813	0.039
Br	0.523	-
Cl	0.537	-
AC	0.128	0.825
H_AC	0.061	0.353

[1]The fragment-specific contributions times the frequency of their occurrence gives the particular metabolic constant. Based on Béliveau et al. [62] and Kamgang et al. [63].

Table 10. Fragment-specific contributions to intrinsic clearance normalized to P450 CYP2E1 content in liver[1].

Fragment in molecule	Contribution to Log CL_{int} (CYP2E1)
CH_3	1.552
CH_2	0.514
CH	0.078
C	-0.871
C=C	0.591
H	0.383
Br	1.000
Cl	0.522
F	0.000
AC	-7.646
H on AC	1.535

[1] Based on Béliveau et al. [81]

2.10. Figures

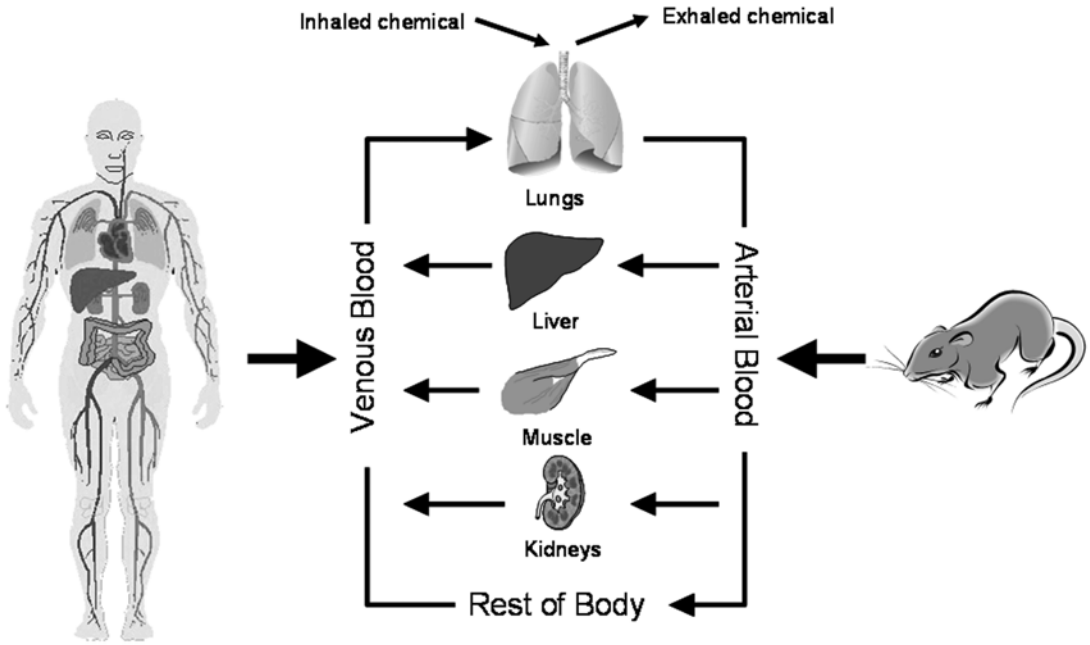

Figure 1. Conceptual representation of a PBPK model for an inhaled toxicant in rats and humans.

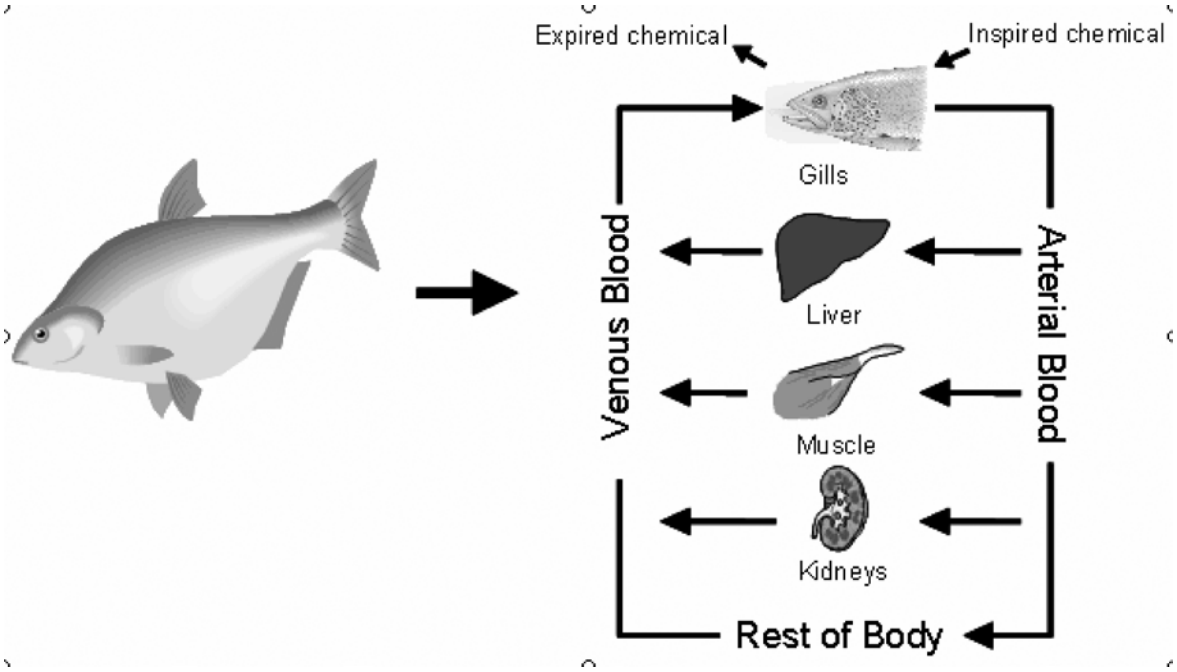

Figure 2. Conceptual representation of a fish PBPK model.

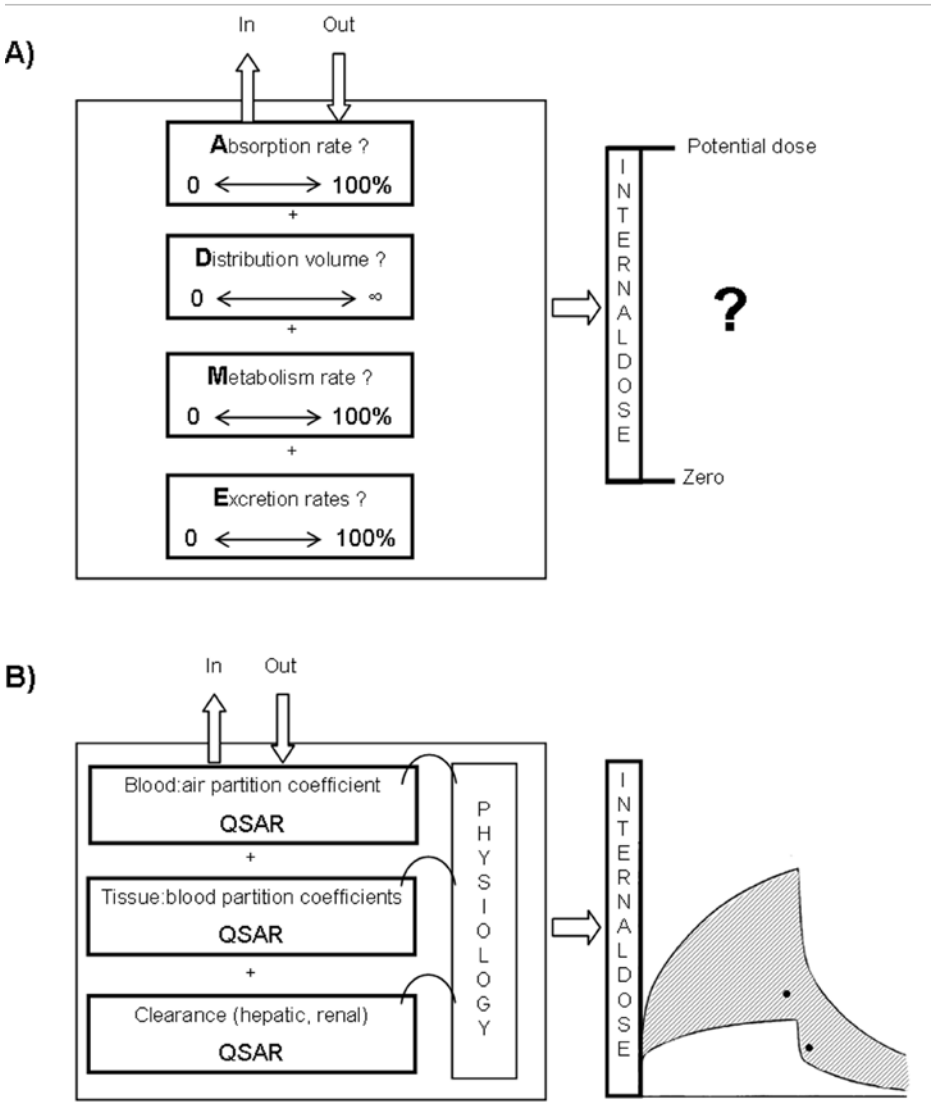

Figure 3. Uncertainty in internal dose calculations for an inhaled toxicant (e.g. target tissue concentration *vs.* time) as a function of the knowledge of pharmacokinetic processes and determinants.

(A) A situation characterized by a total lack of experimental or modelled data on pharmacokinetic processes. (B) A situation characterized by the availability of QSAR-based estimates of input parameters and animal physiology, which are integrated within a PBPK modelling framework.

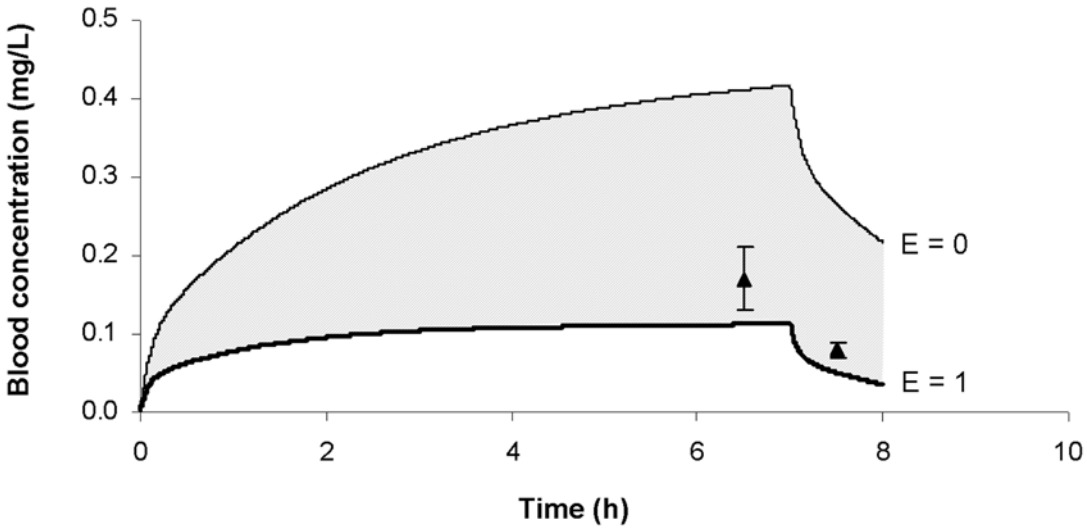

Figure 4. Comparison between the experimental data (symbols) and the envelope of trichloroethylene venous blood concentration simulated by human QSAR-PBPK model (exposure condition: 12.1 ppm, 7 h) [120] using values of 0 and 1 for the hepatic extraction ratio (*E*).

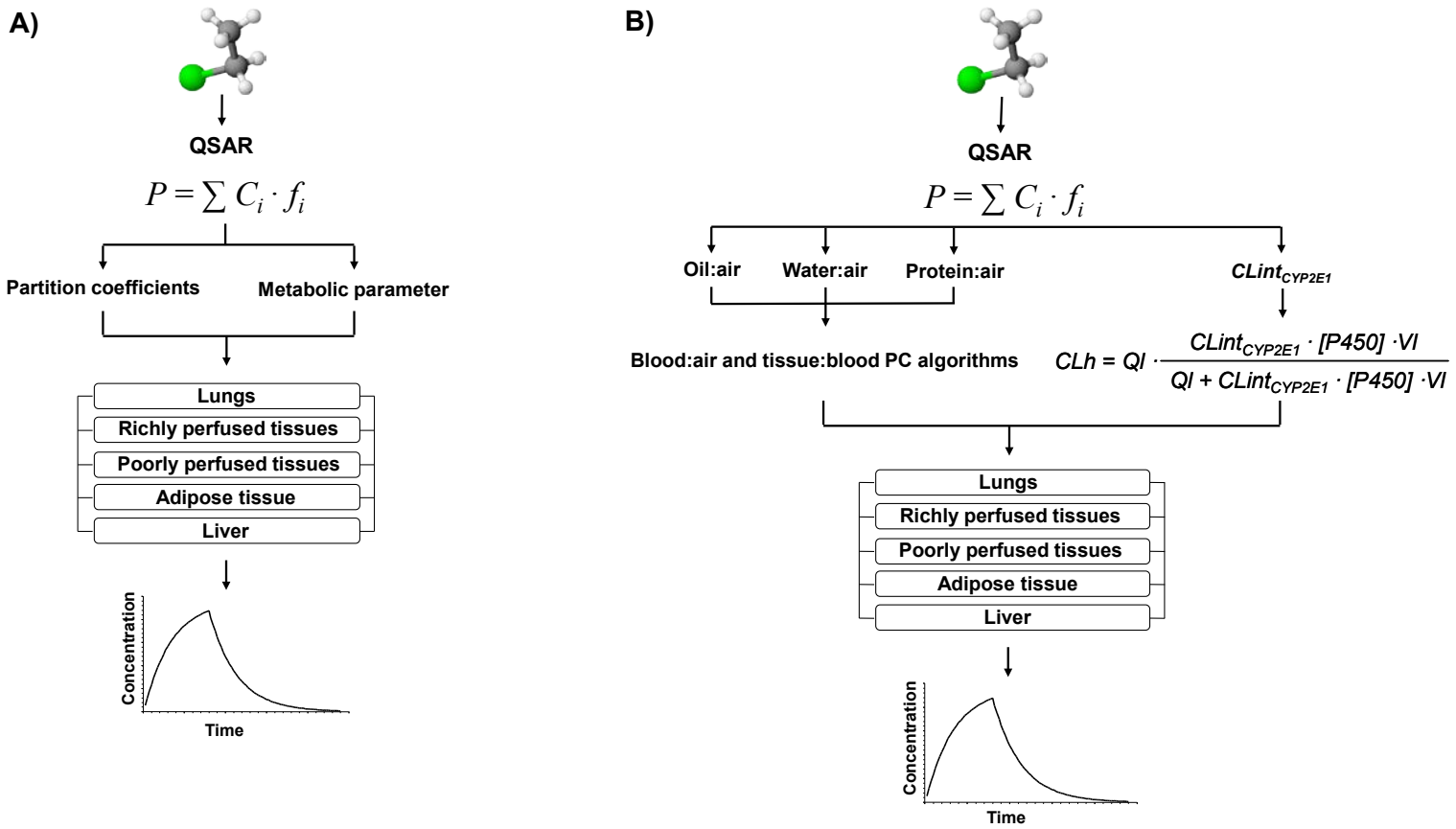

Figure 5. Illustration of the two approaches (A, B) for the development of PBPK models based on QSARs for chemical-specific input parameters.

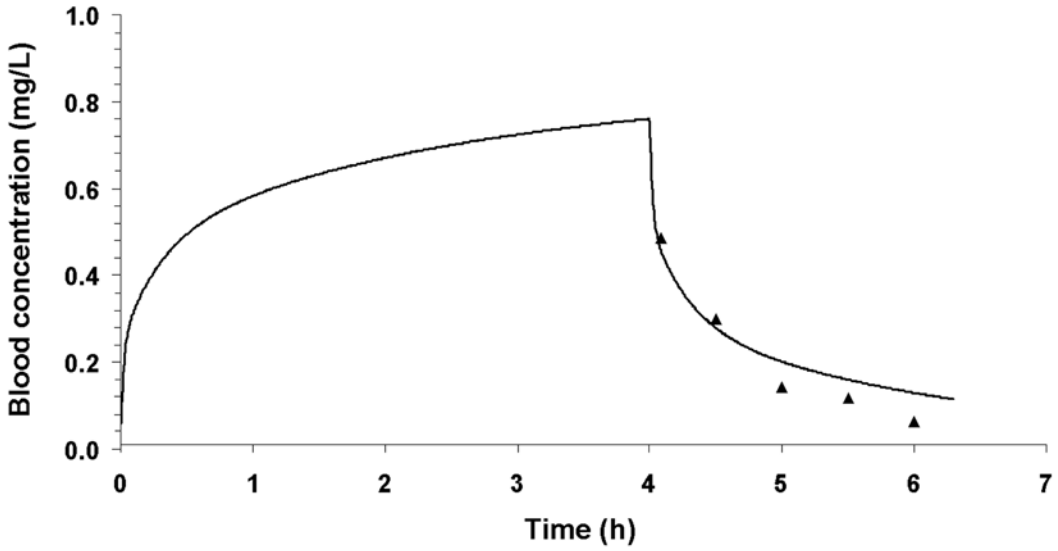

Figure 6. Comparison between the experimental data (symbols) and the QSAR-PBPK model predictions (solid line) of toluene venous blood concentration for 50 ppm, 4 h inhalation exposure in rat. Based on Béliveau et al. [62].

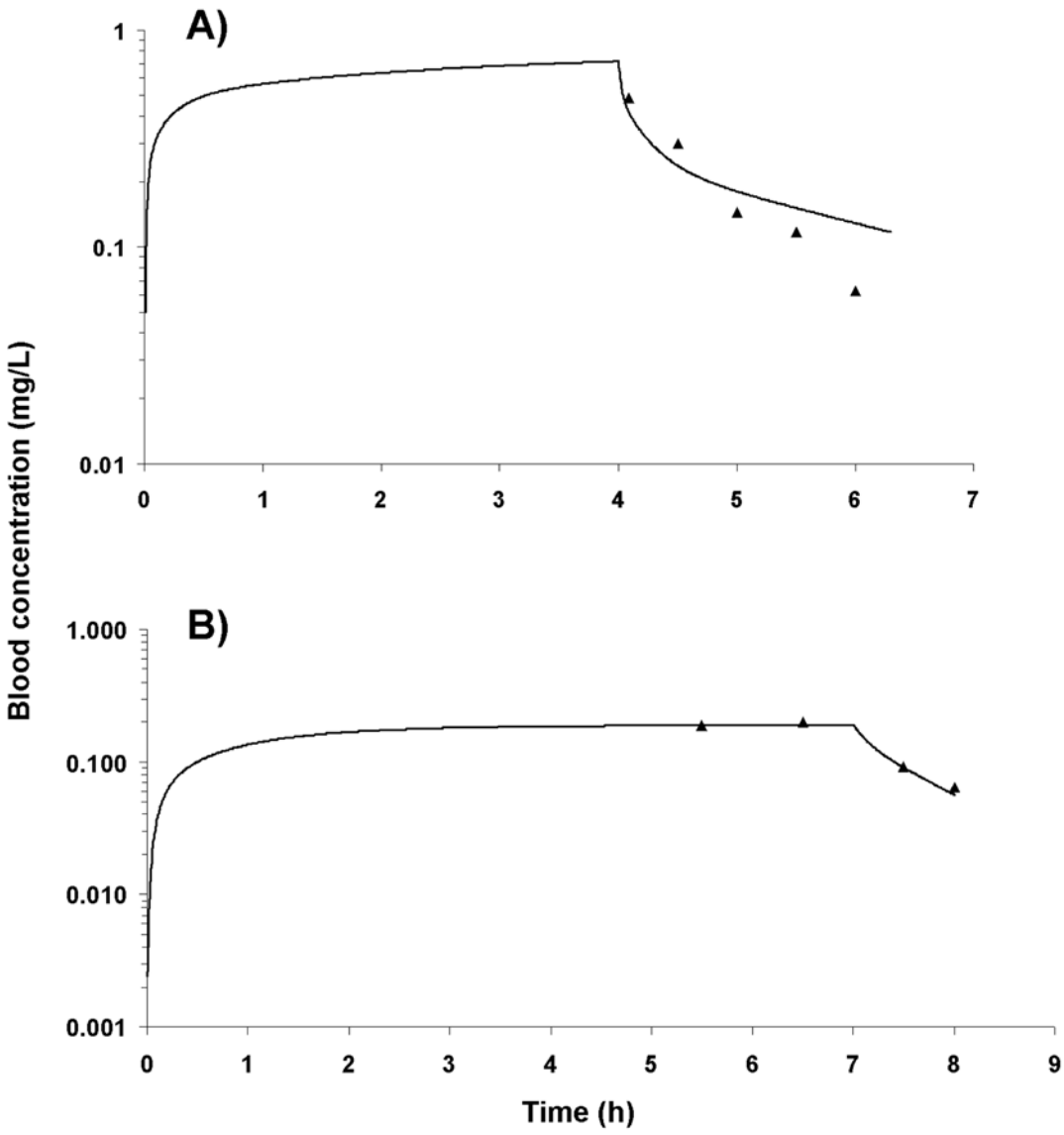

Figure 7. Comparison between the experimental data (symbols) and the QSAR-PBPK model predictions (solid line) of toluene venous blood concentration for inhalation exposures. (A) 50 ppm, 4 h in the rat; (B) 17 ppm, 7 h in humans. Based on Béliveau et al. [81].

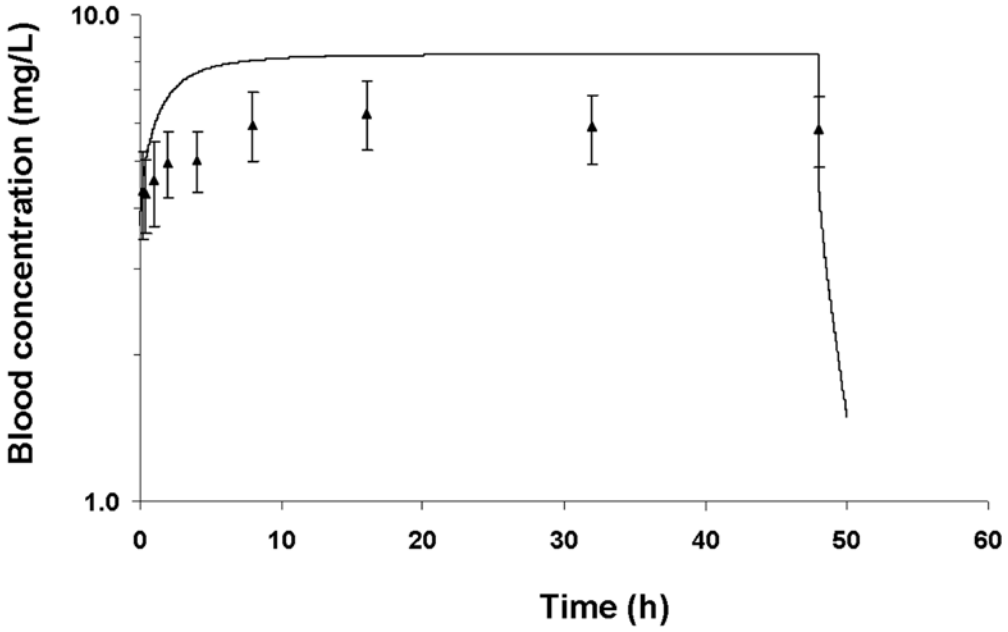

Figure 8. Comparison between the experimental data (symbols) and the QSAR-PBPK predictions (solid line) of arterial blood concentration in rainbow trout exposed to 1.06 mg 1,1,2,2-tetrachloroethane/L water during 48 h. Data from Nichols et al. [42].

Chapitre 3. A unified algorithm for predicting partition coefficients for PBPK modeling of drugs and environmental chemicals

Peyret, T., Poulin, P., and Krishnan, K. (2010). A unified algorithm for predicting partition coefficients for PBPK modeling of drugs and environmental chemicals.
Toxicol. Appl. Pharmacol. 249, 197-207.

A unified algorithm for predicting partition coefficients for PBPK modeling of drugs and environmental chemicals

Thomas Peyret[a], Patrick Poulin[b] and Kannan Krishnan[a]

[a] DSEST, Université de Montréal, Canada H3T 1A8
[b] Consultant, 4009 rue Sylvia Daoust, Québec City, Québec, Canada G1X 0A6

Received 28 June 2010;
revised 30 August 2010;
accepted 16 September 2010.
Available online 23 September 2010.

3.1. Abstract

The algorithms in the literature focusing to predict tissue:blood PC (P_{tb}) for environmental chemicals and tissue:plasma PC based on total (K_p) or unbound concentration (K_{pu}) for drugs differ in their consideration of binding to hemoglobin, plasma proteins and charged phospholipids. The objective of the present study was to develop a unified algorithm such that P_{tb}, K_p and K_{pu} for both drugs and environmental chemicals could be predicted. The development of the unified algorithm was accomplished by integrating all mechanistic algorithms previously published to compute the PCs. Furthermore, the algorithm was structured in such a way as to facilitate predictions of the distribution of organic compounds at the macro (i.e. whole tissue) and micro (i.e. cells and fluids) levels. The resulting unified algorithm was applied to compute the rat P_{tb}, K_p or K_{pu} of muscle (n = 174), liver (n = 139) and adipose tissue (n = 141) for acidic, neutral, zwitterionic and basic drugs as well as ketones, acetate esters, alcohols, aliphatic hydrocarbons, aromatic hydrocarbons and ethers. The unified algorithm reproduced adequately the values predicted previously by the published algorithms for a total of 142 drugs and chemicals. The sensitivity analysis demonstrated the relative importance of the various compound properties reflective of specific mechanistic determinants relevant to prediction of PC values of drugs and environmental chemicals. Overall, the present unified algorithm uniquely facilitates the computation of macro and micro level PCs for developing organ and cellular-level PBPK models for both chemicals and drugs.

Keywords: Partition coefficients; PBPK modeling; Tissue distribution; Tissue:blood; Tissue:plasma

Abbreviations: PC = partition coefficient; P_{tb} = tissue:blood PC; P_{ct} = tissue cell:water PC; P_{it} = tissue interstitial fluid:water PC; P_e = erythrocyte:water PC; P_p = plasma:water PC; F_{ct} = fractional content of cells in tissue; F_{it} = fractional content of interstitial fluid in tissue; F_e = fractional content of erythrocyte; F_p = fractional content of plasma; C_m = concentration in matrix m; C_{nw} = concentration of the non-ionic form in water; F_{wm} = fractional content of water equivalent in the matrix; F_{nlm} = fractional content of neutral lipids equivalent in the matrix; F_{aplm} = fractional content of acidic phospholipids in the matrix; F_{prm} = fractional content of binding proteins in the matrix; P_{ow} = vegetable oil (or *n*-octanol):water PC; P_{aplw} = acidic phospholipids:water PC; P_{prw} = protein:water PC; P_{mw} = matrix:water PC; I_m = ionization term for the aqueous phase of the matrix m; P_{Hbw} = hemoglobin:water PC; P_{bw} = blood:water PC; subscripts e = hemoglobin; p = plasma; c = cell; I = interstitial fluid; w = water m = muscle; f = adipose tissue.

3.2. Introduction

Volume of distribution is a key determinant of the pharmacokinetics and concentration-time course behaviour of chemicals and drugs in target sites. The volume of distribution at steady-state is computed as the plasma or blood volume plus the tissue volumes times the tissue:plasma or tissue:blood partition coefficients (PCs). The tissue:blood or tissue:plasma PCs are used in physiologically-based pharmacokinetic (PBPK) models to compute the uptake and distribution kinetics of chemicals and drugs. The PCs used in PBPK models correspond either to the tissue:blood PCs (P_{tb}) based on total concentration for environmental chemicals or to the tissue:plasma PCs based on total (k_p) or unbound concentration (K_{pu}) in the case of drugs. For volatile organic chemicals (VOCs), the P_{tb} has frequently been obtained as the ratio of tissue:air PC to blood:air PC. These PCs indicate the degree of accumulation of a compound in a tissue compared to another under steady-state condition. A number of methods have been developed by the toxicology and

pharmaceutical communities to estimate/calculate the PCs required for PBPK modeling (Krishnan and Andersen, 2007). The mechanistic algorithms or tissue composition-based equations developed for calculating P_{tb}, K_p and/or K_{pu} values are based on the fundamental principle that the concentration (or solubility) of a compound in a biological matrix can be expressed as the sum of its concentration in the respective components of the matrix (i.e. water, neutral lipids, charged phospholipids, hemoglobin and/or plasma proteins). These equations were initially developed for neutral organic solvents and pollutants for which the generic hydrophobic interactions with neutral lipids and hemoglobin were taken into account (Poulin and Krishnan, 1995a; Poulin and Krishnan, 1995b; Poulin and Krishnan, 1996a; Poulin and Krishnan, 1996b; Poulin and Theil, 2000; Poulin et al., 2001; Payne and Kenny, 2002). Recent advances extended these equations, which focused initially on hydrophobic interactions for drugs, by including ionic interactions with the charged phospholipids and binding to plasma proteins (Poulin and Theil, 2002; Rodgers et al., 2005; Rodgers and Rowland, 2006). The existing algorithms developed for predicting PCs of environmental chemicals and drugs differ in their consideration of binding to plasma proteins and charged phospholipids. Diverse input parameters routinely determined *in vitro* were used in these algorithms to estimate the hydrophobic interactions with neutral lipids (e.g., *n*-octanol:buffer PC), the ionic binding with charged phospholipids or hydrophobic binding to hemoglobin (e.g., erythrocyte:buffer or blood:air PC) and the binding to plasma proteins (e.g., unbound fraction in plasma), which facilitated the applicability of these mechanistic equations (Poulin and Krishnan, 1996a; Poulin and Krishnan, 1996b; Poulin and Theil, 2002; Rodgers et al., 2005; Rodgers and Rowland, 2006; Schmitt, 2008). In parallel, *in silico*-based approaches have also been developed for parameterizing the biological algorithms in view of predicting P_{tb} of organic pollutants (Béliveau and Krishnan, 2003).

At the present time, the prediction of P_{tb}, K_p and K_{pu} for a given molecule could be conducted using each of the published algorithms separately (Table 1). In other words, there is no algorithm unifying all the mechanisms involved in the distribution of both the

environmental chemicals and drugs. Moreover, the most recent effort in this regard is limited to the computation of K_p of drugs only (Schmitt, 2008). This later study developed a unified algorithm to predict the tissue:plasma (or erythrocyte:plasma) PCs of drugs by considering their distribution in cells and interstitial fluids. In this approach, however, the plasma was not described with a mechanistic equation, which considers separately drug partitioning into each component (i.e. water, lipids, and proteins) as it did for tissues. Consequently, only the measured or modeled unbound fraction in plasma (fu_p) could be used to account for the partitioning into the plasma. Nevertheless, Schmitt (2008) successfully predicted the K_p of various drugs but did not apply it to predict K_p or P_{tb} of environmental pollutants. Due to the growing interest in cellular toxicity testing and high-throughput assays, it would be relevant to predict distribution parameters also at the cellular level. In this case, it is essential to predict the PCs for both the macro (i.e. whole tissue and whole blood) and micro (i.e., cells and fluids) levels for both drugs and chemicals.

The objective of the present study was to develop a unified algorithm such that the PCs for both drugs and environmental chemicals could be predicted at the macro and micro levels from readily available data. This study basically intended to reproduce the predictions of each of the previous published algorithms using a single, unified description of the mechanisms underlying the distribution of diverse groups of drugs and chemicals. We also report the results of a sensitivity analysis for the proposed unified algorithm.

3.3. Methods

The development of a unified algorithm was performed by integrating key, original tissue composition-based algorithms in the literature, which have been demonstrated to predict the P_{tb} of environmental chemicals (Poulin and Krishnan, 1995a; Poulin and Krishnan, 1995b; Poulin and Krishnan, 1996a; Poulin and Krishnan, 1996b) as well as K_p and K_{pu} of drugs (Poulin and Theil, 2000; Poulin et al., 2001; Rodgers et al., 2005; Rodgers and Rowland,

2006) (Table 1). Accordingly, the resulting single algorithm would reproduce the values of P_{tb}, K_p and K_{pu} using the same assumptions and input parameters of the published algorithms. In this study, three tissues were considered, namely, muscle, liver and adipose. Following the development of the unified algorithm, a sensitivity analysis on the input parameters of the unified algorithm was conducted to identify the most sensitive parameters for selected chemicals and drugs.

3.3.1 Development of the unified algorithm

P_{tb} can be estimated by dividing the predicted concentration of an organic compound in tissue by its predicted concentration in blood at equilibrium (Poulin and Krishnan, 1995a,b). The concentration of a chemical in tissue would be equal to the sum of its volume-adjusted concentration in tissue cells and interstitial fluid. Similarly, the concentration of a chemical in blood would in turn be equal to the sum of the volume-adjusted concentration in the erythrocytes and plasma (Poulin and Krishnan, 1995a,b). The concentration of a chemical in these four matrices (i.e. tissue cells; interstitial fluid; erythrocyte and plasma) as well as the P_{tb} could be computed from matrix:water PCs (i.e., cell:water, interstitial fluid:water, plasma:water and erythrocyte:water) as follows:

$$P_{tb} = \frac{P_{ct} \cdot F_{ct} + P_{it} \cdot F_{it}}{P_p \cdot F_p + P_e \cdot F_e} \quad (1)$$

where P_{ct}: tissue cell:water PC; P_{it}: tissue interstitial fluid:water PC; P_e: erythrocyte:water PC; P_p: plasma:water PC; F_{ct}: fractional content of cells in tissue; F_{it}: fractional content of interstitial fluid in tissue; F_e: fractional content of erythrocyte in blood; and F_p: fractional content of plasma in blood.

In essence, Eq. (1) calculates the ratio of the chemical concentration in cellular and interstitial components to the chemical concentration in plasma and erythrocytes, taking into account the volume differences of the various components. In other terms, the product of a matrix:water PC times the fractional content of the matrix (e.g., $P_{ct} \cdot F_{ct}$) equals the volume-adjusted matrix:water PC. In Eq. (1), the numerator corresponds to an algorithm for calculating the tissue:water PC, which corresponds to K_{pu} (or the tissue:plasma water PC). The denominator corresponds to the algorithm used for calculating the blood:water PC as required for the prediction of P_{tb}. Therefore, the whole tissue:blood PCs as required in PBPK models of environmental chemicals can be calculated by dividing the numerator (i.e., tissue:water PC) with the denominator (i.e., blood:water PC) of Eq. (1). Similarly, the tissue:plasma PC (K_p) can be calculated by dividing the numerator of Eq. (1) (i.e., tissue:water PC) with the first term in the denominator of Eq. (1) (i.e., plasma:water PC). Here the term water may also refer to the buffer solution commonly used in the experimental analyses.

Eq. (1) also provides the advantage of describing the PCs at the micro level. For example, the cell:blood PC can be predicted by dividing the tissue cell:water PC (i.e., first term in the numerator of Eq. (1)) with the blood:water PC (i.e., denominator of Eq. (1)), whereas the interstitial fluid:blood PC can be calculated from the tissue interstitial fluid:water PC (i.e., second term in the numerator of Eq. (1)) along with the blood:water PC. Similarly, the erythrocyte:plasma PC of a chemical can be predicted by dividing the erythrocyte:water PC by the plasma:water PC using Eq. (1).

In order to use the Eq. (1), diverse matrix:water PCs need to be defined (i.e., P_{ct}, P_{it}, P_e and P_p). Each matrix:water PC was defined on the basis of the corresponding fractional content of and partitioning/binding into: water, neutral lipids, phospholipids (neutral and acidic) and proteins, as defined by the conceptual model presented in Fig. 1. Accordingly, in each biological matrix, the central compartment is water where ionizable molecules exist in ionic and non-ionic forms, which equilibrate with the other constituents. More specifically, intracellular and extracellular water represent the sites of dissociation of ionizable

molecules; therefore both ionic and non-ionic forms are present in this constituent (Rodgers et al., 2005; Rodgers and Rowland, 2006). Similarly, in the hydrophilic group of the phospholipids, (e.g. phosphomonoester) both ionic and non-ionic forms are assumed to be present. The non-ionic form of all classes of chemicals is solubilized in the neutral lipids and the hydrophobic group (e.g., glyceride) of the neutral phospholipids (Poulin and Krishnan, 1995b; Rodgers et al., 2005). The ions produced by the dissociation of bases have electrostatic interactions with acidic phospholipids (phosphatidylserine, mono- and diphosphatidylglycerol, phosphatidylinositol, and phosphatidic acid). The accumulation of cations in the acidic phospholipids would appear to be a major mechanism of distribution of a strong basic drug (at least one pKa $\geq$ 7) (Rodgers et al., 2005). Consequently, for a neutral compound the binding to acidic phospholipids is neglected. The acids, zwitterions with an acidic behaviour, and weak bases bind to albumin whereas the neutral drugs are assumed to bind to lipoproteins (Rodgers and Rowland, 2006). For neutral volatile organic chemicals, the binding to these macromolecules was neglected since the hemoglobin appears to be the principal binding protein (Béliveau and Krishnan, 2003). In this regard, it has been observed that relatively hydrophobic (log $P > 1$) volatile organic compounds with a low molecular volume (< 300 $Å^3$) bind significantly to the hydrophobic pockets of rat hemoglobin (Poulin et al., 1999).

3.3.2 Computation of the volume-adjusted matrix:water PCs

In order to solve each of the four terms of Eq. (1) (i.e., volume-adjusted matrix:water PCs), the fractional volumes of the four constituents (i.e., F_{ct}, F_{it}, F_p, F_e) as well as the matrix:water PCs for these four constituents (i.e., P_{ct}, P_{it}, P_p, P_e) are required. The terms F_{ct} and F_{it} for rat were estimated from data on the whole tissues (Kawai et al., 1994). The fractional volume F_{ct} was obtained by subtracting F_{it} and vascular space from the whole tissue space. The sum of F_{ct} and F_{it} was in turn set equal to unity. The fractional volume of cells and interstitial fluid of the adipose tissue, liver and muscle is presented in Table 2. The

fractional content of erythrocyte (F_e) and plasma (F_p) in the rat was set equal to 0.4 and 0.6, respectively (Poulin and Krishnan, 1995a).

Each matrix:water PC of Eq. (1) (i.e. P_{ct}, P_{it}, P_e and P_p) can be computed on the basis of the concentration of non-ionic form in the water phase as per (Poulin and Krishnan, 1995a), (Poulin and Theil, 2000), (Rodgers et al., 2005), (Rodgers and Rowland, 2006) and (Schmitt, 2008), as follows:

$$C_m = C_{nw} \cdot (1 + I_m) \cdot F_{wm} + C_{nw} \cdot P_{ow} \cdot F_{nlm} + C_{nw} \cdot I_m \cdot P_{aplw} \cdot F_{aplm} + C_{nw} \cdot (1 + I_m) \cdot P_{prw} \cdot F_{prm} \quad (2)$$

where C_m: concentration in the matrix m; C_{nw}: concentration of the non-ionic form in water; F_{wm}: fractional volume of water equivalent in the matrix; F_{nlm}: fractional volume of neutral lipids equivalent in the matrix; F_{aplm}: fractional volume of acidic phospholipids in the matrix; F_{prm}: fractional volume of binding proteins in the matrix; I_m: ionization term for the aqueous phase of the matrix m; P_{ow}: vegetable oil:water PC or n-octanol:water PC; P_{aplw}: acidic phospholipids:water PC; and P_{prw}: protein:water PC.

In Eq. (2), the term F_{wm} equals the sum of the fractional volume of water plus 70% of the content of neutral phospholipids, whereas, the term F_{nlm} corresponds to the fractional volume of neutral lipids plus 30% of the content of neutral phospholipids (Poulin and Krishnan, 1995a,b). The ionization term of the matrix I_m was calculated using the Henderson–Hasselbach equation as follows (Rodgers and Rowland, 2007):

$I_m = 0$ for neutrals (3)

$I_m = 10^{pKa-pH}$ for monoprotic bases (4)

$$I_m = 10^{pH-pKa} \text{ for monoprotic acids} \quad (5)$$

$$I_m = 10^{pKa2-pH} + 10^{pKa1+pKa2-2pH} \text{ for diprotic bases} \quad (6)$$

$$I_m = 10^{pH-pKa1} + 10^{2pH-pKa1-pKa2} \text{ for diprotic acids} \quad (7)$$

$$I_m = 10^{pKabase-pH} + 10^{pH-pKaacide} \text{ for zwitterions} \quad (8)$$

Dividing Eq. (2) by the chemical or drug concentration in water yields, after rearrangement, the following algorithm for computing a matrix:water PC (i.e., cell:water; interstitial fluid:water; plasma:water and erythrocyte:water):

$$P_{mw} = \frac{\left(1+I_m\right)\cdot F_{wm} + P_{ow}\cdot F_{nlm} + I_m \cdot P_{aplw}\cdot F_{aplm} + \left(1+I_m\right)\cdot P_{prw}\cdot F_{prm}}{\left(1+I_w\right)} \quad (9)$$

where P_{mw}: matrix:water PC; I_m and I_w are the ionization term for the matrix and water, respectively.

This unified equation of a matrix:water PC (Eq. (9)) can be used to compute cell:water PC, interstitial fluid:water PC, erythrocyte:water PC and plasma:water PC, simply by using the corresponding physiological input parameters. Furthermore, it can be applied to predict P_{tb}, K_p or K_{pu} of any compound using chemical-specific input parameters (P_{ow}, P_{aplw}, P_{prw}, I_m, and I_w).

3.3.3 Estimation of the physiological input parameters

Table 3 presents the values of the physiological input parameters on tissue composition, specifically for cells (*c*), interstitial fluid (*i*), erythrocytes (*e*) and plasma (*p*) of the rat. The derivation of these parameters from the literature is described in detail below.

Tissue cells

The critical components are: water, neutral lipids (including neutral phospholipids), acidic phospholipids and binding proteins (Rodgers et al., 2005 and Rodgers and Rowland, 2006). The cellular fractions of neutral lipids, neutral phospholipids and acidic phospholipids were derived from values reported for the whole tissue (Poulin and Krishnan, 1995a and Rodgers et al., 2005). Considering that the presence of lipids is negligible in the interstitial fluid (Aukland and Nicolaysen, 1981), the values reported for the whole tissue were corrected for the cellular fraction. For the adipocytes, a fractional volume of neutral lipids of 0.954 was used in order to avoid the sum of fractions of the components of this matrix exceeding unity. For all tissues, the fractional content of neutral phospholipids in the cells was obtained by subtracting the fractional content of acidic phospholipids (Rodgers et al., 2005) from the fractional content of total phospholipids (Poulin and Krishnan, 1995a). Similarly, the values of the fractional content of acidic phospholipids in the cells of muscle, liver, adipose tissue and erythrocytes were obtained by dividing the fractional content observed for the whole tissue (Rodgers et al., 2005) with the fractional volume of cells in the corresponding tissues. The volume fraction of water in adipocytes corresponds to the average of the values reported by DiGirolamo and Owens (1976). As for the values of the fractional volume of water in liver and muscle cells, they were obtained from the study of Cieslar et al. (1998). The fractional content of proteins of the liver and muscle cells were obtained from Lesser et al. (1980). The fractional content of proteins used for the adipocytes was obtained by dividing the fractional content of intracellular proteins in the adipose tissue reported by Mattacks et al. (2003) by the fractional volume of cells in this tissue.

Interstitial fluid

The interstitial fluid consists mainly of water and plasma proteins (Aukland and Nicolaysen, 1981). The binding to tissue proteins is considered to occur principally in the

interstitial fluid where the organic compounds can interact with the plasma proteins such as albumin and lipoproteins (Poulin and Theil, 2000; Rodgers and Rowland, 2006). The fractional content of water in the interstitial fluid was assumed to be the same for all tissues (Aukland and Nicolaysen, 1981). The fractional content of plasma proteins (i.e. albumin and lipoproteins) in the interstitial fluid of each rat tissue was calculated from their fractional content in plasma corrected for the corresponding interstitial fluid:plasma concentration ratios. The later ratios were estimated from whole tissue values reported by Rodgers and Rowland (2006).

Erythrocytes

The chemical partitioning into erythrocyte is determined by its content of water, neutral lipids, neutral phospholipids, proteins and acidic phospholipids (Poulin and Krishnan, 1995a, Rodgers et al., 2005; Rodgers and Rowland, 2006). The fractional contents of neutral lipids, total phospholipids and water in rat were taken from Poulin and Krishnan (1995a). The fractional content of neutral phospholipids was in turn obtained by subtracting the fractional content of acidic phospholipids (Rodgers et al., 2005) from the fractional content of total phospholipids. The fractional content of acidic phospholipids in the red blood cells (Rodgers et al., 2005) was derived as described previously for the tissue cell. The fractional content of binding proteins (0.327) corresponds to the fraction of hemoglobin in the whole blood (0.147) (Long, 1961) divided by the hematocrit (= 0.45).

Plasma

A review of the literature did not reveal significant amount of acidic phospholipids in the plasma in contrast to other tissue matrices. Therefore, partitioning into plasma is determined by its content of water, neutral lipids, neutral phospholipids and the two major binding proteins, namely, albumin and lipoproteins. The values of the fractional content of

neutral lipids, phospholipids and water in plasma were gathered from Poulin and Krishnan (1995a). For plasma proteins, the fractional content of albumin was obtained from Long (1961) whereas the fractional content of lipoproteins was assumed to be the sum of the fractions of VLDL, IDL, LDL, and HDL as reported by Dory and Roheim (1981).

3.3.4 Estimation of the chemical-specific input parameters

The values of the chemical-specific input parameters are listed in Table 4, Table 5, Table 6, Table 7, Table 8 and Table 9. The generic lipophilicity parameter (P_{ow}), which corresponds to the vegetable oil:water PC, was calculated as the ratio between olive oil:air PC and water:air PC determined *in vitro* for volatile organic chemicals (VOCs) (Gargas et al., 1989; Johanson and Filser, 1993; Kaneko et al., 1994; Poulin and Krishnan, 1996b). For drugs, this parameter corresponds to oil:water PC for adipose tissue, whereas for non-adipose tissues it refers to *n*-octanol:water PC, as proposed by Poulin and Theil (2002) and Rodgers and Rowland (2006). The difference between VOCs and drugs in terms of the use of P_{ow} arises from the fact that the experimental PC values relative to air were only available for olive oil for VOCs. The present study did not prefer one solvent (olive oil) compared to another (*n*-octanol) because, the main objective is to reproduce the published algorithms using the same assumptions and input parameters.

The values of pKa and the unbound fraction in plasma (fu_p) determined *in vitro* for each drug were also obtained from the literature (Poulin and Theil, 2000; Poulin et al., 2001; Rodgers et al., 2005; Rodgers and Rowland, 2006). The fu_p values were used in the calculation of P_{aplw} as well as plasma and interstitial P_{prw}. However, for VOCs, the value fu_p was set equal to 1, and there is no pKa value since they are in the neutral form at the physiological pH.

A pH value of 7, 7.4, 7.22 and 7.4 was used for cells, interstitial fluid, erythrocytes and plasma, respectively (Rodgers et al. 2005). Therefore, the ionization term I_m for these matrixes was calculated at these pH values using the Henderson–Hasselbach equations and the pKa values. For water (aqueous phase or buffer), a pH value of 7.4 was used. Consequently, I_w was calculated at this pH.

Calculation of P_{prw}

It is known that for small chemical molecules, distribution is typically driven by nonspecific binding in tissues; however, pharmacological target binding is generally of minor relevance in terms of their contribution to the volume of distribution. Therefore, the binding to intracellular proteins has not been characterised routinely in efforts focusing to predict PCs. In other words, the extent of binding to the proteins in tissue cellular matrix was set equal to zero for all compounds (i.e., $P_{prw} = 0$).

For the interstitial fluid and plasma, P_{prw} refers to the albumin:water PC for the acidic compounds (acids and acidic zwitterions) and weak bases or lipoprotein:water PC for the neutral drugs. This parameter was obtained from the information on the unbound fraction measured *in vitro* in plasma (fu_p) for drugs as suggested previously by Rodgers and Rowland (2006):

$$P_{prwp} = \left(\frac{1}{fu_p} - 1 - \frac{P_{ow} \cdot F_{nlp}}{(1 + I_P)} \right) \cdot \frac{1}{F_{prp}} \qquad (10)$$

where subscript p refers to plasma; F_{nl}: fractional content of neutral lipids equivalent; and F_{pr}: fraction of protein.

The same value of P_{prw} was used for plasma and interstitial fluid since it was assumed that the binding macromolecules are the same in both matrices, which should represent a similar binding affinity and capacity (Rodgers and Rowland, 2006). The underlying principle is that the plasma and interstitial fluid contain these binding macromolecules that provide high-affinity binding sites for drugs.

For erythrocyte, P_{prw} refers to the hemoglobin:water PC (P_{Hbw}) only for relatively hydrophobic VOCs (Poulin and Krishnan, 1996a). It was estimated from the blood:water PC (P_{bw}) determined *in vitro* (i.e., the ratio between blood:air PC and water:air PC obtained from the literature (Gargas et al., 1989; Johanson and Filser, 1993) as suggested by Poulin and Krishnan (1996a):

$$P_{Hbw} = \frac{\left(\frac{P_{bw} - f_P \cdot P_p}{f_e}\right) \cdot (1 + I_w) - \left((1 + I_e) \cdot F_{we} + P_{ow} \cdot F_{nle} + I_e \cdot P_{aplw} \cdot F_{aple}\right)}{F_{pre}} \qquad (11)$$

where subscript *e* refers to erythrocyte.

The underlying principle is that VOC binding to rat erythrocytes is due to the presence of lipophilic binding pockets (Poulin and Krishnan, 1996a).

Calculation of P_{aplw}

P_{aplw} refers to the acidic phospholipid:water PC, and was used only for the strong basic drugs and basic zwitterions with at least one pKa ≥ 7 as previously stated. Rodgers et al. (2005) used the blood:plasma ratio determined *in vitro* to estimate the extent of binding to acidic phospholipids in tissues. The main reason is that the erythrocyte also contains such lipids that provide high-affinity binding sites for basic drugs. Accordingly, the

blood:plasma ratio, which has been converted to erythrocyte:water PC (P_{ew}) using the value of fu_p and the erythrocyte content in blood, was used to estimate P_{aplw} of tissue cells for all basic drugs having at least one pKa ≥ 7 based on Rodgers et al. (2005):

$$P_{aplw} = \left[P_{ew} - \frac{(1 + I_e) \cdot F_{we} + P_{ow} \cdot F_{nle}}{1 + I_p} \right] \cdot \frac{1 + I_p}{I_e \cdot F_{aple}} \qquad (12)$$

where *e*: erythrocyte; F_{apl}: fractional content of acidic phospholipids equivalent; F_{nl}: fractional content of neutral lipid equivalent; and F_w: fractional content of water equivalent.

Since it is assumed that there are no acidic phospholipids in the interstitial fluid and plasma, the value of P_{alpw} was set equal to 0 for these two matrices.

3.3.5 Comparison with published algorithms

The values of P_{tb} of chemicals along with K_p and K_{pu} of drugs were calculated using the unified algorithm and compared with the predictions of individual algorithms. The dataset consisted of 142 drugs and chemicals (Table 4, Table 5, Table 6, Table 7, Table 8 and Table 9) for which experimental data on P_{tb} (chemicals), K_p (drugs) and K_{pu} (drugs) were available in the peer-reviewed literature and used by the original study authors for comparing with the predictions of their algorithms (Gargas et al., 1989; Kaneko et al., 1994; Poulin and Krishnan, 1995a; Poulin and Krishnan, 1996a,b; Rodgers et al., 2005; Rodgers and Rowland, 2006).

In the present study,

- predictions of P_{tb} of liver, muscle and adipose tissue for the twenty-two organic chemicals (diethyl ether, 5 ketones, 8 alcohols, and 8 acetates) presented in Table 4

were compared with those of the published algorithm of Poulin and Krishnan (1995a);

■ predictions of P_{tb} of liver, muscle and adipose tissue for fifty-three volatile organic chemicals (1 ether, 2 nitropropanes, 32 alkanes, 10 alkenes, and 8 aromatic hydrocarbons) presented in Table 5 were compared to the predictions of the algorithms of Poulin and Krishnan (1996a,b);

■ predictions of K_p of muscle for the 33 drugs listed in Table 6 were compared with the predictions of the algorithm published by Poulin and Theil (2000);

■ predictions of K_p of adipose tissue for the 11 drugs listed in Table 7 were compared to the predictions of Poulin et al. (2001);

■ predictions of K_{pu} of liver, muscle and adipose tissue for 28 strong bases (Table 8) were compared to the predictions of the published algorithms of Rodgers et al. (2005); and

■ predictions of K_{pu} of liver, muscle and adipose tissue for the 8 zwitterions, 7 weak bases, 21 acids and 4 neutrals (Table 9) were compared to the estimates of the algorithms of Rodgers and Rowland (2006).

3.3.6 Sensitivity analysis

A sensitivity analysis was conducted to identify those input parameters of the algorithm that influenced the predicted PC values the most. This analysis then aimed to ascertain the key parameters in the calculation of PCs for a given tissue and chemical. The sensitivity analysis was carried on the muscle and adipose tissue:blood PCs of one hydrophilic VOC (methanol), one lipophilic VOC (*n*-hexane), one neutral drug (cyclosporine), one basic drug (phencyclidine) and one acid drug (tenoxicam). These compounds are identified in Table 4, Table 5, Table 6, Table 7, Table 8 and Table 9. The sensitivity ratios (SR) were calculated as follows:

$$\mathrm{SR} = \frac{\Delta_Y / Y_0}{\Delta_X / X_0} \tag{13}$$

where Δ_Y is the difference between the value of the response Y, which was calculated using a varied value for one parameter X and Y_0, the value of the response calculated using initial values for all parameters; and Δ_X is the difference between the varied and the initial (X_0) values of the parameter X. The variation of the parameter corresponded to a 10% reduction of the value of X_0, i.e., the value of Δ_X/X_0 was equal to -0.1. For each scenario investigated, the top 3 of the most sensitive parameters were compiled (i.e., the three parameters with the highest absolute value of SR).

3.4. Results

3.4.1 Prediction of PCs

Fig. 2 presents the relationship between the values of PCs predicted with the unified algorithm and those predicted with the previously published algorithms for adipose, muscle and/or liver tissues. The unified algorithm reproduced adequately the predictions provided by the published algorithms. The ratio of the values predicted in this study to those predicted by published algorithms (pred/pred) is equal to 1 ± 0 for the muscle, liver and adipose tissue P_{tb} of the 22 chemicals that do not bind to hemoglobin (i.e., hydrophilic VOCs) (Fig. 2a). When comparing the predictions of the unified algorithm with the one published by (Poulin and Krishnan, 1996a,b), the ratio pred/pred equals 1 ± 0 for the rat P_{tb} of 53 lipophilic VOCs (Fig. 2b). The pred/pred ratio was also equal to 1 ± 0 for the muscle K_p of 33 drugs from Poulin and Theil (2000) (Fig. 2c). Similarly, the ratio pred/pred = 1 ± 0 for the 11 fat:plasma PCs of drugs studied by Poulin et al. (2001) (Fig. 2d). For basic drugs, the unified algorithm reproduced the predictions of Rodgers et al. (2005) as demonstrated

by a pred/pred ratio of unity (Fig. 2e). The same level of accuracy was obtained for the weak bases, neutrals, and zwitterions from Rodgers and Rowland (2006) study (Fig. 2f).

3.4.2 Sensitivity analyses

Table 10 presents the top 3 of the most sensitive parameters for each model chemical or drug investigated. The values of SRs are presented in brackets. A negative (positive) value indicates that the parameter influences negatively (positively) the value of the outcome.

For *n*-hexane, methanol and cyclosporine, the fractional content of cells in tissue was found to be the most sensitive parameter of muscle:blood PC. Similarly, it was also a very sensitive parameter of the adipose:blood PC for *n*-hexane and cyclosporine. The second most sensitive parameter was the fractional content of neutral lipids, which was relevant particularly for muscle:blood and adipose:blood PCs of cyclosporine and adipose:blood PC of *n*-hexane. Furthermore, the fractional content of protein of the erythrocytes (F_{pre}) and the hemoglobin:water PC (P_{Hbw}) had strong impact on the *n*-hexane tissue:blood PCs. P_{ow} was the third most sensitive parameter of muscle:blood and fat:blood PCs of cyclosporine and *n*-hexane. For methanol, the muscle:blood PC was mainly influenced by the fractional content of water in the cells and plasma. Whereas for the adipose:blood PC of methanol, the fractional content of water in plasma, interstitial fluid, and erythrocytes along with the fractional content of interstitial fluid of adipose tissue, were the most sensitive parameters.

For the acidic drug tenoxicam, the most sensitive parameters of the muscle:blood and fat:blood PCs were roughly the same. Namely, the pH value of plasma and interstitial fluid had the most impact, followed by the fractional content of plasma proteins and the plasma protein:water PC. For the fat:blood PC, the pKa of the acid was also a very sensitive parameter, whereas for the muscle:blood PC, the fractional content of interstitial fluid (F_i) was a sensitive parameter. For phencyclidine, however, the most sensitive parameters of muscle:blood PC were related to the pH of the intracellular water, plasma and interstitial

fluid along with the fractional content of cells (F_c). For the fat:blood PC of phencyclidine, the most sensitive parameters were: pKa and pH of plasma and interstitial fluid as well as the fractional content of neutral lipids.

3.5. Discussion

Physiologically-based pharmacokinetic (PBPK) models make use of tissue:blood or tissue:plasma PCs to predict the kinetics of uptake and distribution in tissues. The experimental measurement of PCs for new and emerging contaminants or drugs is often viewed as a time- and resource-consuming effort. In this regard, a number of algorithms have been developed over the last few years to facilitate an initial estimate of the PCs for PBPK modeling of environmental chemicals (Poulin and Krishnan, 1995a,b; Poulin and Krishnan, 1996a,b) as well as pharmaceutical compounds (Poulin and Theil, 2000; Poulin et al., 2001; Rodgers et al., 2005; Rodgers and Rowland, 2006; Schmitt, 2008). The unified algorithm developed in this study reproduced adequately the predictions provided by the previously published algorithms. Fig. 2 indicates that we reproduced the predictions of other models, which were essentially identical to the predictions of our unified algorithm. It was possible because we used the same mechanistic assumptions and tissue composition as the published models. This implies that the prediction performance of the unified algorithm is essentially the same as that of the previously published algorithms for environmental chemicals and drugs. The unified algorithm developed in this study allowed the prediction of the PCs for various combinations of matrices by integrating mechanisms that were only described in isolation in the algorithms for drugs and environmental chemicals (Poulin and Krishnan, 1995a; Poulin and Krishnan, 1996a,b; Rodgers et al., 2005; Rodgers and Rowland, 2006).

The tissue composition algorithms for predicting PCs have evolved over the years. In the initial form, the algorithm was used to calculate whole tissue:whole blood PCs ([Poulin and

Krishnan, 1995a,b; Poulin and Krishnan, 1996a,b). Subsequently, Poulin and Theil (Poulin and Theil, 2000 and Poulin et al., 2001) adapted this algorithm to compute whole tissue:whole plasma PCs (for drug molecules). Further developments by Rodgers and colleagues (Rodgers et al., 2005 and Rodgers and Rowland, 2006) focused on the calculation of whole tissue:plasma water PCs. The present study focused on integrating and reproducing all these previous algorithms and their outputs, using a single algorithm and a single set of input parameters defined using water as the reference phase. In this process then, re-estimation of certain parameters (i.e., P_{prwp}, P_{prwi}, P_{Hbw}) was essential to translate the various input parameters of the existing algorithms to a common form that has water as the reference phase.

A key difference between the only unified algorithm existing in the literature (Schmitt, 2008) and the present unified algorithm relates to the consideration of plasma. Schmitt (2008) predicted only the tissue:plasma PCs of drugs without describing the plasma based on its composition and distribution mechanisms. The present study, however, described the partitioning into each of the following four components: tissue cell, interstitial fluid, erythrocyte, and plasma, so as to facilitate the prediction of the diverse PCs (P_{tb}, K_p, and K_{pu}) of both drugs and environmental chemicals.

The ability of the unified algorithm to predict the PCs also at the micro level represents an advantage compared to the previously published algorithms that only predict the PCs for the whole tissue (macro level). In other terms, an original concept of the unified algorithm resides in the use and combination of several compartments (i.e., cells, interstitial fluid, erythrocytes and plasma) to facilitate the computation of macro and micro level PCs (e.g., cells to plasma PC, whole tissue to whole blood PC). Due to this characteristic, the unified algorithm can facilitate the prediction of intracellular concentration of a chemical which can be particularly useful for developing pharmacodynamic models as well as for interpreting the toxicity data from high-throughput and cell culture assays. The rising use of high-throughput assays and *in vitro* tests, following the National Academy of Sciences' vision for toxicity testing in 21st century, requires the development of computational tools

to interpret such data (National Research Council, 2007; National Research Council, 2010; Andersen and Krewski, 2009). In this regard, the unified algorithm developed in the present study should facilitate the prediction of cell:media PCs for *in vivo* to *in vitro* extrapolation purposes. The division into different matrix:water PCs might also be used to refine the prediction of PCs for different cell types or organelles where the pollutants or drugs are distributed (Waddell, 2010). Subsequently, the cells may be further subdivided into other specific components as the cytosol and other organelles (e.g., nucleus, REG, REL, golgi, mitochondria).

Refining the unified algorithm may consist of adding specific binding site(s) for a more detailed and realistic description of K_{pu}, for example. The binding to alpha1-acid glycoprotein can be predominant for basic drugs that are lipophilic (Israili and Dayton, 2001; Rodgers and Rowland, 2006; Ishizaki et al., 2010). Therefore, the global protein:water PC (P_{prw}) used in the unified algorithm might be expanded to represent the binding to alpha1-acid glycoprotein in addition to albumin and lipoproteins in the interstitial fluid. For this purpose, the corresponding fractional volume of total binding proteins in rat plasma (i.e., F_{prp}) is available, as well as its components (i.e., alpha1-acid glycoprotein (0.0082) (Long, 1961), lipoproteins (0.0006) and albumin (0.029)). One would also expect then the alpha1-acid glycoprotein binding could probably be saturable because of capacity limitations. Thus, if the binding to alpha1-acid glycoprotein is saturated with increasing concentrations for particular drugs, it would indicate a small capacity binding site.

In this study, a sensitivity analysis was carried out using the biologically-based algorithm for partition coefficients. In general, this analysis revealed that specific physiological descriptors play an important role, which is in accordance with the compound properties. In other words, the more lipophilic compounds are principally influenced by the tissue fractions associated with lipids, and inversely, the more hydrophilic compounds by the fractions associated with water. Thus, the current sensitivity analysis confirmed the assumptions of the mechanistic algorithms, consistent with compound properties and

physiological descriptors that determine the PCs. The ionized compounds were influenced by their pKa value and/or pH value associated with diverse tissue and plasma components. For example, the pKa was a very sensitive parameter for the adipose tissue:blood PC for a basic and an acidic compound because this parameter influences the concentration of non-ionic form in the neutral lipid, a major constituent of the adipose tissue. The value of pH, in turn, influenced mostly the concentration in the aqueous phase, the major constituent of muscle tissue and cells, which probably explained the strong impact of this parameter on the muscle PC. For a neutral lipophilic compound, as expected, the lipophilicity parameter P_{ow} and the fractional volume of neutral lipid were the most sensitive input parameters. Since the present sensitivity analyses are only based on five model compounds (cyclosporine, *n*-hexane, methanol, phencyclidine and tenoxicam), these findings would only represent a limited chemical space covered by these candidate substances. Such sensitivity analysis with newer chemicals or drugs can facilitate the identification of input parameters for which characterization of uncertainty and variability would be most useful. Such a sensitivity analysis with the biologically-based algorithms for predicting PCs was not conducted previously. Finally, the sensitivity analysis can be a useful tool to investigate the key determinants of the distribution of chemicals and drugs with mixed/complex physicochemical properties (e.g. relatively hydrophobic, moderately ionized as well as bound to albumin).

In conclusion, the unified algorithm allows the prediction of PCs for both chemicals (P_{tb}) and drugs (K_p and K_{pu}), whereas the sensitivity analysis demonstrated the critical role of specific compound-related properties. The sensitivity analysis applied to the unified algorithm should facilitate the identification and prioritization of the determinants of partitioning at the macro and micro levels. Quantitative structure–activity relationship (QSAR) models on the chemical-specific input parameters (i.e. oil:water, plasma protein:water, hemoglobin:water and acidic phospholipid:water PCs) could potentially be integrated within the unified algorithm to develop first-generation of PBPK models for emerging chemical contaminants and drugs. In other words, it would be feasible to include

molecular structure information in the unified algorithm such that, for any untested chemical and drugs, the PCs can be estimated. Overall, the present unified algorithm uniquely facilitates the computation of macro and micro level PCs for developing organ and cellular-level PBPK models based on the chemicals and drugs tested in this study.

3.6. Acknowledgments

Financial support by Agence française de sécurité sanitaire de l'environnement et du travail (AFSSET) and Natural Sciences and Engineering Research Council of Canada (NSERC) is acknowledged.

3.7. References

Andersen, M. E., and Krewski, D. (2009). Toxicity Testing in the 21st Century: Bringing the Vision to Life. *Toxicol. Sci.* **107**, 324-330.

Aukland, K., and Nicolaysen, G. (1981). Interstitial fluid volume: local regulatory mechanisms. *Physiol. Rev.* **61**, 556-643.

Béliveau, M., and Krishnan, K. (2003). In Silico approaches for developing physiologically based pharmacokinetic (PBPK) models. In *Alternative toxicological methods* (H. Salem, and S. A. Katz, Eds.), pp. 479-532. CRC Press, Boca Raton, Fla.

Cieslar, J., Huang, M.-T., and Dobson, G. P. (1998). Tissue spaces in rat heart, liver, and skeletal muscle in vivo. *Am J Physiol Regul Integr Comp Physiol* **275**, R1530-1536.

DiGirolamo, M., and Owens, J. L. (1976). Water content of rat adipose tissue and isolated adipocytes in relation to cell size. *The American journal of physiology* **231**, 1568-1572.

Dory, L., and Roheim, P. S. (1981). Rat plasma lipoproteins and apolipoproteins in experimental hypothyroidism. *J. Lipid Res.* **22**, 287-296.

Gargas, M. L., Burgess, R. J., Voisard, D. E., Cason, G. H., and Andersen, M. E. (1989). Partition coefficients of low-molecular-weight volatile chemicals in various liquids and tissues. *Toxicol. Appl. Pharmacol.* **98**, 87-99.

Haddad, S., Poulin, P., and Krishnan, K. (2000). Relative lipid content as the sole mechanistic determinant of the adipose tissue:blood partition coefficients of highly lipophilic organic chemicals. *Chemosphere* **40**, 839-843.

Ishizaki, J., Fukaishi, A., Fukuwa, C., Yamazaki, S., Tabata, M., Ishida, T., Suga, Y., Arai, K., Yokogawa, K., and Miyamoto, K.-i. (2010). Evaluation of Selective Competitive Binding of Basic Drugs to alpha;1-Acid Glycoprotein Variants. *Biological & pharmaceutical bulletin* **33**, 95-99.

Israili, Z. H., and Dayton, P. G. (2001). Human alpha-1-glycoprotein and its interactions with drugs. *Drug Metabolism Reviews* **33**, 161-235.

Johanson, G., and Filser, J. G. (1993). A physiologically based pharmacokinetic model for butadiene and its metabolite butadiene monoxide in rat and mouse and its significance for risk extrapolation. *Arch Toxicol* **67**, 151-163.

Kaneko, T., Wang, P. Y., and Sato, A. (1994). Partition coefficients of some acetate esters and alcohols in water, blood, olive oil, and rat tissues. Occup. Environ. Med. 51, 68-72.

Kawai, R., Lemaire, M., Steimer, J. L., Bruelisauer, A., Niederberger, W., and Rowland, M. (1994). Physiologically based pharmacokinetic study on a cyclosporin derivative, SDZ IMM 125. *J Pharmacokinet Biopharm* **22**, 327-365.

Krishnan, K., and Andersen, M. E. (2007). Physiologically based Pharmacokinetic modeling in toxicology. In *Principles and methods of toxicology* (A. W. Hayes, Ed.), pp. 231-292. Taylor & Francis, Boca Raton.

Lesser, G. T., Deutsch, S., and Markofsky, J. (1980). Fat-free mass, total body water, and intracellular water in the aged rat. *Am J Physiol Regul Integr Comp Physiol* **238**, R82-90.

Long, C. (1961). *Biochemists' handbook*. Van Nostrand, Princeton, N.J.

Mattacks, C. A., Sadler, D., and Pond, C. M. (2003). The cellular structure and lipid/protein composition of adipose tissue surrounding chronically stimulated lymph nodes in rats. *J. Anat.* **202**, 551-561.

National Research Council (2007). *Toxicity testing in the 21st century : a vision and a strategy*. National Academies Press, Washington, DC.

National Research Council (2010). Toxicity-pathway-based risk assessment: preparing for paradigm change, a symposium summary. National Academies Press, Washington, DC.

Payne, M. P., and Kenny, L. C. (2002). Comparison of models for the estimation of biological partition coefficients. *J Toxicol Environ Health A* **65**, 897-931.

Poulin, P., Béliveau, M., and Krishnan, K. (1999). Mechanistic animal replacement appoaches for predicting pharmacokinetics of organic chemicals. In *Toxicity assessment alternatives : methods, issues, opportunities* (H. Salem, and S. A. Katz, Eds.), pp. 115-139. Humana Press, Totowa, N.J.

Poulin, P., and Krishnan, K. (1995a). An algorithm for predicting tissue: blood partition coefficients of organic chemicals from *n*-octanol: water partition coefficient data. *J Toxicol Environ Health* **46**, 117-129.

Poulin, P., and Krishnan, K. (1995b). A biologically-based algorithm for predicting human tissue: blood partition coefficients of organic chemicals. *Hum. Exp. Toxicol.* **14**, 273-280.

Poulin, P., and Krishnan, K. (1996a). A mechanistic algorithm for predicting blood:air partition coefficients of organic chemicals with the consideration of reversible binding in hemoglobin. *Toxicol. Appl. Pharmacol.* **136**, 131-137.

Poulin, P., and Krishnan, K. (1996b). A tissue composition-based algorithm for predicting tissue:air partition coefficients of organic chemicals. *Toxicol. Appl. Pharmacol.* **136**, 126-130.

Poulin, P., Schoenlein, K., and Theil, F.-P. (2001). Prediction of adipose tissue: Plasma partition coefficients for structurally unrelated drugs. *J. Pharm. Sci.* **90**, 436-447.

Poulin, P., and Theil, F. P. (2000). A priori prediction of tissue:plasma partition coefficients of drugs to facilitate the use of physiologically-based pharmacokinetic models in drug discovery. *J. Pharm. Sci.* **89**, 16-35.

Poulin, P., and Theil, F. P. (2002). Prediction of pharmacokinetics prior to in vivo studies. 1. Mechanism-based prediction of volume of distribution. *J. Pharm. Sci.* **91**, 129-156.

Poulin, P., and Theil, F.-P. (2009). Development of a novel method for predicting human volume of distribution at steady-state of basic drugs and comparative assessment with existing methods. J. Pharm. Sci. 98, 4941-4961.

Rodgers, T., Leahy, D., and Rowland, M. (2005). Physiologically based pharmacokinetic modeling 1: predicting the tissue distribution of moderate-to-strong bases. *J. Pharm. Sci.* **94**, 1259-1276.

Rodgers, T., and Rowland, M. (2006). Physiologically based pharmacokinetic modelling 2: predicting the tissue distribution of acids, very weak bases, neutrals and zwitterions. *J. Pharm. Sci.* **95**, 1238-1257.

Rodgers, T., and Rowland, M. (2007). Mechanistic approaches to volume of distribution predictions: understanding the processes. *Pharm Res* **24**, 918-933.

Schmitt, W. (2008). General approach for the calculation of tissue to plasma partition coefficients. *Toxicol In Vitro* **22**, 457-467.

Waddell, W. J. (2010). Commentary on "Toxicity Testing in the 21st Century: A vision and a Strategy". *Human and Experimental Toxicology* **29**, 31-32.

3.8. Tables

Table 1. The capability of the published algorithms in relation to the proposed unified algorithm

Algorithm	Environmental PCs Organics (VOC, contaminants)			Pharmaceutical PCs Drugs			
	Algorithms			Algorithms			
	Tissue:air	Blood:air	Tissue:blood	Tissue:plasma			
				A	B	N	Z
Poulin and Krishnan (1995a,b)			X				
Poulin and Krishnan (1996b)	X						
Poulin and Krishnan (1996a)		X					
Haddad et al. (2000)			X				
Poulin and Theil (2002)				X	X	X	X
Rodgers *et al*. (2005)					X		
Rodgers and Rowland (2006)				X		X	X
Schmitt (2008)				X	X	X	X
Poulin and Theil (2009)					X		
Present study (unified algorithm)	X	X	X	X	X	X	X

A: acid, B: base, N: neutral, Z: zwitterion

Table 2. The fractional content of interstitial and intracellular spaces in rat tissues (Kawai *et al.*, 1994)

Tissue	Fraction of cellular matrix volume	
	Intracellular space	Interstitial space
Adipose	0.864	0.136
Liver	0.816	0.184
Muscle	0.877	0.123

Table 3. Tissue composition of various matrices of rat tissues and blood

(Long, 1961; DiGirolamo and Owens, 1976; Lesser et al., 1980; Aukland and Nicolaysen, 1981; Dory and Roheim, 1981; Poulin and Krishnan, 1995a; Cieslar et al., 1998; Mattacks et al., 2003; Rodgers et al., 2005; Rodgers and Rowland, 2006).

Matrix	Fraction of matrix volume				
	Neutral lipids	Neutral phospholipids	Acidic phospholipids	Water	Proteins
Tissue matrices					
Tissue cells					
Adipose	0.954	0.002	0.0005	0.035	0.008
Liver	0.0427	0.0253	0.0056	0.527	0.192
Muscle	0.0099	0.0094	0.0017	0.636	0.178
Interstitial fluid					
Adipose	0	0	0	0.89	0.010 A; 0.0003 L
Liver	0	0	0	0.89	0.014 A; 0.0005 L
Muscle	0	0	0	0.89	0.015 A; 0.0003 L
Blood matrices					
Erythrocyte	0.0012	0.0034	0.0005	0.63	0.327
Plasma	0.0015	0.0008	0	0.96	0.029 A; 0.0060 L

A: albumin, L: lipoproteins.

Table 4. Chemical-specific input parameters used in the unified algorithm for the computation of tissue:blood PCs (liver, muscle and adipose) of VOCs investigated by Poulin and Krishnan (1995a)

Compound name	P_{ow}[a]	P_{aplw}	P_{prw}[b]		
			P_{prwp}	P_{Hbw}	P_{prwc}
Diethyl ether	4.88	0	0	0	0
Dimethyl ketone	0.32	0	0	0	0
Methyl ethyl ketone	1.20	0	0	0	0
Methyl *n*-propyl ketone	4.47	0	0	0	0
Methyl isobutyl ketone	12.9	0	0	0	0
Methyl *n*-pentyl ketone	41.7	0	0	0	0
Methanol*	0.03	0	0	0	0
Ethanol	0.05	0	0	0	0
n-Propanol	0.16	0	0	0	0
Isopropanol	0.10	0	0	0	0
n-Butanol	0.58	0	0	0	0
Isobutanol	0.42	0	0	0	0
n-Pentanol	1.29	0	0	0	0
Isopentanol	1.2	0	0	0	0
Methyl acetate	0.79	0	0	0	0
Ethyl acetate	2.45	0	0	0	0
n-Propyl acetate	9.55	0	0	0	0
Isopropyl acetate	8.91	0	0	0	0

Table 4. Continued

Compound name	P_{ow} [a]	P_{aplw}	P_{prw} [b]		
			P_{prwp}	P_{Hbw}	P_{prwc}
n-Butyl acetate	49	0	0	0	0
Isobutyl acetate	49	0	0	0	0
n-Pentyl acetate	162	0	0	0	0
Isopentyl acetate	132	0	0	0	0

[a]: All values correspond to oil:water PCs

[b]: P_{prwp}: Plasma and interstitial fluid protein:water PC; P_{Hbw}: hemoglobin:water PC; P_{prwc}: tissue cell binding protein:water PC

*: Compound submitted to the sensitivity analysis

Table 5. Chemical-specific input parameters used in the unified algorithm for the computation of tissue:blood PCs (liver, muscle and adipose) following Poulin and Krishnan, (1996a,b) algorithms

Compound name	P_{ow}[a]	P_{aplw}	P_{prw}[b]		
			P_{prwp}	P_{Hbw}	$P_{prw,c}$
Methyl chloride	9.74	0	0	15.1	0
Dichloromethane	22	0	0	18.3	0
Chloroform	119	0	0	39.2	0
Carbon tetrachloride	1.07×10^3	0	0	77.3	0
Difluoromethane	3.63	0	0	2.96	0
Chlorofluoromethane	7.24	0	0	6.2	0
BromoChloromethane	41.7	0	0	29.9	0
Dibromomethane	66.5	0	0	32.2	0
Chlorodibromomethane	366	0	0	110	0
Chloroethane	35.7	0	0	21.9	0
1,1-Dichloroethane	75.9	0	0	27.7	0
1,2-Dichloroethane	32.1	0	0	13.7	0
1,1,1-Trichloroethane	393	0	0	46.9	0
1,1,2-Trichloroethane	134	0	0	25.2	0
1,1,1,2-Tetrachloroethane	761	0	0	73.3	0
1,1,2,2-Tetrachloroethane	272	0	0	36.3	0
Pentachloroethane	2.88×10^3	0	0	296	0
Hexachloroethane	7.60×10^3	0	0	613	0
1,2-Dibromoethane	73.8	0	0	45.5	0
1-Bromo-2-chloroethane	63.9	0	0	38.2	0
Chlorotrifluoroethane	57.1	0	0	16	0
1,1,1-Trifluoro-2-bromo-2-chloroethane	396	0	0	68.7	0

Table 5. Continued

Compound name	P_{ow} [a]	P_{aplw}	P_{prw} [b]		
			P_{prwp}	P_{Hbw}	$P_{prw,c}$
1-Chloropropane	101	0	0	30.7	0
2-Chloropropane	85.2	0	0	21.5	0
1,2-Dichloropropane	156	0	0	43.6	0
1-Bromopropane	189	0	0	53.4	0
Isopropylbromide	152	0	0	33.8	0
n-Hexane*	5.96×10^3	0	0	584	0
n-Heptane	2.25×10^3	0	0	164	0
Cyclohexane	1.95×10^3	0	0	36.3	0
2,3,4-Trimethyl pentane	2.76×10^5	0	0	7.97×10^3	0
2,2,4-Trimethyl pentane	2.61×10^5	0	0	5.89×10^3	0
Vinyl chloride	56.7	0	0	22.8	0
1,1-Dichloroethylene	184	0	0	101	0
cis-1,2-Dichloroethylene	85.5	0	0	43.5	0
trans-1,2-Dichloroethylene	126	0	0	44	0
Trichloroethylene	666	0	0	187	0
Tetrachloroethylene	2.70×10^3	0	0	138	0
Vinyl bromide	127	0	0	62.6	0
Benzene	169	0	0	40.9	0
Chlorobenzene	779	0	0	145	0
Toluene	603	0	0	63.9	0
Styrene	2.52×10^5	0	0	176	0
m-Methylstyrene	7.47×10^3	0	0	634	0
o-Xylene	1.33×10^3	0	0	103	0
m-Xylene	1.69×10^3	0	0	153	0
p-Xylene	1.88×10^3	0	0	146	0

Table 5. Continued

Compound name	P_{ow} [a]	P_{aplw}	P_{prw} [b]		
			P_{prwp}	P_{Hbw}	$P_{prw,c}$
Allyl chloride	52.9	0	0	57.4	0
Isoprene	42	0	0	61.5	0
1,3-butadiene	605	0	0	373	0
1-nitropropane	8.36	0	0	7.01	0
2-nitropropane	6.51	0	0	7.85	0
Isoflurane	141	0	0	16.1	0

[a]: All values correspond to oil:water PCs

[b]: P_{prwp}: Plasma and interstitial fluid protein:water PC; P_{Hbw}: hemoglobin:water PC; P_{prwc}: tissue cell binding protein:water PC

*: Compound submitted to the sensitivity analysis

Table 6. Chemical-specific input parameters used in the unified algorithm for the computation of muscle:plasma PCs following Poulin and Theil (2000) algorithm

Compound name	pKa^a	$P_{ow}{}^b$	P_{aplw}	$P_{prw}{}^c$			
				P_{prwp}	P_{prwi}	P_{Hbw}	P_{prwc}
Alfentanil	-	123	0	207	2.93×10^3	0	0
Biperiden	-	2.29×10^3	0	257	1.12×10^4	0	0
Cefazolin	-	1.12×10^{-2}	0	198	1.13×10^3	0	0
Ceftazidime	-	8.51×10^{-4}	0	3.59	20.4	0	0
Clobazam	-	69.2	0	36.3	395	0	0
Cotinine	-	0.562	0	1	5.73	0	0
Diazepam	-	1.05×10^3	0	938	3.42×10^4	0	0
Dicloxacillin	-	77.6	0	1.19×10^3	1.36×10^4	0	0
2,3-Dideoxyinosine	-	2.14×10^{-3}	0	0.66	3.75	0	0
Digoxin	-	1.19	0	4.83	28.0	0	0
Ethoxybenzamide	-	0.347	0	3.19	18.3	0	0
Fentanyl	-	1.62×10^4	0	4.73×10^3	2.43×10^5	0	0
Fleroxacin	-	9.12×10^{-2}	0	10.8	61.3	0	0
Flurazepam	-	1.86×10^3	0	140	5.87×10^3	0	0
Glycyrrhetinic acid	-	1.86×10^6	0	2.04×10^6	1.08×10^8	0	0
Glycyrrhizin	-	58.9	0	678	6.90×10^3	0	0
Hexobarbital	-	7.41	0	14	88.4	0	0
n-Hexylbarbital	-	112	0	177	2.40×10^3	0	0
Medazepam	-	8.32×10^4	0	4.84×10^3	2.54×10^5	0	0

Table 6. Continued

Compound name	pKa^a	$P_{ow}{}^b$	P_{aplw}	$P_{prw}{}^c$			
				P_{prwp}	P_{prwi}	P_{Hbw}	P_{prwc}
N-Methylpentobarbital	-	490	0	60.6	1.68×10^3	0	0
Neostigmine	-	0.007	0	32.3	184	0	0
Nicotine	-	9.55	0	1.73	11.2	0	0
n-Nonylbarbital	-	1.70×10^3	0	1.29×10^4	5.31×10^5	0	0
Norfloxacin	-	3.63×10^{-3}	0	23.4	133	0	0
Pefloxacin	-	9.77×10^{-2}	0	8.07	46.0	0	0
Penicillin	-	2.40×10^{-5}	0	183	1.04×10^3	0	0
Pentazocine	-	2.14×10^2	0	50.3	943	0	0
Pentobarbital	-	5.75	0	16.8	104	0	0
Phenobarbital	-	1	0	9.12	52.6	0	0
Phenytoin	-	9.12	0	514	3.31×10^3	0	0
p-Phenylbenzoic acid	-	646	0	2.25×10^3	6.96×10^4	0	0
Pipemidic acid	-	2.14×10^{-4}	0	5.7	32.4	0	0
Prazepam	-	1.29×10^4	0	776	3.95×10^4	0	0
Procainamide	-	5.25	0	2.83	17.4	0	0
Pyridostigmine	-	1.86×10^{-4}	0	32.3	184	0	0
Salicylic acid	-	10	0	49.3	321	0	0
Tetrachlorodibenzo-p-dioxin	-	9.12×10^3	0	559	2.80×10^4	0	0
Tetracycline	-	1.82×10^{-3}	0	32.3	184	0	0
Theophyllin	-	0.447	0	32.3	185	0	0

Table 6. Continued

Compound name	pKa^a	$P_{ow}{}^b$	P_{aplw}	$P_{prw}{}^c$			
				P_{prwp}	P_{prwi}	P_{Hbw}	P_{prwc}
Thiobarbital	-	2.29	0	32.4	191	0	0
Thiopental	-	63.1	0	108	1.13×10^3	0	0
Tolbutamide	-	18.2	0	106	757	0	0

[a]: In reproducing the K_p values of Poulin and Theil (2000), drug ionisation was neglected as done the original study authors (i.e., $I_p = 0$) and similarly the binding of a drug to the acidic phospholipids and proteins of cells was neglected (i.e., P_{apli} and $P_{prwc} = 0$).

[b]: values correspond to the oil:water PCs reported by Poulin and Theil (2000).

[c]: P_{prwp}: Plasma protein:water PC; P_{prwi}: interstitial fluid protein:water PC; P_{Hbw}: hemoglobin:water PC; P_{prwc}: tissue cell binding protein:water PC; P_{prwp} and P_{prwi}, for reproducing PCs reported by Pouin and Theil, were re-calculated with reference to total concentration in water and lipids as follows:

$P_{prwp} = [P_{ow} \cdot (F_{nlp} + 0.3 \cdot F_{nplp}) + (F_{wp} + 0.7 \cdot F_{nplp})] \cdot (1/fu_p - 1) / F_{prp}$

where F_{nlp}: fractional content of neutral lipids in plasma; F_{nplp}: fractional content of phospholipids in plasma; F_{wp}: fractional content of water in plasma; fu_p: unbound fraction in plasma; F_{prp}: fractional content of proteins (i.e. albumin + lipoprotein) in plasma.

$P_{prwi} = \{[Fct \cdot (P_{ow} \cdot F_{nlc} + F_{wc}) + F_{it} \cdot F_{wi}] \cdot (1/fu_i - 1)\} / (F_{pri} \cdot F_{it})$

where F_{ct}: fractional volume of cells in tissue; F_{it}: fractional content of interstitial fluid in tissue; F_{nlc}: fractional content of neutral lipids equivalent in the tissue cell; F_{wc}: fractional content of water equivalent in the tissue cell; F_{wi}: fractional content of water equivalent in the interstitial space; fu_i: unbound fraction in the interstitial space which is equal to $1 / (1+(((1 - fu_p)/fu_p) \cdot 0.5))$ according to Poulin and Theil (2002); and F_{pri}: fractional content of proteins (i.e. albumin + lipoproteins) in the interstitial space.

*: Compound submitted to the sensitivity analysis.

Table 7. Chemical-specific input parameters used in the unified algorithm for the computation of adipose:plasma PCs following Poulin et al. (2001) algorithm[a]

Compound name	*pKa*	P_{ow}	P_{aplw}	P_{prw}[b]			
				P_{prwp}	P_{prwi}	P_{Hbw}	P_{prwc}
Imipramine	-	85.11	0	118	0	0	0
Nicotine	-	0.39	0	6.15	0	0	0
Pentazocine	-	6.73	0	18.4	0	0	0
Pentobarbital	-	4.47	0	139	0	0	0
Phenobarbital	-	0.57	0	37.9	0	0	0
Phenytoin	-	8.00	0	38.4	0	0	0
Procaine	-	0.34	0	0	0	0	0
Roche A (base)	-	2.69	0	130	0	0	0
Roche B (base)	-	0.60	0	13.8	0	0	0
Thiobarbital	-	2.30	0	20.7	0	0	0
Thiopental	-	63.10	0	204	0	0	0

[a]: P_{ow} values correspond to oil:water PCs; see foot note of Table 6.

[b]: P_{prwp}: Plasma protein:water PC; P_{prwi}: interstitial fluid protein:water PC; P_{Hbw}: hemoglobin:water PC; P_{prwc}: tissue cell binding protein:water PC

*: Compound submitted to the sensitivity analysis.

Table 8. Chemical-specific input parameters used in the unified algorithm for the computation of unbound tissue:plasma PCs (liver, muscle and adipose) for strong basic drugs investigated by Rodgers et al. (2005)

Compound name	*pKa*	P_{ow} [a]	P_{aplw}	P_{prw} [b]		
				P_{prwp}	P_{Hbw}	P_{prwc}
Acebutolol-R	9.7	5.50 (74.1)	747	0	0	0
Acebutolol-S	9.7	5.50 (74.1)	590	0	0	0
Betaxolol-R	9.4	34.7 (389)	7.17×10^3	0	0	0
Betaxolol-S	9.4	34.7 (389)	6.19×10^3	0	0	0
Biperiden	8.8	2.45×10^3 (1.78×10^4)	8.16×10^3	0	0	0
Bisoprolol-R	9.4	5.50 (74.1)	1.55×10^3	0	0	0
Bisoprolol-S	9.4	5.50 (74.1)	1.55×10^3	0	0	0
Carvedilol-R	8.1	2.09×10^3 (1.55×10^4)	3.79×10^4	0	0	0
Carvedilol-S	8.1	2.09×10^3 (1.55×10^4)	3.34×10^4	0	0	0
Fentanyl	9	1.48×10^3 (1.12×10^4)	4.72×10^3	0	0	0
Imipramine	9.5	1.00×10^4 (6.31×10^4)	1.11×10^4	0	0	0
Inaperisone	9.1	617 (5.25×10^3)	1.50×10^4	0	0	0
Lidocaine	8	23.4 (275)	5.29×10^3	0	0	0
Metoprolol-R	9.7	11.2 (141)	2.31×10^3	0	0	0
Metoprolol-S	9.7	11.2 (141)	2.23×10^3	0	0	0
Nicotine	7.8; 3	0.891 (14.8)	0	0	0	0
Oxprenolol-R	9.5	12 (151)	1.19×10^3	0	0	0
Oxprenolol-S	9.5	12 (151)	781	0	0	0
Pentazocine	8.5	219 (2.04×10^3)	5.09×10^3	0	0	0
Phencyclidine*	9.4	1.26×10^4 (9.12×10^4)	0	0	0	0
Pindolol-R	8.8	3.98 (56.2)	2.77×10^3	0	0	0
Pindolol-S	8.8	3.98 (56.2)	2.43×10^3	0	0	0

Table 8. Continued

Compound name	*pKa*	P_{ow} [a]	P_{aplw}	P_{prw} [b]		
				P_{prwp}	P_{Hbw}	P_{prwc}
Procainamide	9.2	0.427 (7.59)	181	0	0	0
Propranolol-R	9.5	525 (4.47×10^3)	3.69×10^4	0	0	0
Propranolol-S	9.5	525 (4.47×10^3)	1.55×10^4	0	0	0
Quinidine	10; 5.4	309 (2.75×10^3)	6.26×10^3	0	0	0
Timolol-S	9.2; 8.8	6.03 (81.3)	452	0	0	0
Verapamil	8.5	759 (6.17×10^3)	1.63×10^4	0	0	0

[a]: Values in brackets correspond to *n*-octanol:water PC values used for the prediction of non-adipose PC for drugs, whereas all other values correspond to oil:water PC used for the prediction of adipose tissue for drugs

[b]: P_{prwp}: Plasma and interstitial fluid protein:water PC; P_{Hbw}: hemoglobin:water PC; P_{prwc}: tissue cell binding protein:water PC;

*: Compound submitted to the sensitivity analysis

Table 9. Chemical-specific input parameters used in the unified algorithm for the computation of unbound tissue:plasma PCs (liver, muscle and adipose) for neutrals, acids, weak bases and zwitterions following Rodgers and Rowland (2006) algorithm

Compound name	*pKa*	P_{ow}[a]	P_{aplw}	P_{prw}[b]		
				P_{prwp}	P_{Hbw}	P_{prwc}
Alfentanil	6.5	12.7 (158)	0	269	0	0
Alprazolam	2.4	16.4 (200)	0	51.9	0	0
Chlordiazepoxide	4.7	21.2 (251)	0	180	0	0
Diazepam	3.4	59.2 (631)	0	173	0	0
Flunitrazepam	1.8	9.81 (126)	0	95.5	0	0
Midazolam	6	128 (1.26 x 10^3)	0	476	0	0
Triazolam	2	21.2 (251)	0	73.4	0	0
5-*n*-Methyl-5-ethyl barbituric acid	8.1	5.08E-02 (1.12)	0	0	0	0
5-*n*-Ethyl-5-ethyl barbituric acid	7.9	0.269 (5.01)	0	1.58	0	0
5-*n*-Propyl-5-ethyl barbituric acid	7.8	0.348 (6.31)	0	4.86	0	0
5-*n*-Butyl-5-ethyl barbituric acid	7.8	3.51 (50.1)	0	19.8	0	0
5-*n*-Pentyl-5-ethyl barbituric acid	8	12.7 (158)	0	26.8	0	0
5-*n*-Hexyl-5-ethyl barbituric acid	7.7	59.2 (631)	0	121	0	0
5-*n*-Heptyl-5-ethyl barbituric acid	7.8	214 (2.00 x 10^3)	0	401	0	0

Table 9. Continued

Compound name	*pKa*	P_{ow} [a]	P_{aplw}	P_{prw} [b]		
				P_{prwp}	P_{Hbw}	P_{prwc}
5-*n*-Octyl-5-ethyl barbituric acid	7.8	771 (6.31×10^3)	0	1.02×10^3	0	0
5-*n*-Nonyl-5-ethyl barbituric acid	7.8	1.67E+03 (1.26×10^4)	0	3.12×10^3	0	0
Cefazolin	2.3	9.65×10^{-2} (2.00)	0	180	0	0
Dideoxyinosine	9.1	2.05×10^{-3} (6.31×10^{-2})	0	1.06	0	0
Etodolac-R	4.7	461 (3.98×10^3)	0	7.42×10^3	0	0
Etodolac-S	4.7	461 (3.98×10^3)	0	1.98×10^3	0	0
Penicillin	2.7	2.72 (39.8)	0	194	0	0
Phenobarbital	7.4	2.72 (39.8)	0	18.1	0	0
Phenytoin	8.3	27.4 (316)	0	130	0	0
Salicyclic acid	3	12.7 (158)	0	211	0	0
Tenoxicam*	5.3	5.87 (79.4)	0	1.98×10^3	0	0
Thiopental	7.5	76.5 (794)	0	203	0	0
Tolbutamide	5.3	21.2 (251)	0	92.6	0	0
Valproate	4.6	59.2 (631)	0	58.3	0	0
Cyclosporine*	-	76.5 (794)	0	1.60×10^4	0	0
Digoxin	-	0.973 (15.8)	0	1.01×10^3	0	0
Ethoxybenzamide	-	0.348 (6.31)	0	1.13×10^3	0	0
Ftorafur	-	2.07×10^{-2} (0.501)	0	465	0	0
Enoxacin	8.7; 6.1	5.77×10^{-2} (1.26)	1.18×10^3	0	0	0
Lomefloxacin	9.3; 5.8	2.07×10^{-2} (0.501)	803	0	0	0
Ofloxacin	8.2; 6.1	1.60×10^{-2} (0.398)	1.24×10^3	0	0	0

Table 9. Continued

Compound name	*pKa*	P_{ow} [a]	P_{aplw}	P_{prw} [b]		
				P_{prwp}	P_{Hbw}	P_{prwc}
Pefloxacin	7.6; 6.3	0.973 (15.8)	1.68 x 10^3	0	0	0
Pipemidic acid	7.0; 3.5; 4.9	1.57 x 10^{-4} (6.31 x 10^{-3})	2.06 x 10^3	0	0	0
Tetracycline	9.7; 7.7; 3.3	4.82 x 10^{-2} (1.07)	1.39 x 10^3	0	0	0
Ceftazidime	3.8; 2.5; 1.9	1.24 x 10^{-2} (0.316)	0	3.81	0	0
Nalidixic acid	3.3; 5.1	0.752 (12.6)	0	84.0	0	0

[a]: Values in brackets correspond to *n*-octanol:water PCs used for the prediction of non-adipose PC for drugs, whereas all other values correspond to oil:water PC used for the prediction of adipose tissue for drugs

[b]: P_{prwp}: Plasma and interstitial fluid protein:water PC; P_{Hbw}: hemoglobin:water PC; P_{prwc}: tissue cell binding protein:water PC;

*: Compound submitted to the sensitivity analysis

Table 10. Top three sensitive parameters of the unified algorithm used for predicting tissue:blood PCs, as well as the corresponding sensitivity ratios (SRs)

Compound	Tissue:blood PCs	
	Muscle	**Fat**
n-Hexane	F_{cm} (1) F_{pre} and P_{Hbw} (-0.94) P_{ow} (0.87)	F_{cf} and F_{nlfc} (1) F_{pre} and P_{Hbw} (-0.94) P_{ow} (0.88)
Methanol	F_{cm} (0.82) F_{wmc} (0.81) F_{wp} (-0.75)	F_{wp} (-0.75) F_{wi} and F_{if} (0.7) F_{we} (-0.31)
Cyclosporine	F_{cm} (0.99) F_{nlmc} (0.72) P_{ow} (0.34)	F_{cf} and F_{nlfc} (1) P_{ow} (0.41) F_{nlp} (-0.29)
Tenoxicam	pH_p and pH_i (-1.99) F_{prp} and P_{prwp} (-1.09) F_{im} (0.95)	pH_P and pH_i (-6.12) F_{prp} and P_{prwp} (-1.09) pKa (1.03)
Phencyclidine	pH_{mc} (-34.2) pH_p and pH_i (5.68) F_{cm} (0.99)	pKa (-31.46) pH_p and pH_i (5.88) F_{nlfc} (0.98)

c: cell; *e*: erythrocyte; *p*: plasma; *mc*: muscle cell; *fc*: fat cell

[a]: The numbers in brackets correspond to SR. Values of SR are classified in decreasing order. Negative values indicate a decrease of the PC values whereas positive values indicate an increase of the PC values following the sensitivity analysis.

3.9. Figures

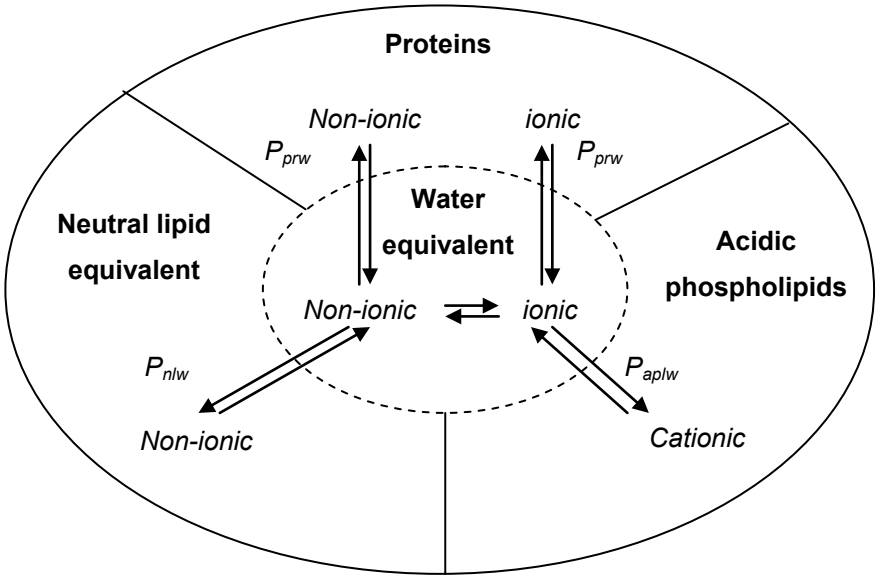

Figure 1. Conceptual representation of the distribution of an organic compound in a biological matrix.

***P_{aplw}*: acidic phospholipids:water PC; *P_{nlw}*: neutral lipids:water PC; *P_{prw}*: protein:water PC.**

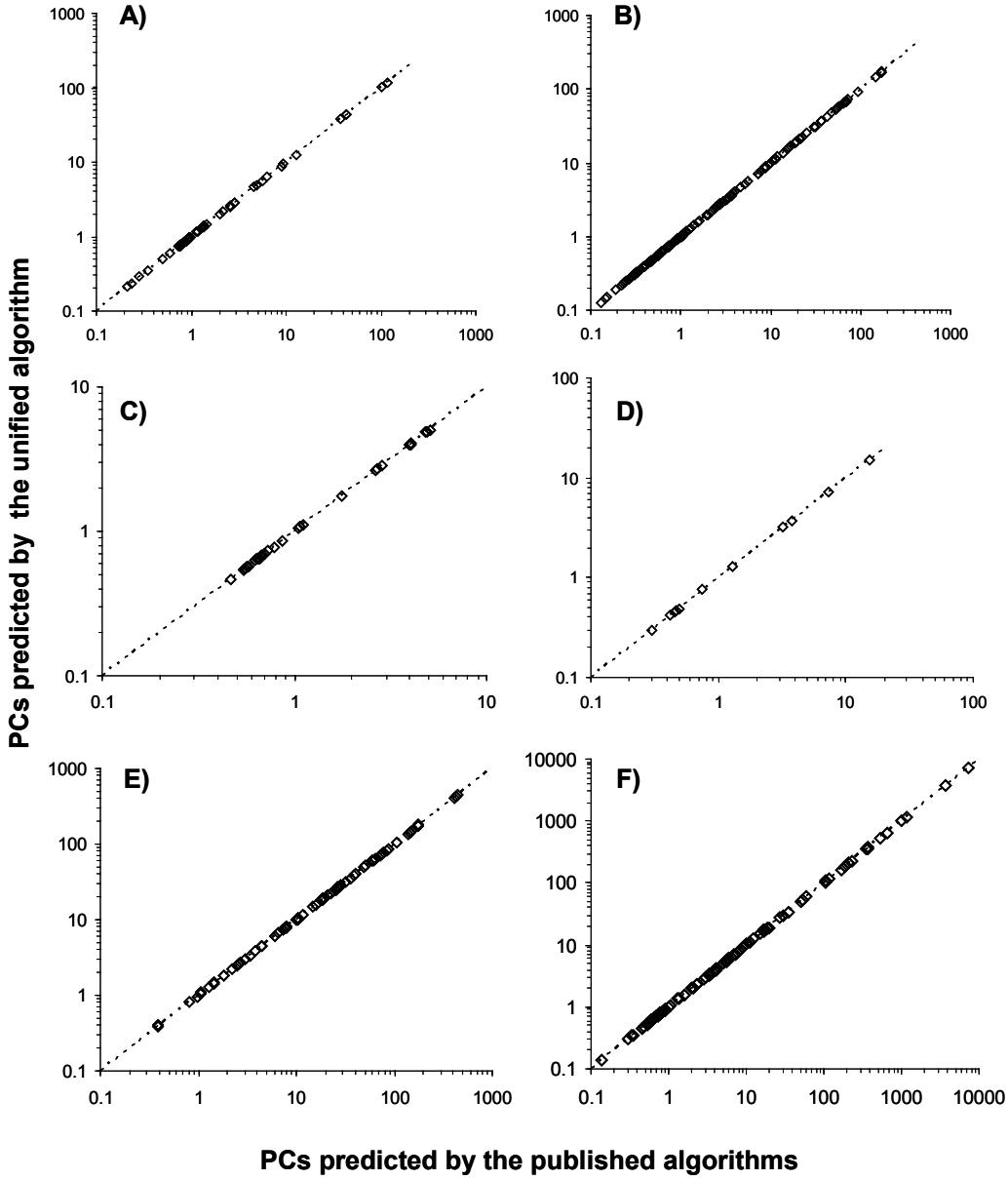

Figure 2. Comparison between the predicted values of the unified algorithm (present study; Equation 1) and the published algorithms for P_{tb}, K_p and K_{pu}.

(A: Poulin and Krishnan (1995a); B: Poulin and Krishnan (1996a 1996b); C: Poulin and Theil (2000); D: Poulin et al. (2001) E: Rodgers et al. (2005); F: Rodgers and Rowland (2006)).

Chapitre 4. Quantitative property-property relationship for screening-level prediction of intrinsic clearance of volatile organic chemicals in rats and its integration within PBPK models to predict inhalation pharmacokinetics in humans

Peyret, T. and Krishnan, K. 2012. Quantitative property-property relationship for screening-level prediction of intrinsic clearance of volatile organic chemicals in rats and its integration within PBPK models to predict inhalation pharmacokinetics in humans. J Toxicol. 22p. doi:10.1155/2012/286079.

Peyret, T. and Krishnan, K

Département de santé environnementale et santé au travail,
Université de Montréal, Montréal, Canada

(Received 31 October 2011; Revised 13 January 2012; Accepted 13 January 2012)

4.1. Abstract

The objectives of this study were (i) to develop a screening-level Quantitative property-property relationship (QPPR) for intrinsic clearance (CL_{int}) obtained from *in vivo* animal studies and (ii) to incorporate it with human physiology in a PBPK model for predicting the inhalation pharmacokinetics of VOCs. CL_{int}, calculated as the ratio of the *in vivo* V_{max} (μmol/h/kg bw rat) to the K_m (μM), was obtained for 26 VOCs from the literature. The QPPR model resulting from stepwise linear regression analysis passed the validation step (R^2 = 0.8; leave-one-out cross-validation Q^2 = 0.75) for CL_{int} normalized to the phospholipid (PL) affinity of the VOCs. The QPPR facilitated the calculation of CL_{int} (L PL/h/kg bw rat) from the input data on log P_{ow}, log blood: water PC and ionization potential. The predictions of the QPPR as lower and upper bounds of the 95% mean confidence intervals (LMCI and UMCI, resp.) were then integrated within a human PBPK model. The ratio of the maximum (using LMCI for CL_{int}) to minimum (using UMCI for CL_{int}) AUC predicted by the QPPR-PBPK model was 1.36 ± 0.4 and ranged from 1.06 (1,1-dichloroethylene) to 2.8 (isoprene). Overall, the integrated QPPR-PBPK modeling method developed in this study is a pragmatic way of characterizing the impact of the lack of knowledge of CL_{int} in predicting human pharmacokinetics of VOCs, as well as the impact of prediction uncertainty of CL_{int} on human pharmacokinetics of VOCs.

4.2. Introduction

The evolving scientific and regulatory activities in Europe and North America emphasize the need for the development of tools that refine, replace, or reduce the use of animals and human volunteers in pharmacokinetic and toxicity tests [1–3]. The ability to base the toxic responses on the target tissue dose or internal concentration of the toxic moiety of the chemicals is key to the predictive tools reflective of the current state of science. Therefore, physiologically based pharmacokinetic (PBPK) models that are capable of providing *a*

priori prediction of the time course of chemicals in blood and tissues is of tremendous interest [4]. PBPK models are mechanistically based mathematical descriptions of the absorption, distribution, metabolism, and excretion of chemicals or pharmaceutical compounds. In PBPK models, the organism is represented as a set of several tissue compartments interconnected by blood flows. In these models, the internal dose measures (e.g., blood or tissue concentrations, amount metabolized) of a chemical are described on the basis of mass-balance differential equations requiring species-specific properties (e.g., alveolar ventilation rate, cardiac output, regional blood flows, and tissue volumes) and chemical-specific input parameters (e.g., partition coefficients and metabolic constants). Although the species-specific values of several physiological parameters are available in the literature [4–6], the partition coefficients (PCs) and metabolic constants need to be determined experimentally or calculated by using animal-replacement methods for each chemical individually [7]. The values of tissue : blood or tissue : plasma partition coefficients essential for developing PBPK models have been estimated for a wide range of chemicals and chemical classes, including drugs, with the use of tissue composition-based algorithms or QSAR methods (e.g., [8–19]).

Regarding the metabolism parameters (i.e., hepatic clearance, intrinsic clearance, V_{max}, K_m, K_{cat}, free energy of binding, energy of activation, or activation enthalpy), some studies have developed 2-D and 3-D QSARs but with a specific focus on either a single isozyme, a single reaction or a single class of substances [8, 20–38]. None of these past efforts succeeded in predicting both V_{max} and K_m (or CL_{int}) of environmental chemicals for direct incorporation within animal or human PBPK models. Alternatively, few studies utilized the group contribution method of Gao [39–43], to predict metabolic rates for PBPK models. In this method, the chemical is decomposed into different structural fragments or groups, the contributions of which are obtained by regression analysis [39]. Accordingly, these publications demonstrated the feasibility of developing structure-property relationships for the metabolism rates. The group contribution method was successfully used to develop quantitative structure-property relationships (QSPRs) for the tissue : air partition coefficients as well as intrinsic (CL_{int}) and hepatic clearance (CL_h) for a group of low-

molecular-weight volatile organic chemicals (VOCs) in rats [41, 42]. These QSPR models, in turn, were incorporated within PBPK models to predict reasonably well the blood kinetics of inhaled VOCs in rats. As these QSPRs are species specific, they could not be used to conduct interspecies extrapolations. To overcome this limitation, Béliveau et al. [40] developed biologically based algorithms for PCs and CL_h to conduct rat to human extrapolations of the inhalation toxicokinetics of VOCs. In this study, QSPRs based on the group contribution method were developed for the chemical-specific input parameters of the biological algorithms for PCs (i.e., oil : air, water : air, and blood protein : air) and CL_{int} (intrinsic clearance normalized for cytochrome P450 2E1 content). More recently, QSPRs were developed for the metabolic constants Vmax (maximum velocity of reaction) and K_m (Michaelis constant) [43] and were further incorporated within a rat PBPK model to predict the toxicokinetics of mixtures of VOCs. Despite the successful use of the group contribution method in QSPR modeling of metabolism rates, their principal limitation relates to the fact that the chemical space they cover is extremely limited (low-molecular-weight VOCs containing one or more of the following fragments: CH_3, CH_2 , CH, C, C=C, H, Br, Cl, F, benzene ring, and H on benzene ring). More experimental data on diverse chemicals would be needed to determine the contributions of other molecular fragments, as has been done with P_{ow} (e.g., estimation of the contribution of 130 fragments (i.e., groups) required 1200 measurements of P_{ow}) [44]. To extend the currently available QSPR for CL_{int} to cover more diverse fragments and at the same time respect a reasonable ratio of the number of parameters to the number of observations, extensive experimental data would be required.

Since the critical limitation in the construction of PBPK models for new substances continues to be the metabolism rate, a pragmatic approach —particularly for inhaled VOCs— is to evaluate the maximum and minimum possible blood concentration profiles in exposed individuals. Thus, using a hepatic extraction ratio (E) of 0 and 1 in the PBPK models, Poulin and Krishnan [45] obtained simulations of the physiological limits (i.e., maximal and minimal blood concentration profiles) for inhaled VOCs in humans. Assuming the conceptual PBPK model and the values of its physiological parameters are

reliable, the real answer, that is, the actual concentrations and kinetic curve, would be somewhere in between the theoretical limits simulated with these PBPK models [45]. The uncertainty associated with these theoretical bounds can be reduced by developing better estimates of the metabolism constants. This could be done, at a practical level, by developing *in silico* tools that provide a range of plausible values, in lieu of a single accurate point estimate. Such a tool might be of use for the toxicokinetic screening of substances, until the time when the chemical-specific measurements are obtained *in vivo*, *in vitro,* or with a highly precise mechanistic *in silico* method.

Since human exposures to environmental contaminants in most cases do not attain levels that approach or exceed saturation, it is not crucial to predict V_{max} and K_m separately, particularly for simulating kinetics in humans exposed to low atmospheric concentrations of VOCs. Therefore, the availability of *in silico* approaches based on easily available parameters to predict plausible range of CL_{int} would be desirable as a screening-level tool. The objective of this study was therefore to develop a quantitative property-property relationship (QPPR) model of animal data to generate initial estimates (or bounds) of intrinsic clearance of VOCs, for eventual incorporation within a human PBPK model to simulate blood concentration profiles associated with inhalation exposures. In this regard, we focused on evaluating the impact of the uncertainty associated with QPPR predictions of CL_{int} on the blood kinetics of VOCs in humans, relative to that of the uncertainty associated with the total lack of knowledge of the metabolic rate in humans.

Furthermore, the reliability of applying the QPPR to predict the area under the blood concentration versus time curve (AUC) of parent chemicals was evaluated, as a function of the sensitivity of the metabolism parameter in the PBPK model and the prediction uncertainty of QPPR model.

4.3. Methods

A QPPR model for CL_{int} was developed using a calibration set of 26 VOCs. The QPPR predictions were then compared with experimental data for several VOCs and the pharmacokinetics in humans were simulated using integrated QPPR-PBPK models for these 26 VOCs. The predictions of QPPR were evaluated further with an external data set of CL_{int} for 11 VOCs.

4.3.1 QPPR Modeling for Intrinsic Clearance

Chemicals and Data Sources.

The development of a global QPPR model for metabolism was initially undertaken using experimental data on the *in vivo* intrinsic clearance of 26 VOCs in rats, collated and evaluated in previous studies by Béliveau et al. [40, 41] (1,1,1,2-tetrachloroethane; 1,1,2,2-tetrachloroethane; 1,1,2-trichloroethane; 1,1-dichloroethane; 1,1-dichloroethylene; 1,2-dichloroethane; benzene; bromochloromethane; bromodichloromethane; carbon tetrachloride; chloroethane; chloroform; *cis*-1,2-dichloroethylene; dibromomethane; dichloromethane; ethylbenzene; hexachloroethane; isoprene; methyl chloride; *m*-xylene; *n*-hexane; pentachloroethane; styrene; toluene; trichloroethylene; vinyl chloride) [24, 46–53].

Subsequently, the resulting QPPR model was evaluated with experimental *in vivo* data on CL_{int} for 11 additional VOCs in rats (1,1,1-trichloroethane; 1,2,4-trimethylbenzene; bromoform; dibromochloromethane; furan; halothane; *o*-xylene; *trans*-1,2-dichloroethylene; tetrachloroethylene; propylene; ethylene) [46, 48, 54–61]. These 11 chemicals outside the calibration set were also lipophilic, low molecular-weight VOCs and likely substrates of cytochrome P450 2E1 [32, 62]. Moreover except for halothane and 1,2,4-trimethylbenzene, the chemicals of the evaluation dataset possess values of P_{ow}, ionization potential, and blood : water PC within the range of values for the chemicals in the QPPR calibration set.

Modeling Endpoint.

For QPPR modeling, CL_{int} (expressed in units of L blood, $CL_{intblood}$, or L phospholipids, CL_{intPL}) was used as the endpoint. Initially, $CL_{intblood}$ (L blood/h/kg$^{0.75}$) for all the studied chemicals was computed as allometrically scaled *V*max (μmol/h/kg$^{0.75}$)/*Km* (μmol/L blood). Since CYPs are located in the endoplasmic reticulum embedded in the phospholipidic bilayer [63], the CL_{intPL} values reflecting chemical affinity for the phospholipids (PL) were subsequently computed. The values of CL_{intPL} (L phospholipid/h/kg$^{0.75}$) were obtained by dividing V_{max} (μmol/h/kg$^{0.75}$) with *Km* expressed as μmol/L PL. The K_m values in μM of PL were obtained by multiplying the values of K_m expressed as μmol/L blood with the chemical-specific phospholipid : blood partition coefficients (P_{plb}) calculated as follows:

$$P_{plb} = \frac{0.3 \cdot P_{oa} + 0.7 \cdot P_{wa}}{P_{ba}} \quad (1)$$

where P_{oa} is the *n*-octanol : air PC, P_{wa} the water : air PC, and P_{ba} the blood : air PC.

The above equation computes *P*plb as the ratio of phospholipid : air to blood : air PCs of the VOCs, based on Poulin and Krishnan [10, 12].

Input Parameters for Transforming the Endpoint.

The input parameters required for converting the CL_{int} obtained from the literature were P_{oa}, P_{wa}, and P_{ba}.

(1) P_{oa} *and* P_{wa}. The *n*-octanol : air PC (P_{oa}), was calculated as the product of the *n*-octanol :water PC (P_{ow}) and P_{wa} (inverse of Henry's law constant at 37.5◦C). The values of P_{ow} and

*P*wa were predicted using U.S. EPA's freeware EPISUITE (http://www.epa.gov/opptintr/exposure/pubs/episuite.htm).

(2) $P_{ba.}$. Experimental values were used for rat blood : air [54, 56, 59, 64–68]. The calculated values of P_{plb} for the chemicals used for the development and for the evaluation of the QPPR are reported in Table 1.

Variable Selection

A priori list of variables was developed on the basis on mechanistic considerations. The rate and affinity for P450-mediated metabolism would appear to be related to the size, shape, charge, and energy of the substrate; therefore variables that reflect these properties were chosen for the QPPR analysis [21, 23, 27, 28, 32, 69–71]. The descriptors of the size and shape of the molecule were the molecular length, width, depth, volume, surface, and the Kappa 2 index [72], as well as two descriptors used in the work of Lewis et al. [23], namely, the ratio of the molecular length to the molecular width (L/W) and the ratio of the area of the molecule (i.e., length times width) to the square of the depth (a/d^2). The dipole moment and ionization potential (IP) were used as measure of the charge disposition and the energy in the molecule, respectively. The values of all the previously cited descriptors were calculated using commercially available software (Molecular Modeling Pro, Chem SW, Fairfield, CA). Before calculating the molecular descriptors with Molecular Modeling Pro®, the 3D molecules were drawn and minimized using the full MM2 (molecular mechanics program) method provided in the software. The dipole moment and the ionization potential were calculated using MOPAC/PM3 program, included in Molecular Modeling Pro®.

Hydrophobic descriptors such as log P_{ow} (log of the *n*-octanol : water PC) that reflect hydrogen bonding and π-π stacking have already been correlated to the values of metabolic constants [69–71]. In this study, the following physicochemical parameters were chosen to

describe the relative solubility and partitioning into diverse biological media: log P_{ow}, log phospholipid :water PC (log P_{plw}); log blood : water PC (log P_{bw}), and log water : air PC (log P_{wa}). The blood : water and phospholipid :water PCs were obtained by dividing the blood : air and phospholipid : air PCs values by the water : air PC values. The values of P_{ow}, P_{wa}, blood : air, and phospholipid : air PCs were obtained as described for the calculation of P_{plb} (1).

Statistical Analysis

Multilinear regression analysis approach was chosen for the QPPR analysis of CL_{int} because linear regression models are simple, transparent, and easy to reproduce [73]. The regression analysis was performed using SPSS v16 for Windows (SPSS Inc., Chicago, IL). Stepwise regression analysis was performed to select the QPPRs based on the most statistically significant independent variable(s) from an *a priori* list (see Section "Variable Selection"). The coefficient of determination R^2, the adjusted R^2 (R^2_{adj}; adjusted for number of variables) [73], the standard error of the estimate *s*, and the value and significance of the *F* statistic were calculated. The normality of the residuals was checked visually on normal probability plots of the standardized residuals (i.e., expected normal cumulative probability versus observed cumulative probability). Leave-one-out cross-validation was conducted and the results were expressed in terms of Q^2, a measure of precision error of the model. The Q^2 was computed as follows [74]:

$$Q^2 = 1 - \frac{PRESS}{SSY} \qquad (2)$$

where PRESS is that predicted residual sum of squares and SSY the sum of squares of the response values. The statistical significance ($p < 0.05$) of the regression coefficients was estimated by a *t* statistic test. Multicollinearity refers to the occurrence of correlation between two independent variables in the multiple linear regression model.

Multicollinearity of the variables in the model was assessed by calculating the variance inflation factor (VIF) for all independent variables [75]. The value of VIF was calculated as follows [75]:

$$VIF_i = \frac{1}{1 - R^2{}_i} \quad (3)$$

where VIFi is the variance inflation factor of the independent variable i in the multilinear regression model and $R^2{}_i$ the coefficient of determination of the regression between the independent variable i and the other independent variables in the multilinear regression model.

For each model, the application domain was documented by reporting the ranges of values of the descriptors, the modeled response, and the endpoint. A QPPR model was considered adequate when: the values of R^2 and $R^2{}_{adj}$ were ≥0.6 [73], the value of Q^2 was ≥0.6 [76], and the independent variables were not highly correlated (i.e., VIF < 4) [75].

The predictions of the QPPR model were obtained in terms of lower and upper bounds of the 95% mean confidence intervals (LMCI and UMCI, resp.) in order to represent the uncertainty associated with the mean predicted value. The LMCI and UMCI for the 11 VOCs, not in the QSPR calibration dataset, were obtained by adding them in the SPSS file containing the data used for the QPPR, along with the values of their independent variables only.

Translation of QPPR Predicted Intrinsic Clearance Values to In Vivo Metabolism Rate and Integration within Human PBPK Models.

In the PBPK model, the value of intrinsic clearance was calculated as the product of the QPPR value of CL_{intPL} (L of PL/h/kg$^{0.75}$) and the phospholipid : blood PC (values of P_{plb} in Table 1). The intrinsic clearance (L blood/h/kg$^{0.75}$) was used within the human PBPK

models to compute the hepatic clearance. The rate of metabolism was calculated on the basis of hepatic clearance (i.e., hepatic clearance times the arterial concentration) [4, 40, 41, 45]. For chloroethane, dichloromethane, vinyl chloride, and dibromomethane a first-order constant (1, 2, 1, and 0.7 h−1, resp.) was included in the calculation of the hepatic clearance, CL_h (L/h) [41]:

$$CL_h = Q_L \cdot E \tag{4}$$

where $E = (CL_{int} + K_f \cdot V_L)/((CL_{int} + K_f \cdot V_L) + Q_L)$, Q_L is the blood flow through the liver (L/h), CL_{int} the intrinsic clearance (L blood/h), K_f the first order metabolic constant (h^{-1}), and V_L the liver volume (L).

4.3.2 PBPK Modeling

The QPPR values of CL_{int} were included in a human PBPK model for inhaled VOCs [50]. Briefly, the PBPK model consisted in four tissue compartments (i.e., liver, fat, richly, and poorly perfused tissues) and a gas exchange lung, which were interconnected by blood flows. The distribution of VOCs into tissue compartments was described as perfusion limited, and the metabolism was limited to liver. To evaluate the impact of uncertainty on the metabolic rate, for all the chemicals, PBPK simulations were also conducted by setting the value of E to 0.999 (Emax) and then to 0.001 (Emin), respectively.

The human physiological parameters of the PBPK model (i.e., body weight = 70 kg; cardiac output = 18 L/h/$kg^{0.74}$; alveolar ventilation = 18 L/h/$kg^{0.74}$; tissue compartment volumes, fraction of body weight: liver = 0.026; richly perfused tissues = 0.05; poorly perfused tissues = 0.62; fat = 0.19; perfusion of the tissue compartments, fraction of cardiac output: liver = 0.26; richly perfused tissues = 0.44; poorly perfused tissues = 0.25; fat = 0.05) were obtained from Tardif et al. [67]. Table 1 presents the value of the partition

coefficients used in the PBPK model (i.e., blood : air, tissue : blood, and phospholipid : blood PCs). The phospholipid : blood PC was calculated using (1), whereas the blood : air PC and tissue : blood PCs were gathered from the literature [48, 50, 52, 54, 56–59, 61, 66, 67, 77–80].

The PBPK model (differential and algebraic mass-balance equations, physiological parameters, QSPR equations for metabolic constants, and PCs) was written in ACSL (acslX, version 2.5, Aegis Technologies Group, Inc, Huntsville, AL). The model code is included in the supplementary data available online at doi: 10.1155/2012/286079. To compare the impact of different (uncertain) scenarios of rate of metabolism on the pharmacokinetics in human, simulations were carried out by setting (i) the value of CL_{int} equal to the lower and upper bound of the QPPR predicted mean 95% confidence interval, or (ii) the liver extraction ratio to 0.001 (no metabolism) and 0.999 (maximum extraction). The 24 h venous blood kinetics corresponding to the four scenarios of metabolism were simulated for an 8 h exposure to 1 ppm of each VOC. The 24 h area under the curve (AUC_{24}) of the venous blood kinetics was also calculated to compare the four scenarios of metabolism simulated with PBPK models. Additionally, the venous blood kinetics of *m*-xylene, toluene, ethylbenzene, dichloromethane, styrene, 1,2,4-trimethylbenzene, and 1,1,1-trichloroethane were compared to experimental data [61, 67, 81–83].

4.3.3 Analysis of Applicability of the CL_{int} QPPR to PBPK Modeling

The applicability of the QPPR model was evaluated on the basis of the level of uncertainty in the QPPR estimate and the impact (sensitivity) of metabolism on the AUC_{24}. Figure 1 illustrates the role of uncertainty and sensitivity in the reliability of the QPPR-PBPK modeling framework, based on reference [84]. The sensitivity of the metabolism to the AUC was estimated by the ratio of the AUC_{24} obtained with no metabolism (E_{min}) to that obtained with the maximum theoretical metabolism (E_{max}).

The sensitivity of AUC_{24} to metabolism was considered to be low, medium, or high if the ratio (AUC_{Emin}/AUC_{Emax}) was within a factor of 2, within an order of magnitude, or greater. The uncertainty in the QPPR prediction was evaluated by comparing it to the experimental data. The prediction uncertainty was considered to be low, medium or high if the prediction was within a factor of two, within an order of magnitude and above 10-fold of the experimental data, respectively.

This approach was applied to evaluate the reliability of applying the QPPR within the PBPK model for two situations: (i) for the calibration set of chemicals, for which the uncertainty of the QPPR was evaluated by comparing the predictions of CL_{intPL} with the experimentally derived CL_{intPL} values and (ii) for chemicals in the evaluation dataset, for which the uncertainty in the QPPR prediction was considered to be "high", to replicate the "data poor" situations with new or tested chemicals with unknown experimental CL_{int} values.

4.4. Results

4.4.1 QPPR Development

The initial effort to develop a QPPR model for metabolism rate (expressed as $CL_{intblood}$, in units of L blood/hr), based on a stepwise analysis of its relationship to various molecular descriptors and physicochemical properties, was not successful (not shown). Same analysis, repeated for CL_{int} expressed in units of L PL/h (CL_{intPL}), yielded a QPPR that consisted of log P_{plw}, logP_{bw}, and IP (ionization potential, eV) as input parameters. This model satisfied the criteria for an acceptable model in terms of coefficient of determination (R^2 = 0.802; R^2_{adj} = 0.775), leave-one-out cross validation (Q^2 = 0.755), and multicollinearity (VIFs: log P_{plw} = 2.42; log P_{bw} = 2.38; IP = 1.04). The values of the regression coefficients were significant (P value < 0.001 for the constant, log P_{plw} and log P_{bw}, and 0.007 for IP).

However, as the value of log P_{ow} can be obtained more readily than log P_{plw}, the regression analysis was repeated by using log P_{ow}, logP_{bw}, and calculated IP, and it yielded the following QPPR:

$$\log CL_{intPL} = 5.63\,(\pm 1.187) - 1.287\,(\pm 0.149)\cdot \log P_{ow} + 1.08\,(\pm 0.233)\cdot \log P_{bw} - 0.328\,(\pm 0.111)\cdot IP \quad (5)$$

This QPPR model satisfied the criteria for an acceptable model in terms of coefficient of determination (R^2 = 0.796; R^2_{adj} = 0.768), leave-one-out cross validation (Q^2 = 0.748), and multicollinearity (VIFs: log P_{ow} = 2.42; log P_{bw} = 2.38; IP = 1.04). The application domain of the model can be described with [min; max] as follows: log P_{ow} = [1.09; 4.03]; log P_{bw} [0.16; 2.49]; calculated ionization potential [9.13;11.28].

The QPPR (5) was subsequently applied to calculate the CL_{intPL} of the VOCs in the calibration set. Table 2 presents the values of the input parameters, along with the experimental data for the 26 VOCs used in QPPR development. Figure 2 illustrates the comparison of the predicted values of CL_{intPL} (LMCI and UMCI) and the experimental data. The uncertainty in the predicted log CL_{intPL} can be characterized by the difference between the UMCI and the LMCI; this value ranged from 0.37 (1,1-dichloroethane) to 1.23 (*n*-hexane) with a mean of 0.54 and a standard deviation of 0.18. The nearest confidence bounds of the predicted log CL_{intPL} were higher than 5-fold of the experimental value (exp.) for three substances (*cis*-1,2-dichloroethylene, LMCI = 0.55 versus exp . = 0.09; styrene, LMCI = −0.45 versus exp . = −0.09; and 1,1,2-trichloroethane, UMCI = 0.46 versus exp . = 0.02). The impact of the imprecision of these QPPR predictions of the metabolic constants on the pharmacokinetics in humans was then evaluated by PBPK modeling.

Figure 3 presents the predictions of the 24 h blood pharmacokinetics following 8 h exposure to 1 ppm of each of the 26 VOCs used in the QPPR analysis. The bold lines represent the simulations obtained using 0 and 1 as the hepatic extraction ratio, whereas the grey area encompassed by thin lines represents the simulation obtained using LMCI and

UMCI of predicted CL_{int} in PBPK models. Overall, the envelope of the concentrations predicted using the QPPR predictions reduced the region of uncertainty associated with the complete lack of knowledge of hepatic extraction ratio in humans (i.e., ranging from 0 to 1).

The average ratio (± standard deviation) of the PBPK model simulated values of the end-of-exposure blood concentrations (i.e., *C*max) obtained with E_{min} and E_{max} was 4.19 ± 1.81. The lowest and highest ratios, based on the theoretical bounds of hepatic extraction (i.e., E_{min} and E_{max}), were observed for isoprene (1.63) and 1,1,2,2-tetrachloroethane (8.05), respectively. However, the average ratio (± standard deviation) of the PBPK model simulated values of the end-of-exposure blood concentrations, based on QPPR-generated bounds (LMCI, UMCI), was 1.29 ± 0.27. This ratio was the highest for hexachloroethane (2.39) and the lowest for 1,1-dichloroethylene (1.06).

For the 26 VOCs used in the development of the QPPR, the values of AUC_{24}s for a 1 ppm continuous exposure are reported in Table 3. The ratio of the highest to the lowest AUC predicted with *E*min and *E*max was 4.3 ± 1.94 ranging from 1.63 (isoprene) to 8.7 (1,1,2,2-tetrachloroethane). The ratio of the maximum to minimum concentrations predicted using the QPPR metabolism rate was 1.36 ± 0.4 ranging from 1.06 (1,1-dichloroethylene) to 2.8 (isoprene). Figure 4 illustrates the range of predictions of venous blood pharmacokinetics compared to experimental data [67, 81, 82]. Overall, the predicted envelope of concentrations approximated reasonably the experimental data for dichloromethane, ethylbenzene, styrene, toluene, and *m*-xylene.

4.4.2 Analysis of Applicability of the CL_{int}QPPR to PBPK

Modeling. The reliability of applying the QPPR within the PBPK model was assessed for the 26 VOCs in the calibration dataset (Table 4). The uncertainty of the QPPR prediction was estimated as the ratio of predicted CL_{intPL} to experimental CL_{intPL}. For 3 VOCs (isoprene, 1,1-dichloroethylene, and vinyl chloride) the sensitivity of AUC to CL_{int} was low

(ratio of AUCs < 2) whereas uncertainty of the CL_{int} QPPR was low for isoprene and vinyl chloride and medium for 1,1-dichloroethylene. For the other 23 VOCs, the ratio of AUCs was between 2 and 5. For 16 of the later 23 VOCs (benzene; bromochloromethane; bromodichloromethane; chloroform; dibromomethane; 1,2-dichloroethane; hexachloroethane; *n*-hexane; pentachloroethane; styrene; 1,1,1,2-tetrachloroethane; 1,1,2,2-tetrachloroethane; toluene; 1,1,2-trichloroethane; trichloroethylene; *m*-xylene) the prediction uncertainty was low, thus the confidence in using the QPPR in the PBPK model is high for these compounds. The uncertainty was medium for the prediction of CL_{intPL} for 7 VOCs (carbon tetrachloride; chloroethane; 1,1-dichloroethane; *cis*-1,2-dichloroethylene; dichloromethane; ethylbenzene; methyl chloride). Therefore, for these chemicals, the confidence in using the QPPR in an inhalation PBPK model to evaluate the AUC is medium.

4.4.3 QPPR Evaluation.

The QPPR model was applied to predict the CL_{intPL} of 11 VOCs that were not in the calibration dataset. Table 5 presents the values of the input parameters along with the experimental data for the 11 VOCs used in QPPR evaluation. Figure 5 illustrates the comparison of the predicted values of CL_{intPL} (LMCI and UMCI) and the experimental data. The average difference (± standard deviation) between the UMCI and the LMCI was 0.57 ± 0.11 ranging from 0.46 (bromoform) to 0.84 (1,2,4-trimethylbenzene). The highest UMCI-LMCI ranges were obtained for furan (0.62), tetrachloroethylene (0.63), and 1,2,4-trimethylbenzene (0.84). The nearest predicted values of UMCI and LMCI on log CL_{intPL} were greater than 5-fold of the experimental data for tetrachloroethylene (LMCI = 0.02 versus exp = −1.8). As in the QPPR development section, the impact of the imprecision on these log CL_{int} predictions on the pharmacokinetics in humans was evaluated by PBPK modeling.

Figure 6 presents the predictions of the 24 h blood pharmacokinetics following 8 h exposure to 1 ppm of each of the 11 VOCs used in the QPPR evaluation. The bold lines represent the simulations obtained using 0 and 1 as the hepatic extraction ratio, whereas the grey area encompassed by thin lines represents the simulation obtained using LMCI and UMCI of predicted CL_{int} in PBPK models. The reduction of the region of uncertainty associated with the complete lack of knowledge of hepatic extraction ratio in humans (i.e., ranging from 0 to 1) by the envelope of the concentrations predicted using the QPPR predictions was observed for the 11 VOCs.

The mean ratio (± standard deviation) of the PBPK model simulated values of the end-of-exposure blood concentrations obtained with E_{min} and E_{max} was 3.92 ± 2.13 ranging from 1.42 (ethylene) to 7.45 (bromoform). However, the same average ratio (± standard deviation) of PBPK simulated blood concentrations, based on QPPR-generated bounds (LMCI and UMCI) was 1.2 ± 0.1, ranging from 1.07 (ethylene) to 1.33 (bromoform).

Table 6 presents the values of the AUC_{24}s (mg/L-h) for the 11 VOCs used in the evaluation of the QPPR. The average ratio of the highest to lowest AUC predicted using E_{min} and E_{max} was 4.08 ± 2.31 (mean ± SD). The lowest and highest ratios, based on the theoretical bounds of hepatic extraction (i.e., E = 0.001 or 0.999), were observed for ethylene (1.44) and bromoform (7.96), respectively. The ratio of the maximum to minimum concentrations predicted using the QPPR metabolism rate was 1.2 ± 0.1, ranging from 1.07 (propylene) to 1.33 (dibromochloromethane).

Figure 7 illustrates the range of predictions for two of the chemicals in the external dataset (1,2,4-trimethylbenzene and 1,1,1-trichloroethane) venous blood pharmacokinetics compared to experimental data [61, 85]. The QPPR-PBPK model-generated "envelope" of concentrations simulated reasonably the experimental data for 1,2,4-trimethylbenzene whereas the blood concentrations of 1,1,1-trichloroethane were underestimated by about 30%.

4.4.4 Analysis of Applicability of the CL_{int} QPPR to PBPK Modeling

The reliability of applying the QPPR within the PBPK model was assessed for the 11 VOCs in the evaluation dataset, using the framework shown in Figure 1. Considering that the experimental data of CL_{intPL} for new or untested chemicals will be essentially unknown, it is realistic to consider the uncertainty of the QPPR prediction of CL_{intPL} to be high for all chemicals in the evaluation dataset.

The results of the analysis of applicability for the chemicals in the evaluation dataset are reported in Table 7. For 3 VOCs (ethylene; propylene; 1,1,1-trichloroethane) the sensitivity was low (ratio of AUCs < 2) thus the reliability of using their CL_{int} QPPR in the PBPK was considered high. For the other 8 VOCs (bromoform; dibromochloromethane; *trans*-1,2-dichloroethylene; furan; halothane; tetrachloroethylene; 1,2,4-trimethylbenzene; *o*-xylene), the ratio of the maximum to the minimum possible AUCs was between 2 and 5, such that the confidence in using the QPPR in an inhalation PBPK model to evaluate the AUCs is medium for these chemicals.

4.5. Discussion

SARs, QSAR, QSPRs, and QPPRs have been developed for various toxicological and chemical properties but only very few studies have focused on developing such models to parameterize PBPK models [8, 86]. A limitation in developing PBPK models relates to the availability of the metabolic constants (CL_{int}, V_{max}, and K_m) [8]. Quantitative relationships between structure and metabolism rates have been investigated for a limited number of closely related compounds, even though their applicability to PBPK modeling has not been demonstrated (e.g., QSPR models for K_{cat} and $1/K_m$ [87]). Other works in this area relate to the development of quantum chemical or quantum dynamic methods for prediction of activation energy or enthalpy of activation of P450 mediated reactions [20, 25, 26, 31, 36, 38, 88–91], which have not been used to derive metabolism constants for direct incorporation within rodent or human PBPK models.

The use of the group contribution method to develop QSPRs for integration within PBPK models has been successfully demonstrated, particularly for the inhalation toxicokinetics of VOCs [40–43]. This approach however is limited to VOCs containing one or more of the molecular groups or fragments for which the contribution has been evaluated (i.e., CH3, CH2, CH, C, C=C, benzene ring, H on benzene ring, and halogens). In order to extend the applicability domain then, it is important to investigate the feasibility of developing QSPRs based on more global, physicochemical properties. In this regard, the present study investigated the development of a QPPR, that used chemical properties rather than chemical structure as input, and it was calibrated to predict CL_{int} expressed in terms of chemical affinity to phospholipids in the endoplasmic reticulum in which CYP enzymes are embedded [63]. This logical transformation of CL_{int} data, reported here for the first time in literature, facilitated the development of more adequate QPPR than the conventional CL_{int} based on blood concentrations. All efforts to develop QPPRs for predicting CL_{int} based on blood concentrations were unsuccessful. The QPPR based chemical affinity to phospholipids–obtained in this study should be regarded as a screening level tool to provide plausible range of metabolism rates in order to facilitate a first-cut evaluation of the blood concentration of inhaled VOCs in humans. The uncertainty associated with this QPPR tool should be evaluated along with the sensitivity of CL_{int} on the dose metrics of the chemical of interest, in the perspective of intended precision. Accordingly, if the dose metric is highly sensitive to CL_{int} and the QPPR predictions of CL_{int} are highly uncertain, then the present tool is of limited use even for screening purposes. In such cases, then *in vivo* or *in vitro* studies can be undertaken to get chemical-specific estimates of CL_{int}.

The QPPR predictions were reasonably in accordance with experimental values for most but not all chemicals in the calibration and evaluation datasets. For some chemicals, the predicted values of log CL_{int} for 1,1,1-trichloroethane (Figure 5(A)) and tetrachloroethylene (Figure 5(K)) exceeded the experimental values by two orders of magnitude. The QSPR for rat hepatic clearance developed by Béliveau and colleagues [41] also overestimated the metabolic rate of these two VOCs. However the PBPK model for 1,1,1-trichlorethane indicated that the AUC of parent chemical in venous blood is not sensitive to *V*max and *Km*

[92, 93]. This was demonstrated in Figure 6(a), showing that QPPR overestimation of CL_{intPL} of 1,1,1-trichloroethane led only to a minimal impact, in terms of the underestimation of the venous blood concentration. In the case of tetrachloroethylene, a poorly metabolized halogenated VOC, the overestimation of the CL_{intPL} led to a 3-fold underestimation of the C_{max} (Figure 6(k)) or a 4-5-fold underestimation of the AUC_{24} (Table 7). If this magnitude of error is not acceptable for screening-level evaluation, then the metabolic rate should be experimentally determined. The combined assessment of the uncertainty/sensitivity of metabolic constants in PBPK models would facilitate the determination of the applicability of the QPPR model, given the level of precision need for an application (Figure 1).

The QPPR developed in this study is a generic tool to provide initial estimates of CL_{int} of VOCs metabolized by hepatic CYP. It does not take into account stereochemistry or other pathway-specific rates and processes, which may be important for some chemicals (e.g., predicted values of CL_{int} are almost identical for 1,1-dichloroethylene and *cis*-1,2-dichloroethylene but experimental values vary by log units of 1.06). Therefore, predictions of CL_{int} based on generic considerations are likely to be inaccurate for specific chemicals but are of limited use in that the estimates (along with the bounds, representing the level of uncertainty) can be integrated with human physiology to provide a first-cut view of the plausible kinetic profiles.

The utility of the QPPR models depends, in part, on the ability to reproducibly calculate the descriptors [74]. Hence, in this study, the descriptors that could be easily calculated and interpreted were chosen and obtained using EPISUITE (for log P_{ow} and P_{wa}) and MMPro (for the ionization potential). However, the blood solubility parameter (i.e., blood : air PC) is additionally required and this can either be obtained experimentally *in vitro* or using other QSARs that account for protein (i.e., haemoglobin and plasma protein) binding in addition to solubility considerations. There are some algorithms and QSARs available in this regard, but further development is necessary to adequately account for the protein binding phenomena in human blood for various classes of chemicals [8].

The QPPR developed in this study computes CL_{intPL}, which can then be converted to $CL_{intblood}$ for use in PBPK modeling. In an effort to evaluate whether the same input parameters can be used to relate to $CL_{intblood}$, additional analyses were performed. These yielded the following equation (significant terms only):

$$\log CL_{intblood} = 5.117 - 0.305 \cdot \log P_{ow} - 0.324 \cdot IP \qquad (6)$$

Even though (5) and (6) give almost identical results (one for CL_{intPL} and the other for $CL_{intblood}$) despite the differing R^2 values (0.796 versus 0.402), it should be noted that (5) was obtained based on statistical analysis of calibration dataset (i.e., modeling) whereas (6) was derived simply by fitting $CL_{intblood}$ to the specific input parameters. Further rearrangements and simplifications of the QPPR, as well as the loss of accuracy associated with such attempts, were not performed in the current study.

The output of the QPPR developed in the present study is log CL_{int}, which is useful for simulating pharmacokinetics in humans of chemicals at low levels of exposure. CL_{int} is applicable to first-order situations (i.e., when blood levels in humans are much lower than the K_m for metabolizing enzyme) and is derived by dividing the V_{max} (i.e., the enzyme turn-over) with K_m (representing the affinity of the substrate for the enzyme). The input parameters of the QPPR, namely, log P_{ow} and log P_{bw}, are estimates of the relative solubility in octanol, water, and blood. Then, an interpretation of the model for CL_{int} could be that the binding to the P450 enzyme is a result of hydrophobic interactions [94] which, in turn, can be estimated with parameters reflective of the solubility in *n*-octanol and blood. The solubility in blood is the sum of the solubility in its components (water, phospholipids, neutral lipids, and proteins). Most of the studied VOCs are likely to bind to hemoglobin because of their lipophilicity (log P_{ow} value above 1) and low molecular volume [40]. The P_{bw}, thus, is likely an indicator of the binding to proteins, whereas the log P_{ow} reflects more the affinity for biotic lipids in the metabolism microenvironment. Similar to log P_{ow}, the ionization potential has already been correlated with metabolic rates, namely, the V_{max} and V_{max}/k_m [23], as this latter parameter could be correlated with the energy needed to break a covalent bond for the oxidation of the substrate.

The QSPR model for CL_{int} developed in this study has a defined theoretical endpoint, is nonambiguous, has a defined domain of application, was analyzed using appropriate goodness-of-fit (R^2) and robustness (Q^2), and has an attempt of mechanistic interpretation. The *in vivo* dataset on 26 VOCs used for the QPPR calibration was chosen because it was previously collated and used in QSPR analyses [40, 41]. These values were taken mainly from the work of Gargas et al. [24]. The QSPR analysis was also attempted with the entire dataset of 37 VOCs (calibration + external dataset) but it did not improve the goodness-of-fit statistics (not shown).

The predicted bounds of the 95% confidence interval of intrinsic clearance were incorporated within a PBPK model to predict the blood toxicokinetics of VOCs. The simulations of blood kinetics were comparable to experimental data for 6 VOCs (toluene, *m*-xylene, ethylbenzene, styrene, dichloromethane, 1,2,4-trimethylbenzene, and 1,1,1-trichloroethane, Figures 4 and 7). The simulations obtained in the present study, using lower and upper confidence intervals on the mean predicted CL_{int}, reduced clearly the uncertainty bounds associated with the total lack of knowledge (i.e., E ranging anywhere between 0 and 1). Furthermore, the present study incorporated the QPPR predictions of CL_{int} along with physiological parameters, such that impact on *in vivo* kinetics could be simulated. In effect, in some cases where the uncertainty on CL_{int} predictions was high, it did not translate into a proportionate error on the predictions of kinetics, due to the additional consideration of physiological constraints, and such observations are critical in data-poor situations for designing focused studies to generate chemical-specific data *in vitro* or *in vivo*.

The QPPR developed in this study approximated the experimental rat metabolic constants for the various low molecular-weight VOCs; and it was used along with the human physiology to generate initial or screening level values of CL_{int} to construct human PBPK models that could be of potential use to interpret data such as measured biomarker levels or for designing kinetic studies to reduce database uncertainty. As shown with some VOCs (e.g., Figure 3: 1,1,1,2-tetrachloroethane, hexachloroethane, and *n*-hexane), the blood

concentration profile is extremely influenced by CL_{int}, such that metabolism cannot be neglected in simulating or interpreting human exposure data. And in such cases, the ability to generate at least a range of plausible values of CL_{int}, as done in the present study, would facilitate first in human simulations of pharmacokinetics of parent chemicals. Integrating information on the impact of metabolism on dose metrics (i.e., AUC) along with prediction uncertainty of the QPPR facilitates the determination of the level of confidence in using this screening level tool. Depending upon the overall confidence in the QPPR application for predicting dose metrics (low, medium, and high) relative to the use purposes, decisions can be made as to the specific studies needed.

Overall, the QPPR developed in the present study allows to predict the CL_{int} of VOCs on the basis of generic molecular descriptors rather than with fragment constants as done previously. The chemical concentration in phospholipids, for the first time, was found to be a dose metric amenable to QPPR analysis. The QPPR was then used to generate range of values of CL_{int}; the level of confidence in these estimates was assessed by considering the impact of CL_{int} on the simulated dose metrics (i.e., AUC of parent chemical in venous blood). For other dose metrics and situations, a more robust QPPR needs to be developed, and such efforts can be based on the methodological developments accomplished in this study. The QPPR-based simulation of pharmacokinetics reduced the range of uncertainty for few substances relative to complete lack of knowledge of the CL_{int}, but it needs to be evaluated/refined with much larger dataset should this screening-level approach be adopted for providing more precise estimates of metabolism rates. Overall, the integrated QPPR-PBPK model developed in this study is a potentially useful tool for characterizing and reducing the uncertainty associated with the complete lack of knowledge of CL_{int} in predicting human pharmacokinetics of inhaled VOCs.

4.6. Acknowledgments

Financial support by Agence Française de Sécurité Sanitaire de l'Environnement et du Travail (AFSSET; EST-2007-85) and Natural Sciences and Engineering Research Council of Canada (NSERC; Discovery grant 138195-2007 RGPIN) is acknowledged.

4.7. References

[1] Commission des communautés européennes, *LIVRE BLANC Strat´egie pour la future politique dans le domaine des substances chimiques*, 2001.

[2] CEPA, "Loi canadienne sur la protection de l'environnement (1999), Règlement sur les renseignements concernant les substances nouvelles (substances chimiques et polymères)," in *Gazette du Canada partie II*, pp. 1850–2221, Queen's Printer for Canada, Ottawa, Canada, 2005.

[3] United States Environmental Protection Agency, "The U.S. Environmental Protection Agency's strategic plan for evaluating the toxicity of chemicals," Tech. Rep. EPA/100/K-09/001, Office of the Science Advisor, Science Policy Council, Washington, DC, USA, 2009.

[4] K. Krishnan and M. E. Andersen, "Physiologically based pharmacokinetic modeling in toxicology," in *Principles and Methods of Toxicology*, A. W. Hayes, Ed., pp. 231–292, Taylor & Francis, Boca Raton, Fla, USA, 2007.

[5] A. D. Arms and C. C. Travis, "Reference physiological parameters in pharmacokinetic modeling," Tech. Rep. EPA/600/6-88/004, United States Environmental Protection Agency, Washington, DC, USA, 1988.

[6] R. P. Brown, M. D. Delp, S. L. Lindstedt, L. R. Rhomberg, and R. P. Beliles, "Physiological parameter values for physiologically based pharmacokinetic models," *Toxicology and Industrial Health*, vol. 13, no. 4, pp. 407–484, 1997.

[7] M. Béliveau and K. Krishnan, "In Silico approaches for developing physiologically based pharmacokinetic (PBPK) models," in *Alternative Toxicological Methods*, H. Salemand S. A. Katz, Eds., pp. 479–532, CRC Press, Boca Raton, Fla, USA, 2003.

[8] T. Peyret and K. Krishnan, "QSARs for PBPK modelling of environmental contaminants," *SAR and QSAR in Environmental Research*, vol. 22, no. 1-2, pp. 129–169, 2011.

[9] J. DeJongh, H. J. M. Verhaar, and J. L. M. Hermens, "A quantitative property-property relationship (QPPR) approach to estimate in vitro tissue blood partition coefficients of organic chemicals in rats and humans," *Archives of Toxicology*, vol. 72, no. 1, pp. 17–25, 1997.

[10] P. Poulin and K. Krishnan, "An algorithm for predicting tissue:blood partition coefficients of organic chemicals from *n*-octanol:water partition coefficient data," *Journal of Toxicology and Environmental Health*, vol. 46, no. 1, pp. 117–129, 1995.

[11] P. Poulin and K. Krishnan, "A biologically-based algorithm for predicting human tissue: blood partition coefficients of organic chemicals," *Human and Experimental Toxicology*, vol. 14, no. 3, pp. 273–280, 1995.

[12] P. Poulin and K. Krishnan, "A tissue composition-based algorithm for predicting tissue:air partition coefficients of organic chemicals," *Toxicology and Applied Pharmacology*, vol. 136, no. 1, pp. 126–130, 1996.

[13] P. Poulin and K. Krishnan, "A mechanistic algorithm for predicting blood: air partition coefficients of organic chemicals with the consideration of reversible binding in hemoglobin," *Toxicology and Applied Pharmacology*, vol. 136, no. 1, pp. 131–137, 1996.

[14] P. Poulin and F. P. Theil, "A priori prediction of tissue:plasma partition coefficients of drugs to facilitate the use of physiologically-based pharmacokinetic models in drug discovery," *Journal of Pharmaceutical Sciences*, vol. 89, no. 1, pp. 16–35, 2000.

[15] P. Poulin and F. P. Theil, “Prediction of pharmacokinetics prior to in vivo studies. 1. Mechanism-based prediction of volume of distribution,” *Journal of Pharmaceutical Sciences*, vol. 91, no.1, pp. 129–156, 2002.

[16] T. Rodgers, D. Leahy, and M. Rowland, “Physiologically based pharmacokinetic modeling 1: predicting the tissue distribution of moderate-to-strong bases,” *Journal of Pharmaceutical Sciences*, vol. 94, no. 6, pp. 1259–1276, 2005.

[17] T. Rodgers and M. Rowland, “Physiologically based pharmacokinetic modelling 2: predicting the tissue distribution of acids, very weak bases, neutrals and zwitterions,” *Journal of Pharmaceutical Sciences*, vol. 95, no. 6, pp. 1238–1257, 2006.

[18] W. Schmitt, “General approach for the calculation of tissue to plasma partition coefficients,” *Toxicology in Vitro*, vol. 22, no.2, pp. 457–467, 2008.

[19] T. Peyret, P. Poulin, and K. Krishnan, “A unified algorithm for predicting partition coefficients for PBPK modeling of drugs and environmental chemicals,” *Toxicology and Applied Pharmacology*, vol. 249, no. 3, pp. 197–207, 2010.

[20] P. Rydberg, U. Ryde, and L. Olsen, “Prediction of activation energies for aromatic oxidation by cytochrome P450,” *Journal of Physical Chemistry A*, vol. 112, no. 50, pp. 13058–13065, 2008.

[21] D. Zhou, L. Afzelius, S. W. Grimm, T. B. Andersson, R. J. Zauhar, and I. Zamora, “Comparison of methods for the prediction of the metabolic sites for CYP3A4-mediated metabolic reactions,” *Drug Metabolism and Disposition*, vol. 34, no. 6, pp. 976–983, 2006.

[22] C. Hansch, S. B. Mekapati, A. Kurup, and R. P. Verma, “QSAR of Cytochrome P450,” *Drug Metabolism Reviews*, vol. 36, no. 1, pp. 105–156, 2004.

[23] D. F. V. Lewis, C. Sams, and G. D. Loizou, “A quantitative structure-activity relationship analysis on a series of alkyl benzenes metabolized by human cytochrome P450 2E1,” *Journal of Biochemical and Molecular Toxicology*, vol. 17, no. 1, pp. 47–52, 2003.

[24] M. L. Gargas, P. G. Seybold, and M. E. Andersen, "Modeling the tissue solubilities and metabolic rate constant V_{max} of halogenated methanes, ethanes, and ethylenes," *Toxicology Letters*, vol. 43, no. 1–3, pp. 235–256, 1988.

[25] K. R. Korzekwa, J. P. Jones, and J. R. Gillette, "Theoretical studies on cytochrome P-450 mediated hydroxylation: a predictive model for hydrogen atom abstractions," *Journal of the American Chemical Society*, vol. 112, no. 19, pp. 7042–7046, 1990.

[26] H. Yin, M. W. Anders, K. R. Korzekwa et al., "Designing safer chemicals: predicting the rates of metabolism of halogenated alkanes," *Proceedings of the National Academy of Sciences of the United States of America*, vol. 92, no. 24, pp. 11076–11080, 1995.

[27] C. L. Waller, M. V. Evans, and J. D. Mckinney, "Modeling the cytochrome P450-mediated metabolism of chlorinated volatile organic compounds," *Drug Metabolism and Disposition*, vol. 24, no. 2, pp. 203–210, 1996.

[28] J. Ishizaki, K. Yokogawa, E. Nakashima, and F. Ichimura, "Relationships between the hepatic intrinsic clearance or blood cell-plasma partition coefficient in the rabbit and the lipophilicity of basic drugs," *Journal of Pharmacy and Pharmacology*, vol. 49, no. 8, pp. 768–772, 1997.

[29] D. F. V. Lewis, "Modelling human cytochromes P450 for evaluating drug metabolism: an update," *DrugMetabolism and Drug Interactions*, vol. 16, no. 4, pp. 307–324, 2000.

[30] D. F. V. Lewis, "Quantitative structure-activity relationships (QSARs) within the cytochrome P450 system: QSARs describing substrate binding, inhibition and induction of P450s," *Inflammopharmacology*, vol. 11, no. 1, pp. 43–73, 2003.

[31] J. P. Jones, M. Mysinger, and K. R. Korzekwa, "Computational models for cytochrome P450: a predictive electronic model for aromatic oxidation and hydrogen atom abstraction," *Drug Metabolism and Disposition*, vol. 30, no. 1, pp. 7–12, 2002.

[32] D. F. V. Lewis, "On the recognition ofmammalian microsomal cytochrome P450 substrates and their characteristics: towards the prediction of human P450 substrate

specificity and metabolism," *Biochemical Pharmacology*, vol. 60, no. 3, pp. 293–306, 2000.

[33] D. F. V. Lewis, S. Modi, and M. Dickins, "Structure-activity relationship for human cytochrome P450 substrates and inhibitors," *Drug Metabolism Reviews*, vol. 34, no. 1-2, pp. 69–82, 2002.

[34] K. V. Balakin, S. Ekins, A. Bugrim et al., "Quantitative structure-metabolism relationship modeling of metabolic Ndealkylation reaction rates," *Drug Metabolism and Disposition*, vol. 32, no. 10, pp. 1111–1120, 2004.

[35] S. Ekins, S. Andreyev, A. Ryabov et al., "Computational prediction of human drug metabolism," *Expert Opinion on Drug Metabolism and Toxicology*, vol. 1, no. 2, pp. 303–324, 2005.

[36] P. N. D'Yachkov, N. V. Kharchevnikova, A. V. Dmitriev, A. V. Kuznetsov, and V. V. Poroikov, "Quantum chemical simulation of cytochrome P450 catalyzed aromatic oxidation: metabolism, toxicity, and biodegradation of benzene derivatives," *International Journal of Quantum Chemistry*, vol. 107, no. 13, pp. 2454–2478, 2007.

[37] G. P. Miller, "Advances in the interpretation and prediction of CYP2E1 metabolism from a biochemical perspective," *Expert Opinion on Drug Metabolism and Toxicology*, vol. 4, no. 8, pp. 1053–1064, 2008.

[38] A. N. Mayeno, J. L. Robinson, R. S. H. Yang, and B. Reisfeld, "Predicting activation enthalpies of cytochrome-P450-mediated hydrogen abstractions. 2. Comparison of semiempirical PM3, SAM1, and AM1 with a density functional theory method," *Journal of Chemical Information and Modeling*, vol. 49, no. 7, pp. 1692–1703, 2009.

[39] C. Gao, R. Goind, and H. H. Tabak, "Application of the group contribution method for predicting the toxicity of organic chemicals," *Environmental Toxicology and Chemistry*, vol. 11, no. 5, pp. 631–636, 1992.

[40] M. Béliveau, J. Lipscomb, R. Tardif, and K. Krishnan, "Quantitative structure-property relationships for interspecies extrapolation of the inhalation pharmacokinetics

of organic chemicals," *Chemical Research in Toxicology*, vol. 18, no. 3, pp. 475–485, 2005.

[41] M. Béliveau, R. Tardif, and K. Krishnan, "Quantitative structure-property relationships for physiologically based pharmacokinetic modeling of volatile organic chemicals in rats," *Toxicology and Applied Pharmacology*, vol. 189, no. 3, pp. 221–232, 2003.

[42] E. Kamgang, T. Peyret, and K. Krishnan, "An integrated QSPR-PBPK modelling approach for in vitro-in vivo extrapolation of pharmacokinetics in rats," *SAR and QSAR in Environmental Research*, vol. 19, no. 7-8, pp. 669–680, 2008.

[43] K. Price and K. Krishnan, "An integrated QSAR-PBPK modelling approach for predicting the inhalation toxicokinetics of mixtures of volatile organic chemicals in the rat," *SAR and QSAR in Environmental Research*, vol. 22, no. 1-2, pp. 107–128, 2011.

[44] W. M. Meylan and P. H. Howard, "Atom/fragment contribution method for estimating octanol-water partition coefficients," *Journal of Pharmaceutical Sciences*, vol. 84, no. 1, pp. 83–92, 1995.

[45] P. Poulin and K. Krishnan, "Molecular structure-based prediction of the toxicokinetics of inhaled vapors in humans," *International Journal of Toxicology*, vol. 18, no. 1, pp. 7–18, 1998.

[46] S. Haddad, G. C. Tardif, and R. Tardif, "Development of physiologically based toxicokinetic models for improving the human indoor exposure assessment to water contaminants: trichloroethylene and trihalomethanes," *Journal of Toxicology and Environmental Health A*, vol. 69, no. 23, pp. 2095–2136, 2006.

[47] N. Ali and R. Tardif, "Toxicokineticmodeling of the combined exposure to toluene and *n*-hexane in rats and humans," *Journal of Occupational Health*, vol. 41, no. 2, pp. 95–103, 1999.

[48] R. Tardif and G. Charest-Tardif, "The importance of measured endpoints in demonstrating the occurrence of interactions: a case study with methylchloroform and *m*-xylene," *Toxicological Sciences*, vol. 49, no. 2, pp. 312–317, 1999.

[49] M. L. Gargas, M. E. Andersen, and H. J. Clewell III, “A physiologically based simulation approach for determining metabolic constants from gas uptake data,” *Toxicology and Applied Pharmacology*, vol. 86, no. 3, pp. 341–352, 1986.

[50] J. C. Ramsey and M. E. Andersen, “A physiologically based description of the inhalation pharmacokinetics of styrene in rats and humans,” *Toxicology and Applied Pharmacology*, vol. 73, no. 1, pp. 159–175, 1984.

[51] M. L. Gargas, H. J. Clewell III, and M. E. Andersen, “Metabolism of inhaled dihalomethanes in vivo: differentiation of kinetic constants for two independent pathways,” *Toxicology and Applied Pharmacology*, vol. 82, no. 2, pp. 211–223, 1986.

[52] J. G. Filser, G. A. Csanády, B. Denk et al., “Toxicokinetics of isoprene in rodents and humans,” *Toxicology*, vol. 113, no. 1–3, pp. 278–287, 1996.

[53] S. Haddad, R. Tardif, G. Charest-Tardif, and K. Krishnan, “Physiological modeling of the toxicokinetic interactions in a quaternary mixture of aromatic hydrocarbons,” *Toxicology and Applied Pharmacology*, vol. 161, no. 3, pp. 249–257, 1999.

[54] J.G. Filser, R. Schmidbauer, F. Rampf, C.M. Baur,C. Putz, and G. A. Csanady, “Toxicokinetics of inhaled propylene in mouse, rat, and human,” *Toxicology and Applied Pharmacology*, vol. 169, no. 1, pp. 40–51, 2000.

[55] M. L. Gargas, H. J. Clewell, and M. E. Andersen, “Gas uptake inhalation techniques and the rates of metabolism of chloromethanes, chloroethanes and chloroethylenes in the rat,” *Inhalation Toxicology*, vol. 2, no. 3, pp. 295–319, 1990.

[56] G. L. Kedderis and S. D. Held, “Prediction of furan pharmacokinetics from hepatocyte studies: comparison of bioactivation and hepatic dosimetry in rats, mice, and humans” *Toxicology and Applied Pharmacology*, vol. 140, no. 1, pp. 124–130, 1996.

[57] R. H. Reitz, M. L. Gargas, A. L. Mendrala, and A. M. Schumann, “*In vivo* and *in vitro* studies of perchloroethylene metabolism for physiologically based pharmacokinetic modeling in rats, mice, and humans,” *Toxicology and Applied Pharmacology*, vol. 136, no. 2, pp. 289–306, 1996.

[58] R. J.Williams, A. Vinegar, J. N.Mcdougal, A.M. Jarabek, and J. W. Fisher, "Rat to human extrapolation of HCFC-123 kinetics deduced from halothane kinetics: a corollary approach to physiologically based pharmacokineticmodeling," *Fundamental and Applied Toxicology*, vol. 30, no. 1, pp. 55–66, 1996.

[59] G. A. Csanády, B. Denk, C. Pütz et al., "A physiological toxicokinetic model for exogenous and endogenous ethylene and ethylene oxide in rat, mouse, and human: formation of 2-hydroxyethyl adducts with hemoglobin and DNA," *Toxicology and Applied Pharmacology*, vol. 165, no. 1, pp. 1–26, 2000.

[60] J. E. Dennison, M. E. Andersen, and R. S. H. Yang, "Characterization of the pharmacokinetics of gasoline using PBPK modeling with a complex mixtures chemical lumping approach," *Inhalation Toxicology*, vol. 15, no. 10, pp. 961–986, 2003.

[61] A. M. Hissink, J. Krüse, B. M. Kulig et al., "Model studies for evaluating the neurobehavioral effects of complex hydrocarbon solvents. III. PBPK modeling of white spirit constituents as a tool for integrating animal and human test data," *NeuroToxicology*, vol. 28, no. 4, pp. 751–760, 2007.

[62] D. F. V. Lewis, *Guide to Cytochromes P450: Structure and Function*, Taylor & Francis, London, UK, 2001.

[63] A. I. Archakov and G. I. Bachmanova, Eds., *Cytochrome P-450 and Active Oxygen*, Taylor & Francis, London, UK, 1990.

[64] Z. Fang, J. Sonner, M. J. Laster et al., "Anesthetic and convulsant properties of aromatic compounds and cycloalkanes: implications for mechanisms of narcosis," *Anesthesia and Analgesia*, vol. 83, no. 5, pp. 1097–1104, 1996.

[65] P. D. Lilly, M. E. Andersen, T. M. Ross, and R. A. Pegram, "Physiologically based estimation of in vivo rates of bromodichloromethane metabolism," *Toxicology*, vol. 124, no. 2, pp. 141–152, 1997.

[66] M. L. Gargas, R. J. Burgess, D. E. Voisard, G. H. Cason, and M. E. Andersen, "Partition coefficients of low-molecular-weight volatile chemicals in various liquids and tissues," *Toxicology and Applied Pharmacology*, vol. 98, no. 1, pp. 87–99, 1989.

[67] R. Tardif, G. Charest-Tardif, J. Brodeur, and K. Krishnan, "Physiologically based pharmacokinetic modeling of a ternary mixture of alkyl benzenes in rats and humans," *Toxicology and Applied Pharmacology*, vol. 144, no. 1, pp. 120–134, 1997.

[68] M. Béliveau and K. Krishnan, "Estimation of rat blood: air partition coefficients of volatile organic chemicals using reconstituted mixtures of blood components," *Toxicology Letters*, vol. 116, no. 3, pp. 183–188, 2000.

[69] C. Hansch and L. Zhang, "Quantitative structure-activity relationships of cytochrome P-450," *DrugMetabolism Reviews*, vol. 25, no. 1-2, pp. 1–48, 1993.

[70] D. F. V. Lewis and M. Dickins, "Baseline lipophilicity relationships in human cytochromes P450 associated with drug metabolism," *Drug Metabolism Reviews*, vol. 35, no. 1, pp. 1–18, 2003.

[71] D. F. V. Lewis and Y. Ito, "Human P450s involved in drug metabolism and the use of structural modelling for understanding substrate selectivity and binding affinity," *Xenobiotica*, vol. 39, no. 8, pp. 625–635, 2009.

[72] L. B. Kier, "A shape index from molecular graphs," *Quantitative Structure-Activity Relationships*, vol. 4, no. 3, pp. 109–116, 1985.

[73] Organisation for Economic Co-operation and Development, "Guidance document on the validation of (quantitative) structure-activity relationship [(Q)SAR] models," Tech. Rep., OECD-OCDE, Paris, France, 2007, OECD Environment Health and Safety Publications, Editor.

[74] P. Gramatica, "Principles of QSAR models validation: Internal and external," *QSAR and Combinatorial Science*, vol. 26, no. 5, pp. 694–701, 2007.

[75] S. A. Glantz and B. K. Slinker, *Primer of Applied Regression and Analysis of Variance*, McGraw-Hill, New York, NY, USA, 2nd edition, 2001.

[76] S. Wold, "Validation of QSARs," *Quantitative Structure Activity Relashionship*, vol. 10, pp. 191–193, 1991.

[77] C. J. W. Meulenberg and H. P. M. Vijverberg, "Empirical relations predicting human and rat tissue: air partition coefficients of volatile organic compounds," *Toxicology and Applied Pharmacology*, vol. 165, no. 3, pp. 206–216, 2000.

[78] S. Batterman, L. Zhang, S.Wang, and A. Franzblau, "Partition coefficients for the trihalomethanes among blood, urine, water, milk and air," *Science of the Total Environment*, vol. 284, no. 1–3, pp. 237–247, 2002.

[79] L. M. da Silva, G. Charest-Tardif, K. Krishnan, and R. Tardif, "Influence of oral administration of a quaternary mixture of trihalomethanes on their blood kinetics in the rat," *Toxicology Letters*, vol. 106, no. 1, pp. 49–57, 1999.

[80] M. E. Andersen, H. J. Clewell, M. L. Gargas, F. A. Smith, and R. H. Reitz, "Physiologically based pharmacokinetics and the risk assessment process for methylene chloride," *Toxicology and Applied Pharmacology*, vol. 87, no. 2, pp. 185–205, 1987.

[81] J. C. Ramsey, J. D. Young, R. J. Karbowski, M. B. Chenoweth, L. P. McCarty, and W. H. Braun, "Pharmacokinetics of inhaled styrene in human volunteers," *Toxicology and Applied Pharmacology*, vol. 53, no. 1, pp. 54–63, 1980.

[82] M. E. Andersen, H. J. Clewell, M. L. Gargas et al., "Physiologically based pharmacokinetic modeling with dichloromethane, its metabolite, carbon monoxide, and blood carboxyhemoglobin in rats and humans," *Toxicology and Applied Pharmacology*, vol. 108, no. 1, pp. 14–27, 1991.

[83] T. M. Cahill, I. Cousins, and D. Mackay, "Development and application of a generalized physiologically based pharmacokinetic model for multiple environmental contaminants," *Environmental Toxicology and Chemistry*, vol. 22, no. 1, pp. 26–34, 2003.

[84] International Programme on Chemical Safety, *Characterization and Application of Physiologically Based Pharmacokinetic Models in Risk Assessment*, International Programme on Chemical Safety, 2010.

[85] C. J. MacKay, L. Campbell, A. M. Samuel et al., "Behavioral changes during exposure to 1,1,1-trichloroethane: timecourse and relationship to blood solvent levels," *American Journal of Industrial Medicine*, vol. 11, no. 2, pp. 223–239, 1987.

[86] M. T. D. Cronin and D. Livingstone, *Predicting Chemical Toxicity and Fate*, CRC Press, Boca Raton, Fla, USA, 2004.

[87] H. Gao and C.Hansch, "QSAR of P450 oxidation: on the value of comparing kcat and km with kcat/km," *Drug Metabolism Reviews*, vol. 28, no. 4, pp. 513–526, 1996.

[88] J. P. Jones, K. R. Korzekwa, F. J. Eric, and R. W. Michael, "Predicting the rates and regioselectivity of reactions mediated by the P450 superfamily," in *Methods in Enzymology*, pp. 326–335, Academic Press, New York, NY, USA, 1996.

[89] D. L. Harris, J.-Y. Park, L. Gruenke, and L. Waskell, "Theoretical study of the ligand-CYP2B4 complexes: effect of structure on binding free energies and heme spin state," *Proteins*, vol. 55, no. 4, pp. 895–914, 2004.

[90] L. Olsen, P. Rydberg, T. H. Rod, and U. Ryde, "Prediction of activation energies for hydrogen abstraction by cytochrome P450," *Journal of Medicinal Chemistry*, vol. 49, no. 22, pp. 6489–6499, 2006.

[91] D. N. Kim, K. H. Cho, W. S. Oh et al., "EaMEAD: activation energy prediction of cytochrome p450 mediated metabolism with effective atomic descriptors," *Journal of Chemical Information and Modeling*, vol. 49, no. 7, pp. 1643–1654, 2009.

[92] Y. Lu, S. Rieth, M. Lohitnavy et al., "Application of PBPK modeling in support of the derivation of toxicity reference values for 1-trichloroethane," *Regulatory Toxicology and Pharmacology*, vol. 50, no. 2, pp. 249–260, 2008.

[93] R. H. Reitz, J. N. McDougal, M. W. Himmelstein, R. J. Nolan, and A.M. Schumann, "Physiologically based pharmacokinetic modeling with methylchloroform: implications for interspecies, high dose/low dose, and dose route extrapolations," *Toxicology and Applied Pharmacology*, vol. 95, no. 2, pp. 185–199, 1988.

[94] M. H. Wang, D. Wade, L. Chen, S. White, and C. S. Yang, "Probing the active sites of rat and human cytochrome P450 2E1 with alcohols and carboxylic acids," *Archives of Biochemistry and Biophysics*, vol. 317, no. 1, pp. 299–304, 1995.

4.8. Tables

Table 1. Partition coefficients used in the human PBPK models

Chemicals[a]	Partition coefficient (PC)[b]						Reference
	P_{ba}	P_{lb}	P_{rb}	P_{pb}	P_{fb}	P_{plb}	
Benzene	8.19	2.08	2.08	1.26	60.93	4.55	[66]
Bromochloromethane	10.4	2.81	2.81	1.07	31.5	2	[66];[78]
Bromodichloromethane	26.6	1.15	1.15	0.47	19.77	2.48	[77];[79]
Carbon tetrachloride	2.73	5.2	5.2	1.67	131.5	8.57	[66]
Chloroethane	2.69	1.34	1.34	1.2	14.3	4.42	[66]
Chloroform	6.85	3.08	3.08	2.03	29.6	1.93	[66]
Dibromomethane	19.9	3.42	3.42	2.03	39.8	1.78	[66];[78]
Dichloroethane (1,1-)	4.94	2.19	2.19	1.04	33.2	4.27	[66]
Dichloroethane (1,2-)	19.5	1.83	1.83	1.2	17.64	9.25	[66]
Dichloroethylene (1,1-)	0.81	5.46	5.46	2.53	84.69	4.82	[66];[78]
Dichloroethylene (*cis*-1,2)	9.85	1.55	1.55	0.62	23	5.2	[66]
Dichloromethane	9.7	1.46	1.46	0.82	12.4	1.79	[80]
Ethylbenzene	28	2.99	2.15	0.93	55.6	13.2	[67]
Hexachloroethane	52.4	7.04	7.04	1.43	63.4	156	[66]
Hexane (*n*-)	2.13	5.2	5.2	2.9	159	1.89	[95]
Isoprene	0.75	2.57	2.45	1.97	82	11.84	[52]
Methyl chloride	2.48	1.4	1.4	0.39	5.44	3.04	[66]
Pentachloroethane	50.3	5.17	5.17	1.44	81.9	21.7	[66];[78]
Styrene	52	2.7	5.7	1	50	30.2	[50]
Tetrachloroethane (1,1,1,2-)	30.2	2.92	2.92	1.31	71.1	37.3	[66]
Tetrachloroethane (1,1,2,2-)	116	1.69	1.69	0.87	32.47	14.3	[66]
Toluene	15.6	5.36	5.36	1.77	65.4	13.8	[67]
Trichloroethane (1,1,2-)	35.7	2.05	2.05	0.64	40.3	10.1	[66]
Trichloroethylene	8.11	3.35	3.35	1.24	68.3	5.73	[66]
Vinyl chloride	1.16	1.38	1.38	1.81	17.2	4.87	[66]
Xylene (*m*-)	26.4	3.44	3.44	1.59	70.4	15.1	[67]
Bromoform	102.3	2.06	2.06	1.12	40.4	2.44	[77];[79]
Dibromochloromethane	49.2	2.56	2.56	1.13	38.96	1.48	[77];[79]
*Dichloroethylene (*trans-*1,2-)*	6.04	1.48	1.48	0.58	24.5	11.7	[66]
Ethylene	0.22	2.05	2.18	2.95	8.73	1.05	[59]

Table 1. Continued

Chemicals[a]	Partition coefficient (PC)[b]						Reference
	P_{ba}	P_{lb}	P_{rb}	P_{pb}	P_{fb}	P_{plb}	
Furan	6.59	0.9	0.9	0.64	9.72	2.75	[56]
Halothane	3.3	2.42	2.42	2.91	44.2	5.82	[58]
Propylene	0.44	1.09	1.2	1.25	11.7	1.52	[54]
Tetrachloroethylene	10.3	5.88	5.88	3.1	119.1	11.1	[57]
Trichloroethane (1,1,1-)	2.53	1.24	3.4	3.4	103.9	21.7	[48]
Trimethylbenzene (1,2,4-)	85	4.4	4.4	2.11	109	19	[61]
*Xylene (*o-*)*	34.9	3.09	3.09	1.47	53.8	22.6	[66]

[a]: Chemicals in italics were not included in the dataset for the calibration of the model.
[b]: P_{ba}: Blood:air PC; P_{lb}: liver blood PC; P_{rb} Richly perfused tissues:blood PC; P_{pb}: poorly perfused tissues:blood PC; P_{fb}: Fat:blood PC; P_{plb}: phospholipids:blood PC.

Table 2. Input parameters and experimental data of log CL_{intPL}.

Chemical	Input parameters			Log Cl_{intPL} [a] (L_{PL}/h/kg)	Ref V_{max}, K_m
	log P_{ow}	log P_{bw}	Ionization potential (eV)		
Benzene	1.99	0.820	9.743	0.667	[53]
Bromochloromethane	1.43	0.642	10.562	1.118	[49]
Bromodichloromethane	1.61	0.717	10.676	1.029	[46]
Carbon tetrachloride	2.44	0.988	10.985	-0.700	[24]
Chloroethane	1.58	0.438	10.410	0.987	[24]
Chloroform	1.52	0.741	10.839	1.192	[24]
Dibromomethane	1.52	0.777	10.587	1.275	[51]
Dichloroethane (1,1-)	1.76	0.624	10.577	0.974	[24]
Dichloroethane (1,2-)	1.83	0.356	10.446	0.163	[24]
Dichloroethylene (1,1-)	2.12	0.922	9.748	1.223	[24]
Dichloroethylene (*cis*-1,2)	1.98	0.752	9.493	0.092	[24]
Dichloromethane	1.34	0.608	10.582	0.777	[24]
Ethylbenzene	3.03	1.386	9.406	-0.334	[49]
Hexachloroethane	4.03	1.315	10.843	-1.767	[24]
Hexane (*n*-)	3.29	2.492	11.276	0.252	[95]
Isoprene	2.58	0.987	9.349	0.472	[52]
Methyl chloride	1.09	0.160	10.473	0.299	[24]
Pentachloroethane	3.11	1.251	10.763	-0.297	[24]
Styrene	2.89	0.889	9.130	-0.088	[50]
Tetrachloroethane (1,1,1,2-)	2.93	0.836	10.728	-0.693	[24]
Tetrachloroethane (1,1,2,2-)	2.19	0.519	10.736	0.051	[24]
Toluene	2.54	0.879	9.442	0.282	[49]
Trichloroethane (1,1,2-)	2.01	0.491	10.689	0.018	[24]
Trichloroethylene	2.47	1.192	9.368	0.916	[24]
Vinyl chloride	1.62	0.433	9.833	0.741	[24]
Xylene (*m*-)	3.09	1.388	9.308	0.218	[48]

[a]: EXP.: Experimental data (references in the methods); LMCI and UMCI: Lower and upper bound of the 95 % mean confidence interval, respectively.

Table 3. Area-under-the-curve for four metabolic scenarios for the VOCs used in the QPPR development

Chemicals	Area under the curve (mg/L-h)			
	Metabolic scenario[a]			
	E_{min}	E_{max}	LMCI	UMCI
Benzene	0.437	0.125	0.155	0.138
Bromochloromethane	0.913	0.229	0.305	0.257
Bromodichloromethane	2.380	0.356	0.523	0.422
Carbon tetrachloride	0.34	0.153	0.224	0.186
Chloroethane	0.156	0.069	0.084	0.076
Chloroform	0.599	0.185	0.257	0.211
Dibromomethane	1.659	0.336	0.466	0.384
Dichloroethane (1,1-)	0.391	0.138	0.181	0.158
Dichloroethane (1,2-)	1.142	0.205	0.305	0.241
Dichloroethylene (1,1-)	6.98×10^{-2}	4.22×10^{-2}	4.76×10^{-2}	4.47×10^{-2}
Dichloroethylene (*cis*-1,2)	0.702	0.174	0.214	0.188
Dichloromethane	0.65	0.157	0.206	0.174
Ethylbenzene	1.247	0.216	0.32	0.246
Hexachloroethane	3.071	0.494	1.774	0.738
Hexane (*n*-)	0.15	0.073	0.129	0.084
Isoprene	4.59×10^{-2}	2.81×10^{-2}	0.084	2.95×10^{-2}
Methyl chloride	0.119	0.054	0.064	0.057
Pentachloroethane	2.584	0.418	0.929	0.595
Styrene	1.497	0.222	0.322	0.246
Tetrachloroethane (1,1,1,2-)	1.911	0.337	0.739	0.457
Tetrachloroethane (1,1,2,2-)	3.337	0.384	0.717	0.495

Table 3. Continued

Chemicals	Area under the curve (mg/L-h)			
	Metabolic scenario[a]			
	E_{min}	E_{max}	LMCI	UMCI
Toluene	0.74	0.168	0.223	0.188
Trichloroethane (1,1,2-)	1.876	0.284	0.474	0.355
Trichloroethylene	0.721	0.209	0.267	0.227
Vinyl chloride	6.68×10^{-2}	3.79×10^{-2}	4.25×10^{-2}	3.98×10^{-2}
Xylene (*m*-)	1.117	0.209	0.308	0.236

[a]: E_{min}: non metabolism; E_{max}: maximum hepatic extraction; LMCI and UMCI: lower and upper bound of the 95 % mean confidence interval, respectively.

Table 4. Reliability analysis of the QPPR for CL_{int} on the PBPK predicted AUC

		Impact of metabolism on AUC (AUC_{Emin} / AUC_{Emax})[a]		
		Low (< 2)	**Medium (2-5)**	**High (> 5)**
QPPR prediction uncertainty (Pred. / Exp. CL_{intPL})[b]	**Low (< 2)**	Isoprene, vinyl chloride	benzene; bromochloromethane; bromodichloromethane; chloroform; dibromomethane; 1,2-dichloroethane; hexachloroethane; *n*-hexane; pentachloroethane; styrene; 1,1,1,2-tetrachloroethane; 1,1,2,2-tetrachloroethane; toluene; 1,1,2-trichloroethane; trichloroethylene; *m*-xylene	
	Medium (2-5)	1,1,-dichloroethylene	carbon tetrachloride; chloroethane; 1,1-dichloroethane; *cis*-1,2-dichloroethylene; dichloromethane; ethylbenzene; methyl chloride	
	High (> 5)			

[a]: calculated as the ratio of the PBPK simulations of 24-h AUC (of venous blood concentration, 1 ppm VOC, 24-h exposure) by setting E = 0 (i.e. CL_{int} = 0) to that setting E = 1 (i.e., CL_{int} = 1000)

[b]: calculated as the ratio of the predicted to the experimental values of CL_{intPL}

Table 5. Input parameters and experimental data on log CL_{int} for VOCs of QPPR evaluation.

Chemical	Input parameters			Log CL_{intPL}[a] (L_{PL}/h/kg)	Ref V_{max}, K_m
	log P_{ow}	log P_{bw}	IP (eV)		
Bromoform	1.79	0.896	10.837	1.006	[46]
Dibromochloromethane	1.70	1.025	10.702	1.108	[46]
Dichloroethylene (*trans*-1,2-)	1.98	0.484	9.512	0.438	[55]
Ethylene	1.27	0.776	10.638	1.208	[59]
Furan	1.36	0.441	9.375	1.773	[56]
Halothane	2.26	0.977	11.039	1.104	[58]
Propylene	1.68	0.995	10.103	1.118	[54]
Tetrachloroethylene	2.97	1.404	9.217	-1.804	[57]
Trichloroethane (1,1,1-)	2.68	0.823	10.751	-2.467	[48]
Trimethylbenzene (1,2,4-)	3.63	1.829	9.084	-0.132	[61]
Xylene (*o*-)	3.09	1.213	9.304	0.163	[60]

[a]: Experimental data (references in section 3.3)

Table 6. Area under the curve for four metabolic scenarios, for VOCs in the evaluation dataset

Chemicals	24 h Area under the curve			
	Metabolic scenario[a]			
	E_{min}	E_{max}	LMCI	UMCI
Bromoform	2.122	0.267	0.434	0.328
Dibromochloromethane	3.114	0.45	0.7	0.527
Dichloroethylene (*trans*-1,2-)	0.472	0.149	0.185	0.16
Ethylene	5.87×10^{-3}	4.08×10^{-3}	4.55×10^{-3}	4.23×10^{-3}
Furan	0.388	0.113	0.131	0.118
Halothane	0.523	0.22	0.325	0.266
Propylene	1.76×10^{-2}	1.16×10^{-2}	1.3×10^{-2}	$1.21E \times 10^{-2}$
Tetrachloroethylene	0.953	0.266	0.363	0.291
Trichloroethane (1,1,1-)	0.271	0.125	0.184	0.15
Trimethylbenzene (1,2,4-)	1.577	0.249	0.425	0.395
Xylene (*o*-)	1.297	0.218	0.325	0.248

[a]: E_{min}: no metabolism; E_{max}: maximum hepatic extraction; LMCI and UMCI: lower and upper bound of the 95 % mean confidence interval, respectively.

Table 7. Reliability analysis for the chemicals in the QPPR evaluation dataset

		Impact of metabolism on AUC (AUC_{Emin} / AUC_{Emax})[a]		
		Low (< 2)	**Medium (2-5)**	**High (> 5)**
QPPR prediction uncertainty (Pred. / Exp. CL_{intPL})[b]	**Low (< 2)**			
	Medium (2-5)			
	High (> 5)	ethylene; propylene; 1,1,1-trichloroethane	bromoform; dibromochloromethane; trans-1,2-dichloroethylene; furan; halothane; tetrachloroethylene; 1,2,4-trimethylbenzene; *o*-xylene	

[a]: calculated as the ratio of the PBPK simulations of 24-h AUC (of venous blood concentration, 1 ppm VOC, 24-h exposure) by setting E = 0 (i.e. CL_{int} = 0) to that setting E = 1 (i.e., CL_{int} = 1000)

[b]: calculated as the ratio of the predicted to the experimental values of CL_{intPL}

4.9. Figures

Confidence in the QPPR-PBPK model		Impact of metabolism on AUC (AUC_{Emin} / AUC_{Emax})		
		Low (< 2)	Medium (2-10)	High (> 10)
QPPR prediction uncertainty (Pred. CL_{intPL} / exp. CL_{intPL})	Low (<2)	High	High	High
	Medium (2-10)	High	Medium	Medium
	High (> 10)	High	Medium	Low

Figure 1. Evaluation of the confidence in applying the QPPR for CL_{intPL} in a PBPK model using a sensitivity/uncertainty approach.

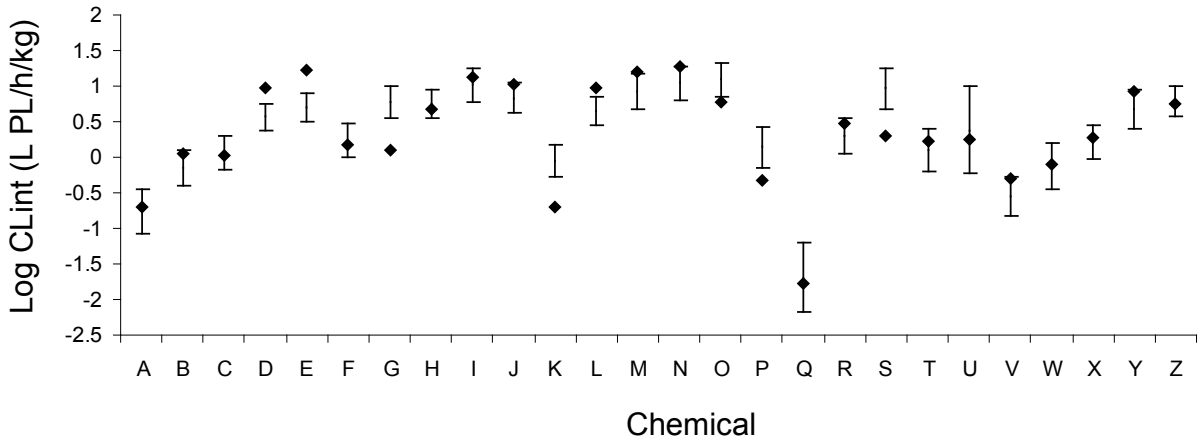

Figure 2. Experimental and predicted values of log CL_{int} for 26 VOCs.

The horizontal bars represent the QPPR predicted LMCI and UMCI, the symbols represent the experimental data. A: 1,1,1,2-tetrachloroethane; B: 1,1,2,2-tetrachloroethane; C: 1,1,2-trichloroethane; D: 1,1-dichloroethane; E: 1,1-dichloroethylene; F: 1,2-dichloroethane; G: 1,2-dichloroethylene (*cis*-); H: benzene; I: bromochloromethane; J: bromodichloromethane; K: carbon tetrachloride; L: chloroethane; M: chloroform; N: dibromomethane; O: dichloromethane; P: ethylbenzene; Q: hexachloroethane; R: isoprene; S: methyl chloride; T: *m*-xylene; U: *n*-hexane; V: pentachlorethane; W: styrene; X: toluene; Y: trichlorethylene; Z: vinyl chloride.

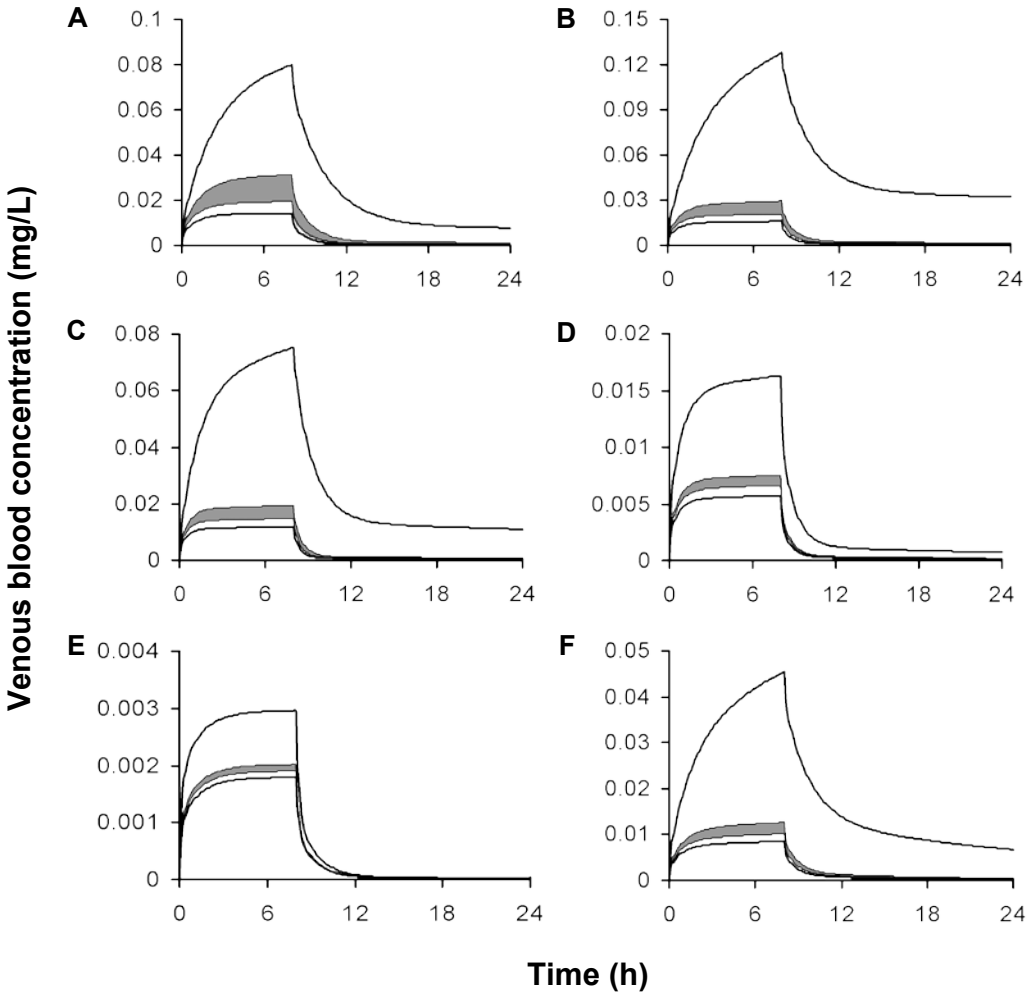

Figure 3. 24 hour simulation of the venous blood concentration following inhalation exposure to 1 ppm, 8 h for 26 volatile organic compounds considering maximum and minimum (bold lines) and QPPR-based hepatic extraction (grey area).

A: 1,1,1,2-tetrachloroethane; B: 1,1,2,2-tetrachloroethane; C: 1,1,2-trichloroethane; D: 1,1-dichloroethane; E: 1,1-dichloroethylene; F: 1,2-dichloroethane; G: 1,2-dichloroethylene (*cis*-); H: benzene; I: bromochloromethane; J: bromodichloromethane; K: carbon tetrachloride; L: chloroethane; M: chloroform; N: dibromomethane; O: dichloromethane; P: ethylbenzene; Q: hexachloroethane; R: isoprene; S: methyl chloride; T: *m*-xylene; U: *n*-hexane; V: pentachlorethane; W: styrene; X: toluene; Y: trichlorethylene; Z: vinyl chloride.

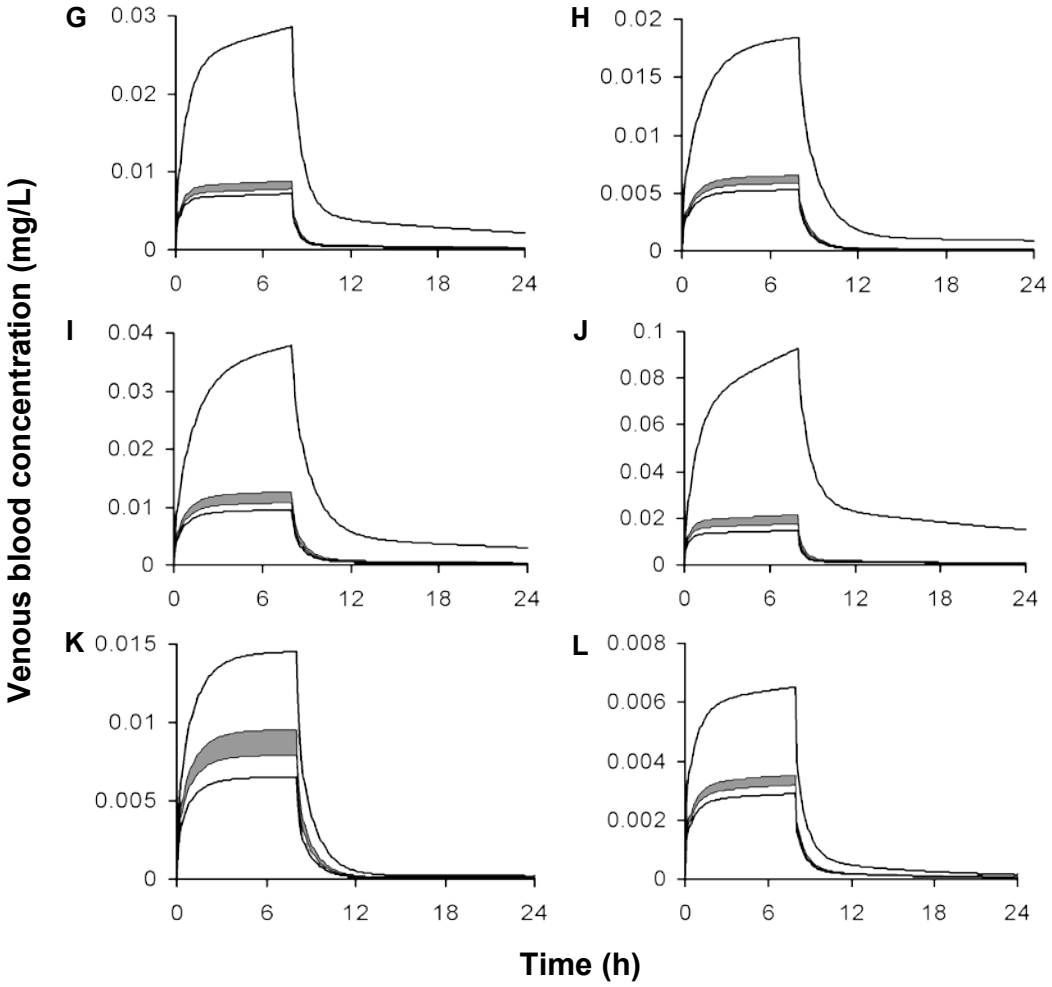

Figure 3. Suite

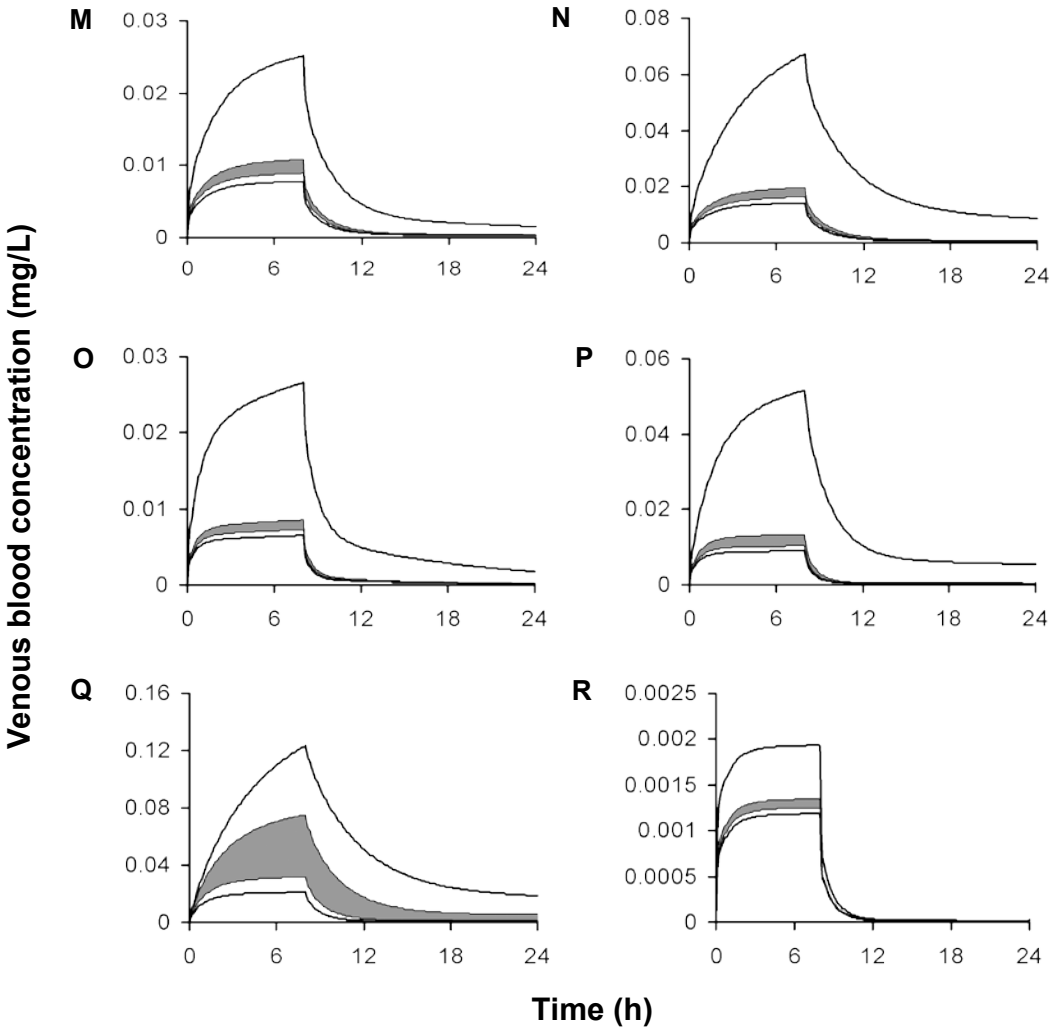

Figure 3. Suite

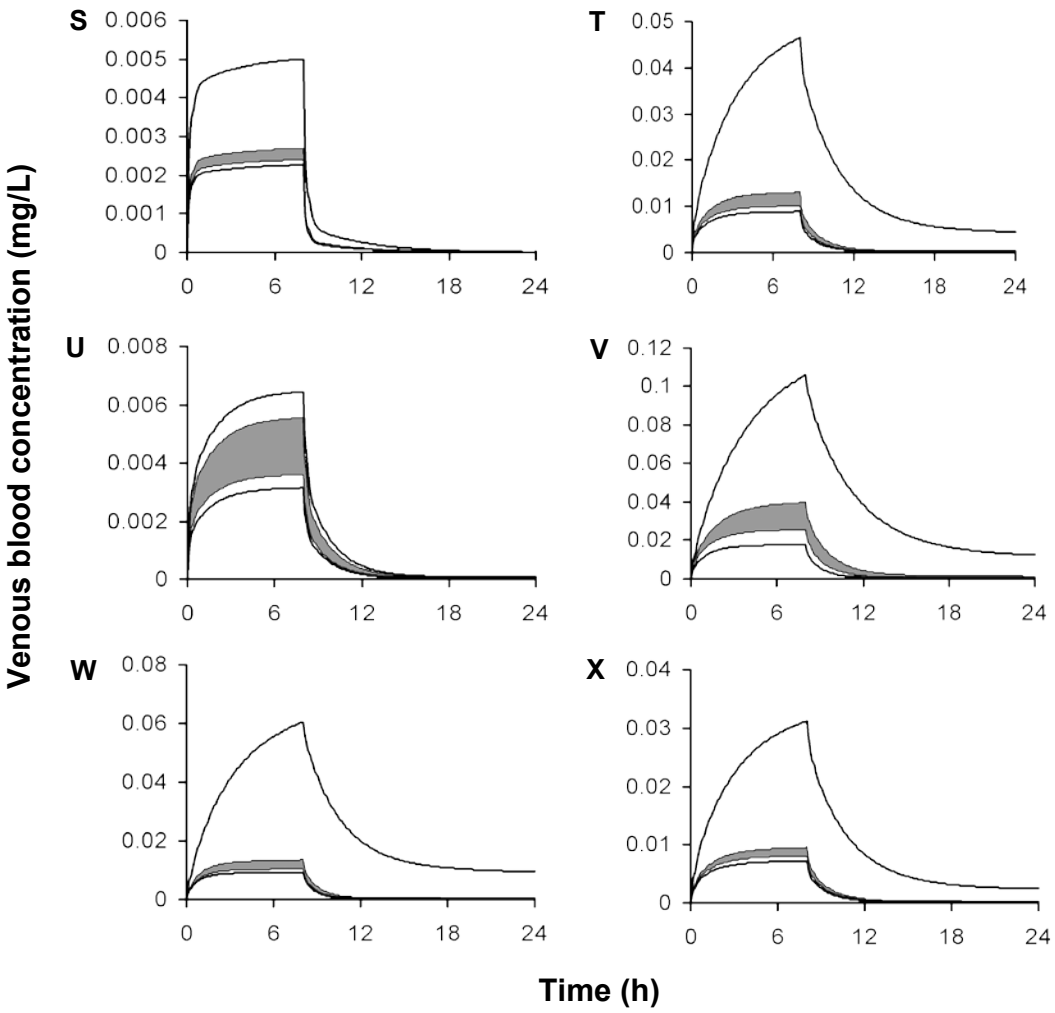

Figure 3. Suite

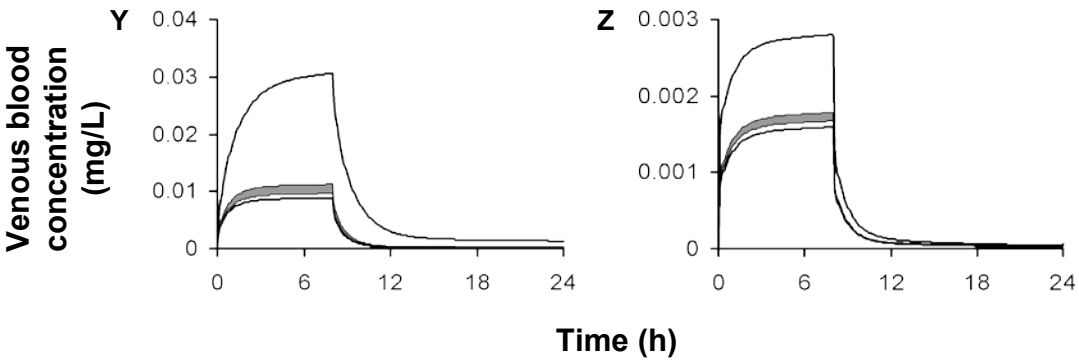

Figure 3. Suite

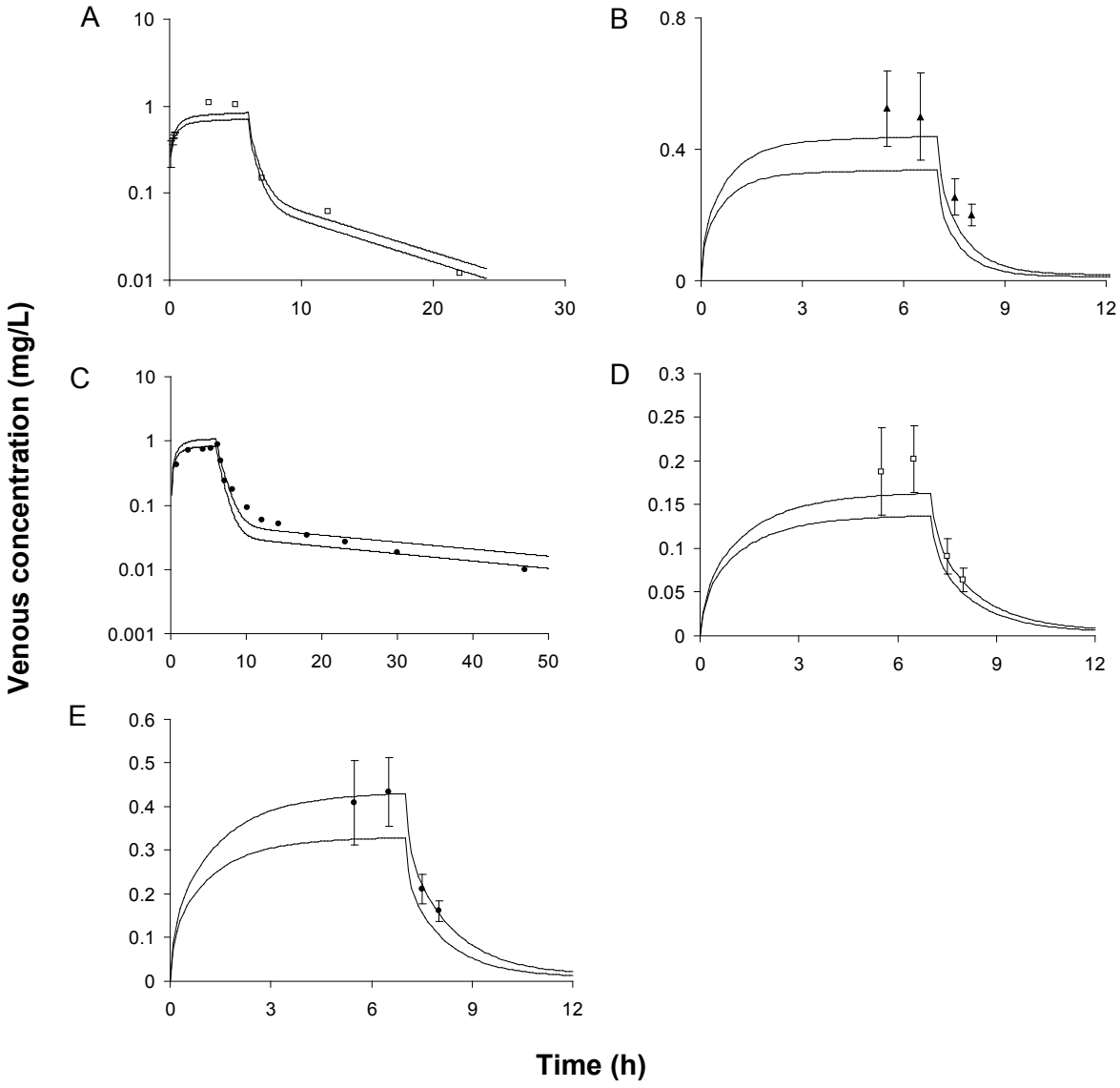

Figure 4. Comparison of PBPK model simulation with experimental data of venous blood concentration following inhalation exposure

to: A) 100 ppm, 6h dichloromethane [78]; B) 33 ppm, 7 h ethylbenzene [67]; C) 80 ppm, 6h styrene [77]; D) 17 ppm, 7 h toluene [67]; E) 33 ppm, 7 h m-xylene [67]. Bold lines: predicted LMCI and UMCI for CL_{int}.

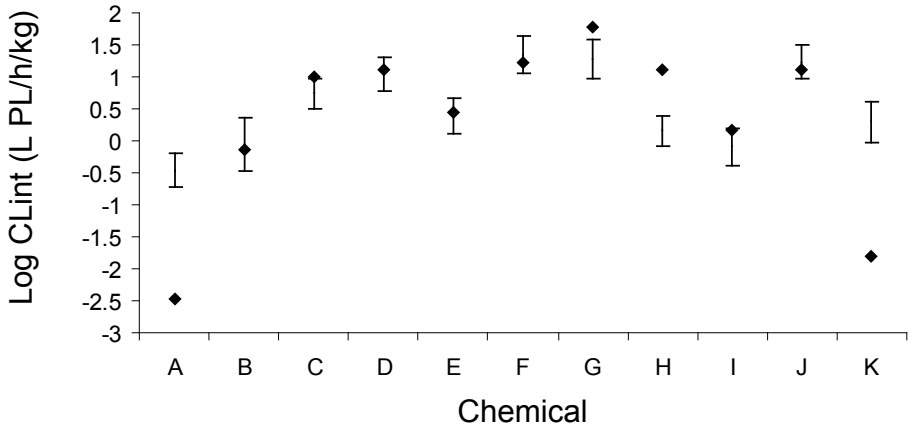

Figure 5. Comparison of the predicted log CL_{int} (LMCI and UMCI) with the experimental data on 11 VOCs.

The bars represent the QPPR predictions, the symbols the experimental values. A: 1,1,1-trichlororoethane; B: 1,2,4-trimethylbenzene; C: 1,2-dichloroethylene (trans-); D: bromoform; E: dibromochloromethane; F: ethylene ; G: furan; H: halothane; I: o-xylene; J: propylene; K: tetrachloroethylene.

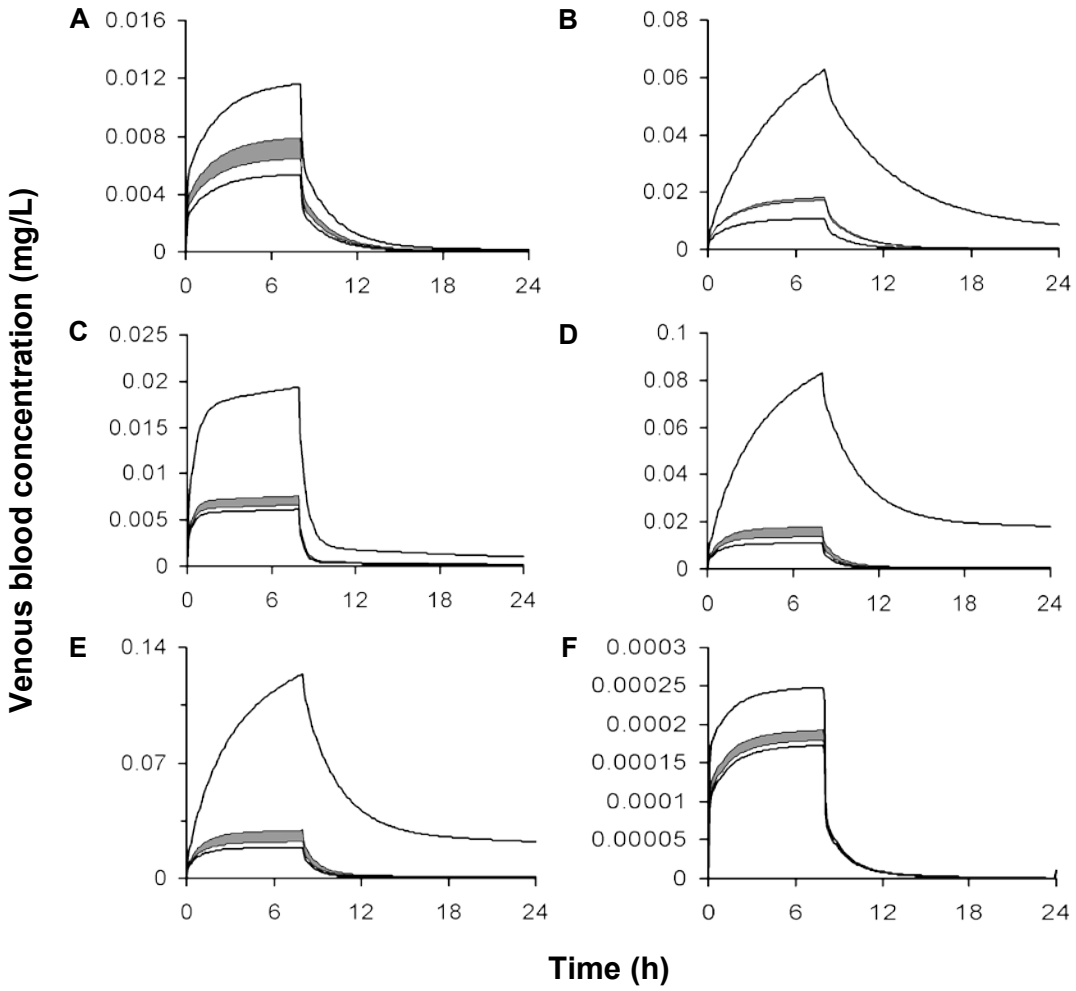

Figure 6. 24 hour simulation of the venous blood concentration following inhalation exposure to 1 ppm, 8 h for 11 volatile organic compounds considering maximum and minimum (bold lines) and QPPR-based hepatic extraction (grey area).

A: 1,1,1-trichlororoethane; B: 1,2,4-trimethylbenzene; C: 1,2-dichloroethylene (*trans*-); D: bromoform; E: dibromochloromethane; F: ethylene ; G: furan; H: halothane; I: *o*-xylene; J: propylene; K: tetrachloroethylene.

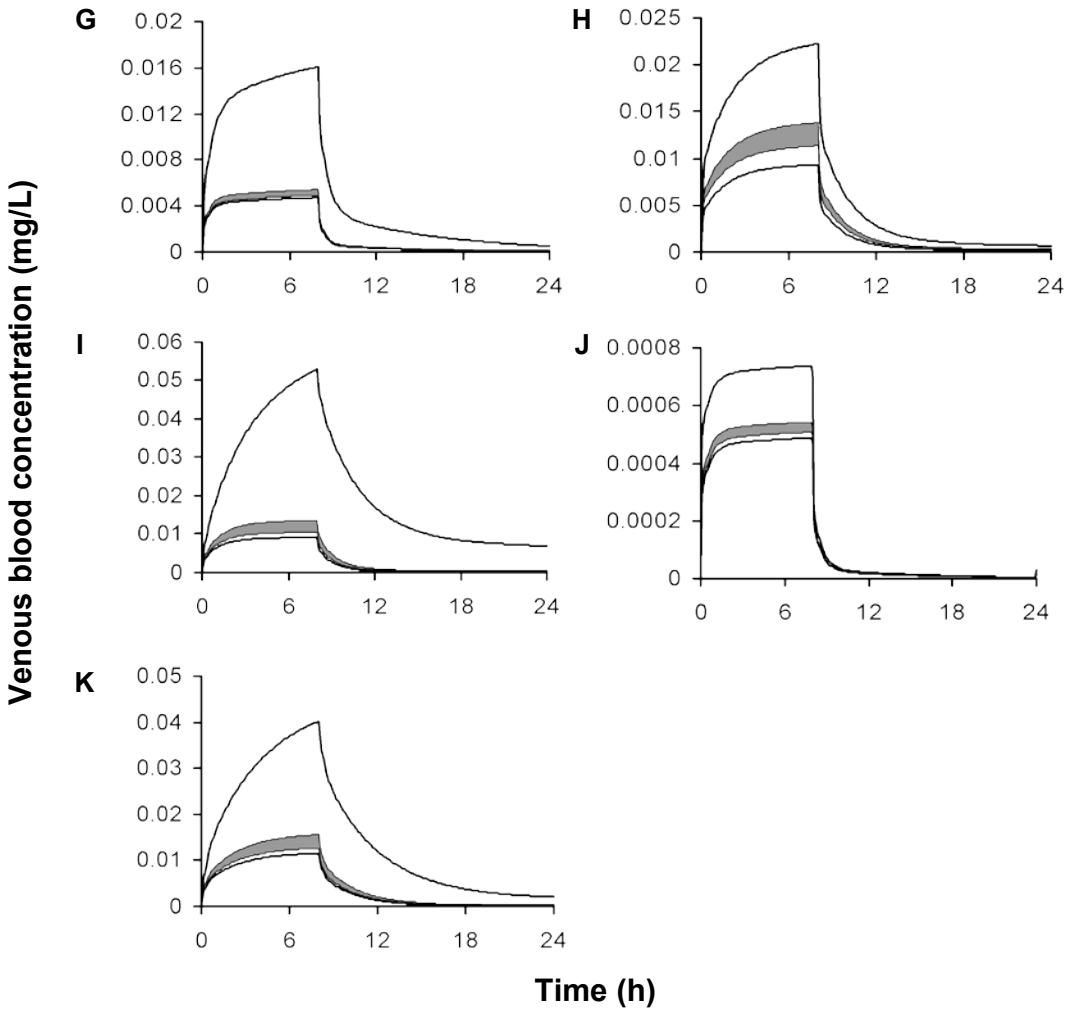

Figure 6. 24 hour simulation of the venous blood concentration following inhalation exposure to 1 ppm, 8 h for 11 volatile organic compounds considering maximum and minimum (bold lines) and QPPR-based hepatic extraction (grey area). A: 1,1,1-trichlororoethane; B: 1,2,4-trimethylbenzene; C: 1,2-dichloroethylene (*trans*-); D: bromoform; E: dibromochloromethane; F: ethylene ; G: furan; H: halothane; I: *o*-xylene; J: propylene; K: tetrachloroethylene.

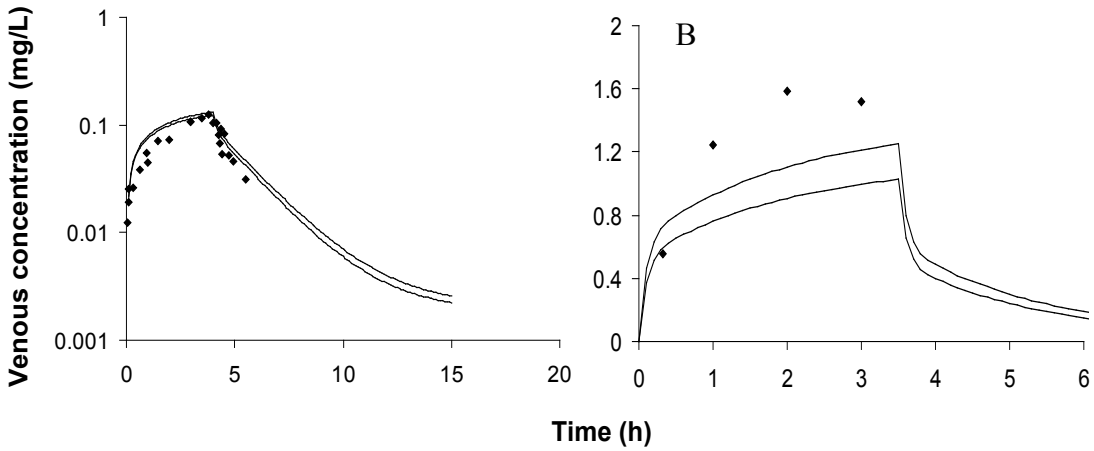

Figure 7. Comparison of PBPK model simulations (Bold lines: predicted LMCI and UMCI for CL_{int}) with experimental data of venous blood concentration following inhalation exposure to A) 8 ppm, 4h 1,2,4-trimethylbenzene [59], B) 175 ppm, 3.5 h 1,1,1-trichloroethane [85].

4.10. Supplementary data

The code of the human PBPK model for inhaled VOCs is provided in this supplemental material. The model is written in advance continuous simulation language to be run in ACSL® (acslX®, version 2.5, Aegis Technologies Group, Inc, Huntsville, AL). The model parameters are defined in the "initial" section and the differential equations are written in the "dynamic" section. PBPK consisted in four tissue compartments (liver, fat, richly, and poorly perfused tissues) and a gas exchange lung interconnected by blood flows. Two descriptions of hepatic clearance are available: one using the intrinsic clearance (CL_{int}) and the other the extraction ratio.

INITIAL

```
constant BW = 70.          ! Body weight (kg)
constant conc = 0          ! Exposition dose (ppm)
constant MW = 0            ! Molecular weight
constant SV = 24.450       ! Standard volume mL/mol
constant DUREE= 0          ! Exposure lenght (h)
constant periode = 0       ! Period between two exposures (h)
```

! Tissue volumes (fraction of body weight)

```
constant VLc = 0.026 ! Liver (fraction of body weight)
constant VRc = 0.05  ! Richly perfused tissues (fraction of body weight)
constant VSc = 0.62  ! Poorly perfused tissues (fraction of body weight)
constant VFc = 0.19  ! Fat (fraction of body weight)

VL = VLc*BW              ! Liver (L)
```

```
VR = VRc*BW              ! Richly perfused tissues (L)
VS = VSc*BW              ! Poorly perfused tissues (L)
VF = VFc*BW              ! Fat (L)
```

! Flows

```
constant QPc = 18 ! Alveloar ventilation (L/h/kg)
constant QCc = 18 ! Cardiac output (L/h/kg)

QP = QPc*BW**0.74 ! Alveloar ventilation (L/h)
QC = QCc*BW**0.74 ! Cardiac output (L/h)

constant QLc = 0.26 ! Liver (fraction of QC)
constant QRc = 0.44 ! Richly perfused tissues (fraction of QC)
constant QSc = 0.25 ! Poorly perfused tissues (fraction of QC)
constant QFc = 0.05 ! fat (%QC)

QL = QLc*QC ! Liver (L/h)
QR = QRc*QC ! Richly perfused tissues (L/h)
QS = QSc*QC ! Poorly perfused tissues (L/h)
QF = QFc*QC ! fat (L/h)
```

! Partition coefficients (PCs)

```
constant PB = 0.0      ! Blood:air
constant PLB = 0.0     ! Liver:blood
constant PRB = 0.0     ! RPT:blood
constant PSB = 0.0     ! PPT:blood
constant PFB = 0.0     ! Fat:blood
```

! Metabolism constants

constant logclint = 0.0 ! log CLint (L PL/h/kg)
CLintPL = 10**logclint ! CLint L PL/h/kg
constant pplb = 0.0 ! Phospholipids:blood PC

CLint = CLintPL * pplb * BW**0.75 ! CLint (L bloob/h)
constant KFC = 0.0 ! First order metabolism (h-kg)-1
KF = KFC * BW**0.3 ! First order metabolism (h-1)

! Hepatic clearance based on CLint and Kf
CLH = QL * (CLINT + KF * VL)/(QL + CLINT + KF * VL)

! Hepatic clearance based extraction ratio (E)
constant E = 0.0 ! Extraction ratio
! CLH = QL * E

END ! INITIAL

DYNAMIC
! Exposure scenario
JOURNE=PULSE(0.,periode,DUREE) ! 24 h exposure

CI=JOURNE*conc *MW / SV /1000 ! Inhaled concentration (mg/L)

! Blood concentrations

```
CA = (CI*QP+QC*CV)/(QC+QP/PB)        ! Arterial mg/L
CV = (QL*CVL+QR*CVR+QS*CVS+QF*CVF)/QC       ! Venous mg/L
AUC = INTEG(CV, 0.0)       ! Venous blood area under the curve (mg/L-h)

CALV = CA/PB*SV/MW*1000                ! Alveolar air PPM

! Tissue compartments

! Liver

rAL = QL*(CA-CVL) - CLH * CA   ! Rate of amount (mg/h)
AL = integ (rAL,0.0)                   ! Amount (mg)
CL = AL/VL                             ! Liver concentration (mg/L)
CVL = CL/PLB                           ! Liver venous blood concentration (mg/L)

! Richly perfused tissues

rAR = QR*(CA-CVR)          ! Rate of amount (mg/h)
AR = integ (rAR, 0.0)! Amount (mg)
CR = AR/VR                     ! Richly perfused tissues concentration (mg/L)
CVR = CR/PRB        ! Richly perfused tissues venous blood concentration (mg/L)

! Slowly perfused tissues

rAS = QS*(CA-CVS)! Rate of amount (mg/h)
AS = integ (rAS, 0.0) ! Amount (mg)
CS = AS/VS                     ! Poorly perfused tissues concentration (mg/L)
CVS = CS/PSB         ! Poorly perfused tissues venous blood concentration (mg/L)
```

! Fat

```
rAF = QF*(CA-CVF)          ! Rate of amount (mg/h)
AF = integ (rAF, 0.0)      ! Amount (mg)
CF = AF/VF                 ! Fat concentration (mg/L)
CVF = CF/PFB               ! Fat venous blood concentration (mg/L)

END ! DYNAMIC
```

Chapitre 5. Quantitative property-property relationships for predicting macro level and micro level pharmacokinetics of inhaled chemicals in rats

Article en préparation pour Chemical Research in Toxicology

Quantitative property-property relationships for predicting macro level and micro level pharmacokinetics of inhaled chemicals in rats

Thomas Peyret and Kannan Krishnan

Département de santé environnementale et santé au travail,

Université de Montréal, Canada H3T 1A8

Corresponding author : Kannan Krishnan, Pavillon Marguerite-d'Youville, 2375, chemin de la Côte Ste-Catherine, local 4095, H3T 1A8, Montréal, Québec, Canada

5.1. Abstract

The available quantitative structure-property relationships (QSPRs) and quantitative property-property relationships (QPPRs) for developing physiologically-based pharmacokinetic (PBPK) models have only been applied to predict macro level kinetics (i.e., tissue level). The objective of this study was to develop and integrate QPPRs within PBPK models to predict both the macro level (i.,e., whole body and tissues) and micro level (i.e., cells and fluids) pharmacokinetics of VOCs in rats. To predict the amount of chemical at the cellular level, each tissue was subdivided into 3 compartments namely the tissue cells, the interstitial fluid, and the vascular space, containing blood (plasma and erythrocytes) which were interconnected by permeation area cross products. QSPRs were developed to predict oil:air (P_{oa}) and hemoglobin:water (P_{hbw}) partition coefficients (PCs) on the basis of calculated values of octanol:water and water:air PCs. The QSPRs predicted reasonably well the experimental data on these PCs ($R^2 = 0.865$, $n = 148$ for P_{oa}; $R^2 = 0.732$, $n = 50$ for P_{hbw}; $Q^2 = 0.861$ for P_{oa}; $Q^2 = 0.727$ for P_{hbw}). The QSPRs were used along with predicted water:air PCs as input parameters in biologically-based algorithm for PCs (blood:air, interstitial fluid:blood and cell:insterstitial fluid PCs). The QSPRs and PC algorithms were then incorporated within a PBPK model along with a QPPR for intrinsic clearance (based on log P_{ow}, log P_{bw}: log blood:water PC and *IP*: ionization potential). The predicted inhalation toxicokinetics were within a 3 fold factor of experimental data for 7 VOCs. Overall, this study demonstrated the feasibility to predict the macro and micro level pharmacokinetics of inhaled chemicals in rats on the basis of molecular properties and descriptors.

Keywords: Quantitative structure property relationships; Physiologically based pharmacokinetic; Cellular dosimetry; Toxicokinetics; Volatile organic compounds

5.2. Introduction

There is growing interest in the development and use of predictive tools to screen the pharmacokinetic behavior of chemicals (*1, 2*). Physiologically based pharmacokinetic models have proven their ability to predict the internal dose of chemicals on the basis of mechanistic mathematical descriptions of the chemical's absorption, distribution, metabolism and excretion (*3*). Although these models can now be developed using readily available data on physiological parameters (e.g. tissue volumes, rates of blood perfusion, and alveolar ventilation), there are few experimental data available for the chemical-specific parameters (e.g. tissue:blood partition coefficients and metabolic constants), particularly for new compounds. Previously, quantitative structure-property relationship (QSPR) models were developed for those parameters and integrated within physiological based pharmacokinetic (PBPK) models to predict the toxicokinetics of VOCs on the basis of molecular structure information (*4-7*). The later QSPR models were based on the group contribution method of Gao (*8, 9*). This approach consisted of describing the molecule on the basis of particular molecular fragments or groups. Each fragment has a unique contribution to the endpoint or modeled response. The contributions of the groups are estimated from the experimental values of the endpoint of interest by multi-linear regression analysis. The QSPRs developed to be incorporated within PBPK models can be used when the available groups (CH_3, CH_2, CH, C, C=C, H, benzene ring, H on benzene ring, Br, Cl, F; in refs (*4-7*)) are alone sufficient to describe a given molecule. Accordingly, these QSPRs are limited to aliphatic and aromatic hydrocarbons and halogenated hydrocarbons. Hence, more experimental data are needed to increase the number of groups in the QSPR to enrich the applicability domain of the group contribution-based QSPRs. For example, a fragment-based QSPR developed by Meylan and Howard to predict the *n*-octanol:water partition coefficient (P_{ow}) has a wide domain of applicability because 130 molecular fragments are available to describe the molecule (*10*). The regression coefficients of the fragments were estimated using hundreds of experimental measures of the log P_{ow}.

Therefore, the development of QSPRs for PBPK parameters is limited by the poor availability of experimental data on PCs and metabolic constants. Using different molecular descriptors might lead to QSPRs for PBPK parameters with a wider domain of applicability. A QSPR model was recently developed to predict the hepatic intrinsic clearance (CL_{int}) on the basis of generic molecular descriptors (e.g. log P_{ow}, log blood:water PC, and calculated ionization potential) for VOCs (*11*). The incorporation of the bounds of the 95th confidence interval around the mean predicted CL_{int} within a PBPK model was useful in characterizing the impact of uncertainty in the metabolic rates on the toxicokinetics of inhaled VOCs in humans.

In some QSPR-PBPK models for VOCs (*4, 7*), the partition coefficients were calculated using biologically based algorithms. Such algorithms have the advantage of facilitating interspecies extrapolations (*4*). Due to the growing interest in cellular toxicity testing and high-throughput assays, it would be relevant to adapt the PBPK models to predict the internal dose at the cellular level. Such a cellular dosimetry model could be of potential interest in the context of *in vitro-in vivo* extrapolations. In this regard, a biologically based algorithm was developed to predict the PCs of environmental chemicals and drugs at both the macro (i.e., tissue) and micro (i.e., cell, fluids) levels (*12*). The input parameters of this algorithm consist of partition coefficients (i.e., the neutral lipids:water PC, the hemoglobin:water PC, the plasma proteins:water PC and the acidic phospholipid:water PC) and information on tissue composition (i.e., the volumes of neutral lipids, neutral phospholipids, acidic phospholipids, water, and proteins). The latter chemical-specific parameters in biologically based algorithms for PCs need to be determined experimentally or estimated with animal-alternative methods. Since most of the volatile environmental pollutants of current interest are neutral compounds and do not significantly bind to plasma proteins, the values of their plasma protein:water and acidic phospholipid:water PCs are negligible. The biotic neutral lipid:water PC can be approximated by the oil:water or the *n*-octanol:water PC (*13, 14*). Nevertheless, the oil:water PC should be preferred to the *n*-octanol:water PC because the former overestimates the partitioning of hydrophilic

compounds (e.g. alcohols and ketones) into the biotic neutral lipids (*14*). The phospholipid:water PC is calculated as 30 percent of the value of the neutral lipid:water PC plus 0.7, based on the phosphatidylcholine hydrophilic/lipophilic balance (*15*). Consequently, for a molecular-structure-based estimation of the PCs with a mechanistic algorithm, two chemical-specific input parameters (i.e. oil:water, hemoglobin:water) need to be predicted using QSPR models. Béliveau *et al*. (*4*) developed QSPR models for the oil:air, water:air and blood protein (i.e., hemoglobin, for relatively hydrophobic VOCs):air PCs based on the occurrence of structural groups; however, there are no QSPRs predicting these endpoints on the basis of other molecular descriptors. Some solvent-solvent relationships between the oil:water and *n*-octanol:water PCs are available in the literature (*16*-*18*). For adequate reproducibility of the predictions made by the model, however, the value of the *n*-octanol:water PC should be obtained from the same source as was used to develop the model, and the domain of the application should be documented (*19*). Therefore, it could be interesting to calibrate a QSPR for the partitioning in oil with a validated and easy-to-access predictive tool for the *n*-octanol:water PC, such as KOWWIN (EPI SUITE^{TM}, USEPA, http://www.epa.gov/oppt/exposure/pubs/episuite.htm). QSPRs are not available to predict the hemoglobin:water PCs of VOCs, apart from a limited group contribution approach. Consequently, QSPR models must be developed for the neutral lipid:water and hemoglobin:water PCs to estimate the PCs for PBPK models solely on the basis of molecular information.

The objective of the present study was to develop a tool to predict the pharmacokinetics of VOCs at both the micro (i.e., cells and fluids) and macro (i.e. tissues) levels on the basis of molecular structure in rats. For this purpose, i) QSPR models were developed for the oil:water and hemoglobin:water PCs, ii) a cellular dosimetry QSPR-PBPK model was developed for rats, and iii) a QPPR model for CL_{int} and a QSPR model for PCs were incorporated within the cellular dosimetry model to predict the toxicokinetics of inhaled VOCs in rats.

5.3. Methods

5.3.1 QSPR for PCs

The PCs, representing the relative distribution of a chemical between two matrices (e.g., matrix:water PCs), can be predicted follows (*12*):

$$P_{mw} = F_{wm} + P_{ow} \cdot F_{nlm} + P_{prw} \cdot F_{prm} \quad [1]$$

where P_{mw} is the matrix:water PC; F_{wm} is the fractional volume of water-equivalent in the matrix; F_{nlm} is the fractional volume of neutral lipid-equivalent in the matrix; F_{prm} is the fractional volume of binding proteins in the matrix; P_{ow} is the vegetable oil:water PC; and P_{prw} is the protein:water PC.

The volume of water-equivalent corresponds to the sum of the volumes of water and 70% of the neutral phospholipids, whereas the neutral lipid-equivalent volume refers to the sum of the volumes of the neutral lipids and 30% of the neutral phospholipids (*15*). The compositions of the tissue cells, interstitial fluid, plasma and erythrocytes (F_{nl}, F_w, F_{pr}) in rats were obtained from the literature (*12*). Due to lack of experimental evidence, binding of VOCs in the tissue cells, interstitial fluid and plasma, was assumed to be negligible; accordingly, the protein:water PC was set equal to 0 for these matrices. Then, for all the tissue and blood compartments (i.e. tissue cells and interstitial fluid for tissue; erythrocytes and plasma for blood), the matrix:water PCs were calculated on the basis of the QSPRs for the oil:water PC (P_{ow}) and the hemoglobin:water PC. The neutral lipid:water PC was calculated as the ratio of the oil:air PC to the water:air PC predicted by HENRYWIN (EPISUITE™, US EPA). The QSPR models for P_{oa} and hemoglobin:water PC (P_{hbw}) were both developed in the present study.

QSPR for hemoglobin:water PC

Chemicals and data source

The QSPR analysis of P_{hbw} was undertaken for 50 alkanes, halogenated alkanes, alkenes, aromatic hydrocarbons, halogenated aromatic hydrocarbons [Chemical name (CAS RN): 1,1,1,2-tetrachloroethane (630-20-6); 1,1,1-trichloroethane (71-55-6); 1,1,1-trifluoro-2-chloroethane (151-67-7); 1,1,2,2-tetrachloroethane (79-34-5); 1,1,2-trichloroethane (79-00-5); 1,1-dichloroethane (75-34-3); 1,1-dichloroethylene (75-35-4); 1,2-dibromoethane (106-93-4); 1,2-dichloroethane (107-06-2); 1,2-dichloropropane (78-87-5); 1-bromo-2-chloroethane (107-04-0); 1-chloropropane (540-54-5); 2,2,4-trimethylpentane (540-84-1); 2,3,4-trimethylpentane (565-75-3); 2-chloropropane (75-29-6); allyl chloride (107-05-1); benzene (71-43-2); bromochloromethane (74-97-5); carbon tetrachloride (56-23-5); chlorobenzene (108-90-7); chloroethane (75-00-3); chlorofluoromethane (593-70-4); chloroform (67-66-3); chloromethane (74-87-3); *cis*-1,2-dichloroethylene (156-59-2); cyclohexane (110-82-7); dibromochloromethane (124-48-1); dibromomethane (74-95-3); dichloromethane (75-09-2); halothane (75-88-7); hexachloroethane (67-72-1); isoprene (78-79-5); isopropylbromide (75-26-3); *m*-methylstyrene (100-80-1); *m*-xylene (108-38-3); *n*-heptane (142-82-5); *n*-hexane (110-54-3); *n*-propyl bromide (106-94-5); *o*-xylene (95-47-6); pentachloroethane (76-01-7); *p*-methylstyrene (622-97-9); *p*-xylene (106-42-3); styrene (100-42-5); tetrachloroethylene (127-18-4); toluene (108-88-3); *trans*-1,2-dichloroethylene (156-60-5); trichloroethylene (79-01-6); JP-10 (2825-82-3); vinyl bromide (593-60-2); vinyl chloride (75-01-4)]. The P_{hbw} was calculated from experimental values of the rat blood:air, oil:air and saline:air PCs (*20*) for selected VOCs. Any chemicals with a log P_{ow} value below 1 (i.e., 1- and 2-nitropropanes, difluoromethane) as predicted by KOWWIN (EPI SUITE^{TM}, US EPA) or containing oxygen (i.e., diethyl ether, isoflurane and the nitropropanes) were not included in the dataset because they are not thought to significantly bind to hemoglobin (*21*).

Modeling endpoint

The protein:water PC, P_{prw}, required for solving the PC algorithm (Eq. 1) corresponds to P_{hbw} (in the case of blood), which was calculated as follows (*12*):

$$P_{hbw} = \frac{\left(\frac{P_{bw} - F_P \cdot P_{pw}}{F_e}\right) - \left(F_{we} + P_{ow} \cdot F_{nle}\right)}{F_{pre}} \quad [2]$$

where F_p is the fractional volume of plasma in the blood; F_e is the fractional volume of erythrocyte in the blood; P_{hbw} is the hemoglobin:water PC; P_{bw} is the blood:water PC; P_{pw} is the plasma:water PC; F_{nle} is the fractional content of the neutral lipid-equivalent in the erythrocyte; F_{we} is the fractional content of the water-equivalent in the erythrocyte; F_{pre} is the fractional content of proteins (hemoglobin) in the erythrocyte.

In Eq. 2, the value of P_{bw} was calculated as the ratio of the experimental measures of blood:air PC to saline:air PC. The plasma:water PC (P_{pw}) was calculated using Eq. 1. The values of the rat blood composition parameters (i.e. F_{nle}, F_{we}, F_{pre}, F_e, $F_{p,}$ along with the plasma composition) were obtained from the literature (*12*).

Variable selection

Previous studies have reported that VOCs bind to hydrophobic pockets in hemoglobin (*21, 22*). Moreover, the size and/or shape of the chemical can limit its crossing through the erythrocyte membrane (*23*) and, consequently, its docking to the hemoglobin binding site.

Therefore, the variables used to describe the hydrophobicity, size and shape of the chemicals were log P_{ow}, the length, width, and depth of the molecule, and the Kappa-2 index (*24*). The values of log P_{ow} were estimated using KOWWIN (EPI SUITE^{TM}, US

EPA, http://www.epa.gov/), while the other molecular descriptors were calculated with commercially available software (Molecular Modeling Pro, ChemSW, Inc. Fairfield, CA).

QSPR for oil:air PC

Chemicals and data source

Experimental data on the oil:air PC were collected from the literature for 150 halogenated and/or non-halogenated alkanes, alkenes, aromatic hydrocarbons, nitropropanes, ethers, epoxy compounds, ketones, acetates, alcohols [Chemical name (CAS RN): 1,1,1,2-tetrachloroethane (630-20-6); 1,1,1,2-tetrafluoroethylmonofluorochloromethyl ether (56885-28-0); 1,1,1-trichloroethane (71-55-6); 1,1,1-trifluoro-2-chloroethane (75-88-7); 1,1,1-trifluoroethyl-difluoro-monochloromethyl ether (33018-78-9); 1,1,2,2-tetrachloroethane (79-34-5); 1,1,2,2-tetrachloroethylene (127-18-4); 1,1,2-trichlorethane (79-00-5); 1,1-dichloro-1-fluoroethane (1717-00-6); 1,1-dichloroethane (75-34-3); 1,1-dichloroethylene (75-35-4); 1,1-difluoro-2-chloroethylene (359-10-4); 1,2,3-trimethylbenzene (526-73-8); 1,2,4-trifluorobenzene (367-23-7); 1,2,4-trimethylbenzene (95-63-6); 1,2-dibromoethane (106-93-4); 1,2-dichloroethane (107-06-2); *cis*-1,2-dichloroethylene (156-59-2); *trans*-1,2-dichloroethylene (156-60-5); 1,2-dichloropropane (78-87-5); 1,3,5-trifluorobenzene (372-38-3); 1,3,5-trimethylbenzene (108-67-8); 1,3-butadiene (106-99-0); 1-bromo-2-chloroethane (107-04-0); 1-bromopropane (106-94-5); 1-chlorobutane (109-69-3); 1-chloropentane (543-59-9); 1-chloropropane (540-54-5); 1-methoxy-2-propanol (107-98-2); 1-nitropropane (108-03-2); 2,2,4-trimethylpentane (540-84-1); 2,2-dichloro-1,1,1-trifluoroethane (306-83-2); 2,2-dimethylbutane (75-83-2); 2,3,4-trimethyl pentane (565-75-3); 2-bromo-1,1,1,2-tetrafluoroethane (124-72-1); 2-butoxyethanol (111-76-2); 2-chloro-1,1,1-trifluoroethane (1330-45-6); 2-chloropropane (75-29-6); 2-cyanoethylene oxide (4538-51-6); 2-ethoxyethanol (110-80-5); 2-isopropoxyethanol (109-59-1); 2-methoxyethanol (109-86-4); 2-methylpentane (107-83-5); 2-nitropropane (79-46-9); 3-methylhexane (589-34-4); 3-methylpentane

(96-14-0); acetone (67-64-1); acrylic acid (79-10-7); acrylonitrile (107-13-1); aliflurane (56689-41-9); allyl chloride (107-05-1); allylbenzene (300-57-2); benzene (71-43-2); bromochloromethane (74-97-5); butadiene monoxide (930-22-3); carbon dioxide (124-38-9); chlorobenzene (108-90-7); chlorodifluoromethane (75-45-6); chloroethane (75-00-3); chlorofluoromethane (593-70-4); chloroform (67-66-3); chloromethane (74-87-3); cumene (98-82-8); cycloheptane (291-64-5); cyclohexane (110-82-7); cyclopentane (287-92-3); cyclopropane (75-19-4); dibromochloromethane (124-48-1); dibromomethane (74-95-3); dichloromethane (75-09-2); diethyl ether (60-29-7); diethyl ketone (96-22-0); difluoromethane (75-10-5); divinyl ether (109-93-3); enflurane (13838-16-9); epoxybutene (930-22-3); ethane (68475-58-1); ethanol (64-17-5); ethyl acetate (141-78-6); ethyl *t*-butyl ether (637-92-3); ethyl *t*-pentyl ether (919-94-8); ethylbenzene (100-41-4); ethylene (74-85-1); ethyne (74-86-2); fluorobenzene (462-06-6); fluroxene (406-90-6); halopropane (679-84-5); halothane (151-67-7); hexachloroethane (67-72-1); hexafluorobenzene (392-56-3); isobutanol (78-83-1); isobutyl acetate (110-19-0); isoflurane (26675-46-7); isopentanol (123-51-3); isopentyl acetate (123-92-2); isopropanol (67-63-0); isopropyl acetate (108-21-4); isopropylbromide (75-26-3); JP-10 (2825-82-3); *m*-dichlorobenzene (541-73-1); methane (74-82-8); methanol (67-56-1); methoxyflurane (76-38-0); methyl acetate (79-20-9); methyl ethyl ketone (78-93-3); methyl isobutyl ketone (108-10-1); methyl *n*-pentyl ketone (110-43-0); methyl *n*-propyl ketone (107-87-9); Methyl t-butyl ether (1634-04-4); Methylcyclopentane (96-37-7); methyl-n-butyl ketone (591-78-6); methylpentafluorobenzene (771-56-2); *m*-methylstyrene (100-80-1); *m*-xylene (108-38-3); *n*-butane (106-97-8); *n*-butanol (71-36-3); *n*-butyl acetate (123-86-4); *n*-decane (124-18-5); *n*-heptane (142-82-5); *n*-hexane (110-54-3); *n*-hexanol (25917-35-5); *n*-octane (111-65-9); *n*-octanol (111-87-5); *n*-pentane (109-66-0); *n*-pentanol (71-41-0); *n*-pentyl acetate (628-63-7); *n*-propanol (71-23-8); *n*-propyl acetate (109-60-4); *o*-dichlorobenzene (95-50-1); *o*-difluorobenzene (367-11-3); *o*-xylene (95-47-6); *p*-chlorobenzotrifluoride (98-56-6); *p*-difluorobenzene (540-36-3); pentachloroethane (76-01-7); pentafluorobenzene (363-72-4); *p*-methylstyrene (622-97-9); propylbenzene

(103-65-1); *p*-xylene (106-42-3); sevoflurane (28523-86-6); styrene (100-42-5); *t*-butanol (75-65-0); teflurane (124-72-1); tetrachloroethylene (127-18-4); tetrachloromethane (56-23-5); thiomethoxyflurane (2045-53-6); toluene (108-88-3); trichloroethylene (79-01-6); vinyl bromide (593-60-2); vinyl chloride (75-01-4)] (*14, 20, 25-43*). In the studies that used literature data (*27, 38*), the source of the data was verified to avoid duplicates from the same study. In other words, for a given chemical, the value of P_{oa} was taken from one of these studies only if it was the sole reference for P_{oa}. For all chemicals, when different values were reported, the average was used for the QSPR analysis.

Variable selection

The oil:air PC was calculated as the product of the oil:water PC times the water:air PC. Both log P_{ow} and log P_{wa} at 37°C as predicted by EPI SUITE™ (US EPA, http://www.epa.gov/) were used as predictors of the oil:air PC (*16*, *18*).

Evaluation of QSPR for PCs

The QSPR models for PCs were evaluated by comparing the predictions of the fat:air, muscle:air, liver:air and blood:air PCs to the experimental data on 76 VOCs (1,1,1,2-tetrachloroethane; 1,1,1-trichloroethane; 1,1,1-trifluoro-2-chloroethane; 1,1,2,2-tetrachloroethane; 1,1,2-trichloroethane; 1,1-dichloroethane; 1,1-dichloroethylene; 1,2-dibromoethane; 1,2-dichloroethane; 1,2-dichloropropane; 1-bromo-2-chloroethane; 1-chloropropane; 1-nitropropane; 2,2,4-trimethylpentane; 2,3,4-trimethylpentane; 2-chloropropane; 2-nitropropane; allylchloride; benzene; bromochloromethane; carbon tetrachloride; chlorobenzene; chloroethane; chlorofluoromethane; chloroform; chloromethane; *cis*-1,2-dichloroethylene; cyclohexane; dibromochloromethane; dibromomethane; dichloromethane; diethyl ether; difluoromethane; dimethyl ketone; ethanol; ethyl acetate; halothane; hexachloroethane; isobutanol; isobutyl acetate; isoflurane;

isopentanol; isopentyl acetate; isoprene; isopropanol; isopropyl acetate; isopropylbromide; JP-10; methanol; methyl acetate; methyl ethyl ketone; methyl isobutyl ketone; *m*-methylstyrene; methyl *n*-pentyl ketone; methyl *n*-propyl ketone; *m*-xylene; *n*-butanol; *n*-butyl acetate; *n*-heptane; *n*-hexane; *n*-pentanol; *n*-pentyl acetate; *n*-propanol; *n*-propyl acetate; *n*-propyl bromide; o-xylene; pentachloroethane; *p*-methylstyrene; *p*-xylene; styrene; tetrachloroethylene; toluene; *trans*-1,2-dichloroethylene; trichloroethylene; vinyl bromide; and vinyl chloride) in rats (*14, 20, 32, 44*). The QSPR predictions of P_{hbw}, P_{ow} and P_{wa}, along with the rat tissue and blood composition data, were incorporated within an algorithm to calculate the tissue:air PC (Eq. 3) and blood:air PCs (Eq. 4), as follows:

$$P_{ta} = \left[F_{ct} \cdot \left(P_{ow} \cdot F_{nlct} + F_{wct}\right) + F_{it} \cdot F_{wit}\right] \cdot P_{wa} \quad [3]$$

$$P_{ba} = \left[F_{e} \cdot \left(P_{ow} \cdot F_{nle} + F_{we} + P_{hbw} \cdot F_{pre}\right) + F_{p} \cdot \left(P_{ow} \cdot F_{nlp} + F_{wp}\right)\right] \cdot P_{wa} \quad [4]$$

where F_{ct} is the fractional volume of cells in the tissue; F_{it} is the fractional volume of interstitial fluid in the tissue; F_e is the fractional volume of erythrocyte in the blood; F_p is the fractional volume of plasma in the blood; F_{nlct} is the fractional content of the neutral lipid-equivalent in the tissue cell; F_{nle} is the fractional content of the neutral lipid-equivalent in the erythrocyte; F_{nlp} is the fractional content of the neutral lipid-equivalent in the plasma; F_{wct} is the fractional content of the water-equivalent in the tissue cell; F_{wct} is the fractional content of the water in the interstitial fluid; F_{we} is the fractional content of the water-equivalent in the erythrocyte; F_{wp} is the fractional content of the water-equivalent in the plasma; F_{pre} is the fractional content of binding proteins (hemoglobin) in the erythrocyte; P_{ta} is the tissue:air PC; P_{ba} is the blood:air PC; P_{hbw} is the hemoglobin:water PC; P_{ow} is the oil:water PC; and P_{wa} is the water:air PC.

Statistical analysis of quantitative relationship models

A multiple linear regression approach was used to develop the QSPR models. The regression analysis was performed using SPSS v16 for Windows (SPSS Inc., Chicago, IL). A stepwise method was used to include the variables in the model. The coefficient of determination (R^2) and the adjusted R^2 (R^2_{adj}) were calculated. Like the R^2, the R^2_{adj} is an indicator of the goodness of fit, but it accounts for the degree of freedom in the model. Data points were considered to be outliers when the absolute value of their studentized residual was equal to 3 or above (*45*). The normality of the residuals was checked by normal probability plots of the standardized residuals (i.e. expected normal cumulative probability versus observed cumulative probability). Leave-one-out cross validation was conducted, and the results were expressed in terms of Q^2 (Q^2 = 1 – the predicted residual sum of squares / the sum of squares of the response values). The statistical significance ($p < 0.05$) of the independent variables was estimated by a *t* statistic test. The high correlation between two independent variables in the model refers to multicollinearity, which can lead to the calculation of erroneous values for regression coefficients and non-significant *t* tests (*45*). The multicollinearity of the variables in the model was assessed by calculating the variance inflation factor (VIF) for all independent variables (*45*). For each model, the application domain was documented by reporting the ranges of values of the descriptors and the modeled response.

A QSPR model was considered adequate when the values of R^2 and R^2_{adj} were above 0.6 (*46*), the value of Q^2 was 0.6 or greater (*47*), and the independent variables were not highly correlated (i.e., VIF < 4, (*45*)).

5.3.2 Cellular dosimetry modeling

Model representation

The cellular dosimetry model for inhaled VOCs in rats is illustrated in Figure 1. In this PBPK model, the organism was described by four tissue compartments (i.e. liver, fat, richly perfused tissues, poorly perfused tissues) and a lung exchange compartment interconnected by systemic circulation (*48*). To predict the amount of chemical at the cellular level, each tissue was subdivided into 3 compartments, namely, the tissue cells, the interstitial fluid and the vascular space, which contained blood (plasma and erythrocytes). These compartments were interconnected by permeation-area cross products (*49*).

The amount of VOC in the tissue intracellular space was calculated from the concentration of the chemical in the interstitial fluid and the cell:interstitial fluid PC.

For non-metabolizing tissues, the rate of accumulation of VOC in cells was calculated as follows:

$$\frac{dA_{ct}}{dt} = PA_{cif_t} \cdot \left(C_{if} - \frac{C_{ct}}{P_{cif_t}} \right) \qquad [5]$$

where A_{ct} is the amount of VOC in the intercellular compartment of tissue t cell (μmol); $PA_{cif\,t}$ is the permeation area cross product between the tissue cell and interstitial fluid (L/h); C_{if} is the concentration of chemical in the interstitial fluid of the tissue (μM); C_{ct} is the concentration of chemical in the cells of the tissue (mg/L); and $P_{cif\,t}$ is the tissue cell:interstitial fluid PC.

The metabolism of VOCs in hepatocytes, based on the mass balance differential equation, was computed as follows:

$$\frac{dA_{cl}}{dt} = PA_{cif\ l} \cdot \left(C_{ifl} - \frac{C_{cl}}{P_{clif\ l}} \right) - \frac{dA_{met}}{dt} \qquad [6]$$

where A_{cl} is the amount of VOC in hepatocytes in liver (l) (µmol); A_{met} is the amount metabolized VOCs (µmol); $PA_{cif\ l}$ is the permeation area cross product between the hepatocyte and the interstitial fluid (L/h); C_{ifl} is the concentration in the interstitial fluid of the liver (µM); C_{cl} is the intracellular concentration in the liver; and P_{clifl} is the hepatocyte:interstitial fluid PC.

In the hepactocytes, the rate of metabolism, dAmet/dt (Eq. 6), was described as a linear process involving intrinsic clearance (3).

The mass-balance differential equation for the amount of chemical in the interstitial fluid was calculated from the interstitial fluid:blood PC and the concentrations of the blood and tissue cells, as follows:

$$\frac{dA_{ift}}{dt} = PA_{bif} \cdot \left(C_{vt} - \frac{C_{if\ t}}{P_{ib}} \right) + PA_{cif\ t} \cdot \left(\frac{C_{c\ t}}{P_{cif\ t}} - C_{if\ t} \right) \qquad [7]$$

where A_{ift} is the amount in the interstitial fluid of tissue t (µmol); C_{vt} is the concentration in blood leaving the tissue; PA_{bif} is the permeation area cross product between the blood and the interstitial fluid (L/h); $PA_{cif\ t}$ is the permeation area cross product between the tissue cell and the interstitial fluid (L/h); C_{ift} is the concentration in the interstitial fluid of the tissue (µM); C_{ct} is the intracellular concentration of the tissue (µM); P_{ib} is the interstitial fluid:blood PC; and P_{cift} is the tissue cell:interstitial fluid PC.

The rate of the amount of VOC in the vascular subcompartment of the tissue was calculated as follows:

$$\frac{dA_{bt}}{dt} = Q_t \cdot \left(C_a - C_{vt}\right) + PA_{bif} \cdot \left(\frac{C_{ift}}{P_{ib}} - C_{vt}\right) \quad [8]$$

where A_{bt} is the amount in tissue vascular space (μmol); Q_t is the tissue blood flow; PA_{bif} is the permeation area cross product between the blood and the interstitial fluid (L/h); C_a is the arterial concentration; C_{vt} is the concentration in blood leaving the tissue; C_{ift} is the concentration in the interstitial fluid of the tissue (μM); and P_{ib} is the interstitial fluid:blood PC.

Physiological parameters

The rat cardiac output, alveolar ventilation, blood flow and tissue volume were obtained from the literature (*48*). Table 1 presents the numerical values of the volumes of the tissue subcompartments (i.e., interstitial space, tissue cell and vascular space) as fraction of the tissue volume. The values of interstitial fluid and vascular spaces were obtained from Kawai *et al*. (*50*). The fractional volume of cells was estimated by subtracting the interstitial and vascular spaces from the whole tissue space. For the poorly perfused tissues, the values for the fraction of the tissue volume occupied by the interstitial fluid and vascular spaces correspond to the average for muscle and skin. For the richly perfused tissues, the values of fractional content are the means of the data for kidney, thymus, lung, heart, stomach, gut, spleen and pancreas. The perfusion-limited tissue uptake was obtained by setting the values of the permeation area cross product coefficients >> Q_t (tissue blood flow, Eq. 8). Therefore, for each tissue compartment *t*, the value of these coefficients (PA_{bif} *and* PA_{cif}, Eq. 5-7) were equal to 1000 x Q_t.

Partition coefficients

The partition coefficients used in the PBPK model (i.e. interstitial fluid:blood, P_{ib} and tissue cell:interstitial fluid, P_{ci}) were estimated using a biologically based algorithm by combining diverse matrix:water PCs (Eq. 1) (*12*). The value of P_{ci} was calculated as the ratio of the cell:water PC (P_{cw}) to the interstitial fluid:water PC (P_{iw}), whereas P_{ib} was calculated as follows (*12*):

$$P_{ib} = \frac{P_{iw}}{P_{pw} \cdot F_p + P_{ew} \cdot F_e} \qquad [9]$$

where P_{ib} is the interstitial fluid:blood PC; P_{iw} is the tissue interstitial fluid:water PC; P_{ew} is the erythrocyte:water PC; P_{pw} is the plasma:water PC; F_e is the fractional content of erythrocytes in the blood; and F_p is the fractional content of plasma in the blood.

The denominator of Eq. 9 refers to the blood:water PC, which is the mean of P_{ew} and P_{pw} weighted on the relative volumes of erythrocytes and plasma. P_{cw}, P_{iw}, P_{pw}, P_{ew} were calculated according to Eq. 1 using QSPR predictions for P_{ow}, and P_{hbw}, along with the composition of cells and fluid in the tissue and vascular space (*12*). The proportions of erythrocytes (F_e) and plasma (F_p) in the blood were 40% and 60%, respectively.

In the PBPK model, the value of the blood:air PC was calculated as the QSPR prediction of the blood:water PC times the water:air PC. The value of P_{wa} at 37.5°C was predicted with HENRYWIN (EPI SUITE^{TM}, US EPA, http://www.epa.gov/).

Metabolic constants

In the PBPK model, the rate of metabolism was described on the basis of intrinsic clearance. The value of CL_{int} (L PL/h/kg$^{0.75}$) was calculated with a previously developed

QPPR and converted to L blood/h/kg$^{0.75}$ by multiplying it by P_{plb} (*11*). The CL_{int} (L PL/h/kg$^{0.75}$) was calculated as follows:

$$\log CL_{intPL} = 5.63\,(\pm 1.187) - 1.287\,(\pm 0.149)\cdot \log P_{ow} + 1.08\,(\pm 0.233)\cdot \log P_{bw} - 0.328\,(\pm 0.111)\cdot IP \quad [10]$$

where log P_{ow} is the log of the *n*-octanol:water PC; log P_{bw} is the log of the blood:water PC; and *IP* is the ionization potential.

The value of P_{bw} was calculated as the experimental blood:air PC values (*20, 48, 51-55*) divided by the calculated water:air PC (P_{wa}) values at 37.5 °C (*11*).

Predicted values of log P_{ow} and P_{wa} were obtained from U.S. EPA's freeware EPISUITE™ (http://www.epa.gov/opptintr/exposure/pubs/episuite.htm).

The values of the ionization potential were calculated using commercially available software (Molecular Modeling Pro®, Chem SW, Fairfield, CA). Before calculating the molecular descriptors with Molecular Modeling Pro®, the 3D molecules were drawn and minimized using the full MM2 (molecular mechanics program) method provided in the software. The ionization potential was calculated using the MOPAC/PM3 program, which was included in Molecular Modeling Pro®.

A first-order constant, K_f, describing GSH conjugation was used for chloroethane (K_f= 1 h^{-1}/kg$^{0.3}$), dibromomethane (K_f = 0.7 h^{-1}/kg$^{0.3}$), dichloromethane (K_f = 2 h^{-1}/kg$^{0.3}$) and vinyl chloride (K_f = 1 h^{-1}/kg$^{0.3}$). The values of K_f were obtained from the literature (*56, 57*). The rate of metabolism in the hepatocytes was calculated as follows:

$$RAM = \left(CL_{intcell} + K_f \cdot \frac{V_l}{F_{cl}} \right) \cdot C_{cl} \qquad [11]$$

where RAM is the rate of the amount metabolized (mg/h); $CL_{intcell}$ is the hepatocellular intrinsic clearance (L/h); K_f is the first-order constant (h^{-1}); V_l is the liver volume (L); F_{cl} is the cell fraction of the liver volume; and C_{cl} is the concentration of the chemical in a liver cell.

In Eq. 10, $CL_{intcell}$ was obtained by dividing the CL_{int} predicted for the whole liver by the volume of cells in this tissue and then multiplying by the estimated liver cell:blood PC, which was calculated as follows (*12*):

$$P_{clb} = \frac{P_{clw}}{P_{pw} \cdot F_p + P_{ew} \cdot F_e} \qquad [12]$$

where P_{clb} is the hepatocyte:blood PC; P_{clw} is the hepatocyte:water PC; P_{ew} is the erythrocyte:water PC; P_{pw} is the plasma:water PC; F_e is the fractional volume of erythrocytes in blood; and F_p is the fractional volume of plasma in blood.

In Eq. 12, P_{clw}, P_{ew} and P_{pw} were calculated using Eq. 1.

Thus, the CL_{int} (L PL/h/kg) value was calculated using a QPPR based on log P_{ow}, log P_{bw} and the calculated ionization potential (IP). This value of CL_{int} was converted to units of L blood/h/kg, yielding the predicted intrinsic clearance for the whole liver, which was scaled to the liver cell metric using P_{clb} and the fraction of cells in the liver volume. The values of the input parameters to calculate the $CL_{intcell}$ are presented in Table 2.

PBPK model simulations

PBPK simulations were conducted for the chemicals within the application domain of the QSPR-QPPR models used. Therefore, the venous blood concentration kinetics were

simulated and compared to published experimental data in rats for the chemicals included in the QPPR calibration set (benzene, 1,2-dichloroethane, dichloromethane, *m*-xylene, toluene and styrene) (*52, 58-60*) for the metabolic constants and for the chemicals outside this dataset (1,1,1-trichloroethane and 1,2,4-trimethylbenzene) (*61, 62*).

In an effort to further validate these data, the 24-h venous blood kinetics were simulated for a 24-h exposure to 1 ppm of the VOCs listed in Table 2. For each compound, the 24-h area-under-the-curve (AUC_{24}) of the venous blood kinetics was also calculated and compared to that obtained using a validated QSPR-PBPK model for inhaled VOCs (*4*).

5.4. Results

5.4.1 Development of QSPR for PCs

QSPR for hemoglobin:water PC

The following model was obtained by the stepwise analysis of selected predictors:

$$Log\ P_{hbw} = 0.68\ (\pm 0.059) \cdot \log P_{ow} + 0.21\ (\pm 0.15) \qquad [13]$$

$R^2 = 0.732$; $R^2_{adj} = 0.727$; $Q^2 = 0.709$; $s = 0.328$; $F = 131.23$; $n = 50$

The numbers between brackets are standard errors of the coefficients of regression. The *p* values of the coefficients of regression were < 0.001 for log P_{ow} and 0.169 for the constant. The comparison between the predictions and the experimental values is illustrated in Figure 2. The ratio of the predicted/observed values (pred/exp, mean ± SD [minimum;maximum]) was 1.03 ± 0.18 [0.72;1.65]. The QSPR for P_{hbw} was developed for chemicals with values

of log P_{ow} between 1.03 and 4.09 and experimentally derived log P_{hbw} values ranging from 1.03 and 4.09. The predicted responses (log P_{hbw}) ranged from 0.91 to 2.99.

QSPR for oil:air PC

The following QSPR model, which relates the values of log P_{ow} and log P_{wa} to the log P_{oa}, was obtained:

$$Log\ P_{oa} = 0.95\ (\pm 0.042) \cdot \log P_{ow} + 0.675\ (\pm 0.031) \cdot \log P_{wa} + 0.325\ (\pm 0.102) \quad [14]$$

$R^2 = 0.801$; $R^2_{adj} = 0.798$; $Q^2 = 0.79$; $s = 0.441$; F = 296.024; n = 150

The values of the regression coefficients were significant for log P_{ow} ($p < 0.001$), log P_{wa} ($p < 0.001$) and for the constant ($p = 0.002$). P_{oa} and P_{wa} were not highly correlated (VIF = 1.79). Figure 3 presents the predictions of log P_{oa} obtained with Eq. 14, along with the values of the input parameters and the experimental values. Overall, using this equation, the ratio pred/exp was 1.13 ± 0.92 [-0.16;9.14] (mean ± standard deviation [minimum;maximum]). The predictions were more than twice the experimental values for 8 of the 150 chemicals (compound, pred/exp: 2-cyanoethylene oxide, 0.12; carbon dioxide, 9.14; difluoromethane, 0.16; ethane, 2.91; ethylene, 7.77; ethyne, 3.15; isoprene, 2.43; methane, -0.16). The studentized residual values of 2-cyanolethylene oxide, and isoprene were above 3 (6.3, -3.1); thus, these chemicals could be considered to be outliers (*45*). Discarding these chemicals from the calibration dataset improved the statistics of the model and changed the values of the coefficients as follows:

$$Log\ P_{oa} = 1.016\ (\pm 0.035) \cdot \log P_{ow} + 0.694\ (\pm 0.026) \cdot \log P_{wa} + 0.174\ (\pm 0.086) \quad [15]$$

$R^2 = 0.865$; $R^2_{adj} = 0.863$; $Q^2 = 0.861$; $s = 0.362$; F = 462.85; n = 148

The p values of the constant and coefficients in Eq. 15 were significant ($p = 0.046$ for the constant and $p < 0.001$ for log P_{ow} and log P_{wa}). The comparison between the predictions of log P_{oa} (using Eq. 15) and the experimental data is reported in Figure 3. Using this equation, the ratio pred/exp was 1.11 ± 0.82 [-0.03;8.39] (mean ± standard deviation [minimum;maximum]). As for Eq. 14, the predicted values of log P_{oa} for carbon dioxide, difluoromethane, ethane, ethylene, ethyne and methane were more than twice the experimental values. Despite the differences in the values of the regression coefficients between Eq. 14 and 15, both models provided comparable predictions (Figure 3). However, Eq. 15 was used in the QSPR-PBPK modeling because its coefficients of regression estimates more precise (i.e., have lower standard errors).

5.4.2 Evaluation of QSPR for PCs

Equations 13 and 15 and the prediction of P_{wa} were used to predict values of P_{hbw} and P_{ow}. The values of P_{hbw}, P_{ow} and P_{wa}, along with the rat tissue and blood composition data, were incorporated into an algorithm to calculate the tissue:air PC and the blood:air PC (Eq. 3 and 4). Figure 4 illustrates the comparison between the QSPR predictions and the experimental data for the fat:air PC (Figure 4A), the liver:air PC (Figure 4B), the muscle:air PC (Figure 4C) and the blood:air PC (Figure 4D) for 76 halogenated and non halogenated alkanes, alkenes aromatic hydrocarbons along with alcohols acetates ethers and ketones in rats. Table 3

5.4.3 QSPR-PBPK modeling

The QSPRs for log P_{oa} and log P_{hbw}, the predictions of P_{wa} and information on rat tissue composition were used to estimate the PCs that were to be incorporated into the PBPK model (using Eq. 1 and 8). The mean QPPR values of V_{max} and K_m were incorporated within the PBPK models for inhaled VOCs in rats.

The comparison between the experimental and simulated venous blood kinetics is presented in Figure 5 for 8 chemicals of the calibration set used for metabolism constants (Figure 5A: benzene, 50 ppm, 4-h; Figure 5B: 1,2-dichloroethane, 50 ppm, 6-h; Figure 5C: dichloromethane 200 ppm, 4-h; Figure 5D: *m*-xylene, 50 ppm, 4-h; Figure 5E: styrene, 80 ppm, 6-h; Figure 5F: toluene, 50 ppm, 4-h) (*52, 58-60*) and 2 chemicals outside this dataset (Figure 5G: 1,1,1-trichloroethane, 400 ppm, 4 h; Figure 5H: 1,2,4-trimenthylbenzene, 10, 40 ppm, 6 h) (*61, 62*). The simulations fit the data reasonably for all chemicals (prediction within 2- to 3-fold of the experimental data), except for styrene. For this compound, the predictions were more than 5 times the experimental concentrations at the 18-h and 24-h time points.

For 26 VOCs, the AUC_{24}s predicted with the QSPR-PBPK model are presented in Table 4, along with the predictions obtained using a published QSPR model (*4*). Overall, the predictions of the QSPR-PBPK model developed in the present study are comparable to those obtained with the published QSPR-PBPK model. The ratio of the predicted AUCs using the present QSPR-PBPK model to those predicted with the published one were 0.99 ± 0.37 (mean ± standard deviation). The predictions using the present QSPR-PBPK model were within of factor of 2 of those obtained using the other QSPR-PBPK, except for *n*-hexane (4-fold) and carbon tetrachloride (3-fold).

Table 5 presents, as an example, predicted 24-h concentrations at both micro and macro levels for a continuous exposure to 1 ppm of 1,1,1,2-tetrachloroethane, bromochloromethane, methyl chloride, *m*-xylene and vinyl chloride. The results show that at all tissue levels, for comparable $CL_{intcell}$, (1,1,1,2-tetrachloroethane and bromochloromethane) the higher the P_{ow}, the higher the concentrations and for comparable values of P_{ow}, the higher the $CL_{intcell}$, the lower the concentration.

5.5. Discussion

Physiologically based pharmacokinetic modeling has proven its usefulness in the risk assessment of chemicals (*63, 64*). Few tools, however, are available to predict the pharmacokinetics of chemicals on the basis of their structure and/or properties. The use of QSAR, QSPR or QPPR models to predict the input parameters of PBPK models might be of potential interest in the risk assessment of data-poor chemicals. QSPR-PBPK models have been developed to predict the toxicokinetics of VOCs in rats and humans on the basis of molecular structural group information (*4-7*). In the present study, QSPR models for PCs were incorporated into a PBPK model, along with a QPPR for CL_{int}, to predict the pharmacokinetics of VOCs in rats. The approach used was similar to that employed in the study by Béliveau et al. (*4*) because it uses biologically based algorithms for PCs and QSPR or QPPR models for the input parameters, however, the major difference from the study of Béliveau and colleagues relates to the novel QSPR/QPPR modeling approach used for P_{oa}, P_{hbw}, P_{wa} and the metabolic constants, to expand the application domain. Furthermore, the PBPK model developed in this study allows for predictions of cellular-level dose metrics. Therefore, this modeling framework can also be used for *in vitro-in vivo* extrapolations. The need for using such extrapolations may increase because high-throughput assays are encouraged in the new paradigm of toxicity testing (*2*). Expect the results shown in Table 5, simulations of the toxicokinetics at the cellular level were not reported due to the lack of experimental cellular data to compare with for a validation

purpose. Nevertheless, this cellular dosimetry model is potentially useful for further research, such as *in vitro-in vivo* extrapolation of cellular toxicity. Moreover, the concentration in plasma water (i.e., the free concentration in blood), whole plasma and erythrocytes can be calculated using the estimated water:blood, plasma:blood and erythrocyte:blood PCs, respectively.

The prediction of metabolism constants is a major limitation in early predictive or screening toxicokinetic research (*65*). The group contribution method has been successfully applied to develop QSPR models for hepatic clearance, intrinsic clearance, V_{max} and K_m (*4-7*); however, the application of these QSPRs is limited by the available groups (i.e., CH_3, CH_2, CH, C, C=C, H, benzene ring, H on a benzene ring, F, Br, and Cl). Recently, a QPPR model was developed to predict the rat intrinsic clearance (*11*). This model was incorporated into a human PBPK for inhaled chemicals to predict the blood kinetics accounting for the uncertainty in the metabolism prediction. Predictive models for V_{max} and K_m are necessary to estimate the toxicokinetics associated with high-dose exposures, for which saturation of the enzymatic system occurs. When the same approach used for developing the QPPR for the log CL_{int} was applied to develop QPPRs for K_m and V_{max} (of CYP2E1 substrates), it was unsuccessful because no model was found to predict the V_{max}, and the range of experimental K_m values was very narrow to allow the development of a reasonable model for this endpoint.

Recently, a unified algorithm was developed, allowing for the prediction of PCs at the micro (i.e. cells and fluids) and macro levels (i.e. tissues) on the basis of information on the tissue compartment composition and the physicochemical parameters (*12*). For a new chemical, if the P_{ow}, P_{wa} and P_{hbw} (or the blood:air PC) are unknown, QSPRs can be used to calculate *a priori* estimate of the PCs for PBPK models. In the present study, a QSPR model was developed for the hemoglobin:water PC. The model showed reasonably good

statistics in terms of goodness-of-fit. The values of the endpoint (P_{hbw}) were derived from blood:air PC measurements using a biologically based algorithm for PCs. Therefore, it is possible that the error associated with the model prediction is partly due to the combination of the uncertainties related to the measurements of the oil:air PC, the water:air PC and the blood:air PC, along with the uncertainty related to the predictions of the algorithm for PCs and the values of its physiological parameters. For example, a value of 40% was used for hematocrit, which is known to vary from 36 to 48% (*66*). This variation can impact the prediction of P_{hbw}. The value of P_{hbw} was correlated to that of log P_{ow} (Eq. 12) according to the hypothesis of hydrophobic binding to hemoglobin (*21, 22*); thus, the model has a reliable mechanistic basis.

A reasonably good QSPR was developed to predict the oil:air PC. This model is an update of previously reported solvent-solvent relationships (*16, 18*), although in the present study, a medium:air PC was used instead of oil:water with input parameters (Log P_{ow} and log P_{wa}) estimated using a user-friendly and freely available tool. As the applicability domain of the model and the estimation of the variables are documented, the predictive power of the model can be noted for further use or development. The oil:air PC was chosen because the uncertainty associated with the experimental values of the water:air PC necessary to calculate the oil:water PC could enhance the uncertainty associated with the endpoint value. The regression coefficients of log P_{ow} (Eq. 14 and 15), however, are comparable to those reported by Poulin and Theil (*18*) (log $P_{oil:water}$ = 1.115 x log P - 1:35) and Leo *et al*. (*16*) (log $P_{oils:water}$ = 1.119 x log P – 0.325 for hydrogen-bond-acceptor solutes and 1.099 x log P – 1.310 for hydrogen-bond-donor solutes). The QSPR for log P_{oa} might be interpreted as follows: the oil:air PC of a chemical is the product of its oil:water and water:air PCs. The oil:water PC is known to be correlated to the *n*-octanol:water PC (*16*); thus, log P_{oa} is correlated with log P_{ow} and log P_{wa}. The use of the *n*-octanol:air PC predicted from KOWWIN rather than oil:air PC as a surrogate for solubility in neutral lipids was evaluated. Overall, all the predictions of tissue:air and blood:air PCs were closer to the

experimental value when using the QSPR for oil:air instead of the predicted value of *n*-octanol:air PC (pred/exp = 1.88 ± 2.20, 0.87 ± 0.60, 0.86 ± 0.82 and 1.16 ± 0.93, for fat:air, liver:air, muscle:air and blood:air PCs, respectively) as input parameter in the mechanistic algorithm.

Using Eq. 14, 2-cyanoethylene oxide and isoprene were outliers (i.e. their studentized residuals were higher than 3) possibly because the predictions of log P_{ow} and log P_{wa} obtained from EPISUITE were not comparable the experimental values (exp.) of oil:air/water:air and water:air (*20*, *42*). For 2-cyanoethylene oxide, the log P_{ow} predicted from EPISUITE was -1.1 whereas the log (exp. P_{oa}/exp. P_{wa}) was -0.32 and the log P_{wa} predicted from EPISUITE was 1.62 vs exp log P_{oa} 3.38 (*42*). For isoprene, the log P_{ow} predicted from EPISUITE was -2.58 whereas the log (exp. P_{oa}/exp. P_{wa}) was 1.62 and the log P_{wa} predicted from EPISUITE was -0.87 vs exp log P_{oa} -0.68.

The QSPRs developed for P_{hbw} and P_{oa} are in accordance with the validation criteria of the OECD for QSAR models because they have a defined endpoint and are unambiguous, their domain of applicability is documented, appropriate goodness-of-fit measurements (R^2, R^2_{adj}, Q^2) were used, and mechanistic interpretation was provided (*46*). The application of QSPR models for P_{hbw} and P_{oa} to predict the tissue:air and blood:air PCs with a mechanistic algorithm was evaluated. Overall, the tissue:air and blood:air PCs predictions agreed well with the data (Figure 4). Considering the chemicals for which the miss-predicted PC was more than 3 fold for more than one PC (i.e., with superscript b in Table 3), for a given chemical, the pred. / exp. ratio was always positive or negative. For these chemicals, the more lipophilic i.e., with log P_{ow} > 1.5, for which tissue or blood:air PCs were underestimated also shown underestimated P_{oa} (i.e., 1,1,1-trifluoro-2-chloroethane; dibromomethane; isobutyl acetate ester; isopentyl acetate ester; JP-10; methyl *n*-pentyl ketone; *n*-hexane). Similarly, the chemicals with lower log P_{ow} which tissue or blood:air PCs were underestimated had underestimated P_{wa} (dichloromethane; difluoromethane). The P_{oa} of hexachloroethane was 8 times overestimated using Eq. 15, this explains the high

overestimation of the tissue:air and blood:air PCs for this highly lipophilic chemical. These results are consistent with the underlying assumptions of the mechanistic algorithm for tissue:air and blood:air PC that the PC value is sensitive to the water content and the water:air PC values for hydrophilic chemicals and to the neutral lipid content and the oil:air PC for lipophilic chemicals.

The PCs of acetate ester were not adequately fitted using mechanistic algorithm for PCs such as that used in this study (*14*). Perhaps the algorithm did not describe adequately all the mechanism of distribution for this chemical group. However, the experimental study on tissue:air PCs for these acetate esters reported no evident relation between the molecular structure and the PC (*32*).

The QSPRs developed in this study were incorporated, along with QPPR for intrinsic clearance, in a PBPK model for inhaled VOCs in rats. For 8 chemicals, the PBPK models provided reasonably good estimates of the blood toxicokinetics when compared to experimental data. The predictions of the 24-h AUC for a continuous exposure to 1 ppm of VOCs were also comparable with those obtained with a published QSPR-PBPK model (*4*). As the QSPR-PBPK model of Béliveau and colleagues was validated with experimental data, this result confirms the validity of the QS(P)PR-PBPK model. More importantly, the present PBPK modeling framework allowed for the prediction of inhalation toxicokinetics of VOCs on the basis of four molecular properties/descriptors, namely, log P_{ow}, log P_{wa}, log P_{bw} and the calculated ionization potential.

The uncertainty on QPPR estimates for the rat hepatic clearance could be accounted by simulating the limits of the mean predicted confidence interval (e.g., 95 %) and by analysing the confidence of using the QPPR for CL_{int} to predict the blood levels of the studied chemicals, as undertaken in a previous study (*11*).

The present QS(P)PR-PBPK model represents the first alternative to the QSPR-PBPK models based on the group contribution method of Gao (*8, 9*); thus, they enrich this poorly studied modeling area. Furthermore, QPPR and QSPRs were developed using data on oxygenated and fluorinated hydrocarbons, expanding the application domain of the presently available QS(P)PR-PBPK models. The applicability domain of the QSPR-PBPK model developed herein is log P_{ow} = [1.09; 4.03], log P_{wa} = [-2.65; 4.59]; and calculated ionization potential [9.13;11.28]. Moreover, the uncertainty in the prediction could be higher for acetate esters, ketones fluorated hydrocarbons and highly halogenated alkanes (e.g. hexachloroethane).

The QS(P)PR-PBPK model developed in this study might be applied to humans by substituting the values of the physiological parameters and tissue composition. Such a human cellular dosimetry model could be developed to study the extrapolation from an *in vitro* concentration-response relationship to an *in vivo* dose-response relationship. A proof-of-concept of such an application has been recently demonstrated using toluene as model chemical (*67*).

Overall, in this study, QPPR for CL_{int} and QSPRs for PCs were incorporated into a cellular-level PBPK model for inhaled VOCs in rats. The modeling framework was used to predict the blood toxicokinetics, as well as with the predictions of a previously validated QSPR-PBPK model. The present modeling tool provided simulation results comparable with that of existing QSPR-PBPK models.

5.6. References

(1) Commission des communautés européennes. (2001) LIVRE BLANC Stratégie pour la future politique dans le domaine des substances chimiques, Bruxelles. p 37.

(2) National Research Council (2007) *Toxicity testing in the 21st century : a vision and a strategy*, National Academies Press, Washington, DC.

(3) Krishnan, K. and Andersen, M. E. (2007) Physiologically based Pharmacokinetic modeling in toxicology, In *Principles and methods of toxicology* (Hayes, A. W., Ed.) pp 231-292, Taylor & Francis, Boca Raton.

(4) Béliveau, M., Lipscomb, J., Tardif, R. and Krishnan, K. (2005) Quantitative structure-property relationships for interspecies extrapolation of the inhalation pharmacokinetics of organic chemicals. *Chem. Res. Toxicol. 18*, 475-485.

(5) Béliveau, M., Tardif, R. and Krishnan, K. (2003) Quantitative structure-property relationships for physiologically based pharmacokinetic modeling of volatile organic chemicals in rats. *Toxicol. Appl. Pharmacol. 189*, 221-232.

(6) Kamgang, E., Peyret, T. and Krishnan, K. (2008) An integrated QSPR-PBPK modelling approach for in vitro-in vivo extrapolation of pharmacokinetics in rats. *SAR QSAR Environ. Res. 19*, 669 - 680.

(7) Price, K. and Krishnan, K. (2011) An integrated QSAR-PBPK modelling approach for predicting the inhalation toxicokinetics of mixtures of volatile organic chemicals in the rat. *SAR QSAR Environ. Res. 22*, 107-128.

(8) Martin, T. M. and Young, D. M. (2001) Prediction of the acute toxicity (96-h LC50) of organic compounds to the fathead minnow (Pimephales promelas) using a group contribution method. *Chem. Res. Toxicol. 14*, 1378-1385.

(9) Gao, C., Govind, R. and Tabak, H. H. (1992) Application of the group contribution method for predicting the toxicity of organic chemicals. *Environ. Toxicol. Chem. 11*, 631-636.

(10) Meylan, W. M. and Howard, P. H. (1995) Atom/fragment contribution method for estimating octanol-water partition coefficients. *J. Pharm. Sci. 84*, 83-92.

(11) Peyret, T. and Krishnan, K. (2012) Quantitative property-property relationship (QPPR) for screening-level prediction of intrinsic clearance of volatile organic chemicals in rats and its integration within PBPK models to predict inhalation pharmacokinetics in humans. *Journal of Toxicology*. doi: 10.1155/2012/286079.

(12) Peyret, T., Poulin, P. and Krishnan, K. (2010) A unified algorithm for predicting partition coefficients for PBPK modeling of drugs and environmental chemicals. *Toxicol. Appl. Pharmacol. 249*, 197-207.

(13) Poulin, P. and Krishnan, K. (1995) An algorithm for predicting tissue: blood partition coefficients of organic chemicals from n-octanol: water partition coefficient data. *J. Toxicol. Environ. Health 46*, 117-129.

(14) Poulin, P. and Krishnan, K. (1996) A tissue composition-based algorithm for predicting tissue:air partition coefficients of organic chemicals. *Toxicol. Appl. Pharmacol. 136*, 126-130.

(15) Poulin, P. and Krishnan, K. (1995) A biologically-based algorithm for predicting human tissue: blood partition coefficients of organic chemicals. *Hum. Exp. Toxicol. 14*, 273-280.

(16) Leo, A., Hansch, C. and Elkins, D. (1971) Partition coefficients and their uses. *Chem. Rev. 71*, 525-616.

(17) Leo, A. J. and Hansch, C. (1971) Linear free energy relations between partitioning solvent systems. *J. Org. Chem. 36*, 1539-1544.

(18) Poulin, P. and Theil, F. P. (2002) Prediction of pharmacokinetics prior to in vivo studies. 1. Mechanism-based prediction of volume of distribution. *J. Pharm. Sci. 91*, 129-156.

(19) Gramatica, P. (2007) Principles of QSAR models validation: internal and external. *QSAR & Combinatorial Science 26*, 694-701.

(20) Gargas, M. L., Burgess, R. J., Voisard, D. E., Cason, G. H. and Andersen, M. E. (1989) Partition coefficients of low-molecular-weight volatile chemicals in various liquids and tissues. *Toxicol. Appl. Pharmacol. 98*, 87-99.

(21) Poulin, P., Béliveau, M. and Krishnan, K. (1999) Mechanistic animal replacement approaches for predicting pharmacokinetics of organic chemicals, In *Toxicity assessment alternatives : methods, issues, opportunities* (Salem, H. and Katz, S. A., Eds.) pp 115-139, Humana Press, Totowa, N.J.

(22) Lam, C.-W., Galen, T. J., Boyd, J. F. and Pierson, D. L. (1990) Mechanism of transport and distribution of organic solvents in blood. *Toxicol. Appl. Pharmacol. 104*, 117-129.

(23) Sha'afi, R. I., Gary-Bobo, C. M. and Solomon, A. K. (1971) Permeability of Red Cell Membranes to Small Hydrophilic and Lipophilic Solutes. *The Journal of General Physiology 58*, 238-258.

(24) Kier, L. B. (1985) A Shape Index from Molecular Graphs. *Quant. Struct.-Act. Relat. 4*, 109-116.

(25) Andersen, M. E., Clewell, H. J., Gargas, M. L., MacNaughton, M. G., Reitz, R. H., Nolan, R. J. and McKenna, M. J. (1991) Physiologically based pharmacokinetic modeling with dichloromethane, its metabolite, carbon monoxide, and blood carboxyhemoglobin in rats and humans. *Toxicol. Appl. Pharmacol. 108*, 14-27.

(26) Borghoff, S. J., Murphy, J. E. and Medinsky, M. A. (1996) Development of physiologically based pharmacokinetic model for methyl tertiary-butyl ether and tertiary-butanol in male Fisher-344 rats. *Fundam. Appl. Toxicol. 30*, 264-275.

(27) Fiserova-Bergerova, V. (1983) *Modeling inhalation exposure to vapors: uptake, distribution and elimination*, Vol. 1, CRC press, Miami, Florida.

(28) Fang, Z., Sonner, J., Laster, M. J., Ionescu, P., Kandel, L., Koblin, D. D., Eger, E. I., 2nd and Halsey, M. J. (1996) Anesthetic and convulsant properties of aromatic compounds and cycloalkanes: implications for mechanisms of narcosis. *Anesth. Analg. 83*, 1097-1104.

(29) Frederick, C. B., Bush, M. L., Lomax, L. G., Black, K. A., Finch, L., Kimbell, J. S., Morgan, K. T., Subramaniam, R. P., Morris, J. B. and Ultman, J. S. (1998) Application of a hybrid computational fluid dynamics and physiologically based

inhalation model for interspecies dosimetry extrapolation of acidic vapors in the upper airways. *Toxicol. Appl. Pharmacol. 152*, 211-231.

(30) Hallier, E., Filser, J. G. and Bolt, H. M. (1981) Inhalation pharmacokinetics based on gas uptake studies. *Arch. Toxicol. 47*, 293-304.

(31) Johanson, G. and Filser, J. G. (1993) A physiologically based pharmacokinetic model for butadiene and its metabolite butadiene monoxide in rat and mouse and its significance for risk extrapolation. *Arch. Toxicol. 67*, 151-163.

(32) Kaneko, T., Wang, P. Y. and Sato, A. (1994) Partition coefficients of some acetate esters and alcohols in water, blood, olive oil, and rat tissues. *Occup. Environ. Med. 51*, 68-72.

(33) Knaak, J. B., al-Bayati, M. A. and Raabe, O. G. (1995) Development of partition coefficients, Vmax and Km values, and allometric relationships. *Toxicol. Lett. 79*, 87-98.

(34) Knaak, J. B., Smith, L. W., Fitzpatrick, R. D., Olson, J. R. and Newton, P. E. (1998) In vitro hepatic metabolism of PCBTF: development of vmax and km values and partition coefficients and their use in an inhalation PBPK model. *Inhal. Toxicol. 10*, 65 - 85.

(35) Loizou, G. D., Urban, G., Dekant, W. and Anders, M. W. (1994) Gas-uptake pharmacokinetics of 2,2-dichloro-1,1,1-trifluoroethane (HCFC-123). *Drug Metab. Dispos. 22*, 511-517.

(36) Loizou, G. D. and Anders, M. W. (1993) Gas-uptake pharmacokinetics and biotransformation of 1,1-dichloro-1-fluoroethane (HCFC-141b). *Drug Metab. Dispos. 21*, 634-639.

(37) Medinsky, M. A., Leavens, T. L., Csanady, G. A. and Bond, J. A. (1994) In vivo metabolism of butadiene by mice and rats: a comparison of physiological model predictions and experimental data. *Carcinogenesis 15*, 1329-1340.

(38) Meulenberg, C. J. and Vijverberg, H. P. (2000) Empirical relations predicting human and rat tissue:air partition coefficients of volatile organic compounds. *Toxicol. Appl. Pharmacol. 165*, 206-216.

(39) Sato, A. and Nakajima, T. (1979) Partition coefficients of some aromatic hydrocarbons and ketones in water, blood and oil. *Br. J. Ind. Med. 36*, 231-234.

(40) Sato, A. and Nakajima, T. (1979) A structure-activity relationship of some chlorinated hydrocarbons. *Arch Environ Health 34*, 69-75.

(41) Sweeney, L., Schlosser, P., Medinsky, M. and Bond, J. (1997) Physiologically based pharmacokinetic modeling of 1,3-butadiene, 1,2- epoxy-3-butene, and 1,2:3,4-diepoxybutane toxicokinetics in mice and rats. *Carcinogenesis 18*, 611-625.

(42) Teo, S. K. O., Kedderis, G. L. and Gargas, M. L. (1994) Determination of Tissue Partition Coefficients for Volatile Tissue-Reactive Chemicals: Acrylonitrile and Its Metabolite 2-Cyanoethylene Oxide. *Toxicol. Appl. Pharmacol. 128*, 92-96.

(43) Weathersby, P. K. and Homer, L. D. (1980) Solubility of inert gases in biological fluids and tissues: a review. *Undersea Biomed Res 7*, 277-296.

(44) Poulin, P. and Krishnan, K. (1996) A mechanistic algorithm for predicting blood:air partition coefficients of organic chemicals with the consideration of reversible binding in hemoglobin. *Toxicol. Appl. Pharmacol. 136*, 131-137.

(45) Glantz, S. A. and Slinker, B. K. (2001) *Primer of applied regression and analysis of variance*, 2nd ed., McGraw-Hill, Inc, New York.

(46) OECD. (2007) Guidance document on the validation of (quantitative) structure-activity relationship [(Q)SAR] models, (OECD Environment Health and Safety Publications, Ed.) p 154, OECD-OCDE, Paris.

(47) Wold, S. (1991) Validation of QSARs. *Quantitative Structure Activity Relashionship 10*, 191-193.

(48) Tardif, R., Charest-Tardif, G., Brodeur, J. and Krishnan, K. (1997) Physiologically based pharmacokinetic modeling of a ternary mixture of alkyl benzenes in rats and humans. *Toxicol. Appl. Pharmacol. 144*, 120-134.

(49) Gerlowski, L. E. and Jain, R. K. (1983) Physiologically based pharmacokinetic modeling: principles and applications. *J. Pharm. Sci. 72*, 1103-1127.

(50) Kawai, R., Lemaire, M., Steimer, J. L., Bruelisauer, A., Niederberger, W. and Rowland, M. (1994) Physiologically based pharmacokinetic study on a cyclosporin derivative, SDZ IMM 125. *J Pharmacokinet Biopharm 22*, 327-365.

(51) da Silva, L. M., Charest-Tardif, G., Krishnan, K. and Tardif, R. (1999) Influence of oral administration of a quaternary mixture of trihalomethanes on their blood kinetics in the rat. *Toxicol. Lett. 106*, 49-57.

(52) Andersen, M. E., Clewell, H. J., Gargas, M. L., Smith, F. A. and Reitz, R. H. (1987) Physiologically based pharmacokinetics and the risk assessment process for methylene chloride. *Toxicol. Appl. Pharmacol. 87*, 185-205.

(53) Filser, J. G., Csanady, G. A., Denk, B., Hartmann, M., Kauffmann, A., Klesser, W., Kreuzer, P. E., Putz, C., Shen, J. H. and Stei, P. (1996) Toxicokinetics of isoprene in rodents and humans. *Toxicology 113*, 278-287.

(54) Hamelin, G., Charest-Tardif, G., Truchon, G. and Tardif, R. (2005) Physiologically based modeling of n-hexane kinetics in humans following inhalation exposure at rest and under physical exertion: impact on free 2,5-hexanedione in urine and on n-hexane in alveolar air. *J. Occup. Environ. Hyg. 2*, 86-97; quiz D86-87.

(55) Ramsey, J. C. and Andersen, M. E. (1984) A physiologically based description of the inhalation pharmacokinetics of styrene in rats and humans. *Toxicol. Appl. Pharmacol. 73*, 159-175.

(56) Gargas, M. L., Seybold, P. G. and Andersen, M. E. (1988) Modeling the tissue solubilities and metabolic rate constant (Vmax) of halogenated methanes, ethanes, and ethylenes. *Toxicol. Lett. 43*, 235-256.

(57) Gargas, M. L., Clewell, H. J., 3rd and Andersen, M. E. (1986) Metabolism of inhaled dihalomethanes in vivo: differentiation of kinetic constants for two independent pathways. *Toxicol. Appl. Pharmacol. 82*, 211-223.

(58) Haddad, S., Charest-Tardif, G., Tardif, R. and Krishnan, K. (2000) Validation of a physiological modeling framework for simulating the toxicokinetics of chemicals in mixtures. *Toxicol. Appl. Pharmacol. 167*, 199-209.

(59) Sweeney, L. M., Saghir, S. A. and Gargas, M. L. (2008) Physiologically based pharmacokinetic model development and simulations for ethylene dichloride (1,2-dichloroethane) in rats. *Regul. Toxicol. Pharmacol. 51*, 311-323.

(60) Andersen, M. E., MacNaughton, M. G., Clewell, H. J., 3rd and Paustenbach, D. J. (1987) Adjusting exposure limits for long and short exposure periods using a physiological pharmacokinetic model. *Am Ind Hyg Assoc J 48*, 335-343.

(61) Tardif, R. and Charest-Tardif, G. (1999) The importance of measured end-points in demonstrating the occurrence of interactions: a case study with methylchloroform and m-xylene. *Toxicol. Sci. 49*, 312-317.

(62) Hissink, A. M., Kruse, J., Kulig, B. M., Verwei, M., Muijser, H., Salmon, F., Leenheers, L. H., Owen, D. E., Lammers, J. H., Freidig, A. P. and McKee, R. H. (2007) Model studies for evaluating the neurobehavioral effects of complex hydrocarbon solvents III. PBPK modeling of white spirit constituents as a tool for integrating animal and human test data. *Neurotoxicology 28*, 751-760.

(63) U.S. E.P.A. (2006) Approaches for the Application of Physiologically Based Pharmacokinetic (PBPK) Models and Supporting Data in Risk Assessment, (Service, N. T. I., Ed.) p 123, Springfield, VA,.

(64) IPCS (2010) *Characterization and application of physiologically based pharmacokinetic models in risk assessment*.

(65) Peyret, T. and Krishnan, K. (2011) QSARs for PBPK modelling of environmental contaminants. *SAR QSAR Environ. Res. 22*, 129-169.

(66) Mackie, C., Wuyts, K., Haseldonckx, M., Blokland, S., Gysemberg, P., Verhoeven, I., Timmerman, P. and Nijsen, M. (2005) New model for intravenous drug administration and blood sampling in the awake rat, designed to increase quality

and throughput for in vivo pharmacokinetic analysis. *J. Pharmacol. Toxicol. Methods 52*, 293-301.

(67) Peyret, T. and Krishnan, K. (2010) Prediction of in vivo dose-response relationship from in vitro concentration-response relationship using cellular-level PBPK modeling, In *Toxicity-pathway-based risk assessment: preparing for paradigm change, a symposium summary* (Council, N. R., Ed.) pp 114-115, The national academies press, Washington, DC.

5.7. Tables

Table 1. Volumes of the tissue cells, interstitial fluid and vascular spaces used in the cellular dosimetry model.

Tissue	Fraction of tissue volume[a]		
	Cell	**Interstitial fluid**	**Vascular**
Liver	0.722	0.163	0.115
Adipose	0.855	0.135	0.010
Poorly perfused	0.767	0.211	0.023
Richly perfused	0.715	0.138	0.147
Blood	0.40	0.60	–

[a]: from Reference (*50*)

Table 2. QSPR output and input parameters for the calculation of intrinsic clearance in hepatocytes ($CL_{intcell}$)

Chemicals	Input parameters[a]					$CL_{int\ cell}$	Ref.
	log P_{ow}	log P_{bw}	*IP*	P_{plb}	P_{clw}		
1,1,1,2-Tetrachloroethane	2.93	0.84	10.73	37.3	1.79	5.66	(*20*)
1,1,2,2-Tetrachloroethane	2.19	0.52	10.74	14.3	0.6	2.96	(*20*)
1,1,2-Trichloroethane	2.01	0.49	10.69	10.1	0.67	3.82	(*20*)
1,1-Dichloroethane	1.76	0.62	10.58	4.27	0.92	7.06	(*20*)
1,1-Dichloroethylene	2.12	0.92	9.75	4.82	1.82	21.5	(*20*)
1,2-Dichloroethane	1.83	0.36	10.45	9.25	0.64	5	(*20*)
Benzene	1.99	0.82	9.74	4.55	1.09	13.9	(*20*)
Bromochloromethane	1.43	0.64	10.56	2	0.56	5.78	(*20*)
Bromodichloromethane	1.61	0.72	10.68	2.48	0.68	5.59	(*51*)
Carbon tetrachloride	2.44	0.99	10.98	8.57	2.51	9.48	(*20*)
Chloroethane	1.58	0.44	10.41	4.42	0.94	9.05	(*20*)
Chloroform	1.52	0.74	10.84	1.93	0.72	5.65	(*20*)
cis-1,2-dichloroethylene	1.98	0.75	9.49	5.2	0.99	15	(*20*)
Dibromomethane	1.52	0.78	10.59	1.78	0.56	5.27	(*20*)
Dichloromethane	1.34	0.61	10.58	1.79	0.62	6.69	(*52*)
Ethylbenzene	3.03	1.39	9.41	13.2	2.72	24.2	(*48*)
Hexachloroethane	4.03	1.32	10.84	156	4.65	7.14	(*20*)
Isoprene	2.58	0.99	9.35	11.8	3.52	41.8	(*53*)
Methyl chloride	1.09	0.16	10.47	3.04	0.67	9.11	(*20*)
m-xylene	3.09	1.39	9.31	15.1	2.79	25.6	(*48*)
n-hexane	3.29	2.49	11.28	1.89	11.2	49.1	(*54*)
Pentachloroethane	3.11	1.25	10.76	21.7	2.06	6.19	(*20*)
Styrene	2.89	0.89	9.13	30.2	1.81	20.2	(*55*)
Toluene	2.54	0.88	9.44	13.8	1.73	19.2	(*48*)
Trichloroethylene	2.47	1.19	9.37	5.73	1.89	24.7	(*20*)
Vinyl chloride	1.62	0.43	9.83	4.87	1.2	17.4	(*20*)

[a]: log P_{ow}: calculated log n-octanol:water partition coefficient; log P_{bw}: log blood:water partition coefficient; *IP*: calculated ionization potential; P_{plb}: phospholipid:blood partition coefficient; P_{clw}: hepatocyte:blood partition coefficient calculated using Eq. 13; $CL_{intcell}$: intrinsic clearance for hepatocyte, calculated as described in the methods.

Table 3. Chemicals with ratio of predicted / experimental values higher than 3 for blood:air or tissue:air partition coefficients in rats.

Chemical name	Pred. / Exp. value			
	Blood:air	Fat:air	Liver:air	Muscle:air
1,1,1,2-Tetrachloroethane	3.39[a]	1.90	2.35	1.50
1,1,1-Trichloroethane	2.48	2.24	3.47[a]	2.71
1,1,1-Trifluoro-2-chloroethane[b]	0.26[a]	0.77	0.46	0.21[a]
1-Nitropropane	1.31	0.82	0.78	4.00[a]
Allyl chloride[b]	0.27[a]	1.01	0.14[a]	0.18[a]
Chloroform	0.58	0.54	0.36	0.29[a]
Cyclohexane	2.96	1.79	2.66	5.58[a]
Dibromochloromethane[b]	0.37	0.18[a]	0.19[a]	0.22[a]
Dibromomethane[b]	0.53	0.31	0.29[a]	0.29[a]
Difluoromethane[b]	0.04[a]	0.55	0.02[a]	0.03[a]
Hexachloroethane[b]	6.92[a]	9.96[a]	4.46[a]	5.99[a]
Isobutyl acetate ester[b]	0.42	0.64	0.19[a]	0.24[a]
Isoflurane	0.75	0.24[a]	0.34	0.37
Isopentyl acetate ester[b]	0.20[a]	0.66	0.29[a]	0.18[a]
Isopropyl acetate ester	0.88	1.00	0.25[a]	0.40
JP-10[b]	0.12[a]	0.10[a]	0.14[a]	0.02[a]
Methyl-*n*-pentyl ketone[b]	0.24[a]	0.27[a]	0.23[a]	0.27[a]
n Pentyl acetate ester	0.32	0.82	0.39	0.26[a]
n-Butyl acetate ester[b]	0.40	0.79	0.30[a]	0.27[a]
n-Heptane	0.24[a]	0.68	0.85	0.83
n-Hexane	0.21[a]	0.56	0.86	0.42
n-Propyl acetate ester	0.61	0.94	0.25[a]	0.51

[a]: Predicted / experimental value higher than 3; [b]: the chemical had more than one PC for which the pred. / exp. ratio was higher than 3; PC: Partition coefficient; Pred. / Exp.: ratio of Predicted /Experimental PC value

Table 4. Comparison between the present and a previously published QSPR-PBPK model, of the predictions of 24 hours AUC for a continuous exposure to 1 ppm of several VOCs.

Chemical	QSPR-PBPK predicted AUC mg/L-h	
	This study	Published[a]
1,1,1,2-Tetrachloroethane	0.561	0.606
1,1,2,2-Tetrachloroethane	0.961	0.530
1,1,2-Trichloroethane	0.629	0.417
1,1-Dichloroethane	0.258	0.221
1,1-Dichloroethylene	0.151	0.205
1,2-Dichloroethane	0.413	0.275
Benzene	0.200	0.267
Bromochloromethane	0.486	0.408
Bromodichloromethane	0.561	0.546
Carbon tetrachloride	0.269	0.819
Chloroethane	0.120	0.102
Chloroform	0.350	0.490
cis-1,2-Dichloroethylene	0.265	0.205
Dibromomethane	0.712	0.515
Dichloromethane	0.250	0.300
Ethylbenzene	0.294	0.319
Hexachloroethane	0.799	0.748
Isoprene	0.083	0.060
Methyl chloride	0.079	0.086
m-Xylene	0.298	0.450
n-Hexane	0.027	0.123
Pentachloroethane	0.665	0.742
Styrene	0.311	0.340
Toluene	0.250	0.369
Trichloroethylene	0.318	0.317
Vinyl chloride	0.069	0.112

[a]: from reference (*4*)

Table 5. Predictions of 24-h concentrations at the micro- and macro- levels in liver and blood for a continuous exposure to 1 ppm of five VOCs.

Tissue **Tissue level**	**24-h Venous Blood Concentration (mg/L)**				
	1,1,1,2-TCE	**BCM**	**Methyl chloride**	***m*-Xylene**	**Vinyl chloride**
Liver					
Tissue	5.77×10^{-1}	1.43×10^{-3}	2.48×10^{-4}	7.50×10^{-3}	3.39×10^{-4}
Hepatocyte	7.30×10^{-1}	1.39×10^{-3}	2.46×10^{-4}	9.72×10^{-3}	3.96×10^{-4}
Interstitial	1.56×10^{-2}	7.86×10^{-4}	1.64×10^{-4}	1.16×10^{-4}	8.36×10^{-5}
Blood					
Blood	4.15×10^{-1}	1.61×10^{-2}	3.09×10^{-3}	1.60×10^{-2}	2.95×10^{-3}
Erythrocyte	9.74×10^{-1}	3.19×10^{-2}	5.47×10^{-3}	3.70×10^{-2}	6.04×10^{-3}
Plasma	4.25×10^{-2}	5.63×10^{-3}	1.51×10^{-3}	2.04×10^{-3}	8.81×10^{-4}

1,1,1,2-TCE: 1,1,1,2-Tetrachloroethane; BCM: Bromochloromethane

5.8. Figures

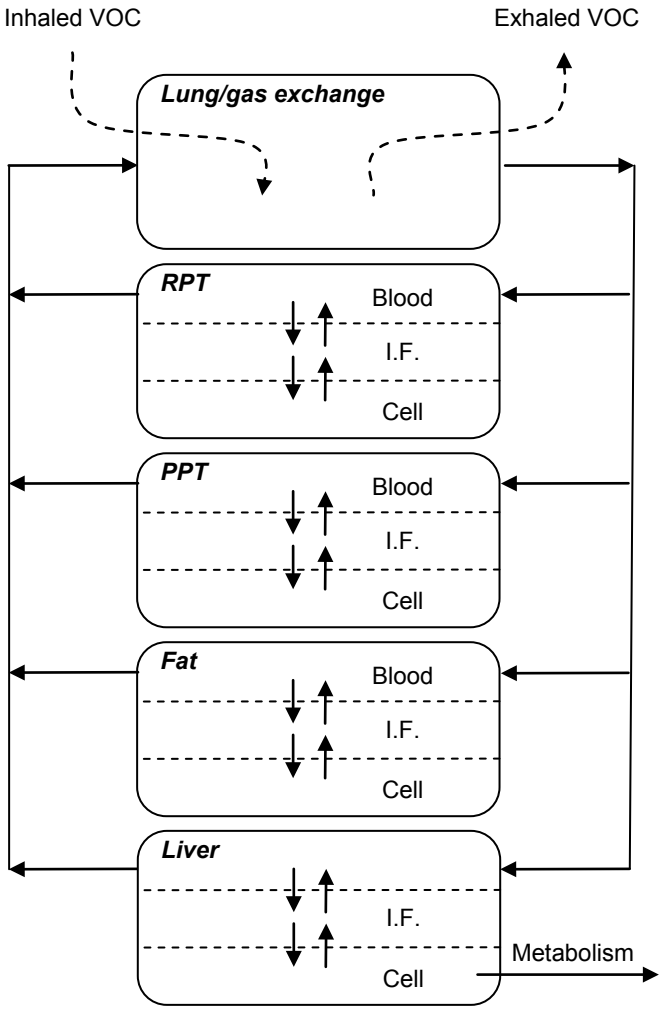

Figure 1. Conceptual representation of the cellular-level PBPK model for inhaled VOCs in rats. (I.F.: Interstitial fluid; PPT: poorly perfused tissues; RPT: richly perfused tissues)

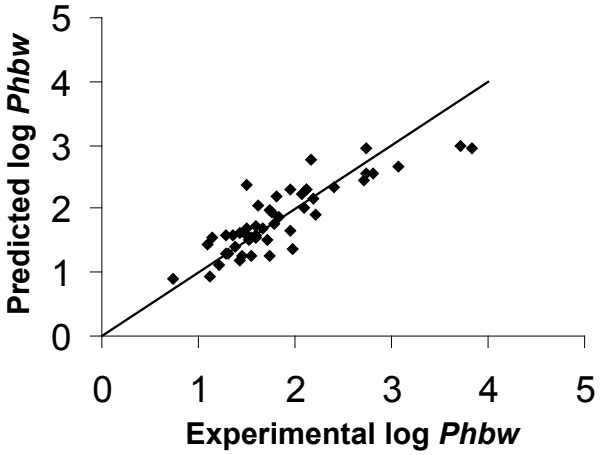

Figure 2. Comparison between the predicted values of log hemoglobin:water PC (log P_{hbw}) with experimental data.

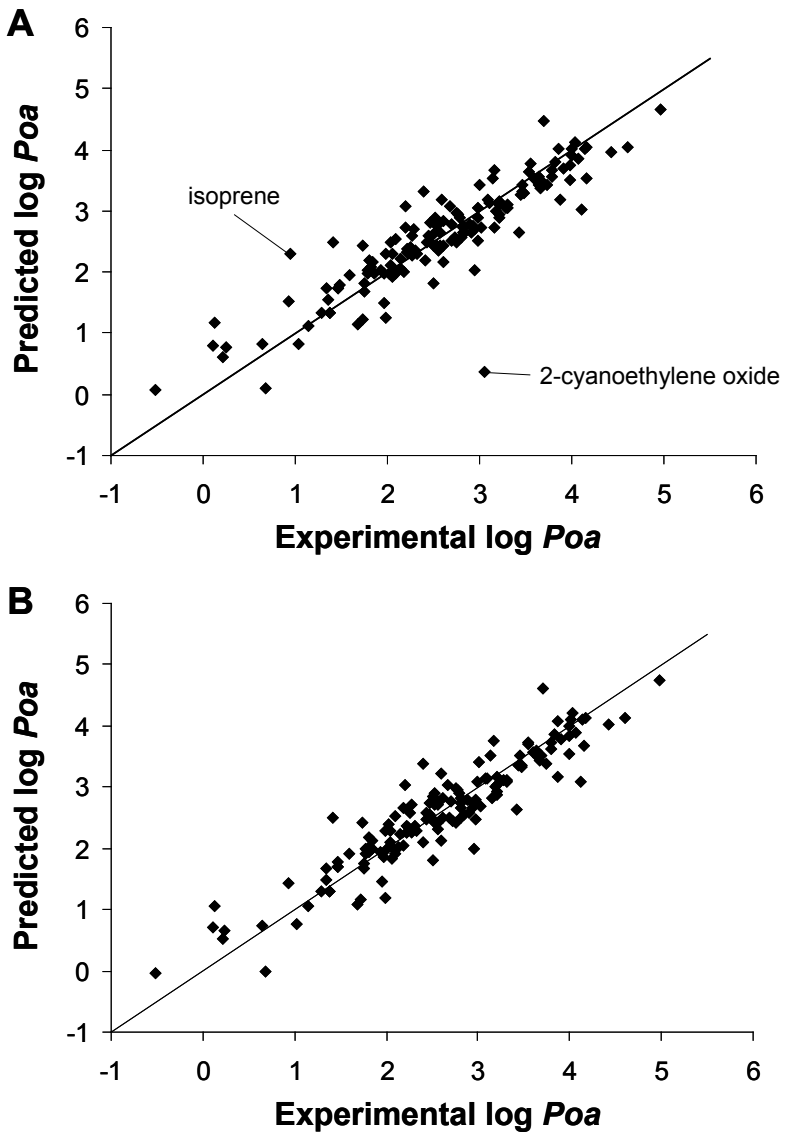

Figure 3. Comparison between the predicted values of log oil:air PC (log P_{oa}) with experimental data. A: using Eq. 14; B: using Eq. 15.

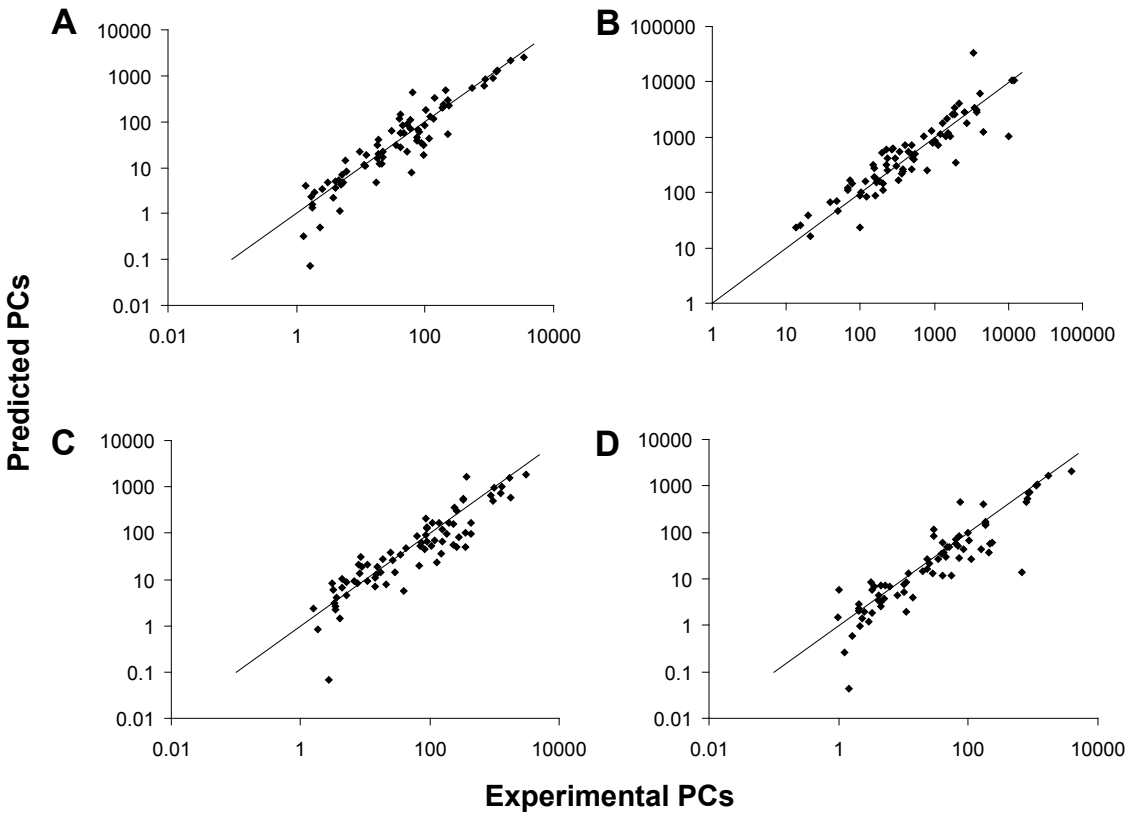

Figure 4. Comparison of predicted values of PCs (using Eq. 3 and 4) with experimental data (*14, 20, 32, 44*).

A) Blood:air PCs; B) Fat:air PCs; C) Liver:air PCs; D) Muscle:air PCs.

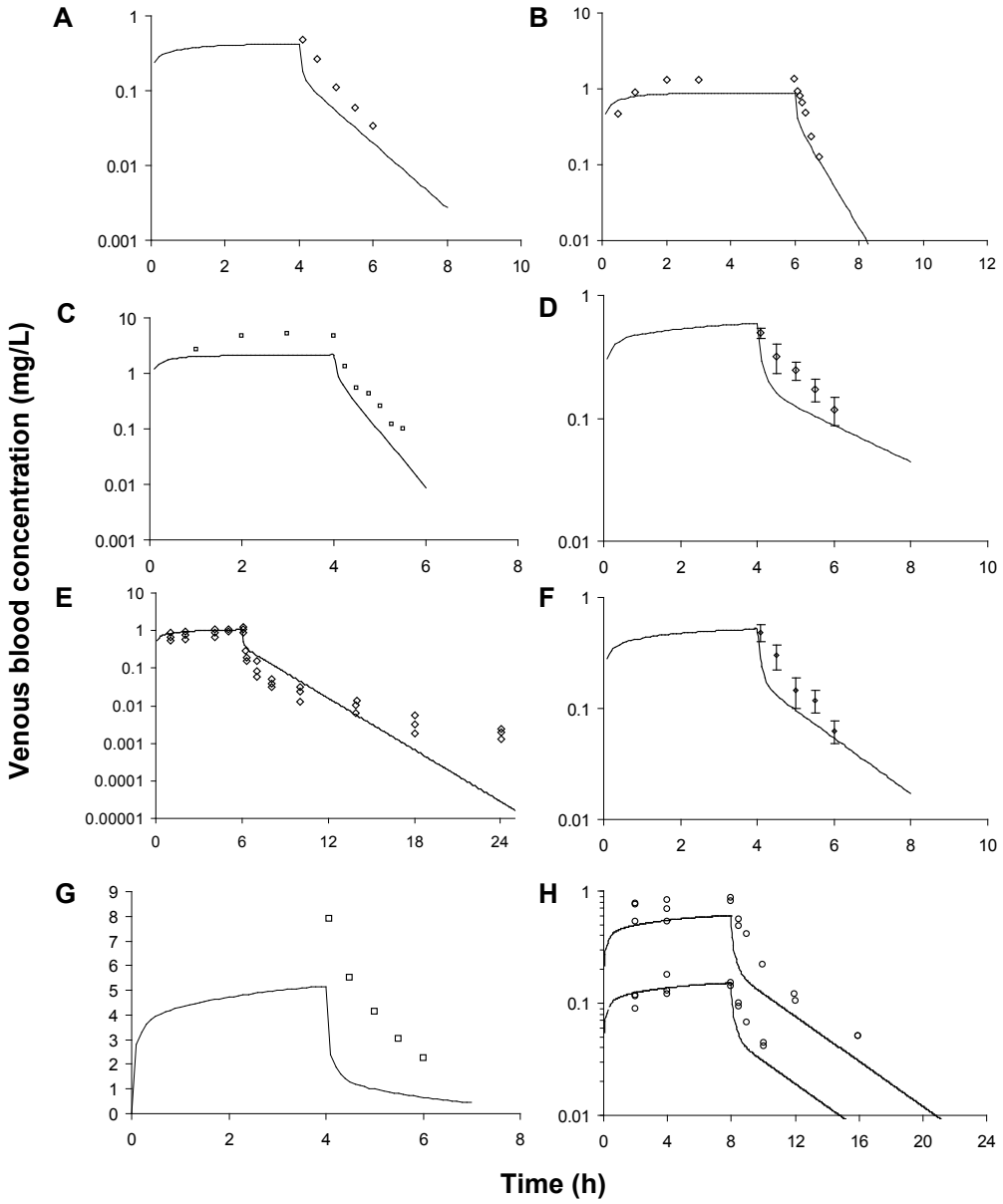

Figure 5. Comparison of the PBPK model simulations (lines) with experimental data (symbols) on venous blood concentrations following the inhalation of VOCs in the rat. A: benzene, 50 ppm, 4-h; B: 1,2-dichloroethane, 50, 6-h; C: dichloromethane 200, 4-h; D: m-xylene, 50 ppm, 4-h; E: styrene, 80, ppm, 6-h; F: toluene, 50 ppm, 4-h; G: 1,1,1-trichloroethane, 400 ppm, 4-h; H: 1,2,4-trimethylbenzene, 10, 40 ppm, 8-h (*52*, *58-62*).

Chapitre 6. Integrating biological variability with chemical property algorithms in PBPK models to simulate distributions of internal dose in humans

Pour soumission à *Regulatory Toxicology and Pharmacology*

Integrating biological variability with chemical property algorithms in PBPK models to simulate distributions of internal dose in humans

Thomas Peyret and Kannan Krishnan

[1]DSEST, Université de Montréal, Canada H3T 1A8

Corresponding author :

Dr. Kannan Krishnan. Département de Santé environnementale et santé au travail. Université de Montréal. C.P. 6128, Succ. Centre-ville. Montréal, Québec, Canada, H3C 3J7. T: +514-343-6581. F: +514-343-2200

6.1. Abstract

Existing mechanistic algorithms use point estimates for blood and tissue composition to predict the blood:air and tissue:air partition coefficients (PCs) required for PBPK modeling. The objectives of this study were: i) to develop a framework to predict the probability of distribution of PCs; and ii) to incorporate them, along with published information on the variability of cytochrome P450 CYP2E1 content and physiological parameters, within a human PBPK model to simulate the variability of toxicokinetics of inhaled VOCs. Previously published human data on toluene and acetone blood:air PCs; fat, liver, and muscle tissue:air PCs for 76 VOCs; and information on oil:air and water:air PCs was used in a Markov chain Monte Carlo (MCMC) approach to characterize the distributions of human blood and rat tissue composition parameters in the mechanistic algorithm for PCs (i.e., neutral lipid- and water-equivalents and protein content of blood). The posteriors distributions resulting from the MCMC analysis were used along with QSPR predicted physicochemical characteristics of benzene, chloroform, styrene and trichloroethylene to compute distributions of the tissue:blood and blood:air PCs. Monte Carlo simulations were then carried out with the PBPK model to predict the blood toxicokinetics. For the four VOCs, the predictions of the PBPK model compared well with experimental data. Overall, this study demonstrated the feasibility to simulate the impact of physiological variability on toxicokinetics using only QSPR and QPPR models for chemical-specific parameters.

Keywords: PBPK; volatile organic compounds; Markov chain Monte Carlo; Monte Carlo; QSPR; QPPR.

6.2. Introduction

In the assessment of health risk related to human exposure to a chemical, the internal (effective) dose is preferred to the potential (exposure) dose in order to reduce the uncertainty in the dose-response relationship. Physiologically based pharmacokinetic (PBPK) models are mathematical descriptions of the physiological, physicochemical and biochemical processes involved in the absorption, distribution, metabolism and excretion (ADME) of chemicals. The PBPK model parameters consist of physiological parameters, including tissue volumes, alveolar air and blood flows, as well as chemical-specific partition coefficients and metabolic constants. PBPK models are useful tools to predict the internal dose associated with the exposure to a substance (Krishnan and Andersen, 2007). For new untested chemicals with unknown pharmacokinetic parameters (e.g., volume of distribution, elimination half-life), the internal dose cannot be reliably estimated. In this case, the actual internal dose associated with a particular exposure scenario could vary from between zero (theoretical minimum) and the potential dose (theoretical maximum) (Peyret and Krishnan, 2011). Because the chemical-specific and physiological parameters determine the pharmacokinetics (particularly the internal dose) of chemicals in biota, this large uncertainty could be reduced by accounting for (i) knowledge of the physiology of the animal species and (ii) estimates of the key chemical-specific determinants of ADME, such as the tissue:blood partition coefficients and metabolic constants (Peyret and Krishnan, 2011). Therefore, integrating quantitative structure-property relationship (QSPR) or quantitative property-property relationship (QPPR) models along with the PBPK models could yield a predictive tool for generating preliminary estimates of the internal dose. The level of accuracy required for the QSPRs would then depend not only upon the intended end-use purpose(s) but also on the sensitivity of the specific input parameters with respect to the model outcome, i.e., predicted internal dose (Peyret and Krishnan, 2011).

However, a single point estimate of the dose metric does not account for the uncertainty or variability of the parameter values. The uncertainty and variability of QSPR-PBPK model

parameters can affect the predictions of internal dose. The variability refers to the inherent variation of a parameter value within or among individuals in a population (intra- and inter-individual variability), whereas the uncertainty relates to the lack of knowledge on the parameter value (U.S. E.P.A., 1997). Uncertainty or variability analysis of PBPK models aim to evaluate the impact of the uncertainty or variability of input parameters on the simulated dose metric (Clewell et al., 2001; Krishnan and Andersen, 2007). The uncertainty analysis can be undertaken using a probabilistic approach such as Monte Carlo (MC) simulations. The MC approach involves generating a distribution of dose metric values on the basis of specified probability distributions for the uncertain PBPK parameters. MC modeling can be performed to quantify the impact of the uncertainty associated with QSPR estimates of chemical-specific parameters and the variability of physiological parameters on a dose metric. Monte Carlo analysis of PBPK models has been conducted to characterize the interindividual variability on dose metrics (e.g., Clewell et al., 2001; Krishnan and Andersen, 2007; Thomas et al., 1996a).

When the rate of metabolism of a chemical in the liver is unknown, this uncertainty can be accounted for in PBPK modeling by setting the hepatic clearance to its physiological limits, namely, between zero and the hepatic blood flow (Béliveau and Krishnan, 2003; Poulin and Krishnan, 1999).

The impact of uncertainty associated with QPPR predictions of hepatic intrinsic clearance (CL_{int}) on the human pharmacokinetics has been studied relative to the impact of maximum uncertainty associated with hepatic clearance (Peyret and Krishnan, 2012). For CYP2E1 substrates, the interindividual variability of the metabolic rate has been modeled using MC simulations based on the variability of the concentration of CYP2E1 in the liver (Lipscomb et al., 2003; Nong and Krishnan, 2007; Nong et al., 2006; Valcke and Krishnan, 2010).

For the MC uncertainty analysis of PBPK models, the distributions of the values of partition coefficients were often estimated on the basis of experimental measurement errors

(Clewell et al., 2001; Thomas et al., 1996a). For VOCs, the values of human tissue:blood PCs used in human PBPK models are often calculated as the ratio of rat tissue:air PCs to human blood:air PC. The underlying assumption is that the rat-human differences are negligible for the value of tissue:air PCs, whereas the difference between these species is significant for the measured values of blood:air PCs of lipophilic VOCs (Gargas et al., 1989).

The tissue:air PCs can be predicted on the basis of the tissue composition (lipids, water, and proteins) along with the solubility in the key tissue constituents (Béliveau and Krishnan, 2003; Peyret and Krishnan, 2011; Peyret et al., 2010). For lipophilic VOCs, the blood:air PC is estimated based on the content and solubility or extent of binding in neutral lipids, neutral phospholipids, water and binding proteins (Béliveau and Krishnan, 2003; Béliveau et al., 2005; Peyret and Krishnan, 2011). The biologically-based algorithms for PCs use point estimates of input parameters to predict the PCs required for PBPK modeling. In a pilot study, the MCMC analysis of the variability on human blood composition parameters was performed using the algorithm described by Béliveau et al. (2005) along with measures of toluene blood:air PC in 26 volunteers (Peyret and Krishnan, 2008). The impact of the distributions of lipid and water content parameters on tissue:air PCs algorithms has not yet been characterized. Prior estimates of the distributions of these parameters could be updated by Markov chain Monte Carlo (MCMC) analysis of published experimental measures of PCs. The distributions of tissue and blood composition parameters, updated by MCMC analysis, could then be used in MC simulations to characterize the distribution of the PCs for PBPK modeling, but this has not been done.

The objective of this study was to develop a screening tool to predict the blood toxicokinetics of inhaled compounds in humans, *a priori,* on the basis of the molecular structure or properties of the substance and the uncertainty/variability associated with the input parameters. For this purpose, an integrated MC/QS(P)PR-PBPK modeling approach was used. The chemical-specific input parameters of the PBPK model were estimated using

QSPR (for partition coefficients) or QPPR (for intrinsic clearance) models. An uncertainty analysis was conducted on the PBPK blood kinetics in humans. For this purpose, Monte Carlo simulations were carried out using the predicted distributions of PCs and published information on the variability of tissue volumes, blood flows and enzyme content.

6.3. Methods

6.3.1 MCMC analysis of partition coefficients

The tissue:air and blood:air PCs were calculated using a biologically based algorithm (Béliveau et al., 2005; Peyret et al., 2010). MCMC analysis of the PCs was performed to characterize the variability of the rat tissue and human blood composition parameters. The resulting probability distributions of parameters were used to predict the uncertainty of tissue:blood and blood:air PCs incorporated within a human PBPK model.

Sensitivity analysis

Prior to the MCMC simulations, a sensitivity analysis for each PC was undertaken to determine which composition parameters most influenced the estimated PC value. Then, prior distributions were assigned to the most sensitive parameters. The sensitivity ratios (SRs) of PCs were calculated using the "backward difference normalized to parameter and response variable" method. The SRs were computed with a 1 % variation in the value of the input parameter value (Peyret et al., 2010).

MCMC modeling

A hierarchical approach was used to describe the variability or/and uncertainty associated with tissue or blood composition parameters (Gelman et al., 2004) (Figure 1).

Two hierarchical levels were used in the Bayesian analysis of rat tissue:air PCs and human blood:air PCs: one level for the population and one level for the experimental data. For the

statistical modeling of human blood (Fig. 1A), the population level contained the distributions of the mean and standard deviation of the blood composition for the human population, and the individual (volunteer) level contained the measured PCs of the same chemical for every individual in an experimental group. For the analysis of rat tissue:air PCs (Fig. 1B), the "population level" consisted of the distributions of the mean and standard deviations of rat tissue composition. Because no measure of PC for individual rats was available, a "chemical-level" computation was used, in which the tissue:air PC was calculated and the input parameter θ was adjusted on the basis of experimental data for diverse VOCs.

The models were written, and the MCMC simulations were run using WinBUGS (MRC Biostatistics Unit, Cambridge, and Imperial College School of Medicine, London). For each simulation, five chains were run until convergence was achieved. The convergence of the chains was monitored using the Gelman-Rubin Statistics (R) monitor included within WinBUGS (Brooks and Gelman, 1998). Convergence was considered to be achieved when the R value approached 1 (Jonsson et al., 2001).

MCMC analysis of human blood:air PCs

Experimental data

Measurements of toluene and acetone blood:air PCs for 73 volunteers were obtained from the literature (Dills et al., 1994). These compounds were chosen because for acetone, the value of blood:air PC was sensitive to the aqueous component of blood whereas the toluene blood:air PC value was primarily driven by the hemoglobin and blood lipid content. Therefore, the variability of water-equivalent content in human blood was analyzed on the basis of acetone blood:air PC values, whereas the variability of the neutral lipid-equivalent and blood-binding protein (hemoglobin) component was analyzed using the measures of toluene blood:air PC. The standard deviations of the PC measures were used to set the residual error of the statistical model. The experimental data (PC mean and standard

deviation) were obtained by digitalizing the graphs from Dills et al., 1994 with Engauge Digitizer (http://digitizer.sourceforge.net/). The quality of the digitalized data was controlled visually and by comparing the descriptive statistics of the digitalized data with those reported in the study.

Human blood:air PC model

The blood:air PCs were calculated using the following tissue level algorithm (Béliveau et al., 2005; Peyret et al., 2010):

$$P_{ba} = f_{nlb} \cdot P_{oa} + f_{wb} \cdot P_{wa} + f_{pb} \cdot P_{hba} \quad (1)$$

where f_{nlb} is the neutral lipid-equivalent fraction of blood volume; f_{wb} is the water-equivalent fraction of blood volume; f_{pb} is the hemoglobin fraction of blood volume; P_{oa} is the oil:air PC; P_{wa} is the water:air PC; and P_{hba} is the hemoglobin:air PC.

The neutral lipid-equivalent volume was calculated as the volume of neutral lipids plus 30 % of the volume of neutral phospholipids. The water-equivalent volume was calculated as the volume of water plus 70 % of the volume of neutral phospholipids (Poulin and Krishnan, 1995). For toluene, the hemoglobin:air PC (P_{hba}) was obtained as the product of the hemoglobin:water PC (P_{hbw}) and the water:air PC. For acetone, P_{hba} was set to zero because this chemical does not bind to hemoglobin (Lam et al., 1990; Poulin and Krishnan, 1996a). Experimental values for vegetable oil:air and water:air PC were used to calculate the PCs for acetone and toluene (Sato and Nakajima, 1979).

Input parameters and prior distributions

At the population level, truncated lognormal prior distributions were used for the blood composition parameters in Eq. 1 (f_{nlb}, f_{wb}, and f_{pb}). The numerical values of these prior distributions are listed in Table 1. The mean values for the whole blood content were

derived from compilations of erythocyte and plasma composition in humans (Poulin and Theil, 2002; Surgenor, 1974). The data on neutral lipid, neutral phospholipid, acidic phospholipid (phosphatidylserine) and hemoglobin content of the erythrocytes were obtained from Surgenor (1974). The fractional content of neutral lipids in the erythrocytes was calculated as the fraction of total lipids minus the fraction of total phospholipids. The value for fractional neutral phospholipid content was the difference between the total phospholipid content and the content of acidic phospholipids. The fraction of volume occupied by water in the erythrocytes corresponds to the difference between unity and the sum of total lipid and protein content according to published values (Heseltine et al., 1988). The values used for the composition of human plasma (neutral lipids, neutral phospholipids and water) were obtained from Poulin and Theil (2002), with the acidic phospholipid content considered negligible in the plasma (Peyret et al., 2010). The whole blood composition in terms of neutral lipids, neutral phospholipids, water and proteins was derived from the composition of erythrocytes and plasma assuming a hematocrit of 0.35, according to Dills et al. (1994). The standard deviations of the prior distributions were calculated assuming 20 % coefficient of variation. The variation in hemoglobin content in blood was obtained from the literature (Surgenor, 1974). The highest coefficient of variation reported by Surgenor (1974) associated with the neutral lipid content of erythrocytes (0.2) was used to define the prior distribution of neutral lipid-equivalent in whole blood (f_{nlb}). For water content in blood (f_{wb}), the prior variability was set to 20 %. All prior distributions were truncated to ± 3 standard deviations except the distribution of f_{wb}, for which the maximum was set equal to one less than the minimum prior content in the other constituents. A 30 % uncertainty was assigned to the prior standard deviation for the population (Σ, Figure 1), assuming the value to be quite uncertain.

For toluene blood:air PC analysis, the prior distributions were assigned to f_{nlb}, f_{pb}, and the hemoglobin:water PC. For this chemical, the proportion of water in blood volume (f_{wb}) was fixed (f_{wb} = 0.82 = 1 – (sum of the min prior values of f_{nlb} and f_{pb} + sum of the proportions acidic phospholipids (0.00015) and plasma proteins (0.0105) in blood). Assigning a

distribution to f_{wb} did not change the posterior distributions of f_{nlb} and f_{wb}. Multiplying the hemoglobin:water PC (63.9) calculated in Peyret et al. (2010) by the P_{wa} (1.75) reported by Gargas et al. (1989) gives a point estimate of 112 for toluene P_{hba}. Because the experimental value of this parameter is unknown, it was assumed to follow a uniform non-informative prior distribution (minimum = 0, maximum = 500). For acetone, however, f_{wb} was subjected to the MCMC analysis, and f_{nlb} was fixed.

MCMC analysis of rat tissue:air PCs

For each tissue:air PC, the VOCs were pooled based on similar sensitivity behavior according to the results of the sensitivity analyses. In other words, the chemicals sharing the same most sensitive parameters were pooled to form a single group.

Experimental data

The variability on rat tissue composition parameters was characterized using *in vitro* values of tissue:air PCs for fat, liver and muscle along with values of oil:air and water:air PCs for 76 volatile chemicals (halogenated hydrocarbons, alkanes, aromatic compounds, ethers, alcohols, ketones and acetate esters) (Gargas et al., 1989; Kaneko et al., 1994; Poulin and Krishnan, 1996b). For cyclohexane, 2,3,4-trimethyl pentane and 2,2,4-trimethyl pentane, the value of water:air PC reported by Meulenberg and Vijverberg (2000) was used because no value was available in the study by Gargas et al. (1989). The measured standard deviations of PCs were included in the Bayesian analysis (σ, figure 1).

Rat tissue:air PC model

The tissue:air PCs were calculated as follows (Béliveau et al., 2005; Peyret et al., 2010):

$$P_{ta} = f_{nlt} \cdot P_{oa} + f_{wt} \cdot P_{wa} \quad (2)$$

where f_{nlt} is the neutral lipid-equivalent fraction of tissue volume; f_{wt} is the water-equivalent fraction of tissue volume; P_{oa} is the oil:air PC; and P_{wa} is the water:air PC.

Input parameters and prior distributions

Truncated lognormal prior distributions were assigned to the population parameters. For all tissues, the mean values of the tissue composition were gathered from the literature (Peyret et al., 2010), and 20-50% variability and uncertainty were assumed. For all the population parameters in the tissue:air PC analyses, 30 % uncertainty was assigned to the prior standard deviation, assuming this value to be quite uncertain.

The prior distributions were truncated at ± 3 standard deviations except when it led to unrealistic values. Table 2 presents the numerical values used in the prior distributions of input parameters for fat, liver and muscle as per Eqn. 2. The compositions of tissue, cell and interstitial content were used to calculate the mean values of the input parameters for the tissue:air algorithm, and prior distributions were assigned to the most sensitive of these parameters.

For the analysis of fat:air PCs in rats, the proportion of neutral lipid-equivalent (f_{nlt}) in adipose tissue was the sole parameter subject to MCMC analysis. The maximum of the f_{nlt} in fat was calculated as 1 – (0.019 = minimum fractional content of water-equivalent + fractional content of acidic phospholipids and proteins). The water-equivalent content (f_{wt}) in fat was used as buffer to maintain the mass balance, specifically f_{wt} in fat = 1- (f_{nlt} + acidic phospholipids + proteins).

For the analysis of liver:air PCs, the value of prior distributions for liver composition parameters are reported in Table 2. The prior distributions were truncated to ± 3 standard deviations. A 30 % coefficient of variation was assumed, to specify the mean standard

deviation on f_{nlt} and f_{wt} for the population. The prior distribution of f_{nlt} in liver was truncated to ± 3 standard deviations. For f_{wt}, the maximum was calculated as 1 – (minimum prior f_{nlt} – fraction of acidic phospholipids + fraction of proteins), and the minimum was set to 0.5 (which was considered more physiologically-plausible value than the 0.06 obtained with mean – 3 standard deviations). During the analysis of liver:air PCs, when one parameter was subject to the analysis (e.g., f_{nlt}), the other (e.g., f_{wt}) was treated as the buffer.

For muscle:air PCs analysis, a 30 % coefficient of variation for the tissue composition parameters (f_{nlt} and f_{wt}) was used as prior information for the population standard deviation. The distribution of f_{nlt} was truncated to ± 3 standard deviations. The maximum of f_{wt} was calculated as 1 – (minimum of f_{nlt} + fraction of acidic phospholipids and proteins). The minimum of f_{wt} was calculated as the mean – 1 standard deviation to obtain a relatively low but plausible value. During the MCMC analysis of the distribution of f_{nlt}, f_{wt} was used as the buffer and vice versa.

6.3.2 PBPK modeling

PBPK model

Figure 2 illustrates the PBPK modeling framework used in this study. A PBPK model for inhaled VOCs was implemented. This PBPK model consisted of four tissue compartments (liver, richly perfused tissues RPT, poorly perfused tissues PPT and fat) interconnected by systemic circulation through a gas exchange compartment (Ramsey and Andersen, 1984). The rate of metabolism was described in the liver compartment using intrinsic clearance. Monte Carlo simulations were performed to characterize the distributions of blood toxicokinetics by accounting for the variability/uncertainty in the PBPK parameters. For this purpose, distributions of partition coefficients, cytochrome P450 enzyme content, tissue volumes, blood and alveolar flows were incorporated within the human PBPK

model. Benzene, chloroform, styrene and trichloroethylene were used as model chemicals. These chemicals where chosen as proof of concept and because they have different physicochemical properties (Benzene, log P_{ow}: 1.99, log P_{wa}: 0.43; Chloroform, log P_{ow}: 1.52, log P_{wa}: 0.58; Styrene, log P_{ow}: 2.89, log P_{wa}: 0.72; Trichloroethylene, log P_{ow}: 2.47, log P_{wa}: 0.15) along with available human PK data in the literature.

Physiological parameters

Log normal distributions were assigned to body weight, cardiac output, alveolar ventilation and the predicted PCs, and normal distributions were assigned to the fractional tissue volumes and tissue blood flows (Clewell et al., 2001; Delic et al., 2000). The numerical values of the distributions of physiological parameters are reported in Table 3. The mean values of the physiological parameters were obtained from Tardif et al. (1997). The coefficient of variations for body weight, cardiac output, alveolar ventilation, tissue volumes and blood flows were obtained from the literature (Clewell et al., 2001). The distributions of body weight, cardiac output, alveolar ventilation, tissue volumes and tissue blood flows were truncated to ± 2 standard deviations. The balance of tissue volumes was controlled by setting the volume of the poorly perfused tissues equal to 0.88 (i.e., total of the mean soft tissue volumes) minus the values of liver, fat and richly perfused tissues expressed as a fraction of body weight. The mass balance of blood flows was maintained by calculating the perfusion through the richly perfused tissues as being equal to 1 minus the fractional cardiac output flowing through the liver, fat and poorly perfused tissues.

Partition coefficients

The posterior distributions obtained after the MCMC analysis of rat tissue and human blood composition were used as input parameters for tissue:blood PC (i.e., Eq. 2 divided by Eq. 1) and blood:air PC (Eq. 1) algorithms. In Eq. 1 and 2, the P_{wa} values for benzene, chloroform, styrene and trichloroethylene were estimated using HENRIWIN program in

EPISUITE™ (http://www.epa.gov/opptintr/exposure/pubs/episuite.htm). The values of P_{oa} and P_{hba} were calculated using QSPR models developed in a previous study (Peyret and Krishnan, in preparation), as described in Appendix 1. For each chemical, a sensitivity analysis was conducted on the tissue:air and blood:air PCs to determine the least sensitive parameter. A fixed value of this parameter was set for the MC simulations.

For benzene, chloroform, styrene and trichloroethylene, the distributions of tissue:blood and blood:air PCs were obtained from 5000 Monte Carlo simulations using Crystal Ball 7 for EXCEL® (Decisioneering, Denver, CO). For the four VOCs, the predicted distributions of blood:air PCs and tissue:blood PCs were compared with the experimentally-derived values. Specifically, the experimental values of tissue:blood PCs were calculated as the ratio of human blood:air PCs to rat tissue:air PCs (Gargas et al., 1989; Ramsey and Andersen, 1984).

Metabolism

In the PBPK model, hepatic metabolism was computed from the intrinsic clearance (CL_{int}) normalized to the concentration of cytochrome P450 CYP2E1 (CL_{int2E1}) in human liver (Béliveau et al., 2005). First, the CL_{int2E1} was estimated on the basis of a quantitative property-property relationship (QPPR) (Peyret and Krishnan, 2012). The derivation of CL_{int2E1} is described in the Appendix. The distribution of intrinsic clearance was obtained by multiplying the point estimate of CL_{int2E1} with the distributions of the concentration of CYP2E1 in human liver. The distribution of CYP2E1 in microsomal proteins and the distribution of microsomal proteins in human liver (Table 3) were obtained from the literature (Lipscomb et al., 2003).

PBPK simulations

The human PBPK models (differential and algebraic mass-balance equations, parameters distributions) were written and run in ACSL® (acslX®, version 2.5, Aegis Technologies Group, Inc, Huntsville, AL).

For each chemical, the distributions of partition coefficients, physiological parameters and enzyme content were specified within the PBPK models. Five thousand Monte Carlo simulations were conducted to simulate the distribution of the 24-h area under the curve (AUC) associated with a 1-ppm 24-h continuous exposure. Further, the venous blood toxicokinetics in humans were simulated and compared with experimental data for benzene (25 ppm, 2 h), styrene (80 ppm, 6 h) and trichloroethylene (100 ppm, 4h) (Koizumi, 1989; Ramsey et al., 1980; Travis et al., 1990).

6.4. Results

6.4.1 MCMC analysis of partition coefficients

MCMC analysis of human blood:air PCs

Sensitivity analysis

The SRs of the input parameters in Eq. 1 for human blood:air PC are reported in Table 4. For toluene, the most sensitive parameters, i.e., those with the highest value of SR, were the fraction of proteins in blood volume (f_{pb}) and the fraction of neutral lipid-equivalent (f_{nlb}). For acetone, the fraction of water-equivalent (f_{wb}) was the most sensitive parameter. Therefore, in Eq. 1, the distributions of f_{nlb} and f_{pb}, were updated using toluene blood:air PC experimental values, whereas f_{wb} was updated using acetone blood:air PCs.

MCMC analysis

The posterior distributions of human blood composition parameters are presented in Table 5. Using Eq. 1 and toluene blood:air PC measures, the population posterior distribution of f_{nlb} was comparable to its prior distribution: the coefficient of variation was still approximately 20 %, and the mean was slightly reduced. The posterior distribution of f_{pb} had a slightly decreased mean and decreased variability (coefficient of variation = 17 %), compared to its prior distribution. The posterior distribution of hemoglobin:air PC visually showed a normal shape (mean = 242, standard deviation = 12). When using the acetone blood:air PC data, the updated distribution of the water fraction of blood volume (f_{wb}) showed a decreased mean (0.76) and variability (7 % coefficient of variation).

Analysis of rat tissue:air PCs

The SRs calculated for the three tissue:air PCs of 76 VOCs are presented in the Appendix.

Fat:air PC

Sensitivity analysis

Using Eq. 2, the proportion of neutral lipid-equivalent (f_{nlt}) in fat was the most sensitive parameter for 73 of the 76 VOCs studied (Table A1 in the Appendix 2). For all the VOCs except the eight alcohols, methyl acetate ester, dimethyl ketone, and methyl ethyl ketone, the SR of this parameter was above 0.9, and the SR of the water-equivalent fraction of fat volume was below 0.1. Therefore, the MCMC analysis was conducted on the distribution of f_{nlt} for the 65 VOCs with an SR of this parameter > 0.9.

MCMC analysis

Using Eq. 2, the analysis of fat:air PCs yielded a posterior distribution (Table 6) of 0.83 ± 0.12 for the proportion of neutral lipid-equivalent in the adipose tissue of the rat population. Thus, the mean value of this posterior distribution is the same as its prior value, but the

variability is 45 % higher. At the individual (chemical) level, the predictions of fat:air PC were ± 10 % of the experimental values, with the exception of isoprene (10-fold of the experimental value), 1-bromo-2-chloroethane, chloromethane, 1-nitropropane, 2-nitropropane and difluoromethane (2-3 fold of the experimental value).

Liver:air PC

Sensitivity analysis

Using Eq. 2, for the liver:air PC, the content of neutral lipid-equivalent (f_{nlt}) was the most sensitive parameter for 54 VOCs, and the proportion of water-equivalent (f_{wt}) was the primary sensitive parameter for the remaining 22 chemicals (Table A2 in Appendix 2). The f_{nlt} SR values were > 0.7 for 51 compounds, and the SRs of f_{wt} were < 0.7 for 59 VOCs. The MCMC analysis of f_{nlt} was undertaken for the 54 VOCs for which this parameter was the most sensitive. The f_{wt} was updated using the liver:air PC values of the 22 remaining chemicals.

MCMC analysis

After 10,000 iterations, the chains converged, at which time the posterior distributions of f_{nlt} and f_{wt} (Eq 2) were analyzed using every 10^{th} iteration of the last 5000 iterations (i.e., 2500 samples). The values of the posterior distributions of f_{nlt} and f_{wt} for the liver are reported in Table 6. Compared to its prior distribution, the posterior distribution of f_{nlt} for the rat population had a 9 % higher mean value and an increased coefficient of variation (46 %). The predicted values of the liver:air PC for the individual chemicals used in the analysis of f_{nlt} were equal to the experimental values ± 10 %, except for *n*-hexane, isopentyl acetate ester, allyl chloride, *n*-butyl acetate ester, isobutyl acetate ester and isoprene, for which the predicted value / experimental value ranged from 0.26 (isoprene) to 1.11 (*n*-hexane). For the rat population, the posterior distribution of f_{wt} had an increased mean value and a decreased coefficient of variation (19 %) compared to its prior distribution. The liver:air

PCs were predicted within 30 % error, except for 2-nitropropane, diethyl ether, difluoromethane, *n*-pentanol and dimethyl ketone, for which the ratio of the predicted / experimental values ranged from 0.53 (*n*-pentanol) to 1.46 (diethyl ether).

Muscle:air PCs

Sensitivity analysis

The fraction of neutral lipid-equivalent (F_{nlt}) was the most sensitive parameter in Eq. 2 for muscle:air PC for 45 VOCs, and the fraction of water-equivalent was the most sensitive parameter for 31 VOCs (Table A3 in Appendix 2). F_{nlt} was then updated using the 45 chemicals for which the muscle:air PC was the most sensitive. The remaining 31 VOCs were used to characterize the distribution of F_{wt} in muscle.

MCMC analysis

Using Eq. 2, for the population, the posterior distribution obtained for f_{nlt} (Table 6) had a higher mean value and variability than its corresponding prior distribution. During the analysis of f_{nlt} the errors of prediction for muscle:air PCs were within 30 %, except for JP-10, cyclohexane, *n*-pentyl acetate ester, isopentyl acetate ester and vinyl chloride (predicted / observed value between 0.4 and 1.93). The posterior population mean of f_{wt} (0.77, Table 6) was higher than the prior value, and the variability of this parameter was much lower than the prior. The predicted values of muscle:air PCs for the group of chemicals used to update f_{wt} were approximately 30 % of the experimental value, except for dichloromethane, chloromethane, 1-nitropropane, fluorochloromethane, 2-nitropropane, diethyl ether, methyl acetate ester and methanol, which had predicted to experimental ratios ranging from 0.7 (methanol) to 4.17 (1-nitropropane).

6.4.2 PBPK modeling

The values of the predicted distributions of liver:blood, richly perfused tissues:blood, poorly perfused tissues:blood, fat:blood and blood:air PCs, along with experimental values for benzene, chloroform, styrene and trichloroethylene, are reported in Table 7. Almost all of the predicted distributions of partition coefficients encompassed the experimental values. The maximum of the distribution was below or equal to the experimental value for benzene PPT:blood and fat:blood PCs and for chloroform liver:blood/richly perfused tissues:blood, PPT:blood and fat:blood PCs. These maxima were within a factor of two of the experimental values, except for chloroform, for which the predicted PPT:blood PC was 54 % lower than the experimental value. To perform the Monte Carlo simulations, the shapes of the PC distributions, used as input parameter in the PBPK models, were assumed log normal by visual inspection.

Figure 3 presents the distribution of the 24-h AUC associated with a 24-h exposure to 1 ppm for benzene, chloroform, styrene and trichloroethylene. The 24-h AUC (mean ± standard deviation (percentiles), in mg/L-h) was 0.16 ± 0.05 for benzene (50^{th} = 0.16; 95^{th} = 0.25), 0.26 ± 0.07 (50^{th} = 0.25; 95^{th} = 0.37) for chloroform, 0.30 ± 0.11 (50^{th} = 0.28; 95^{th} = 0.51) for styrene, and 0.27 ± 0.08 (50^{th} = 0.26; 95^{th} = 0.42)for trichloroethylene. The uncertainty in the 24-h AUC ranged from 25 % (chloroform) to 37 % (styrene).

Figure 4 illustrates the Monte Carlo simulations of venous blood concentrations along with experimental data for benzene (25 ppm, 2 h), styrene (80 ppm, 6 h) and trichloroethylene (100 ppm, 4 h) (Koizumi, 1989; Ramsey et al., 1980; Travis et al., 1990). For all chemicals, the simulated venous blood toxicokinetics encompassed the experimental data, except for the elimination phase of benzene, for which the concentrations were underestimated.

6.5. Discussion

Physiologically based pharmacokinetic models have proven their usefulness in the risk assessment of chemicals. The limiting factor for development of PBPK models is related to the fairly high number of parameters and to the level of confidence in their value. Monte Carlo simulations are used in the risk assessment of chemicals to quantify the impact of the uncertainty and variability of PBPK parameters on simulated dose metrics (Clewell et al., 2001; Krishnan and Andersen, 2007). For the physiological PBPK parameters, estimates of variability can be obtained from the literature (Clewell et al., 2001; Thomas et al., 1996a). The variability of CYP2E1 enzyme content was used to describe the variability of metabolism rate (Lipscomb et al., 2003; Valcke and Krishnan, 2010). For partition coefficients, the values of coefficient of variation can be estimated on the basis of experimental measurement errors (Clewell et al., 2001; Thomas et al., 1996b). In this study, the distributions of PC values were obtained on the basis of the variability of tissue and blood composition parameters within biologically based algorithms for PCs. Thus, this is the first attempt to compute the variability of PCs based on tissue composition parameters.

The distributions of tissue and blood composition parameters were obtained by MCMC analysis of *in vitro* PC values. The MCMC simulations were performed on tissue:air PCs for fat, liver and muscle. These tissues are often used to study the solubility/distribution of non-polar chemicals in PBPK modeling (Krishnan and Andersen, 2007; Reddy, 2005). The analysis could further be extended to other tissues such as brain and kidneys, which are often described as target tissues in PBPK models for risk assessment. The distributions obtained for rat tissue composition parameter actually reflected both biological variability and uncertainty, eventhough the term uncertainty might be more appropriate, as used in the text of this article, to describe these distributions.

The MCMC analysis yielded distributions for the neutral lipid- and water-equivalent content of human blood as well as the VOC-binding protein (hemoglobin) based on

experimental data in human volunteers. These distributions thus reflect the variability within this human group. Differences in the variability of the posterior distribution from its prior distribution indicate that there was enough information in the data to characterize this variability. The information on the variability could be used in further Monte Carlo simulations to obtain preliminary estimates of the variability of PCs for VOCs. Indeed, except for the water composition parameters (f_{we}, f_{wp} and f_{wb}), the mean of the population posterior distributions was comparable to the prior values that were gathered from the literature. For the water content of blood, the means of f_{we}, f_{wp} or f_{wb} (Eq. 1 and 2) decreased after the MCMC analysis in order to adequately fit the experimental measures of acetone blood:air PC. The means for these distributions did not correspond to the information collected in the literature for the input parameters (Heseltine et al., 1988; Poulin and Theil, 2002; Surgenor, 1974). As long as the method used for measuring the PCs is reproducible, the variability measured might reflect the interindividual variability. Because (i) the variability in the posterior distributions was different from the prior distributions and (ii) the predictions at the individual level fit the data well, it can be assumed that the interindividual variability of the blood:air PC input composition parameters was adequately characterized.

The hematocrit used for the MCMC simulations was set to the known measured value of 0.35 (Dills et al., 1994). Using a standard value of 0.4-0.45 would have biased the characterization of the erythrocyte and plasma composition. However, once the composition of these blood compartments is achieved another hematocrit value can be used to predict the blood:air PC.

The hemoglobin:air PC is the most sensitive determinant in the estimation of blood:air PC for relatively lipophilic VOCs (log P_{ow} > 1). A non-informative prior distribution was assigned to this parameter because a fixed estimated value could influence predictions of the binding to protein. In this regard, the calibration of the hemoglobin:air PC using Eq. 1 or Eq. 2 gave comparable estimates of this parameter. The distributions of the composition

of human blood should be used with caution because (i) the population sample (students and university staff, Caucasian) might not be representative of the general population and (ii) the quality of the measure of PCs, particularly acetone blood:air PCs, was unclear. It is possible that the methods used to measure this PC overestimate its value (Ackerlund, 1990). Additional MCMC analyses of PCs should be carried out to evaluate the robustness of the distributions of tissue composition parameters. However, the method used in this study is an original, scientifically sound method to obtain preliminary estimates of the variability of PCs. This study demonstrated the feasibility of estimating this variability for four VOCs using QSPR estimates of their physicochemical properties.

Since the initial values of hemoglobin:water PC were fitted on rat blood:air PCs, the MCMC analysis of this PC was not possible because the initial values allow a perfect fit of the observed data.

The posterior distributions of tissue and blood composition were used as input parameters in tissue:air and blood:air algorithms to predict the distribution of tissue:blood and blood:air PCs for benzene, chloroform, styrene and trichloroethylene. The resulting distributions compared fairly well with experimental data (Table 7), but some PCs were underestimated (PPT:blood and fat:blood PCs for benzene; liver:blood/richly perfused tissues:blood, PPT:blood and fat:blood PCs for chloroform). This underestimation can be attributed to the underestimation of the oil:air PC (P_{oa}) for benzene and chloroform. The QSPR predictions of P_{oa} were 312.1 and 132.1, whereas the experimental values were 465 and 402 for benzene and chloroform, respectively (Gargas et al., 1989). However, for each VOC, the PC distributions were then incorporated within a human PBPK model, along with distributions of physiological and enzyme content parameters. Monte Carlo simulations were performed to quantify the uncertainty of blood dose metrics (AUC, venous blood concentration). The metabolism rate was estimated using a QPPR model for rat intrinsic clearance but the uncertainty of the predicted CL_{int} QPPR values was not assessed in this study. However, the reliability of this parameter value can be characterized by a confidence

analysis (IPCS, 2010; Peyret and Krishnan, 2012). The simulations of venous blood toxicokinetics underestimated the experimental data for benzene because the predicted value of intrinsic clearance (mean = 629 L/h) was higher than that used by Travis et al. (1990) (83 L/h), which adequately fit the data. These results should be viewed in the context of application in data-poor situations where even a screening level value or a preliminary idea of the kinetics of the substance is desired solely from its structure-property information.

The ratio of 95^{th} to 50^{th} percentile of chloroform (1.48) and trichloroethylene (1.61) are higher but comparable with those predicted with other probabilistic PBPK framework (1.30 for chloroform and 1.37 for trichloroethylene (Valcke and Krishnan, 2010) is comparable with Renwick and Lazarus (1998) collected data on the variability of pharmacokinetic parameters (mostly area under the plasma concentration–time curve following oral administration of drugs) in humans. These authors observed a mean 38 % coefficient of variation, ranging from 9 % to 114 %, which is fairly comparable to the range of uncertainty in the 24-h AUC predicted with the present QSPR-PBPK framework (25 % for chloroform to 37 % for styrene). Therefore the variability of blood metrics estimated with the present framework can be considered plausible.

6.6. Conclusion

MCMC simulations were carried out to characterize the variability of human blood and the uncertainty of rat tissue composition parameters for use within biologically based algorithms for PCs. The distribution of the composition parameters were then used in Monte Carlo simulations to obtain *a priori* distributions of values for PCs on the basis of readily retrievable physicochemical properties (i.e., octanol:water, oil:air; water:air). This study demonstrated the feasibility of conducting *a priori* uncertainty analysis on the blood toxicokinetics of VOCs on the basis of physiological variability, molecular structure, and physicochemical properties.

6.7. Acknowledgment

Financial support by the Natural Sciences and Engineering Research Council of Canada (NSERC) is acknowledged.

6.8. References

Ackerlund, W. S., Variability in blood/air partitioning of volatile organic compounds: effect of concentration and correlation with blood chemistry. Public Health and Community Medecine. University of Washington, Washington, 1990, pp. 104.

Béliveau, M., Krishnan, K., 2003. In Silico approaches for developing physiologically based pharmacokinetic (PBPK) models. in: Salem, H., Katz, S. A., Eds.), Alternative toxicological methods. CRC Press, Boca Raton, FL., pp. 479-532.

Béliveau, M., Lipscomb, J., Tardif, R., Krishnan, K., 2005. Quantitative structure-property relationships for interspecies extrapolation of the inhalation pharmacokinetics of organic chemicals. Chem Res Toxicol. 18, 475-485.

Brooks, S. P., Gelman, A., 1998. Alternative methods for monitoring convergence of iterative simulations. Journal of Computational and Graphical Statistics. 7, 434-455.

Clewell, H. J., Gentry, P. R., Gearhart, J. M., Allen, B. C., Andersen, M. E., 2001. Comparison of cancer risk estimates for vinyl chloride using animal and human data with a PBPK model. Sci Total Environ. 274, 37-66.

Delic, J. I., Lilly, P. D., MacDonald, A. J., Loizou, G. D., 2000. The utility of PBPK in the safety assessment of chloroform and carbon tetrachloride. Regul Toxicol Pharmacol. 32, 144-55.

Dills, R. L., Ackerlund, W. S., Kalman, D. A., Morgan, M. S., 1994. Inter-individual variability in blood/air partitioning of volatile organic compounds and correlation with blood chemistry. J Expo Anal Environ Epidemiol. 4, 229-245.

Gargas, M. L., Burgess, R. J., Voisard, D. E., Cason, G. H., Andersen, M. E., 1989. Partition coefficients of low-molecular-weight volatile chemicals in various liquids and tissues. Toxicol Appl Pharmacol. 98, 87-99.

Gelman, A., Carlin, J. B., Stern, H. S., Rubin, D. B., 2004. Bayesian data analysis. Chapman & Hall/CRC, Boca Raton, Fla. ; London.

Heseltine, D., Thomas, T. H., James, O. F. W., Kesteven, P., Potter, J. F., 1988. High Erythrocyte Water Content Causes Discrepancy between Values of Automated and Micro-Centrifuged Haematocrit. Acta Haematologica. 80, 89-90.

IPCS, 2010. Characterization and application of physiologically based pharmacokinetic models in risk assessment.

Jonsson, F., Bois, F. Y., Johanson, G., 2001. Assessing the reliability of PBPK models using data from methyl chloride-exposed, non-conjugating human subjects. Arch Toxicol. 75, 189-99.

Kaneko, T., Wang, P. Y., Sato, A., 1994. Partition coefficients of some acetate esters and alcohols in water, blood, olive oil, and rat tissues. Occup Environ Med. 51, 68-72.

Koizumi, A., 1989. Potential of physiologically based pharmacokinetics to amalgamate kinetic data of trichloroethylene and tetrachloroethylene obtained in rats and man. Br J Ind Med. 46, 239-249.

Krishnan, K., Andersen, M. E., 2007. Physiologically based Pharmacokinetic modeling in toxicology. in: Hayes, A. W., (Ed.), Principles and methods of toxicology. Taylor & Francis, Boca Raton, pp. 231-292.

Lam, C.-W., Galen, T. J., Boyd, J. F., Pierson, D. L., 1990. Mechanism of transport and distribution of organic solvents in blood. Toxicology and Applied Pharmacology. 104, 117-129.

Lipscomb, J. C., Teuschler, L. K., Swartout, J., Popken, D., Cox, T., Kedderis, G. L., 2003. The impact of cytochrome P450 2E1-dependent metabolic variance on a risk-relevant pharmacokinetic outcome in humans. Risk Anal. 23, 1221-38.

Meulenberg, C. J., Vijverberg, H. P., 2000. Empirical relations predicting human and rat tissue:air partition coefficients of volatile organic compounds. Toxicol Appl Pharmacol. 165, 206-16.

Nong, A., Krishnan, K., 2007. Estimation of interindividual pharmacokinetic variability factor for inhaled volatile organic chemicals using a probability-bounds approach. Regul Toxicol Pharmacol. 48, 93-101.

Nong, A., McCarver, D. G., Hines, R. N., Krishnan, K., 2006. Modeling interchild differences in pharmacokinetics on the basis of subject-specific data on physiology and hepatic CYP2E1 levels: A case study with toluene. Toxicol Appl Pharmacol. 214, 78-87.

Peyret, T., Krishnan, K., 2008. A hierarchical algorithm for computing distributions of human blood: air partition coefficients (PB) of toluene. Abstract 998. The Toxicologist CD—An official journal of the Society of Toxicology. Toxicol. Sci. 102, 205

Peyret, T., Krishnan, K., 2011. QSARs for PBPK modelling of environmental contaminants. SAR and QSAR in Environmental Research. 22, 129-169.

Peyret, T., Krishnan, K., 2012. Quantitative property-property relationship (QPPR) for screening-level prediction of intrinsic clearance of volatile organic chemicals in rats and its integration within PBPK models to predict inhalation pharmacokinetics in humans. Journal of Toxicology. doi: 10.1155/2012/286079.

Peyret, T., Krishnan, K., in preparation. Quantitative structure/property-property relationships for the physiologically based prediction of toxicokinetics for inhaled chemicals in rats (Chapter 4 of this thesis).

Peyret, T., Poulin, P., Krishnan, K., 2010. A unified algorithm for predicting partition coefficients for PBPK modeling of drugs and environmental chemicals. Toxicology and Applied Pharmacology. 249, 197-207.

Poulin, P., Krishnan, K., 1995. A biologically-based algorithm for predicting human tissue: blood partition coefficients of organic chemicals. Hum Exp Toxicol. 14, 273-280.

Poulin, P., Krishnan, K., 1996a. A mechanistic algorithm for predicting blood:air partition coefficients of organic chemicals with the consideration of reversible binding in hemoglobin. Toxicol Appl Pharmacol. 136, 131-7.

Poulin, P., Krishnan, K., 1996b. A tissue composition-based algorithm for predicting tissue:air partition coefficients of organic chemicals. Toxicol Appl Pharmacol. 136, 126-30.

Poulin, P., Krishnan, K., 1999. Molecular structure-based prediction of the toxicokinetics of inhaled vapors in humans. Int J Toxicol. 18, 7-18.

Poulin, P., Theil, F. P., 2002. Prediction of pharmacokinetics prior to in vivo studies. 1. Mechanism-based prediction of volume of distribution. J Pharm Sci. 91, 129-156.

Ramsey, J. C., Andersen, M. E., 1984. A physiologically based description of the inhalation pharmacokinetics of styrene in rats and humans. Toxicol Appl Pharmacol. 73, 159-75.

Ramsey, J. C., Young, J. D., Karbowski, R. J., Chenoweth, M. B., McCarty, L. P., Braun, W. H., 1980. Pharmacokinetics of inhaled styrene in human volunteers. Toxicology and Applied Pharmacology. 53, 54-63.

Reddy, M. B., 2005. Physiologically based pharmacokinetic modeling : science and applications. John Wiley & Sons, Hoboken, N.J.

Renwick, A. G., Lazarus, N. R., 1998. Human variability and noncancer risk assessment-An analysis of the default uncertainty factor. Regul Toxicol Pharmacol. 27, 3-20.

Sato, A., Nakajima, T., 1979. Partition coefficients of some aromatic hydrocarbons and ketones in water, blood and oil. Br J Ind Med. 36, 231-234.

Surgenor, D. M., 1974. The red blood cell. Acad. Pr., New York.

Tardif, R., Charest-Tardif, G., Brodeur, J., Krishnan, K., 1997. Physiologically based pharmacokinetic modeling of a ternary mixture of alkyl benzenes in rats and humans. Toxicol Appl Pharmacol. 144, 120-134.

Thomas, R. S., Bigelow, P. L., Keefe, T. J., Yang, R. S., 1996a. Variability in biological exposure indices using physiologically based pharmacokinetic modeling and Monte Carlo simulation. Am Ind Hyg Assoc J. 57, 23-32.

Thomas, R. S., Yang, R. S., Morgan, D. G., Moorman, M. P., Kermani, H. R., Sloane, R. A., O'Connor, R. W., Adkins, B., Jr., Gargas, M. L., Andersen, M. E., 1996b. PBPK modeling/Monte Carlo simulation of methylene chloride kinetic changes in mice in relation to age and acute, subchronic, and chronic inhalation exposure. Environ Health Perspect. 104, 858-65.

Travis, C. C., Quillen, J. L., Arms, A. D., 1990. Pharmacokinetics of benzene. Toxicol Appl Pharmacol. 102, 400-20.

U.S. E.P.A., Guiding Principles for Monte Carlo Analysis. U.S. Environmental Protection Agency, Washington, DC, 1997, pp. EPA/630/R-97/001.

Valcke, M., Krishnan, K., 2010. An Assessment of the Interindividual Variability of Internal Dosimetry during Multi-Route Exposure to Drinking Water Contaminants. Int J Environ Res Public Health. 7, 4002-4022.

6.9. Tables

Table 1 Prior distributions of the composition parameters for human blood:air PC

Parameter	Values of population distribution			
	Mean	**Standard deviation**	**Minimum**	**Maximum**
f_{nlb}	0.0038	0.001	0.002	0.0061
f_{wb}	0.847	0.169	0.339	0.939
f_{pb}	0.117	0.023	0.070	0.164

f_{nlb}: neutral lipid-equivalent fraction of blood volume; f_{wb}: water-equivalent fraction of blood volume; f_{pb}: hemoglobin fraction of blood volume

Table 2. Values of prior distributions of the input parameters for the tissue:air PC algorithms for fat, liver and muscle[1]

Tissue:air PC	Parameter	Values of population distribution			
		Mean	Standard deviation	Minimum	Maximum
Fat	f_{nlt}	0.825	0.082	0.58	0.98
Liver	f_{nlt}	0.041	0.012	0.004	0.078
	f_{wt}	0.608	0.182	0.500	0.8
Muscle	f_{nlt}	0.011	0.003	0.0011	0.021
	f_{wt}	0.673	0.202	0.471	0.84

[1]: For all parameters the uncertainty (i.e. the standard deviation of the distribution for the population standard deviation) was 30 % coefficient of variation.

f_{nlt}: neutral lipid-equivalent fraction of tissue volume; f_{wt}: water-equivalent fraction of tissue volume

Table 3. Values and distributions of physiological parameters and enzyme content for the PBPK model in humans

Parameter	Mean	Standard deviation	Minimum[a]	Maximum[b]	Shape[c] / Comments
Body weight (kg)	70	21	28	112	logN
Alveolar ventilation ($L/h/kg^{0.74}$)	18	2.88	12.2	23.8	logN
Cardiac output ($L/h/kg^{0.74}$)	18	1.62	14.8	21.2	logN
Tissue blood flows (fraction of cardiac output)					
Liver	0.26	0.091	0.078	0.442	N
Richly perfused tissues	0.44				100 % - rest of tissues
Poorly perfused tissues	0.25	3.75×10^{-2}	0.175	0.325	N
Fat	0.05	0.015	0.02	0.08	N
Tissue volumes (fraction of body weight)					
Liver	0.026	1.3×10^{-3}	2.34×10^{-2}	2.86×10^{-2}	N
Richly perfused tissues	0.05	5×10^{-3}	0.04	0.06	N
Poorly perfused tissues	0.62				88 % - rest of tissues
Fat	0.19	0.057	0.076	0.304	N
Enzyme content[d]					
CYP2E1(pmol/mg MSP[e)]	48.9	1.6	11	130	logN
MSP[e] (mg/g liver)	52.9	1.48	27	108	logN

[a]: Minimum = mean - 2 standard deviations

[b]: Maximum = mean + 2 standard deviations

[c]: logN = log normal distribution; N, normal distribution

[d]: For these parameters, the mean corresponds to the geometric mean.

[e]: Microsomal protein

Table 4. Sensitivity ratios of the human blood:air PC input parameters for acetone and toluene

Parameter	Acetone	Toluene
f_{nlb}	0.00	0.30
f_{wb}	1.00	0.10
f_{pb}	0.00	0.60
P_{oa}	0.00	0.30
P_{wa}	1.00	0.10
P_{hba}	0.00	0.60

f_{nlb}: neutral lipid-equivalent fraction of blood volume; f_{wb}: water-equivalent fraction of blood volume; f_{pb}: hemoglobin fraction of blood volume; P_{oa}: oil:air PC; P_{wa}: water:air PC; P_{hba}: hemoglobin:air PC

Table 5. Posterior distributions of human blood:air PC input parameters

Parameter	Mean	Standard deviation	Uncertainty (%)
f_{nlb}	0.0037	0.0008	3.88
f_{wb}	0.7611	0.051	0.66
f_{hb}	0.1138	0.0193	1.64
P_{hba}	242.5	11.79	

f_{nlb}: neutral lipid-equivalent fraction of blood volume; f_{wb}: water-equivalent fraction of blood volume; f_{pb}: hemoglobin fraction of blood volume; P_{hba}: hemoglobin:air PC

Table 6. Posterior distributions for the rat tissue:air PC input parameters

Tissue:air PC	Parameter	Mean	Standard deviation	Uncertainty (%)
Fat	F_{nlt}	0.827	0.12	1.2
Liver	F_{nlt}	0.045	0.021	3.626
	F_{wt}	0.643	0.124	3.439
Muscle	F_{nlt}	0.015	0.006	4.076
	F_{wt}	0.774	0.052	1.673

f_{nlt}: neutral lipid-equivalent fraction of tissue volume; f_{wt}: water-equivalent fraction of tissue volume

Table 7. Predicted distributions of PCs for benzene, chloroform, styrene and trichloroethylene

Chemical	Partition coefficient[1]	Predicted distribution				Experimental value[3]
		mean	SD[2]	min	max	
Benzene	Blood:air	8.74	0.89	6.56	11.45	8.19
	Liver:blood	1.68	0.56	0.49	3.63	2.08
	PPT:blood	0.71	0.15	0.31	1.26	1.26
	Fat:blood	29.0	4.42	16.4	44.9	60.9
Chloroform	Blood:air	7.11	0.62	5.57	9.09	6.85
	Liver:blood	1.11	0.29	0.48	2.11	3.08
	PPT:blood	0.69	0.06	0.52	0.92	2.03
	Fat:blood	15.1	2.15	8.78	22.5	29.6
Styrene	Blood:air	63.4	7.64	42.0	90.5	52
	Liver:blood	2.72	1.02	0.55	7.04	2.67
	PPT:blood	0.92	0.27	0.24	1.94	0.9
	Fat:blood	52.3	8.76	27.9	93.0	66.8
Trichloroethylene	Blood:air	9.53	1.08	6.48	13.4	8.11
	Liver:blood	2.77	1.02	0.59	6.93	3.35
	PPT:blood	0.97	0.27	0.29	1.97	1.24
	Fat:blood	52.3	8.48	28.4	90.7	68.3

[1]: PPT: Poorly perfused tissues; The richly perfused tissues:blood PC was set equal to that of liver:blood PC.

[2]: SD: Standard deviation; [3]: Tissue:blood PCs= rat tissue:air PC/human blood:air PC; All values from Gargas et al. (1989) except styrene human blood:air PC from Ramsey and Andersen (1984).

6.10. Figures

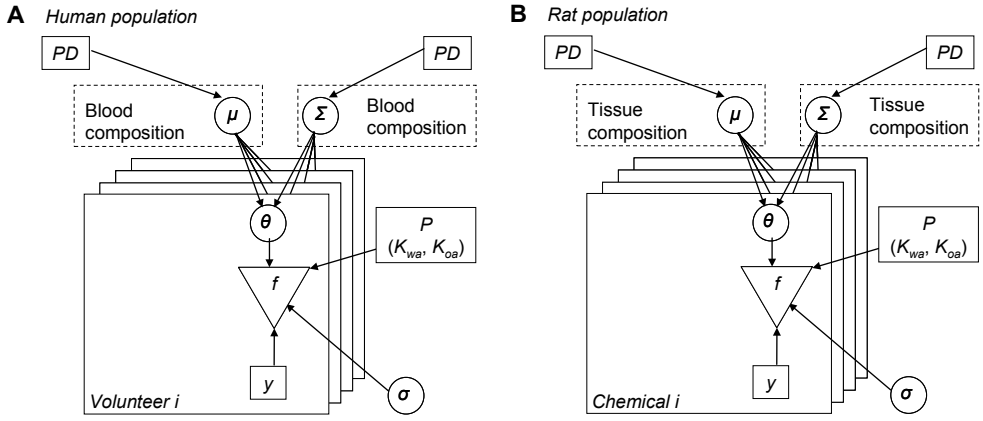

Figure 1. Statistical model for the Bayesian analysis of partition coefficients (PCs).

A) Human blood:air PC analysis; B) Rat tissue:air PC analysis. PD, prior distribution; μ, population mean value of the parameter θ; Σ, standard deviation of the parameter θ in the population; θ, unknown parameters of the PC algorithm (human blood or rat tissue composition in terms of neutral lipids, water and proteins); f, PC algorithm; y, experimental PC data; P, known parameters (Pwa and Poa, constants, from the literature); σ, standard deviation of the data (from the literature).

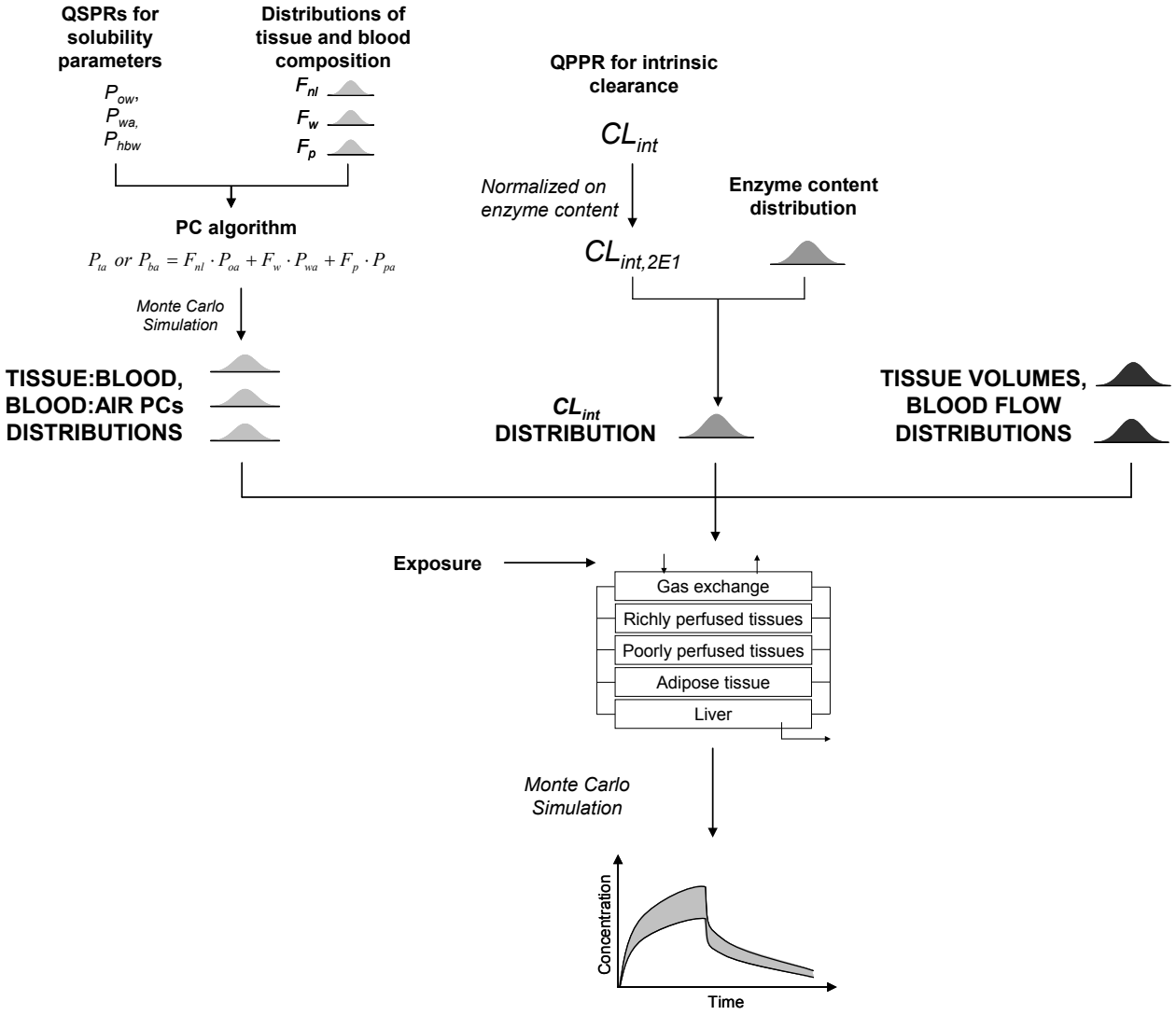

Figure 2. Probabilistic QSPR-PBPK framework presented in this study.

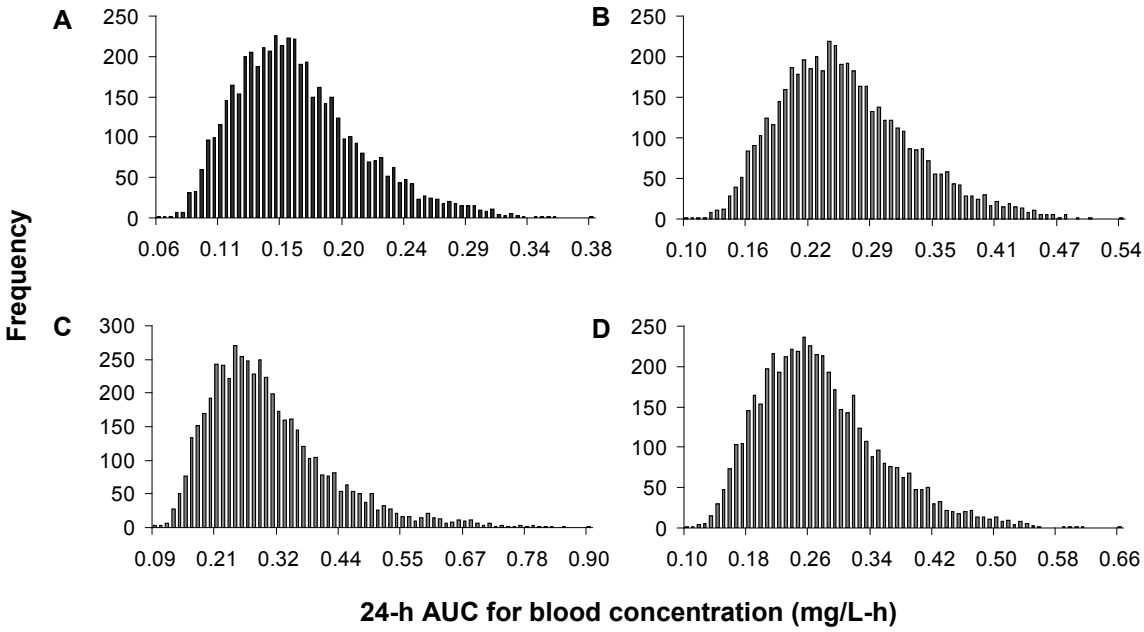

Figure 3. Simulation of 24-h area under the venous blood concentration vs time curve following 24-h exposure to 1 ppm of A) Benzene; B) Chloroform; C) Styrene; and D) Trichloroethylene.

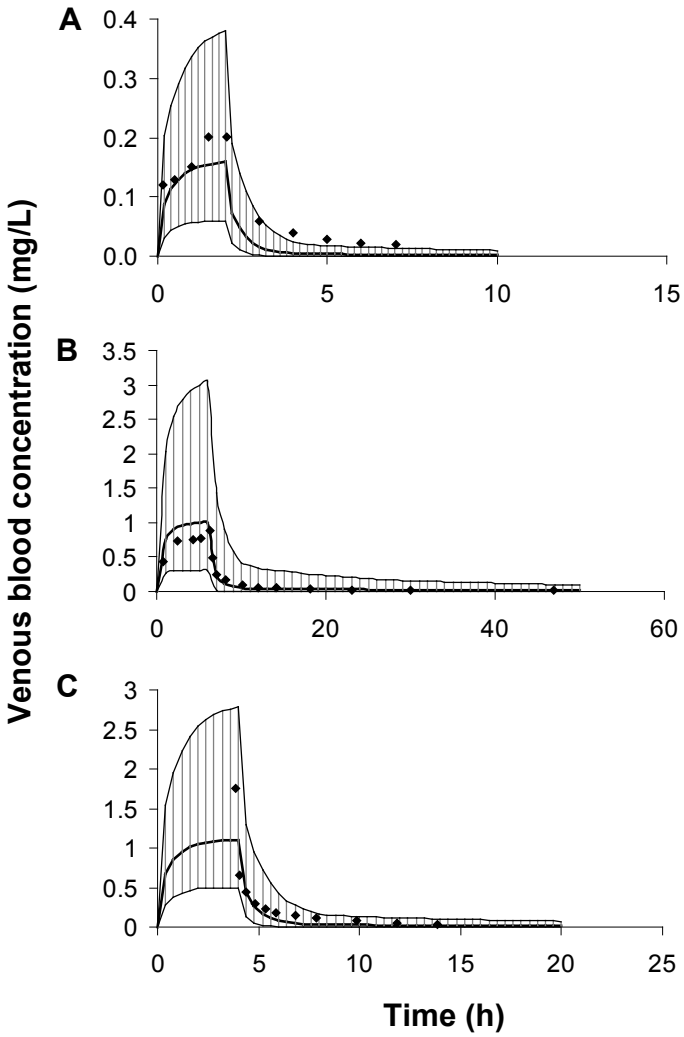

Figure 4. Comparison of 5000 Monte Carlo simulations (lines) with experimental data (symbols) on venous blood concentrations of A) Benzene (25 ppm, 2 h); B) Styrene (80 ppm, 6 h); Trichloroethylene (100 ppm, 4 h). Bold lines and thin lines represent the mean and minimum/maximum of the simulated concentrations, respectively. The dashed area is the envelope of the simulated concentrations.

6.11. Appendix 1

QSPR estimation of oil:air (P_{oa}*) and hemoglobin:water (*P_{hba}*) partition coefficients*

The values of P_{oa} and P_{hba} were calculated using QSPR models developed in a previous study (Peyret and Krishnan, in preparation), as follows:

$$Log\ P_{oa} = 0.95\ (\pm 0.042) \cdot \log P_{ow} + 0.675\ (\pm 0.031) \cdot \log P_{wa} + 0.325\ (\pm 0.102) \quad (3)$$

$$Log\ P_{hbw} = 0.68\ (\pm 0.059) \cdot \log P_{ow} + 0.21\ (\pm 0.15) \quad (4)$$

In Eqs. 3 and 4, the water:air PC (P_{wa} at 37.5°C = 2.69, 3.77, 5.19 and 1.41 for benzene, chloroform, styrene and trichloroethylene, respectively) and the octanol:water PC (P_{ow}) were calculated using HENRYWIN and KOWWIN (EPISUITE™, http://www.epa.gov/opptintr/exposure/pubs/episuite.htm), respectively.

QPPR Estimation of intrinsic clearance (CL_{int}*) normalized to the cytochrome P450 2E1*

For the four VOCs, the value of rat CL_{int} was estimated using a published QPPR as follows (Peyret and Krishnan, in press):

$$\log CL_{intPL} = 5.63 - 1.287 \cdot \log P_{ow} + 1.08 \cdot \log P_{bw} - 0.328 \cdot IP \quad (5)$$

where CL_{intPL}: intrinsic clearance (L phospholipids/h/kg$^{0.75}$); P_{ow}: octanol:water PC; P_{bw}: blood:water PC; and IP: ionization potential.

In Eq. (5) P_{ow} values were estimated using KOWWIN program (EPISUITE™, http://www.epa.gov/opptintr/exposure/pubs/episuite.htm). The values of *IP* (9.74, 10.84, 9.13 and 9.37 for benzene, chloroform, styrene and trichloroethylene, respectively) were estimated using the MOPAC/PM3 program in Molecular Modeling Pro software (Chem SW, Fairfield, CA). The blood:water PCs values (P_{bw} = 6.60, 5.51, 7.74, and 15.6 for benzene, chloroform, styrene and trichloroethylene, respectively) were obtained by dividing the blood:air PC by water:air PC values. The water:air PC were estimated from HENRYWIN program. Experimental values of blood:air PCs (P_{ba} = 17.8, 20.8, 40.2 and 21.9 for benzene, chloroform, styrene and trichloroethylene, respectively) were obtained from Gargas et al. (1989).

To convert intrinsic clearance in L blood/h/kg, the value of CL_{intPL}, obtained using Eq. 5, was multiplied by the phospholipid:blood PC. The phospholipid:blood PC values were 4.55, 1.93, 30.18 and 5.73 for benzene, chloroform, styrene and trichloroethylene, respectively. These values were obtained by dividing the phospholipid:water PC (0.3 x P_{ow} + 0.7) by the blood:water PC.

The value of CL_{int} normalized to cytochrome P450 CYP2E1 content (L/h/µmol CYP2E1) was obtained by dividing the QPPR rat CL_{int} by the content of this enzyme (4.5 µmol/L liver x 0.012 L liver) in rat liver (Béliveau et al., 2005).

6.12. Appendix 2

Table A1. Sensitivity ratios of the input parameters of fat:air PCs

Chemical name	f_{nlt} & P_{oa}	f_{wt} & P_{wa}	Sensitivity group[a]
2,3,4-Trimethyl pentane	1.00	0.00	1
2,2,4-Trimethyl pentane	1.00	0.00	1
Tricyclo[5.2.1.02.6]-decane (JP-10)	1.00	0.00	1
Hexachloroethane	1.00	0.00	1
m-Methylstyrene	1.00	0.00	1
p-Methylstyrene	1.00	0.00	1
n-hexane	1.00	0.00	1
Pentachloroethane	1.00	0.00	1
Tetrachloroethylene	1.00	0.00	1
Styrene	1.00	0.00	1
n-heptane	1.00	0.00	1
cyclohexane	1.00	0.00	1
p-xylene	1.00	0.00	1
m-xylene	1.00	0.00	1
o-xylene	1.00	0.00	1
Carbon tetrachloride	1.00	0.00	1
Chlorobenzene	1.00	0.00	1
1,1,1,2-tetrachloroethane	1.00	0.00	1
Trichloroethylene	1.00	0.00	1
Toluene	1.00	0.00	1
1,1,1-Trifluoro-2-bromo-2-chloroethane	1.00	0.00	1
1,1,1-Trichloroethane	1.00	0.00	1
Chlorodibromomethane	1.00	0.00	1
1,1,2,2-tetrachloroethane	1.00	0.00	1
n-Propyl bromide	1.00	0.00	1
1,1-Dichloroethylene	1.00	0.00	1
Benzene	1.00	0.00	1
n-pentyl acetate ester	1.00	0.00	1
1,2-Dichloropropane	1.00	0.00	1
Isopropylbromide	1.00	0.00	1
Isoflurane	1.00	0.00	1
1,1,2-Trichloroethane	1.00	0.00	1
Isopentyl acetate ester	1.00	0.00	1
Vinyl bromide	1.00	0.00	1
trans-1,2-Dichloroethylene	1.00	0.00	1
Chloroform	1.00	0.00	1
1-Chloropropane	1.00	0.00	1
cis-1,2-Dichloroethylene	1.00	0.00	1
2-Chloropropane	1.00	0.00	1

Table A1. Continued

Chemical name	f_{nlt} & P_{oa}	f_{wt} & P_{wa}	Sensitivity group[a]
1,1-Dichloroethane	1.00	0.00	1
1,2-Dibromoethane	1.00	0.00	1
Dibromomethane	1.00	0.00	1
1-Bromo-2-chloroethane	1.00	0.00	1
1,1,1-Trifluoro-2-chloroethane	1.00	0.00	1
Vinyl chloride	1.00	0.00	1
Allyl chloride	1.00	0.00	1
n-Butyl acetate ester	1.00	0.00	1
Isobutyl acetate ester	1.00	0.00	1
Methyl pentyl ketone	1.00	0.00	1
Isoprene	1.00	0.00	1
BromoChloromethane	1.00	0.00	1
Chloroethane	1.00	0.00	1
1,2-Dichloroethane	1.00	0.00	1
Dichloromethane	0.99	0.01	1
Methyl isobutyl ketone	0.99	0.01	1
Chloromethane	0.99	0.01	1
n-Propyl acetate ester	0.99	0.01	1
Isopropyl acetate ester	0.98	0.02	1
1-Nitropropane	0.98	0.02	1
Fluorochloromethane	0.98	0.02	1
2-Nitropropane	0.98	0.02	1
Diethyl ether	0.97	0.03	1
Methyl propyl ketone	0.97	0.03	1
Difluoromethane	0.96	0.04	1
Ethyl acetate ester	0.95	0.05	1
n-Pentanol	0.90	0.10	-
Methyl ethyl ketone	0.89	0.11	-
Isopentanol	0.89	0.11	-
Methyl acetate ester	0.85	0.15	-
n-Butanol	0.80	0.20	-
Isobutanol	0.75	0.25	-
Dimethyl ketone	0.69	0.31	-
n-Propanol	0.53	0.47	-
Isopropanol	0.42	0.58	-
Ethanol	0.26	0.74	-
Methanol	0.15	0.85	-

[a]: Group 1 was used for the characterization of f_{nlt} distribution; - : not used.

f_{nlt}: neutral lipid-equivalent fraction of tissue volume; f_{wt}: water-equivalent fraction of tissue volume; P_{oa}: oil:air PC; P_{wa}: water:air PC

Table A2. Sensitivity ratios of the input parameters of liver:air PCs

Chemical name	f_{nlt} & P_{oa}	f_{wt} & P_{wa}	Sensitivity group[a]
2,3,4-Trimethyl pentane	1.00	0.00	1
2,2,4-Trimethyl pentane	1.00	0.00	1
Tricyclo[5.2.1.02.6]-decane (JP-10)	1.00	0.00	1
Hexachloroethane	1.00	0.00	1
m-Methylstyrene	1.00	0.00	1
p-Methylstyrene	1.00	0.00	1
n-hexane	1.00	0.00	1
Pentachloroethane	0.99	0.01	1
Tetrachloroethylene	0.99	0.01	1
Styrene	0.99	0.01	1
n-heptane	0.99	0.01	1
Cyclohexane	0.99	0.01	1
p-xylene	0.99	0.01	1
m-xylene	0.99	0.01	1
o-xylene	0.99	0.01	1
Carbon tetrachloride	0.98	0.02	1
Chlorobenzene	0.98	0.02	1
1,1,1,2-tetrachloroethane	0.98	0.02	1
Trichloroethylene	0.98	0.02	1
Toluene	0.97	0.03	1
1,1,1-Trifluoro-2-bromo-2-chloroethane	0.96	0.04	1
1,1,1-Trichloroethane	0.96	0.04	1
Chlorodibromomethane	0.96	0.04	1
1,1,2,2-tetrachloroethane	0.94	0.06	1
n-Propyl bromide	0.92	0.08	1
1,1-Dichloroethylene	0.92	0.08	1
Benzene	0.91	0.09	1
n-Pentyl acetate ester	0.91	0.09	1
1,2-Dichloropropane	0.90	0.10	1
Isopropylbromide	0.90	0.10	1
Isoflurane	0.89	0.11	1
1,1,2-Trichloroethane	0.89	0.11	1
Isopentyl acetate ester	0.89	0.11	1
Vinyl bromide	0.88	0.12	1
trans-1,2-Dichloroethylene	0.88	0.12	1
Chloroform	0.88	0.12	1
1-Chloropropane	0.86	0.14	1
cis-1,2-Dichloroethylene	0.83	0.17	1
2-Chloropropane	0.83	0.17	1
1,1-Dichloroethane	0.82	0.18	1
1,2-Dibromoethane	0.81	0.19	1
Dibromomethane	0.80	0.20	1

Table A2. continued

Chemical name	f_{nlt} & P_{oa}	f_{wt} & P_{wa}	Sensitivity group[a]
1-Bromo-2-chloroethane	0.79	0.21	1
1,1,1-Trifluoro-2-chloroethane	0.77	0.23	1
Vinyl chloride	0.77	0.23	1
Allyl chloride	0.76	0.24	1
n-Butyl acetate ester	0.75	0.25	1
Isobutyl acetate ester	0.74	0.26	1
Methyl pentyl ketone	0.71	0.29	1
Isoprene	0.71	0.29	1
BromoChloromethane	0.71	0.29	1
Chloroethane	0.68	0.32	1
1,2-Dichloroethane	0.65	0.35	1
Dichloromethane	0.56	0.44	1
Methyl isobutyl ketone	0.43	0.57	2
Chloromethane	0.37	0.63	2
n-Propyl acetate ester	0.36	0.64	2
isopropyl acetate ester	0.34	0.66	2
1-Nitropropane	0.33	0.67	2
Fluorochloromethane	0.30	0.70	2
2-Nitropropane	0.28	0.72	2
Diethyl ether	0.22	0.78	2
Methyl propyl ketone	0.21	0.79	2
Difluoromethane	0.18	0.82	2
Ethyl acetate ester	0.13	0.87	2
n-Pentanol	0.07	0.93	2
Methyl ethyl ketone	0.07	0.93	2
Isopentanol	0.07	0.93	2
Methyl acetate ester	0.04	0.96	2
n-Butanol	0.03	0.97	2
Isobutanol	0.02	0.98	2
Dimethyl ketone	0.02	0.98	2
n-Propanol	0.01	0.99	2
Isopropanol	0.01	0.99	2
Ethanol	0.00	1.00	2
Methanol	0.00	1.00	2

[a]: Group 1 was used for the characterization of f_{nlt} distribution, group 2 for f_{wt} distribution.

f_{nlt}: neutral lipid-equivalent fraction of tissue volume; f_{wt}: water-equivalent fraction of tissue volume; P_{oa}: oil:air PC; P_{wa}: water:air PC

Table A3. Sensitivity ratios of the input parameters of muscle:air PCs

Chemical name	f_{nlt} & P_{oa}	f_{wt} & P_{wa}	Sensitivity group[a]
2,3,4-Trimethyl pentane	1.00	0.00	1
2,2,4-Trimethyl pentane	1.00	0.00	1
Tricyclo[5.2.1.02.6]-decane (JP-10)	1.00	0.00	1
Hexachloroethane	0.99	0.01	1
m-Methylstyrene	0.99	0.01	1
p-Methylstyrene	0.99	0.01	1
n-Hexane	0.99	0.01	1
Pentachloroethane	0.98	0.02	1
Tetrachloroethylene	0.98	0.02	1
Styrene	0.98	0.02	1
n-Heptane	0.98	0.02	1
Cyclohexane	0.97	0.03	1
p-Xylene	0.97	0.03	1
m-Xylene	0.97	0.03	1
o-Xylene	0.96	0.04	1
Carbon tetrachloride	0.95	0.05	1
Chlorobenzene	0.93	0.07	1
1,1,1,2-Tetrachloroethane	0.93	0.07	1
Trichloroethylene	0.92	0.08	1
Toluene	0.91	0.09	1
1,1,1-Trifluoro-2-bromo-2-chloroethane	0.87	0.13	1
1,1,1-Trichloroethane	0.87	0.13	1
Chlorodibromomethane	0.87	0.13	1
1,1,2,2-tetrachloroethane	0.83	0.17	1
n-Propyl bromide	0.77	0.23	1
1,1-Dichloroethylene	0.76	0.24	1
Benzene	0.75	0.25	1
n-Pentyl acetate ester	0.74	0.26	1
1,2-Dichloropropane	0.73	0.27	1
Isopropylbromide	0.73	0.27	1
Isoflurane	0.71	0.29	1
1,1,2-Trichloroethane	0.70	0.30	1
Isopentyl acetate ester	0.70	0.30	1
Vinyl bromide	0.69	0.31	1
trans-1,2-Dichloroethylene	0.69	0.31	1
Chloroform	0.68	0.32	1
1-Chloropropane	0.64	0.36	1
cis-1,2-Dichloroethylene	0.60	0.40	1
2-Chloropropane	0.60	0.40	1
1,1-Dichloroethane	0.57	0.43	1
1,2-Dibromoethane	0.57	0.43	1
Dibromomethane	0.54	0.46	1

Table A3. Continued

Chemical name	f_{nlt} & P_{oa}	f_{wt} & P_{wa}	Sensitivity group[a]
1-Bromo-2-chloroethane	0.53	0.47	1
1,1,1-Trifluoro-2-chloroethane	0.50	0.50	1
Vinyl chloride	0.50	0.50	1
Allyl chloride	0.48	0.52	2
n-Butyl acetate ester	0.47	0.53	2
Isobutyl acetate ester	0.47	0.53	2
Methyl pentyl ketone	0.43	0.57	2
Isoprene	0.43	0.57	2
BromoChloromethane	0.42	0.58	2
Chloroethane	0.39	0.61	2
1,2-Dichloroethane	0.36	0.64	2
Dichloromethane	0.28	0.72	2
Methyl isobutyl ketone	0.19	0.81	2
Chloromethane	0.15	0.85	2
n-Propyl acetate ester	0.14	0.86	2
Isopropyl acetate ester	0.13	0.87	2
1-Nitropropane	0.13	0.87	2
Fluorochloromethane	0.11	0.89	2
2-Nitropropane	0.10	0.90	2
Diethyl ether	0.08	0.92	2
Methyl propyl ketone	0.07	0.93	2
Difluoromethane	0.06	0.94	2
Ethyl acetate ester	0.04	0.96	2
n-Pentanol	0.02	0.98	2
Methyl ethyl ketone	0.02	0.98	2
Isopentanol	0.02	0.98	2
Methyl acetate ester	0.01	0.99	2
n-butanol	0.01	0.99	2
Isobutanol	0.01	0.99	2
Dimethyl ketone	0.01	0.99	2
n-Propanol	0.00	1.00	2
Isopropanol	0.00	1.00	2
Ethanol	0.00	1.00	2
Methanol	0.00	1.00	2

[a]: Group 1 was used for the characterization of f_{nlt} distribution, group 2 for f_{wt} distribution.

f_{nlt}: neutral lipid-equivalent fraction of tissue volume; f_{wt}: water-equivalent fraction of tissue volume; P_{oa}: oil:air PC; P_{wa}: water:air PC

Chapitre 7. Discussion générale

La présente thèse avait pour objectif de développer des outils prédictifs de la TK de substances organiques. L'application *in fine* d'un outil prédisant la TK est d'évaluer l'exposition en termes de dose interne chez l'humain. L'approche de modélisation PBPK a été choisie car elle permet de prédire des doses internes sur la base de paramètres physiologiques, physicochimiques et biochimiques sans avoir recours à de nombreuses données TK. Le problème majeur pour prédire la TK de nouvelles substances à l'aide de modèles PBPK est de déterminer la valeur des paramètres qui sont spécifiques à la substance comme les PC et les constantes de métabolisme. Des modèles QSPR-PBPK ont déjà été développés en utilisant l'approche de contribution des groupes ou fragments moléculaires (Béliveau et coll., 2003; 2005; Kamgang et coll., 2008; Price et Krishnan, 2011). Cependant, comme mentionné au long de cette thèse, cette approche ne permet pas d'étendre le domaine d'application sans ajouter de nouveaux groupes structuraux. Les études présentées dans cette thèse rapportent des efforts menés pour résoudre le problème de la détermination des PC et des constantes métaboliques en étudiant une approche par descripteurs moléculaires plus globaux dont le domaine d'application est plus facile à étendre.

7.1. Prédiction des coefficients de partage

L'algorithme développé dans la première étude (chapitre 3) permet de calculer des PC pour une grande diversité de molécules puisqu'il réuni les descriptions des mécanismes clés de distribution de composés acides, basiques et neutres connus à ce jour. La combinaison de différentes matrices biologiques telles que les cellules (du sang, des tissus) et liquides physiologiques (plasma, liquide interstitiel) permet de calculer facilement divers PC aux échelles micro (cellule) et macro (tissu).

Dans le chapitre 3, les paramètres physiologiques de l'algorithme (c'est à dire la composition des matrices biologiques en termes de lipides neutres, phospholipides, eau,

protéines) ont été rapportés pour le foie, le muscle, le sang et le tissu adipeux du rat. En modélisation PBPK, ces trois tissus clés sont souvent utilisés comme base pour prédire la distribution des polluants environnementaux dans les compartiments du foie, du « gras », des tissus richement perfusés et des tissus pauvrement perfusés. La valeur de ces paramètres pour d'autres tissus peut être obtenue par une revue de la littérature. Cependant, cette recherche n'était pas nécessaire pour répondre aux objectifs de la recherche proposée.

Les valeurs des paramètres de composition des tissus dans l'algorithme unifié développé au chapitre 2 ont aussi été collectées chez l'humain. Ces valeurs ont été utilisées pour calculer des PC dans le but de réaliser des extrapolations de relation concentration-réponse mesurée *in vitro* vers des relations dose-réponse *in vivo* (Peyret et Krishnan, 2010a; 2010b). Dans ces études, l'algorithme unifié à été appliqué pour estimer des PC au niveau cellulaire. Des PC cellule:milieu de culture et cellule:liquide interstitiel ont respectivement servi à déterminer les concentrations dans des cellules cultivées *in vitro* et dans les cellules des compartiments tissulaires du modèle PBPK. L'usage de l'approche par PC au niveau micro est potentiellement très intéressant pour extrapoler des relations dose-réponse puisqu'actuellement, la toxicité de nouvelles substances est préférentiellement évaluée sur des cellules humaines cultivées (National Research Council, 2007).

Dans le troisième article de recherche (Chapitre 5), des modèles QSPR ont été développés afin de permettre la prédiction de PC sans avoir besoin de mesures expérimentales pour les paramètres entrants dans l'algorithme unifié (PC huile:air et hémoglobine:eau). L'incorporation des QSPR pour les PC et du QPPR pour la clairance intrinsèque dans un modèle PBPK a permis de simuler la TK de COV inhalés à partir de trois paramètres calculés (P_{ow}, P_{wa}, IP) et d'un paramètre mesuré (PC sang:eau). Le modèle TK obtenu a donné des résultats de simulation de concentration sanguine comparables à ceux d'un modèle basé sur la contribution des groupes moléculaires (Béliveau et al, 2005). Une limite de ce modèle reste la description linéaire du métabolisme qui ne permet pas de simuler la

cinétique pour des expositions à de fortes doses. Néanmoins, cette étude est innovante de par le fait que les paramètres spécifiques au produit de ce modèle à dosimétrie cellulaire ont été estimés *in silico*. Donc ceci démontre la faisabilité de prédire *a priori* la TK de polluants environnementaux (COV).

Une analyse de l'impact de l'incertitude des paramètres du modèle PBPK sur les doses simulées devient cruciale quand il s'agit d'évaluer l'exposition interne chez l'humain, aux fins d'analyse de risque. Pour la première fois, la variabilité des valeurs de coefficients de partage a été dérivée à partir d'information sur la composition des media biologiques dans lesquels se distribuent les polluants environnementaux (chapitre 6). L'approche utilisée pour prédire des distributions de coefficients de partage est originale et peut être un outil intéressant pour la prédiction de l'incertitude reliée aux coefficients de partage avant d'avoir accès à des mesures expérimentales. En effet cette étude démontre la faisabilité d'estimer une incertitude sur des prédictions de coefficients de partage obtenues à partir d'information sur la structure moléculaire.

7.2. Prédiction du métabolisme

Le développement de modèles prédictifs du métabolisme à partir de descripteurs moléculaires plus globaux, comme des propriétés physicochimiques ou des indicateurs de charge, de taille et de forme, a été entrepris dans le chapitre 4. Un modèle quantitatif de relation entre propriété et propriété a été développé pour la clairance intrinsèque de COV chez le rat. En considérant les coefficients de détermination (R^2), qui reflètent l'ajustement des prédictions du modèle aux données observées, le succès de cette approche s'est révélé plutôt limité comparé aux modèles QSPR de constantes métaboliques basés sur l'approche par contribution de groupe (Béliveau et coll., 2003; Béliveau et coll., 2005; Kamgang et coll., 2008; Price et Krishnan, 2011). Cependant, le coefficient de détermination d'un modèle augmente avec le nombre de variables (Livingstone, 2004). Potentiellement, un

modèle ayant 11 variables indépendantes, comme dans le modèle à contribution de groupe, s'ajuste plus facilement aux données qu'un modèle ayant 3 variables, comme dans le modèle à descripteurs plus globaux. Du point de vue de l'interprétation des modèles, l'approche par contribution de groupe pourrait tenir compte de réactions enzymatiques sur différentes sous unités moléculaires disponibles pour des réactions spécifiques (p.ex., oxidation du benzène, du CH_3, de la double liaison). La moins bonne prédiction du taux de métabolisme basée sur les descripteurs plus globaux peut aussi s'expliquer par le fait que ces descripteurs reflètent moins la diversité de réactions potentielles que les fragments de molécule.

La complexité à modéliser le métabolisme nous a mené à diversifier les approches testées. De nombreuses méthodes ont été testées pour prédire différentes mesures de taux de métabolisme (ratio d'extraction hépatique, clairance intrinsèque, V_{max}, K_m, énergie libre d'activation) : modélisation d'arbres de décision, régression linéaire et non linéaire. Ces travaux ont été réalisés en utilisant des données expérimentales publiées de constantes métaboliques (V_{max}, K_m et clairance intrinsèque) sur un plus grand nombre de substances (120, dont des pesticides, BPC, dioxines, COV) que ceux mentionnés dans le chapitre 4 (31 COV). Les efforts pour développer un modèle prédisant les constantes métaboliques de cet ensemble de substances n'ayant pas fourni de modèle satisfaisant, ces substances ont été classées par enzyme dont elles sont le substrat en utilisant les arbres de décisions de Lewis (2000; 2001). Ces travaux ont révélé que les constantes métaboliques ne peuvent être modélisées qu'une fois classées par enzyme responsable de la principale voie de biotransformation (par exemple, cytochromes P450 CYP2E1, CYP2A1, CYP2B1, CYP1A1 d'après observations personnelles). Seul le groupe des substrats du CYP2E1 contenait un nombre assez élevé de données pour permettre le développement d'un modèle statistique raisonnablement robuste. Dans le futur, la modélisation quantitative du métabolisme à partir de la structure moléculaire devrait donc être étudiée en commençant par séparer les molécules selon l'enzyme catalysant la réaction (isoforme de cytochrome,

ADH) puis selon la réaction opérée par l'enzyme (p.ex., hydroxylation de carbone aliphatique ou aromatique, époxydation d'une double liaison, oxygénation d'un hétéro-atome, N-hydroxylation, désalkylation d'un hétéro-atome). Le groupement de substrats par enzyme et par réaction de biotransformation, pourrait être intéressant pour prédire la clairance, les constantes de Michaelis ou d'autres types de constantes comme les microconstantes (vitesses d'association, de dissociation ou de catalyse) voire des paramètres thermodynamiques tels que l'enthalpie standard de réaction ou l'énergie libre standard (Jones et coll., 1996; Olsen et coll., 2006; Rydberg et coll., 2008; Kim et coll., 2009; Mayeno et coll., 2009). Cette approche nécessiterait le développement d'outils de classement (analyse discriminante ou arbres de décision) comme les arbres de décision développés par Lewis (Lewis, 2001). Avec des outils de classement précis et sensibles, la modélisation quantitative des taux de métabolisme pourrait être effectuée avec succès. Le classement des substrats en fonction des enzymes et ensuite le classement des substrats par réaction chimique reste un défi de taille. Un des problèmes majeurs dans l'affection d'une enzyme à un substrat est que bien souvent, une molécule est le substrat de différentes enzymes. Dans ce cas, il est plus facile d'évaluer la principale voie métabolique. De même, une enzyme peut effectuer différentes réactions sur un même substrat, ce qui peut amener un niveau supplémentaire de classement. Une fois les données triées, il est nécessaire que les groupes de substrats aient un nombre d'échantillons assez élevé pour permettre une analyse statistique. Une telle analyse fournirait des données nécessaires au développement de modèles prédictifs de biotransformations spécifiques à une enzyme voire à une réaction. La faible disponibilité de données expérimentales rend difficile la réalisation d'une telle approche.

L'impact de l'incertitude de la prédiction de la biotransformation sur la TK simulée a été évalué par une analyse d'applicabilité du modèle QPPR pour la clairance intrinsèque dans un modèle PBPK. Cette analyse, inspirée des travaux du Programme international sur la sécurité des substances chimiques (PISC), combine une analyse d'incertitude à une analyse

de sensibilité (IPCS, 2010). Dans le chapitre 4, elle aide à décider, pour plusieurs COV, si l'estimé du modèle prédisant la clairance intrinsèque est adapté au niveau de confiance requis dans l'utilisation du modèle PBPK, ou s'il faut mener des études supplémentaires pour réduire l'incertitude reliée au taux de métabolisme. Pour des études préliminaires d'analyse de risque toxicologique de substances chimiques, une telle analyse devrait être systématique dans l'évaluation *in silico* de la TK.

Finalement, le modèle QPPR pour la clairance intrinsèque peut être amélioré par ajout de données supplémentaires sur d'autres substrats du cytochrome P450 CYP2E1. L'obtention d'un outil ayant un potentiel plus élevé d'élargissement du domaine d'application élargi constitue une avancée dans la prédiction du métabolisme.

7.3. Prédiction de la toxicocinétique et de sa variabilité

L'objectif des travaux de recherche présentés était de prédire la TK et sa variabilité pour des substances organiques sur la base de la structure moléculaire ou de propriétés physicochimiques. Plutôt que pour diverses substances organiques, cet objectif a été atteint pour quelques composés organiques volatils. Ceci principalement à cause du domaine d'application restreint du QPPR pour la clairance intrinsèque.

La variabilité de la TK associée à l'inhalation de COV chez l'humain (chapitre 6) a pu être quantifiée pour la première fois uniquement sur la base de la variabilité de paramètres biologiques (c. à d.: volumes des tissus; débits sanguins; composition des tissus et du sang; contenu en cytochrome P450 CYP2E1). Cette approche permet pour la première fois d'obtenir des estimés de la variabilité de la TK sans avoir recours à des données expérimentales celle des coefficients de partage. L'approche de modélisation PBPK probabiliste développée dans le chapitre 6 représente donc un accomplissement de l'objectif de la thèse car elle intègre tous les outils développés dans les travaux de

recherche des chapitres 3 à 5. La Figure 1 présente un modèle conceptuel pour obtenir un premier estimé de la TK d'une substance inhalée et de l'incertitude qui y est associée en reprenant les travaux de recherche de cette thèse. Ce modèle conceptuel, peut être appliqué à l'avenir en y incorporant d'autres modèles prédictifs du métabolisme (QSPR, QPPR, relations allométriques, pour d'autres constantes métaboliques) en fonction des besoins de l'étude et du produit étudié. Il suffit de normaliser la valeur estimée de la constante métabolique sur le contenu enzymatique pour modéliser la variabilité du métabolisme en fonction de ce contenu (Lipscomb et coll., 2003; Valcke et Krishnan, 2010).

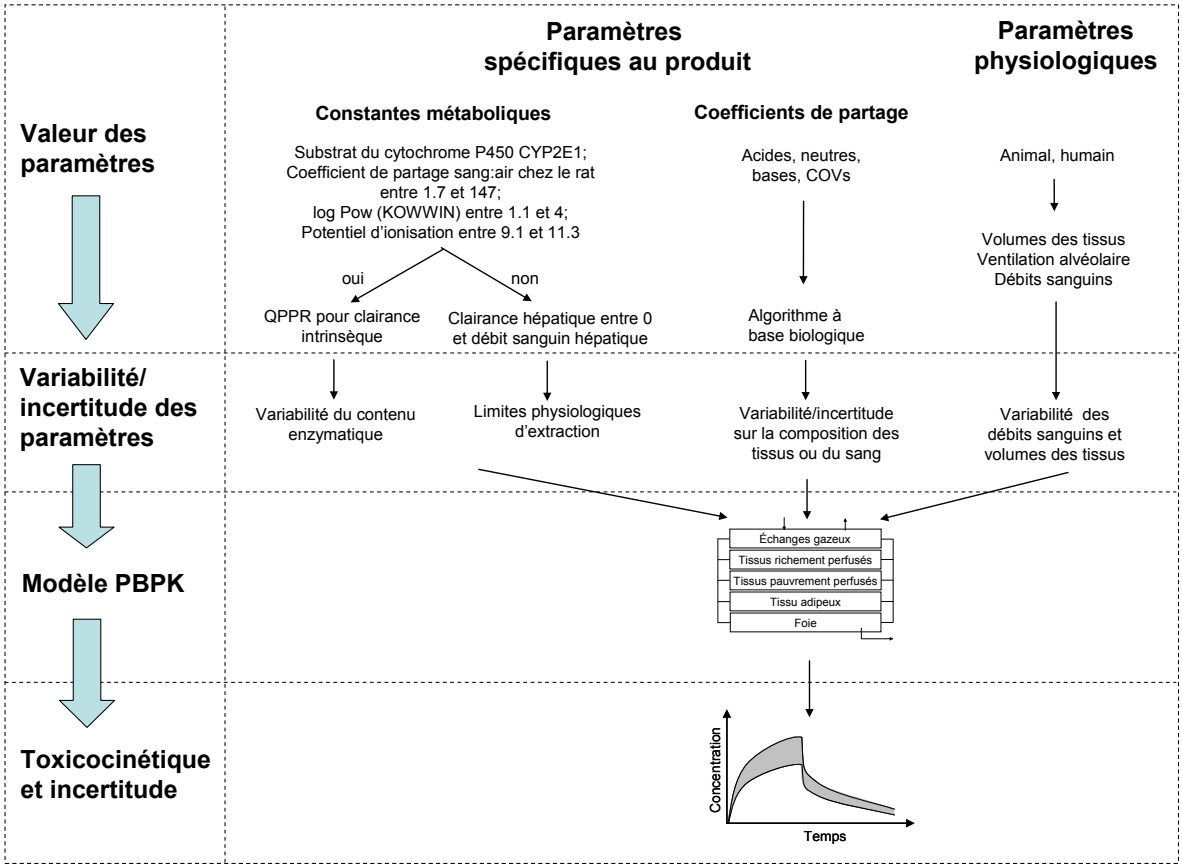

Figure 1. Modèle conceptuel pour une estimation *a priori* de la toxicocinétique de COV par voie inhalée.

L'approche à contribution de groupe peut être privilégiée pour des substances comprises dans le domaine d'application, mais l'approche utilisée dans cette thèse peut être intéressante quand les groupes ne suffisent pas à décrire la molécule. L'approche de descripteurs moléculaires plus globaux peut permettre un développement plus rapide de modèles QPPR ou QSPR avec d'autres données expérimentales (p.e.x., *in vitro*).

Les études effectuées pour prédire les concentrations sanguines en polluants reposent sur l'utilisation de l'approche de modélisation PBPK. Comme mentionné plus haut, les modèles PBPK ont prouvé leur utilité pour mener des extrapolations *in vitro-in vivo*, entre espèces, entre doses et entre voies d'exposition (Andersen, 2003; Krishnan et Andersen, 2007; Blaauboer, 2010; Louisse et coll., 2010). Cependant, d'autres approches auraient pu être utilisées. Pour modéliser des expositions continues, des équations à base physiologique plus simples décrivant l'état stationnaire auraient pu être utilisées (Bogen et McKone, 1988; Pelekis et coll., 1997). De tels algorithmes ont l'avantage d'avoir un nombre moins élevé de paramètres et donc une propagation d'erreur plus faible que celle des modèles PBPK mais leur champ d'application se limite à des expositions continues. La modélisation PK compartimentale aurait aussi pu être utilisée. Dans ce cas, les paramètres nécessaires comme le volume de distribution et la constante d'élimination auraient pu être dérivés à partir des modèles prédisant les coefficients de partage et la clairance intrinsèque (Rodgers et Rowland, 2007). Cependant les équations à l'équilibre et les modèles compartimentaux ne peuvent s'appliquer pour une grande diversité de scénarios d'exposition ni pour des extrapolations entre espèces, souvent nécessaire pour l'analyse de risques en situation pauvre en données.

Les modèles PBPK utilisés dans la présente thèse ne sont applicables que pour des COV principalement substrats du cytochrome CYP2E1. Ces travaux représentent une première étape dans l'élaboration d'outils permettant de prédire la TK d'une plus grande variété de composés organiques. L'algorithme unifié pour les coefficients de partage s'applique à une

grande diversité de substances chimiques et permet de prédire des PC aux niveaux micro et macro.

Dans le chapitre 6, l'incertitude associée aux valeurs des paramètres n'a pas été prise en compte dans les simulations PBPK. L'incertitude reliée aux estimés de clairance intrinsèque n'a pas été simulée. Cette incertitude aurait pu être prise en compte, par exemple en utilisant les limites de l'intervalle de confiance à la moyenne des prédictions. Les distributions des valeurs coefficients de partage, auraient pu être modélisées en tenant compte de l'incertitude sur les estimés QSPR des paramètres physicochimiques entrant dans l'algorithme biologique. L'ajout de l'incertitude sur les paramètres augmente la variation de la réponse simulée de manière plus ou moins importante dépendant de la réponse d'intérêt (dose, temps, exposition). Huizer et coll. (2012) ont étudié l'impact séparé de l'incertitude et de la variabilité des paramètres d'un modèle PBPK pour le 2-propanol et l'acétone. Cette étude a démontré que pendant l'exposition, la variabilité influence le plus la concentration sanguine simulée alors ce l'incertitude a la plus grande influence dans la phase d'élimination de la substance.

Dans le chapitre 6, la variation des prédictions de l'aire sous la courbe concentration-temps correspond à la valeur moyenne observée par Renwick et Lazarus sur des données expérimentales (Renwick et Lazarus, 1998). L'ajout de l'incertitude sur des estimés QSPR, pour lesquels la PK est sensible, pourrait augmenter la variabilité de la réponse mais celle-ci reste limitée par la physiologie. Par exemple de l'incertitude de la clairance hépatique d'un produit sur une dose interne, ne peut engendrer un taux de métabolisme inférieur à zéro ni au delà des limites valeurs limites de débit sanguin hépatique. Les données de variabilité des paramètres physiologiques ont été tirées de la littérature et leur valeur scientifique n'a pas été questionnée (Clewell et coll., 2001). Clewell et coll. (2001) ont basé leur estimés de variabilité sur un report de l'US EPA (Arms et Travis, 1988), les valeurs de coefficients de variation qu'ils ont utilisé pour les débits sanguins et les volumes des tissus

sont comparables à celles utilisées dans d'autres études de modélisation MC-PBPK (Thomas et coll., 1996; Tan et coll., 2006).

L'application de l'outil développé pour prédire la TK est limitée à l'exposition par inhalation. L'ajout de modèles pour prédire les biodisponibilités et les constantes d'absorption orale et cutanée permettrait d'augmenter le domaine d'application de cet outil. Alternativement, des études expérimentales peuvent être conduites pour mesurer les paramètres nécessaires à la modélisation de ces voies d'exposition.

Il y a à peu près 100 000 substances chimiques commercialisées dans le monde (Commission des communautés européennes, 2001). L'évaluation du risque associé à l'exposition à un produit chimique ne peut pas se faire entièrement par des méthodes expérimentales *in vivo* pour des raisons éthiques, économiques et de temps. C'est pourquoi le développement de test de toxicité *in vitro* sur des cellules, de préférence humaines, et le développement de modèles pour réaliser des extrapolations *in vitro-in vivo* est inévitable (National Research Council, 2007).

Les outils de prédictifs de la TK développés dans cette thèse ont diverses applications en analyse de risque. L'utilisation de la relation dose externe-réponse ne renseigne pas sur la dose interne qui provoque la réponse. Par conséquent la relation dose interne-réponse est plus appropriée pour évaluer le risque associé à différents scénarios d'exposition (Clewell et coll., 2002; Krishnan et Johanson, 2005; IPCS, 2010). L'outil prédictif développé dans cette thèse peut être utilisé pour extrapoler des doses toxiques *in vitro,* au niveau cellulaire, à une dose externe produisant les concentrations toxiques observées *in vitro*. Dans des situations pauvres en données de toxicité, des doses toxiques extrapolées de données *in vitro*, comparées à des données d'exposition, pourraient aider à réaliser des évaluations préliminaires du risque. De telles évaluations pourraient servir dans l'établissement de listes

de substances prioritaires pour l'évaluation du risque à la santé comme la liste de substances d'intérêt prioritaire au Canada (CEPA, 1999). Le modèle QSPR-PBPK présentement développé peut aussi être utilisé afin d'interpréter des données de surveillance biologique, c'est-à-dire en évaluant la dose externe produisant les concentrations de biomarqueurs mesurées dans le sang (Aylward et coll., 2010).

Pour conclure, cette étude a permis le développement d'un outil fournissant un premier estimé de la TK de COV par voie inhalée. Les modèles QPPR et QSPR sont basés sur des descripteurs moléculaires globaux, permettant ainsi d'élargir le domaine d'application des modèles QSPR-PBPK. Cet outil peut simuler la variabilité des concentrations internes en COV sur la base de propriétés physicochimiques ou moléculaires mesurées (PC sang:air chez le rat) ou calculées (PC *n*-octanol:eau, eau:air et énergie d'ionisation). Le modèle PBPK développé peut être utilisé pour des études préliminaires d'évaluation de la pharmacocinétique.

Bibliographie

Allen, B. C., Hack, C. E., and Clewell, H. J. (2007). Use of Markov Chain Monte Carlo analysis with a physiologically-based pharmacokinetic model of methylmercury to estimate exposures in US women of childbearing age. *Risk Anal* 27, 947-959.

Andersen, M. E. (2003). Toxicokinetic modeling and its applications in chemical risk assessment. *Toxicol. Lett.* 138, 9-27.

Andersen, M. E., Gargas, M. L., Jones, R. A., and Jenkins Jr, L. J. (1980). Determination of the kinetic constants for metabolism of inhaled toxicants in vivo using gas uptake measurements. *Toxicol. Appl. Pharmacol.* 54, 100-116.

Arms, A. D., and Travis, C. C. (1988). Reference physiological parameters in pharmacokinetic modeling. In *EPA/600/6-88/004*, Washington, DC.

Aylward, L. L., Kirman, C. R., Blount, B. C., and Hays, S. M. (2010). Chemical-specific screening criteria for interpretation of biomonitoring data for volatile organic compounds (VOCs) - Application of steady-state PBPK model solutions. *Regul. Toxicol. Pharmacol.* 58, 33-44.

Beck, B. D., Mattuck, R. L., Bowers, T. S., Cohen, J. T., and O'Flaherty, E. (2001). The development of a stochastic physiologically-based pharmacokinetic model for lead. *Sci. Total Environ.* 274, 15-19.

Béliveau, M., and Krishnan, K. (2003). In Silico approaches for developing physiologically based pharmacokinetic (PBPK) models. In *Alternative toxicological methods* (H. Salem, and S. A. Katz, Eds.), pp. 479-532. CRC Press, Boca Raton, Fla.

Béliveau, M., Lipscomb, J., Tardif, R., and Krishnan, K. (2005). Quantitative structure-property relationships for interspecies extrapolation of the inhalation pharmacokinetics of organic chemicals. *Chem. Res. Toxicol.* 18, 475-485.

Béliveau, M., Tardif, R., and Krishnan, K. (2003). Quantitative structure-property relationships for physiologically based pharmacokinetic modeling of volatile organic chemicals in rats. *Toxicol. Appl. Pharmacol.* 189, 221-232.

Bernillon, P., and Bois, F. Y. (2000). Statistical issues in toxicokinetic modeling: a bayesian perspective. *Environ. Health Perspect.* 108 Suppl 5, 883-893.

Blaauboer, B. J. (2010). Biokinetic Modeling and in Vitro-in Vivo Extrapolations. *Journal of Toxicology and Environmental Health, Part B: Critical Reviews* 13, 242 - 252.

Bogen, K. T., and McKone, T. E. (1988). Linking indoor air and pharmacokinetic models to assess tetrachloroethylene risk. *Risk Anal* 8, 509-520.

Bois, F. Y. (2000a). Statistical analysis of Clewell et al. PBPK model of trichloroethylene kinetics. *Environ. Health Perspect.* 108 Suppl 2, 307-316.

Bois, F. Y. (2000b). Statistical analysis of Fisher et al. PBPK model of trichloroethylene kinetics. *Environ. Health Perspect.* 108 Suppl 2, 275-282.

Bois, F. Y., Gelman, A., Jiang, J., Maszle, D. R., Zeise, L., and Alexeef, G. (1996a). Population toxicokinetics of tetrachloroethylene. *Arch. Toxicol.* 70, 347-355.

Bois, F. Y., Jackson, E. T., Pekari, K., and Smith, M. T. (1996b). Population toxicokinetics of benzene. *Environ. Health Perspect.* 104 Suppl 6, 1405-1411.

Brown, R. P., Delp, M. D., Lindstedt, S. L., Rhomberg, L. R., and Beliles, R. P. (1997). Physiological parameter values for physiologically based pharmacokinetic models. *Toxicol. Ind. Health* 13, 407-484.

CEPA (1999). Loi canadienne sur la protection de l'environnement (1999).http://www.ec.gc.ca/lcpe-cepa/default.asp?lang=En&n=26A03BFA-1. Page consulée le 23-Oct 2012

Chen, H. S. G., and Gross, J. F. (1979). Estimation of tissue-to-plasma partition coefficients used in physiological pharmacokinetic models. *J. Pharmacokinet. Pharmacodyn.* 7, 117-125.

Chiu, W. A., and Ginsberg, G. L. (2011). Development and evaluation of a harmonized physiologically based pharmacokinetic (PBPK) model for perchloroethylene toxicokinetics in mice, rats, and humans. *Toxicol. Appl. Pharmacol.* 253, 203-234.

Chiu, W. A., Okino, M. S., and Evans, M. V. (2009). Characterizing uncertainty and population variability in the toxicokinetics of trichloroethylene and metabolites in mice, rats, and humans using an updated database, physiologically based pharmacokinetic (PBPK) model, and Bayesian approach. *Toxicol. Appl. Pharmacol.* 241, 36-60.

Clewell, H. J., 3rd, and Andersen, M. E. (1996). Use of physiologically based pharmacokinetic modeling to investigate individual versus population risk. *Toxicology* 111, 315-329.

Clewell, H. J., 3rd, Andersen, M. E., and Barton, H. A. (2002). A consistent approach for the application of pharmacokinetic modeling in cancer and noncancer risk assessment. *Environ. Health Perspect.* 110, 85-93.

Clewell, H. J., Gearhart, J. M., Gentry, P. R., Covington, T. R., VanLandingham, C. B., Crump, K. S., and Shipp, A. M. (1999). Evaluation of the uncertainty in an oral reference dose for methylmercury due to interindividual variability in pharmacokinetics. *Risk Anal* 19, 547-558.

Clewell, H. J., Gentry, P. R., Gearhart, J. M., Allen, B. C., and Andersen, M. E. (2001). Comparison of cancer risk estimates for vinyl chloride using animal and human data with a PBPK model. *Sci. Total Environ.* 274, 37-66.

Commission des communautés européennes (2001). LIVRE BLANC Stratégie pour la future politique dans le domaine des substances chimiques, pp. 37.

Cox, L. A., Jr. (1996). Reassessing benzene risks using internal doses and Monte-Carlo uncertainty analysis. *Environ. Health Perspect.* 104 Suppl 6, 1413-1429.

Cronin, W. J. t., Oswald, E. J., Shelley, M. L., Fisher, J. W., and Flemming, C. D. (1995). A trichloroethylene risk assessment using a Monte Carlo analysis of parameter uncertainty in conjunction with physiologically-based pharmacokinetic modeling. *Risk Anal* 15, 555-565.

Dallas, C. E., Bruckner, J. V., Maedgen, J. L., and Weir, F. W. (1986). A method for direct measurement of systemic uptake and elimination of volatile organics in small animals. *J. Pharmacol. Methods* 16, 239-250.

David, R. M., Clewell, H. J., Gentry, P. R., Covington, T. R., Morgott, D. A., and Marino, D. J. (2006). Revised assessment of cancer risk to dichloromethane II. Application of probabilistic methods to cancer risk determinations. *Regul. Toxicol. Pharmacol.* 45, 55-65.

DeJongh, J., and Blaauboer, B. J. (1996a). *In vitro*-based and in vivo-based simulations of benzene uptake and metabolism in rats. *ATLA* 24, 179-190.

DeJongh, J., and Blaauboer, B. J. (1996b). Simulation of toluene kinetics in the rat by a physiologically based pharmacokinetic model with application of biotransformation parameters derived independently in vitro and in vivo. *Fundam. Appl. Toxicol.* 32, 260-268.

Dejongh, J., and Blaauboer, B. J. (1997). Evaluation of In Vitro-based simulations of toluene uptake and metabolism in rats. *Toxicol. In Vitro* 11, 485-489.

Delic, J. I., Lilly, P. D., MacDonald, A. J., and Loizou, G. D. (2000). The utility of PBPK in the safety assessment of chloroform and carbon tetrachloride. *Regul. Toxicol. Pharmacol.* 32, 144-155.

Droz, P.-O., Wu, M. M., Cumberland, W. G., and Berode, M. (1989). Variability in biological monitoring of solvent exposure. I. Development of a population physiological model. *46* 7.

El-Masri, H. A., Bell, D. A., and Portier, C. J. (1999). Effects of glutathione transferase theta polymorphism on the risk estimates of dichloromethane to humans. *Toxicol. Appl. Pharmacol.* 158, 221-230.

Filser, J. G., and Bolt, H. M. (1979). Pharmacokinetics of halogenated ethylenes in rats. *Arch. Toxicol.* 42, 123-136.

Filser, J. G., Kessler, W., and Csanady, G. A. (2004). The Tuebingen Desiccator System, a Tool to Study Oxidative Stress In Vivo and Inhalation Toxicokinetics. *Drug Metab. Rev.* 36, 787-803.

Fiserova-Bergerova, V., and Diaz, M. L. (1986). Determination and prediction of tissue-gas partition coefficients. *Int Arch Occup Environ Health* 58, 75-87.

Gabrielsson, J. L., Paalzow, L. K., and Nordstrom, L. (1984). A physiologically based pharmacokinetic model for theophylline disposition in the pregnant and nonpregnant rat. *J Pharmacokinet Biopharm* 12, 149-165.

Gallo, J. M., Lam, F. C., and Perrier, D. G. (1987). Area method for the estimation of partition coefficients for physiological pharmacokinetic models. *J Pharmacokinet Biopharm* 15, 271-280.

Gargas, M. L., and Andersen, M. E. (1989). Determining kinetic constants of chlorinated ethane metabolism in the rat from rate of extraction. *Toxicol. Appl. Pharmacol.* 99, 344-353.

Gargas, M. L., Andersen, M. E., and Clewell III, H. J. (1986a). A physiologically based simulation approach for determining metabolic constants from gas uptake data. *Toxicol. Appl. Pharmacol.* 86, 341-352.

Gargas, M. L., Burgess, R. J., Voisard, D. E., Cason, G. H., and Andersen, M. E. (1989). Partition coefficients of low-molecular-weight volatile chemicals in various liquids and tissues. *Toxicol. Appl. Pharmacol.* 98, 87-99.

Gargas, M. L., Clewell, H. J., 3rd, and Andersen, M. E. (1986b). Metabolism of inhaled dihalomethanes in vivo: differentiation of kinetic constants for two independent pathways. *Toxicol. Appl. Pharmacol.* 82, 211-223.

Gargas, M. L., Clewell, H. J., and Andersen, M. E. (1990). Gas uptake inhalation techniques and the rates of metabolism of chloromethanes, chloroethanes and chloroethylenes in the rat. *Inhal. Toxicol.* 2, 295-319.

Gargas, M. L., Seybold, P. G., and Andersen, M. E. (1988). Modeling the tissue solubilities and metabolic rate constant (Vmax) of halogenated methanes, ethanes, and ethylenes. *Toxicol. Lett.* 43, 235-256.

Gearhart, J. M., Mahle, D. A., Greene, R. J., Seckel, C. S., Flemming, C. D., Fisher, J. W., and Clewell, H. J., 3rd (1993). Variability of physiologically based pharmacokinetic (PBPK) model parameters and their effects on PBPK model predictions in a risk assessment for perchloroethylene (PCE). *Toxicol. Lett.* 68, 131-144.

Gelman, A., Carlin, J. B., Stern, H. S., and Rubin, D. B. (2004). *Bayesian data analysis*. Chapman & Hall/CRC, Boca Raton, Fla. ; London.

Gentry, P. R., Hack, C. E., Haber, L., Maier, A., and Clewell, H. J., 3rd (2002). An approach for the quantitative consideration of genetic polymorphism data in chemical risk assessment: examples with warfarin and parathion. *Toxicol. Sci.* 70, 120-139.

Gibaldi, M., and Perrier, D. (1982). *Pharmacokinetics*. Dekker, New York.

Gueorguieva, I., Nestorov, I. A., Murby, S., Gisbert, S., Collins, B., Dickens, K., Duffy, J., Hussain, Z., and Rowland, M. (2004). Development of a Whole Body Physiologically Based Model to Characterise the Pharmacokinetics of Benzodiazepines. 1: Estimation of Rat Tissue-Plasma Partition Ratios. *J. Pharmacokinet. Pharmacodyn.* 31, 269-298.

Hamelin, G., Charest-Tardif, G., Truchon, G., and Tardif, R. (2005). Physiologically based modeling of n-hexane kinetics in humans following inhalation exposure at rest and under physical exertion: impact on free 2,5-hexanedione in urine and on n-hexane in alveolar air. *J. Occup. Environ. Hyg.* 2, 86-97; quiz D86-87.

Hilderbrand, R. L., Andersen, M. E., and Jenkins, J. L. J. (1981). Prediction of in vivo kinetic constants for metabolism of inhaled vapors from kinetic constants measured in vitro. *Fundam. Appl. Toxicol.* 1, 403-409.

Huizer, D., Oldenkamp, R., Ragas, A. M. J., van Rooij, J. G. M., and Huijbregts, M. A. J. (2012). Separating uncertainty and physiological variability in human PBPK modelling: The example of 2-propanol and its metabolite acetone. *Toxicol. Lett.* 214, 154-165.

Igari, Y., Sugiyama, Y., Sawada, Y., Iga, T., and Hanano, M. (1983). Prediction of diazepam disposition in the rat and man by a physiologically based pharmacokinetic model. *J Pharmacokinet Biopharm* 11, 577-593.

IPCS (2010). *Characterization and application of physiologically based pharmacokinetic models in risk assessment*.

Johanson, G., and Dynésius, B. (1988). Liquid/Air Partition Coefficients of Six Commonly Used Glycol Ethers. *Br. J. Ind. Med.* 45, 561-564.

Jones, J. P., Korzekwa, K. R., Eric, F. J., and Michael, R. W. (1996). [36] Predicting the rates and regioselectivity of reactions mediated by the P450 superfamily. In *Methods in Enzymology*, pp. 326-335. Academic Press.

Jonsson, F., Bois, F., and Johanson, G. (2001a). Physiologically based pharmacokinetic modeling of inhalation exposure of humans to dichloromethane during moderate to heavy exercise. *Toxicol. Sci.* 59, 209-218.

Jonsson, F., Bois, F. Y., and Johanson, G. (2001b). Assessing the reliability of PBPK models using data from methyl chloride-exposed, non-conjugating human subjects. *Arch. Toxicol.* 75, 189-199.

Jonsson, F., and Johanson, G. (2001a). A Bayesian analysis of the influence of GSTT1 polymorphism on the cancer risk estimate for dichloromethane. *Toxicol. Appl. Pharmacol.* 174, 99-112.

Jonsson, F., and Johanson, G. (2001b). Bayesian estimation of variability in adipose tissue blood flow in man by physiologically based pharmacokinetic modeling of inhalation exposure to toluene. *Toxicology* 157, 177-193.

Jonsson, F., and Johanson, G. (2002). Physiologically based modeling of the inhalation kinetics of styrene in humans using a bayesian population approach. *Toxicol. Appl. Pharmacol.* 179, 35-49.

Kamgang, E., Peyret, T., and Krishnan, K. (2008). An integrated QSPR-PBPK modelling approach for in vitro-in vivo extrapolation of pharmacokinetics in rats. *SAR QSAR Environ. Res.* 19, 669 - 680.

Kaneko, T., Horiuchi, J., and Sato, A. (2000). Development of a physiologically based pharmacokinetic model of organic solvent in rats. *Pharmacol Res* 42, 465-470.

Kaneko, T., Wang, P. Y., and Sato, A. (1994). Partition coefficients of some acetate esters and alcohols in water, blood, olive oil, and rat tissues. *Occup. Environ. Med.* 51, 68-72.

Kim, D. N., Cho, K.-H., Oh, W. S., Lee, C. J., Lee, S. K., Jung, J., and No, K. T. (2009). EaMEAD: Activation Energy Prediction of Cytochrome P450 Mediated Metabolism with Effective Atomic Descriptors. *Journal of Chemical Information and Modeling* 49, 1643-1654.

Klaassen, C. D. (2001). *Casarett and Doull's toxicology : the basic science of poisons*. McGraw-Hill, Medical Pub. Division, New York ; Toronto.

Krishnan, K., and Andersen, M. E. (2007). Physiologically based Pharmacokinetic modeling in toxicology. In *Principles and methods of toxicology* (A. W. Hayes, Ed.), pp. 231-292. Taylor & Francis, Boca Raton.

Krishnan, K., and Andersen, M. E. (2010). *Quantitative modeling in toxicology*. John Wiley & Sons, Chichester, U.K.

Krishnan, K., and Johanson, G. (2005). Physiologically-based pharmacokinetic and toxicokinetic models in cancer risk assessment. *J Environ Sci Health C Environ Carcinog Ecotoxicol Rev* 23, 31-53.

Lam, G., Chen, M. L., and Chiou, W. L. (1982). Determination of tissue to blood partition coefficients in physiologically-based pharmacokinetic studies. *J. Pharm. Sci.* 4, 454-456.

Lewis, D. F. (2000). On the recognition of mammalian microsomal cytochrome P450 substrates and their characteristics: towards the prediction of human p450 substrate specificity and metabolism. *Biochem. Pharmacol.* 60, 293-306.

Lewis, D. F. V. (2001). *Guide to cytochromes P450 : structure and function*. Taylor & Francis, London ; New York.

Liao, K. H., Tan, Y. M., and Clewell, H. J., 3rd (2007a). Development of a screening approach to interpret human biomonitoring data on volatile organic compounds: reverse dosimetry on biomonitoring data for trichloroethylene. *Risk Anal* 27, 1223-1236.

Liao, K. H., Yu-Mei, T., Conolly, R. B., Borghoff, S. J., Gargas, M. L., Andersen, M. E., and Clewell Iii, H. J. (2007b). Bayesian estimation of pharmacokinetic and pharmacodynamic parameters in a Mode-of-Action-based cancer risk assessment for chloroform. *Risk Analysis: An International Journal* 27, 1535-1551.

Lin, J. H., Sugiyama, Y., Awazu, S., and Hanano, M. (1982). In vitro and in vivo evaluation of the tissue-to-blood partition coefficient for physiological pharmacokinetic models. *J Pharmacokinet Biopharm* 10, 637-647.

Lipscomb, J. C., Teuschler, L. K., Swartout, J., Popken, D., Cox, T., and Kedderis, G. L. (2003). The impact of cytochrome P450 2E1-dependent metabolic variance on a risk-relevant pharmacokinetic outcome in humans. *Risk Anal* 23, 1221-1238.

Livingstone, D. (2004). Building QSAR models: A practical guide. In *Predicting chemical toxicity and fate* (M. T. D. Cronin, and D. J. Livingstone, Eds.), pp. 151-170. CRC Press, Boca Raton, Fla.

Louisse, J., de Jong, E., van de Sandt, J. J. M., Blaauboer, B. J., Woutersen, R. A., Piersma, A. H., Rietjens, I. M. C. M., and Verwei, M. (2010). The Use of In Vitro Toxicity Data and Physiologically Based Kinetic Modeling to Predict Dose-Response Curves for In Vivo Developmental Toxicity of Glycol Ethers in Rat and Man. *Toxicol. Sci.* 118, 470-484.

Lowe, E. R., Poet, T. S., Rick, D. L., Marty, M. S., Mattsson, J. L., Timchalk, C., and Bartels, M. J. (2009). The Effect of Plasma Lipids on the Pharmacokinetics of Chlorpyrifos and the Impact on Interpretation of Blood Biomonitoring Data. *Toxicol. Sci.* 108, 258-272.

Lyons, M. A., Yang, R. S., Mayeno, A. N., and Reisfeld, B. (2008). Computational toxicology of chloroform: reverse dosimetry using bayesian inference, markov chain monte carlo simulation, and human biomonitoring data. *Environ. Health Perspect.* 116, 1040-1046.

MacDonald, A. J., Rostami-Hodjegan, A., Tucker, G. T., and Linkens, D. A. (2002). Analysis of solvent central nervous system toxicity and ethanol interactions using a human population physiologically based kinetic and dynamic model. *Regul. Toxicol. Pharmacol.* 35, 165-176.

Marino, D. J., Clewell, H. J., Gentry, P. R., Covington, T. R., Hack, C. E., David, R. M., and Morgott, D. A. (2006). Revised assessment of cancer risk to dichloromethane: part I Bayesian PBPK and dose-response modeling in mice. *Regul. Toxicol. Pharmacol.* 45, 44-54.

Mayeno, A. N., Robinson, J. L., Yang, R. S. H., and Reisfeld, B. (2009). Predicting Activation Enthalpies of Cytochrome-P450-Mediated Hydrogen Abstractions. 2. Comparison of Semiempirical PM3, SAM1, and AM1 with a Density Functional Theory Method. *Journal of Chemical Information and Modeling* 49, 1692-1703.

Mörk, A.-K., Jonsson, F., and Johanson, G. (2009). Bayesian population analysis of a washin-washout physiologically based pharmacokinetic model for acetone. *Toxicol. Appl. Pharmacol.* 240, 423-432.

Mortensen, B., Eide, I., Zahlsen, K., and Nilsen, O. G. (2000). Prediction of in vivo metabolic clearance of 25 different petroleum hydrocarbons by a rat liver head-space technique. *Arch. Toxicol.* 74, 308-312.

Mortensen, B., Løkken, T., Zahlsen, K., and Nilsen, O. G. (1997). Comparison and in vivo Relevance of Two Different in vitro Head Space Metabolic Systems: Liver S9 and Liver Slices. *Pharmacol. Toxicol.* 81, 35-41.

Mortensen, B., and Nilsen, O. G. (1998a). Allometric Species Comparison of Toluene and n–Hexane Metabolism: Prediction of Hepatic Clearance in Man from Experiments with Rodent Liver S9 in a Head Space Vial Equilibration System. *Pharmacol. Toxicol.* 82, 183-188.

Mortensen, B., and Nilsen, O. G. (1998b). Optimization and Application of the Head Space Liver S9 Equilibration Technique for Metabolic Studies of Organic Solvents. *Pharmacol. Toxicol.* 82, 142-146.

National Research Council (2007). *Toxicity testing in the 21st century : a vision and a strategy*. National Academies Press, Washington, DC.

Nichols, J. W., McKim, J. M., Lien, G. J., Hoffman, A. D., and Bertelsen, S. L. (1991). Physiologically based toxicokinetic modeling of three waterborne chloroethanes in rainbow trout (Oncorhynchus mykiss). *Toxicol. Appl. Pharmacol.* 110, 374-389.

Nong, A., and Krishnan, K. (2007). Estimation of interindividual pharmacokinetic variability factor for inhaled volatile organic chemicals using a probability-bounds approach. *Regul. Toxicol. Pharmacol.* 48, 93-101.

Nong, A., McCarver, D. G., Hines, R. N., and Krishnan, K. (2006). Modeling interchild differences in pharmacokinetics on the basis of subject-specific data on physiology and hepatic CYP2E1 levels: A case study with toluene. *Toxicol. Appl. Pharmacol.* 214, 78-87.

Nong, A., Tan, Y.-M., Krolski, M. E., Wang, J., Lunchick, C., Conolly, R. B., and Clewell, H. J. (2008). Bayesian calibration of a physiologically based pharmacokinetic/pharmacodynamic model of carbaryl cholinesterase inhibition. *J. Toxicol. Environ. Health A* 71, 1363 - 1381.

OECD (2012). OECD Cooperative Chemicals Assessment Programme.http://www.oecd.org/env/chemicalsafetyandbiosafety/assessmentofchemicals/oecdcooperativechemicalsassessmentprogramme.htm. Page consulée le 24 Oct 2012

Olsen, L., Rydberg, P., Rod, T. H., and Ryde, U. (2006). Prediction of Activation Energies for Hydrogen Abstraction by Cytochrome P450. *J. Med. Chem.* 49, 6489-6499.

Pelekis, M., Krewski, D., and Krishnan, K. (1997). Physiologically based algebraic expressions for predicting steady-state toxiconetics of inhaled vapors. *Toxicology methods* 7, 205-225.

Pelekis, M., Nicolich, M. J., and Gauthier, J. S. (2003). Probabilistic framework for the estimation of the adult and child toxicokinetic intraspecies uncertainty factors. *Risk Anal* 23, 1239-1255.

Pelekis, M., Poulin, P., and Krishnan, K. (1995). An approach for incorporating tissue composition data into physiologically based pharmacokinetic models. *Toxicol. Ind. Health* 11, 511-522.

Péry, A. R. R., Brochot, C., Hoet, P. H. M., Nemmar, A., and Bois, F. Y. (2009). Development of a physiologically based kinetic model for 99m-Technetium-labelled carbon nanoparticles inhaled by humans. *Inhal. Toxicol.* 21, 1099-1107.

Peyret, T. (2007). Évaluation de la variabilité interindividuelle de la toxicocinétique de composés organiques volatils chez l'humain. Mémoire de Maîtrise, Université de Montréal. Montréal. pp. 121.

Peyret, T., and Krishnan, K. (2010a). *In vitro-in vivo* extrapolation of the human dose-response relationship for cellular perturbations by a binary mixture of toluene (TOL) and *n*-hexane (HEX). *The Toxicologist* 114, 54.

Peyret, T., and Krishnan, K. (2010b). Prediction of in vivo dose-response relationship from in vitro concentration-response relationship using cellular-level PBPK modeling. In *Toxicity-pathway-based risk assessment: preparing for paradigm change, a symposium summary* (N. R. Council, Ed.), pp. 114-115. The national academies press, Washington, DC.

Peyret, T., and Krishnan, K. (2011). QSARs for PBPK modelling of environmental contaminants. *SAR QSAR Environ. Res.* 22, 129-169.

Poet, T. S., Kirman, C. R., Bader, M., van Thriel, C., Gargas, M. L., and Hinderliter, P. M. (2010). Quantitative Risk Analysis for N-Methyl Pyrrolidone Using Physiologically Based Pharmacokinetic and Benchmark Dose Modeling. *Toxicol. Sci.* 113, 468-482.

Portier, C. J., and Kaplan, N. L. (1989). Variability of safe dose estimates when using complicated models of the carcinogenic process. A case study: methylene chloride. *Fundam. Appl. Toxicol.* 13, 533-544.

Poulin, P., Béliveau, M., and Krishnan, K. (1999). Mechanistic animal replacement approaches for predicting pharmacokinetics of organic chemicals. In *Toxicity assessment alternatives : methods, issues, opportunities* (H. Salem, and S. A. Katz, Eds.), pp. 115-139. Humana Press, Totowa, N.J.

Poulin, P., and Krishnan, K. (1999). Molecular structure-based prediction of the toxicokinetics of inhaled vapors in humans. *Int J Toxicol* 18, 7-18.

Price, K., and Krishnan, K. (2011). An integrated QSAR-PBPK modelling approach for predicting the inhalation toxicokinetics of mixtures of volatile organic chemicals in the rat. *SAR QSAR Environ. Res.* 22, 107-128.

Qiu, J., Chien, Y.-C., Bruckner, J. V., and Fisher, J. W. (2010). Bayesian analysis of a physiologically based pharmacokinetic model for perchloroethylene in humans. *Journal of Toxicology and Environmental Health Part A* 73, 74 - 91.

Reddy, M. B. (2005). *Physiologically based pharmacokinetic modeling : science and applications*. John Wiley & Sons, Hoboken, N.J.

Reitz, R. H., Mendrala, A. L., and Guengerich, F. P. (1989). In vitro metabolism of methylene chloride in human and animal tissues: use in physiologically based pharmacokinetic models. *Toxicol. Appl. Pharmacol.* 97, 230-246.

Reitz, R. H., Mendrala, A. L., Park, C. N., Andersen, M. E., and Guengerich, F. P. (1988). Incorporation of in vitro enzyme data into the physiologically-based pharmacokinetic (PB-PK) model for methylene chloride: implications for risk assessment. *Toxicol. Lett.* 43, 97-116.

Renwick, A. G., and Lazarus, N. R. (1998). Human variability and noncancer risk assessment- An analysis of the default uncertainty factor. *Regul. Toxicol. Pharmacol.* 27, 3-20.

Rodgers, T., and Rowland, M. (2007). Mechanistic approaches to volume of distribution predictions: understanding the processes. *Pharm. Res.* 24, 918-933.

Rydberg, P., Ryde, U., and Olsen, L. (2008). Prediction of Activation Energies for Aromatic Oxidation by Cytochrome P450. *The Journal of Physical Chemistry A* 112, 13058-13065.

Sasso, A. F., Georgopoulos, P. G., Isukapalli, S. S., and Krishnan, K. (2012). Bayesian analysis of a lipid-based physiologically based toxicokinetic model for a mixture of PCBs in rats. *J Toxicol*, doi: 10.1155/2012/895391.

Sato, A., and Nakajima, T. (1979a). Partition coefficients of some aromatic hydrocarbons and ketones in water, blood and oil. *Br. J. Ind. Med.* 36, 231-234.

Sato, A., and Nakajima, T. (1979b). A vial-equilibration method to evaluate the drug-metabolizing enzyme activity for volatile hydrocarbons. *Toxicol. Appl. Pharmacol.* 47, 41-46.

Sultatos, L. G. (1990). A physiologically based pharmacokinetic model of parathion based on chemical-specific parameters determined in vitro. *Journal of the American College of Toxicology* 9, 611-619.

Sultatos, L. G., Kim, B., and Woods, L. (1990). Evaluation of estimations in vitro of tissue/blood distribution coefficients for organothiophosphate insecticides. *Toxicol. Appl. Pharmacol.* 103, 52-55.

Sweeney, L. M., Tyler, T. R., Kirman, C. R., Corley, R. A., Reitz, R. H., Paustenbach, D. J., Holson, J. F., Whorton, M. D., Thompson, K. M., and Gargas, M. L. (2001). Proposed occupational exposure limits for select ethylene glycol ethers using PBPK models and Monte Carlo simulations. *Toxicol. Sci.* 62, 124-139.

Tan, Y. M., Liao, K. H., and Clewell, H. J., 3rd (2007). Reverse dosimetry: interpreting trihalomethanes biomonitoring data using physiologically based pharmacokinetic modeling. *J Expo Sci Environ Epidemiol* 17, 591-603.

Tan, Y. M., Liao, K. H., Conolly, R. B., Blount, B. C., Mason, A. M., and Clewell, H. J. (2006). Use of a physiologically based pharmacokinetic model to identify exposures consistent with human biomonitoring data for chloroform. *J. Toxicol. Environ. Health A* 69, 1727-1756.

Tardif, R., Droz, P. O., Charest-Tardif, G., Pierrehumbert, G., and Truchon, G. (2002). Impact of human variability on the biological monitoring of exposure to toluene: I. Physiologically based toxicokinetic modelling. *Toxicol. Lett.* 134, 155-163.

Thomas, R. S., Bigelow, P. L., Keefe, T. J., and Yang, R. S. (1996). Variability in biological exposure indices using physiologically based pharmacokinetic modeling and Monte Carlo simulation. *Am Ind Hyg Assoc J* 57, 23-32.

Timchalk, C., Kousba, A., and Poet, T. S. (2002). Monte Carlo analysis of the human chlorpyrifos-oxonase (PON1) polymorphism using a physiologically based pharmacokinetic and pharmacodynamic (PBPK/PD) model. *Toxicol. Lett.* 135, 51-59.

U.S. E.P.A. (1997). Guiding Principles for Monte Carlo Analysis, pp. EPA/630/R-697/001. U.S. Environmental Protection Agency, Washington, DC.

Valcke, M., and Krishnan, K. (2010). An Assessment of the Interindividual Variability of Internal Dosimetry during Multi-Route Exposure to Drinking Water Contaminants. *Int. J. Environ. Res. Public Health* 7, 4002-4022.

Valcke, M., and Krishnan, K. (2011). Evaluation of the impact of the exposure route on the human kinetic adjustment factor. *Regul. Toxicol. Pharmacol.* 59, 258-269.

Valentin, J. (2002). Basic anatomical and physiological data for use in radiological protection: reference values: ICRP Publication 89. *Annals of the ICRP* 32, 1-277.

Vinegar, A., Jepson, G. W., Cisneros, M., Rubenstein, R., and Brock, W. J. (2000). Setting safe acute exposure limits for halon replacement chemicals using physiologically based pharmacokinetic modeling. *Inhal. Toxicol.* 12, 751-763.

Wilkinson, G. R., and Shand, D. G. (1975). Commentary: a physiological approach to hepatic drug clearance. *Clin. Pharmacol. Ther.* 18, 377-390.

Woodruff, T. J., Bois, F. Y., Auslander, D., and Spear, R. C. (1992). Structure and parameterization of pharmacokinetic models: their impact on model predictions. *Risk Anal* 12, 189-201.